Integrability and higher-Point Functions in AdS/CFT

Dissertation

zur Erlangung des akademischen Grades

Doktor rerum naturalium
(Dr. rer. nat.)

im Fach Physik
Spezialisierung: Theoretische Physik

eingereicht an der

Mathematisch-Naturwissenschaftlichen Fakultät der Humboldt-Universität zu Berlin

von

M.Sc. Dennis Max Dieter le Plat

Präsidentin der Humboldt-Universität zu Berlin
Prof. Dr. Julia von Blumenthal

Dekanin der Mathematisch-Naturwissenschaftlichen Fakultät
Prof. Dr. Caren Tischendorf

Gutachter/innen:
1. Prof. Dr. Matthias Staudacher
2. Dr. Burkhard Eden
3. Prof. Dr. Charlotte Kristjansen

Tag der mündlichen Prüfung: 23. Oktober 2023

Selbstständigkeitserklärung

Hiermit erkläre ich, die Dissertation selbstständig und nur unter Verwendung der angegebenen Hilfen und Hilfsmittel angefertigt zu haben. Ich habe mich nicht anderwärts um einen Doktorgrad in dem Promotionsfach beworben und besitze keinen entsprechenden Doktorgrad. Die Promotionsordnung der Mathematisch-Naturwissenschaftlichen Fakultät, veröffentlicht im Amtlichen Mitteilungsblatt der Humboldt-Universität zu Berlin Nr. 42 am 11. Juli 2018, habe ich zur Kenntnis genommen.

Berlin, den 04.08.2023

Abstract

Integrability proved to be a powerful tool to calculate observables in the AdS/CFT correspondence. At first discovered in the planar spectral problem, methods have since been devised for calculating higher-point functions as well. In this thesis we will consider two instances of the correspondence, that is $\mathrm{AdS}_5/\mathrm{CFT}_4$ as well as $\mathrm{AdS}_3/\mathrm{CFT}_2$, aiming at extending the integrability framework.

In Part I we focus on integrability in $\mathcal{N} = 4$ SYM theory, where the hexagon form factor provides a formalism to calculate three-point functions. For this, the correlator is cut into two hexagonal patches. Considering the local operators in the spin chain picture, the Bethe states also need to be cut, resulting in an entangled state. Most applications in the literature have been restricted to rank-one sectors. In this thesis, we extend the hexagon formalism to higher-rank sectors, while preserving its operator-like structure and importing only a minimum of information from the nested Bethe ansatz. We test this idea against free field theory results for correlators in the so-called SU(3) and SU(1|2) sectors. Further, we investigate the use of the hexagon formalism for the evaluation of correlators in the presence of the β-deformation in SU(1|2) and SU(2) sectors.

Moreover, considering double excitations in the spin chain picture allows us to accommodate for the full set of fields in $\mathcal{N} = 4$ SYM theory. For the Konishi operator we present a tree-level analysis of the related creation amplitudes in the nested Bethe ansatz as well as in the matrix picture, where the excitations scatter via the Beisert S matrix. Remarkably, the local structure of double excitations is hidden in the hexagon calculation. Building on these ideas, we work out Bethe solutions and build the chiral Yang-Mills field strength tensor from four fermions at leading order in the coupling. We put forward a Lagrangian insertion method in the hexagon formalism and perform a first test, namely that the three-point function of the Lagrangian with two half-BPS operators of equal length ought to vanish.

In Part II we propose a hexagon formalism for superstrings in $\mathrm{AdS}_3 \times \mathrm{S}^3 \times \mathrm{T}^4$ backgrounds with an arbitrary mixture or Ramond-Ramond and Neveu-Schwarz-Neveu-Schwarz fluxes. We bootstrap the hexagon form factor for one- and two-particle states from symmetry and give a proposal for the evaluation of many particle states in terms of the theories S matrix. By imposing physical constraints, we find that the hexagons dressing factors are related to those of the S matrix in the spectral problem. In addition, we calculate some correlation functions of protected operators and find agreement with results in the literature.

Finally, we consider the thermodynamic Bethe ansatz (TBA) equations constructed by Frolov and Sfondrini for the spectrum of strings on the pure-Ramond-Ramond $\mathrm{AdS}_3 \times \mathrm{S}^3 \times \mathrm{T}^4$ background. Here we study the small tension limit of the mirror TBA equations and find that the equations simplify considerably. We observe, that the leading-order contribution to the anomalous dimensions is due to massless excitations.

Zusammenfassung

Integrabilität hat sich als ein mächtiges Werkzeug zur Berechnung von Observablen in der AdS/CFT-Korrespondenz erwiesen. Zunächst für das planare Spektralproblem entdeckt, wurden inzwischen auch Methoden zur Berechnung von Mehrpunktfunktionen entwickelt. In dieser Arbeit werden die Realisierungen dieser Korrespondenz für AdS_5/CFT_4 und AdS_3/CFT_2 betrachtet mit dem Ziel, den Anwendungsbereich der Integrabilität zu erweitern.

Teil I behandelt Integrabilität in der $\mathcal{N} = 4$ SYM-Theorie, wo der Hexagon-Formalismus die Berechnung von Dreipunktfunktionen ermöglicht. Hierfür wird der Korrelator in zwei hexagonale Stücke zerlegt. Betrachtet man die lokalen Operatoren dabei im Spinkettenbild, müssen auch die Bethe-Zustände zerschnitten werden, was zu einem verschränkten Zustand führt. Die meisten Anwendungen in der Literatur beschränken sich auf Sektoren vom Rang eins. In dieser Arbeit wird der Hexagon-Formalismus auf Sektoren mit höherem Rang ausgedehnt, wobei die operatorartige Struktur erhalten bleibt und nur ein Minimum an Informationen aus dem verschachtelten Bethe-Ansatz genutzt wird. Diese Idee wird mit Ergebnissen der freien Feldtheorie für Korrelatoren in den sog. SU(3)- und SU(1|2)-Sektoren getestet. Außerdem wird die Anwendung des Hexagon-Formalismus für die Auswertung von Korrelatoren in β-deformierten SU(1|2)- und SU(2)-Sektoren untersucht.

Des Weiteren erlaubt die Betrachtung von Doppelanregungen im Spinkettenbild die Realisierung aller Felder der $\mathcal{N} = 4$ SYM-Theorie. Für den Konishi-Operator werden die zugehörigen Erzeugeramplituden sowohl im verschachtelten Bethe-Ansatz als auch im Matrixbild, wo die Anregungen durch die Beisert S Matrix streuen, auf Baumniveau ausgearbeitet. Die lokale Struktur der Doppelanregungen ist in der Hexagonberechnung verborgen. Es werden Bethe-Lösungen erarbeitet und der chirale Yang-Mills-Feldstärketensor aus vier Fermionen in führender Ordnung der Kopplung konstruiert. Eine Methode zur Einsetzung des Lagrangeoperators im Hexagon-Formalismus wird vorgeschlagen und ein erster Test durchgeführt, nämlich dass die Dreipunktfunktion dieses Operators mit zwei halb-BPS-Operatoren gleicher Länge verschwinden sollte.

Teil II behandelt den Hexagon-Formalismus für Superstrings auf $AdS_3 \times S^3 \times T^4$ Hintergründen mit einer beliebigen Mischung von Ramond-Ramond und Neveu-Schwarz-Neveu-Schwarz Flüssen. Der Hexagon-Formfaktor wird für Ein- und Zwei-Teilchen-Zustände konstruiert und lässt sich für viele Teilchen unter Nutzung der S Matrix verallgemeinern. Weitere physikalische Bedingungen stellen einen Zusammenhang zwischen den Phasenfaktoren der Hexagon-Formfaktoren und denen der S-Matrix im Spektralproblem her. Darüber hinaus werden Korrelationsfunktionen geschützter Operatoren berechnet und Übereinstimmung mit Ergebnissen aus der Literatur gefunden.

Schließlich werden die thermodynamischen Bethe-Ansatz (TBA)-Gleichungen betrachtet, die von Frolov und Sfondrini für das Spektrum von Strings auf reinem Ramond-Ramond $AdS_3 \times S^3 \times T^4$ Hintergrund konstruiert wurden. Bei schwacher Kopplung lassen sich die TBA-Gleichungen erheblich vereinfachen. Der Beitrag zu den anomalen Dimensionen in führender Ordnung ist auf masselose Anregungen zurückzuführen.

List of Publications

This thesis is based on the publications and preprints [1–5], listed chronologically by the date of appearance:

[1] B. Eden, D. le Plat and A. Sfondrini, *Integrable bootstrap for AdS_3/CFT_2 correlation functions*, JHEP **08** (2021) 049, ArXiv:2102.08365.

[2] B. Eden, D. le Plat and A. Spiering, *Higher-rank sectors in the hexagon formalism and marginal deformations*, ArXiv:2212.03211.

[3] B. Eden, D. le Plat and A. Spiering, *Double excitations in the AdS_5/CFT_4 integrable system and the Lagrange operator*, ArXiv2302.02961.

[4] A. Brollo, D. le Plat, A. Sfondrini and R. Suzuki, *The Tensionless Limit of Pure-Ramond-Ramond AdS_3/CFT_2*, ArXiv:2303.02120.

[5] A. Brollo, D. le Plat, A. Sfondrini and R. Suzuki, *More on the Tensionless Limit of Pure-Ramond-Ramond AdS_3/CFT_2*, ArXiv:2308.11576.

The texts were rewritten in order to expand on certain aspects. Moreover, Sec. 3.2 and Sec. 3.3 are based on [2], Sec. 3.4 and Sec. 3.5 are based on [3], Sec. 5 is based on [1] and finally Sec. 6.3 is based on [4] and [5].

Acknowledgement

The last couple of years have been an enthralling journey for me, both academically and personally. I have had the pleasure to meet many fascinating personalities from all over the world and had the chance to learn from them. For these experiences and opportunities I am very grateful.

First of all, I would like to express my gratitude towards Burkhard Eden for being my advisor on this journey. Thank you for all the discussions we had in front of blackboards and teaching me so much. I greatly appreciate the time and support you have given me over the last years.

In addition, I am very thankful to Alessandro Sfondrini. Thank you for taking so much time to discuss and pointing out different research directions to me. I am grateful for your tremendous support along my way and in particular making sure that it crosses yours from time to time.

Furthermore, I would like to thank Matthias Staudacher for having me as a member of his outstanding research group and his support, particularly including writing many reports for my scholarship.

During my PhD I have had the pleasure to collaborate with Alberto Brollo, Burkhard Eden, Maximilian Gottwald, Tristan McLoughlin, Tobias Scherdin, Fiona Seibold, Alessandro Sfondrini, Anne Spiering and Ryo Suzuki. Thank you for all the fruitful discussions and the joint work on the projects this thesis is based on. Further, I would like to thank all the people I have met at conferences and schools as well as those, who always found some time for interesting discussions.

I would also like to thank my office-mates, colleagues and members of staff at the IRIS for the motivating atmosphere. In particular, special thanks go to Jenny Collard for being always on top of administrative matters.

Also I greatly appreciate the effort of Burkhard Eden, Maximilian Gottwald, Tobias Scherdin, Anne Spiering and Alessandro Sfondrini for proof-reading the manuscript, spotting countless misprints and suggesting valuable improvements.

I would also like to thank the organisers and attendees of the KITP program *Integrability in String, Field, and Condensed Matter Theory* for the two extraordinary months in Santa Barbara. It was a pleasure to meet over coffee with Ana, Davide, Deniz, Enrico, Hanno, Moritz and Simon.

I am especially grateful for the scholarship by the *Stiftung der Deutschen Wirtschaft*, which funded my research and made this work possible. The variety of events and seminars I attended as well as the people I met inspired me in many ways. Further, I appreciated the various extracurricular activities for and in particular in cooperation with the foundation. This facilitated a personal growth I cannot possibly asses here.

Ein ganz besonderer Dank gilt schließlich meiner Familie und meinen Freunden. Insbesondere möchte ich mich bei Heike, Timo und Juliane für ihre unermüdliche Unterstützung und die stetige Begleitung auf meinem Weg bedanken. Diese Arbeit ist für Euch!

Contents

1. Introduction **1**

I. Integrability in $\mathcal{N} = 4$ SYM **7**

2. Review of integrability in $\mathcal{N} = 4$ super Yang-Mills theory **8**
2.1. Field theory 8
2.1.1. Field content and the Lagrangian 8
2.1.2. Gauge group 9
2.1.3. Symmetry algebra 10
2.1.4. Correlation functions 13
2.2. The spectral problem and integrability 15
2.2.1. Classical integrability 16
2.2.2. SU(2) spin chain 17
2.2.3. S matrix from symmetries 21
2.2.4. Higher rank models and the nested Bethe Ansatz 22
2.3. Marginal deformations 27
2.3.1. The β-deformed SU(2) sector 28
2.4. Chapter summary 30

3. The hexagon form factor for three-point functions **31**
3.1. Review of the hexagon form formalism 31
3.2. Higher-rank sectors 35
3.2.1. The hybrid formalism 35
3.2.2. Correlators in the SU(3) sector 37
3.2.3. Correlators in the SU(1|2) sector 38
3.3. Marginal deformations 39
3.3.1. Correlators in the SU(1|2) sector 40
3.3.2. Correlators in the SU(2) sector 42
3.4. Double excitations 45
3.4.1. Creation amplitudes for double excitations 46
3.4.2. The Konishi singlet 46
3.5. Lagrangian insertion method 50
3.5.1. The on-shell Lagrangian 50
3.5.2. A simple test of the Lagrangian insertion method 52
3.6. Chapter summary 54

II. Integrability in AdS_3 **57**

4. Review of integrability in $AdS_3 \times S^3 \times T^4$ **58**
4.1. Light-cone gauge fixing of the bosonic string . . . 58
4.2. The Superalgebra . . . 60
4.3. Centrally extended off-shell symmetry algebra . . . 63
4.4. Short representations of the light-cone symmetry algebra . . . 64
4.5. Particle content of the theory . . . 66
4.6. Scattering matrix . . . 72
4.7. Dressing factors and the crossing equation . . . 75
4.8. Chapter summary . . . 79

5. Hexagon form factors in AdS_3 **80**
5.1. The supertranslation operator and the hexagon subalgebra . . . 80
5.2. Bootstrap principle . . . 82
5.2.1. One-particle states . . . 83
5.2.2. Two-particle states . . . 84
5.2.3. General form of the two-particle hexagon form factor . . . 86
5.2.4. Many-particle states . . . 87
5.3. Representations of the hexagon algebra and crossing . . . 87
5.4. The scalar factors . . . 91
5.4.1. The Watson equation . . . 92
5.4.2. Decoupling condition and crossing . . . 93
5.4.3. Cyclic invariance . . . 94
5.4.4. Solution for the scalar factors . . . 96
5.5. An explicit check with protected three-point functions . . . 97
5.5.1. Definition of the correlation functions . . . 97
5.5.2. Hexagon computation . . . 100
5.6. Chapter summary . . . 103

6. Thermodynamic Bethe Ansatz for pure Ramond-Ramond flux **105**
6.1. Review of the Thermodynamic Bethe Ansatz . . . 105
6.2. TBA equations in the pure-RR sector . . . 112
6.2.1. Parametrisation . . . 113
6.2.2. Mirror TBA equations . . . 117
6.3. Simplified TBA equations in the tensionless limit . . . 120
6.3.1. Rewriting of the TBA equations . . . 120
6.3.2. Analysing the scaling in the small-tension limit . . . 121
6.3.3. Simplifying the TBA equations . . . 123
6.4. Chapter summary . . . 128

7. Conclusions **129**

A. Evaluation of the $\mathcal{N} = 4$ SYM hexagon **134**
A.1. Parametrisation and crossing . . . 134
A.2. Dressing phase and measure factor . . . 135
A.3. String and spin chain frame . . . 135

B. S Matrices and kernels for AdS_3 **137**
B.1. S matrices 137
B.2. Dressing factors 139
B.2.1. The BES phase 139
B.2.2. Sine-Gordon dressing factor 139
B.2.3. Massive dressing factors 140
B.2.4. Mixed-mass and massless dressing factors 140

Bibliography **142**

Chapter 1.

Introduction

Quantum field theories (QFT) form the mathematical framework for the description of elementary particles and their interactions in the universe. In particular, Yang-Mills theories have been studied for almost 70 years leading to the Standard Model of particle physics. Its predictions have been tested against data from high-precision measurements, which require the largest machines mankind ever built in order to conduct experiments, such as the Large Hadron Collider. However, most theoretical predictions can only be obtained perturbatively in the coupling constant. The interaction is then considered as a perturbation around the free theory. The terms contributing at each order of the coupling can be represented graphically using Feynman diagrams. In order to obtain predictions with higher precision it is necessary to evaluate the perturbative series to higher orders, which becomes very challenging. On the one hand, the number of diagrams grows factorially with the order. On the other hand, the evaluation of a diagram at a given order involves a certain number of integrals, which are complicated to compute. Furthermore, in physical models like quantum chromodynamics (QCD) at low energy, the coupling constant is not small and a series expansion is not applicable. Hence it is desirable to devise non-perturbative methods, as these would allow to circumvent such problems.

For the purpose of developing these methods it is helpful to consider toy models with a large amount of symmetry. A famous example in this regard is $\mathcal{N} = 4$ supersymmetric Yang-Mills theory ($\mathcal{N} = 4$ SYM). This is the unique maximally supersymmetric gauge theory in four spacetime dimensions. This theory is conformal even at the quantum level and the large amount of symmetry allows us to constrain the form of observables. For instance, the two-point function of scalar operators $\mathcal{O}_j(x)$ with scaling dimension Δ must be of the form

$$\langle \mathcal{O}_j(x_1)\mathcal{O}_k(x_2)\rangle = \frac{\delta_{j,k}}{|x_1 - x_2|^{2\Delta}}\,, \tag{1.1}$$

using an appropriate normalisation of the operators. Moreover, in a similar way the form of three-point functions can be determined in terms of the scaling dimensions Δ_j and the structure constant C_{ijk} of the involved operators. A conformal field theory is characterised by the set $\{\Delta_j, C_{ijk}\}$, since this data captures the dynamical content. Higher-point correlation functions cannot be fully fixed using conformal symmetry, but can be obtained from the *operator product expansion* (OPE). However, the OPE requires the explicit knowledge of the set $\{\Delta_j, C_{ijk}\}$ for actual calculations.

Customarily, for $\mathcal{N} = 4$ SYM theory the gauge group SU(N) is chosen and gauge invariant local operators can be build. The theory simplifies considerably in the large N limit, which is also called the *planar limit*. In [6] 't Hooft observed, that when organising the Feynman diagrams in a $1/N$ expansion, there exists a correspondence to their topology. To have diagrams at a given order in $1/N$ without crossing propagators

one needs to draw them on the topology of a certain genus. When taking the rank N of the gauge group to infinity and the Yang-Mills coupling g_{YM} to zero, while keeping the 't Hooft coupling $\lambda = g_{\mathrm{YM}}^2 N$ finite, only planar diagrams contribute. The large N expansion resembles the sum over worldsheet topologies with the string coupling $g_s \sim 1/N$.

The AdS/CFT correspondence. In 1997 Maldacena conjectured the famous AdS/CFT correspondence [7]. It states a duality between conformal field theories in d dimensions and string theories embedded into a $(d+1)$-dimensional Anti-de-Sitter spacetime. Thus, every observable in the field theory should have a corresponding dual in the string theory. The most famous example for this connection is the duality between $\mathcal{N} = 4$ super Yang-Mills theory and type IIB superstring theory on the $\mathrm{AdS}_5 \times \mathrm{S}^5$ background. Strikingly, both theories share the same global symmetries. The bosonic isometries of AdS_5 and S^5 are given by $\mathfrak{su}(2,2)$ and $\mathfrak{su}(4)$, respectively. Combined with supersymmetry this leads to $\mathfrak{psu}(2,2|4)$, which coincides with the superconformal symmetry algebra of $\mathcal{N} = 4$ SYM. Furthermore, as string theories naturally contain a description of gravity, the duality might also pave a way towards a quantum theory of gravity.

Though the duality is not proven formally, agreement has been found in all the cases considered. For instance, the spectrum of scaling dimensions of local operators corresponds to the energy spectrum of free string states. The 't Hooft coupling λ and the rank of the gauge group N are related to the inverse string tension α' and the radius R of the AdS_5 and S^5 spaces as $\sqrt{\lambda} \sim R^2/\alpha'$ and $g_s \sim \lambda/N$. Further, the AdS/CFT correspondence conjectures a weak/strong duality between λ and the inverse string tension α'. While for weak 't Hooft coupling λ we can use perturbative techniques on the gauge theory side, this corresponds to large inverse tension α' on the side of the string theory. Vice versa, for strong gauge coupling, the inverse string tension is small and a perturbative expansion can be applied. Hence, to study observables at weak or strong coupling, one can choose the side of the correspondence, where perturbative techniques can be used. The drawback is, that the duality cannot be verified by an explicit perturbative calculation on the other side of the correspondence. Fortunately, integrability will help in this regard. A review of the various aspects of integrability in the context of the $\mathrm{AdS}_5/\mathrm{CFT}_4$ correspondence is given in [8].

A further example of the AdS/CFT correspondence is $\mathrm{AdS}_4/\mathrm{CFT}_3$. In the planar limit one has that type IIA string theory on an $\mathrm{AdS}_4 \times \mathbb{C}\mathrm{P}^3$ background is dual to the *ABJM* theory of [9]. Moreover, beyond $\mathrm{AdS}_5/\mathrm{CFT}_4$, in this thesis we will consider $\mathrm{AdS}_3/\mathrm{CFT}_2$ with an $\mathrm{AdS}_3 \times \mathrm{S}^3 \times \mathrm{T}^4$ background. A review is given in [10]. It should be mentioned that for this correspondence there are two further families of backgrounds, namely $\mathrm{AdS}_3 \times \mathrm{S}^3 \times \mathrm{S}^3 \times \mathrm{S}^1$ and $\mathrm{AdS}_3 \times \mathrm{S}^3 \times \mathrm{K3}$. We refer the reader to the reviews [8, 10] for a more detailed discussion of integrability in the context of the AdS/CFT correspondence.

The spectral problem in $\mathcal{N} = 4$ SYM theory. The first objects which were studied in the framework of this correspondence were correlation functions as given in eq. (1.1) of gauge-invariant composite operators [11, 12]. For instance, one could consider the protected half-BPS operators. The scaling dimensions Δ of local operators in a conformal field theory are measured by the *dilataion operator* $\mathfrak{D}$. The scaling dimensions of BPS operators do not receive quantum corrections and are hence given

by their classical values Δ_0. Further, the spectrum problem of *BMN* [13] operators was studied in the large N limit. These operator's scaling dimensions receive quantum corrections, which are also called *anomalous dimensions* γ and depend on the 't Hooft coupling λ and the rank N of the gauge group. The spectral problem amounts then to finding the eigenvalues of the dilatation operator

$$\mathfrak{D}\,\mathcal{O} = \Delta\,\mathcal{O} \qquad \text{with} \qquad \Delta = \Delta_0 + \gamma\,. \tag{1.2}$$

In the AdS/CFT correspondence the anomalous dimensions of the operators are dual to the energy levels of string states. Moreover, in the planar limit $\mathcal{N} = 4$ SYM theory becomes integrable and exact results can be obtained at arbitrary coupling λ. In fact, the dilatation operator of the spectral problem for the SO(6) subsector at one-loop was mapped to the diagonalisation of an integrable nearest-neighbour spin chain Hamiltonian [14] at weak coupling. This allows us to use Bethe ansatz techniques [15] to diagonalise the Hamiltonian and solve the spectral problem. The map to integrable spin chains has then been extended to the full superconformal algebra $\mathfrak{psu}(2,2|4)$ of $\mathcal{N} = 4$ SYM theory [16–18]. The underlying symmetry of the model also permits to find the spin chain S matrix [19] up to an overall dressing phase. By fixing a vacuum, the symmetry is broken and the excitations of the spin chain transform under the remaining $\mathfrak{su}(2|2)^2$ symmetry. The full S matrix $\mathbb{S}$ is then given by two copies of the $\mathfrak{su}(2|2)$ S matrix $\mathcal{S}$, which has to fulfil unitarity constraints. Moreover, the scattering of multi-particle states factorises into several two-particle scattering events. This is a characteristic property of two-dimensional integrable quantum field theories and was first observed by Zamolodchikov and Zamolodchikov in [20]. Further, the result of the scattering process must not depend on the sequence of two-particle scattering events. For three-particles this gives a cubic constraint on the S matrix, which is known as the *Yang-Baxter equation*. The respective overall dressing phase of the S matrix cannot be fixed from symmetries but from physical constraints, as it has to have a certain analytic structure. The solution is known as the Beisert-Eden-Staudacher (BES) dressing phase [21].

Furthermore, integrability was also conjectured to hold at higher loop orders, using the asymptotic Bethe ansatz [22, 23], which includes next-to-nearest-neighbour and higher-neighbouring interactions. However, it should be mentioned, that the form of the full dilatation operator is not completely known beyond one loop. Considering a spin chain of finite length, so called *wrapping effects* have to be taken into account [24]. These effects are suppressed by the length of the spin chain and hence the asymptotic Bethe ansatz is only valid for infinitely long spin chains. In the dual string theory, wrapping effects can be interpreted as virtual particles traveling around the worldsheet and interacting with the physical excitations. These interactions are suppressed by the size of the states and hence start to contribute at a certain loop order. By using the *thermodynamic Bethe ansatz* (TBA) [25] and going to the mirror model wrapping corrections can also be included into the solution of the spectral problem [24, 26–28]. Further, the TBA equations can be simplified [29] and recast into the *Quantum Spectral Curve* (QSC) [30, 31]. In principle, the QSC allows us to calculate the spectrum at weak coupling to arbitrary order in the coupling constant. In [32] this has been done up to including 10th order loop corrections for operators in the $\mathfrak{sl}(2)$ sector. Finally, integrability in $\mathcal{N} = 4$ SYM theory is believed to be related to an underlying symmetry captured by the *Yangian* algebra [33].

As mentioned above, $\mathcal{N} = 4$ SYM theory is rather viewed as a toy model, considered to develop and test new methods. Hence, it seems natural to ask, whether these powerful techniques borrowed from integrability can also be applied to theories with less symmetry. A first step is to study exactly marginal deformations, which preserve conformal invariance. In addition, considering deformations of the type classified by Leigh and Strassler [34] $\mathcal{N} = 1$ supersymmetry can be preserved. A special case is the real β-deformed $\mathcal{N} = 4$ SYM theory, which is integrable [35]. The deformation depends on the internal $\mathfrak{su}(4)$ charges of the fields and hence in the dual string theory the sphere S^5 is deformed. The corresponding string background was found by Lunin and Maldacena [36]. We will consider some three-point functions in the β-deformed theory in this thesis.

Higher-point functions by integrability in $\mathcal{N} = 4$ SYM theory. After the success of integrability in the spectral problem, turning to three-point functions seems a natural next step. In [37] new tools for spin chains were introduced, allowing to calculate tree-level correlators of three closed spin chain states. Here the spin chains, *i.e.* Bethe eigenstates, are cut into subchains and then sewed back together, using an inner product. When cutting the Bethe state, the excitations can end up on either subchain, hence all possible partitions need to be summed. This idea was then further developed to the *hexagon form factor* [38]. Considering the correlator in the dual string theory, the three-point function is given by a worldsheet with three punctures, *i.e.* the operators. This topology can then be cut into two hexagonal patches, which can be evaluated using the hexagon operator. Since the operators are cut in a similar way as in the tailoring picture of [37], the partitions also need to be summed here. The edges of the hexagon corresponding to the operators are also called physical edges, while those coming from the cut worldsheet are called virtual edges. The evaluation in this formalism yields the asymptotic three-point function.

Moreover, the hexagon form factor can be bootstrapped from symmetry constraints and is in fact given in terms of the Beisert S matrix [19]. Wrapping corrections can also be included into this formalism [38–40]. In a sense, by cutting the worldsheet, information is lost and in order to retrieve it, a full set of states needs to be inserted on the virtual edges. The explicit evaluation of these processes has to be done order by order and is rather involved [38–44]. However, these corrections are suppressed by the *bridge lengths*, *i.e.* the number of propagators connecting the respective operators.

In addition, the hexagon formalism paves the way to studying higher-point functions using methods from integrability. The tessellation of four-point functions was considered in [41,45]. In contrast to two- and three-point functions, the form of four-point functions is not fully fixed by symmetry and they depend non-trivially on the conformal cross-ratios. Cutting the latter into four hexagons, the form factor allows to circumvent the operator product expansion (OPE). It is here necessary to sum over all distinct ways to tessellate the correlator. Including the cross-ratio dependence into the hexagon formalism then reproduces the correct dependence for higher-point functions [41, 42, 45]. Further, it was noticed that diagrams calculated by hexagons have to be dressed by their respective $\mathrm{SU}(N)$ colour factors, in order to reproduce field theory results [42], allowing to also include $1/N$ corrections by tessellating higher-genus manifolds [42, 46, 47].

The spectral problem in $\mathbf{AdS_3/CFT_2}$. Another example of the AdS/CFT correspondence it the duality between type IIB superstring theory on an $\mathrm{AdS}_3 \times \mathrm{S}^3 \times \mathrm{T}^4$

background and a two-dimensional CFT_2. Compared to $\mathrm{AdS}_5/\mathrm{CFT}_4$, this background preserves only half the amount of supersymmetry. For the spectral problem in the planar limit, there are two important parameters [48], as the background can be supported by a mixture of Ramond-Ramond (RR) flux h as well as Neveu-Schwarz-Neveu-Schwarz (NSNS) flux k. The background at hand is most similar to the case of $\mathrm{AdS}_5 \times \mathrm{S}^5$ when there is pure RR flux, *i.e.* no NSNS flux. In this case, as well as for mixed flux, the dual CFT_2 is not known. On the other hand, for pure NSNS flux, the model can be described as a worldsheet CFT and is given by a supersymmetric $\mathfrak{sl}(2,\mathbb{R})$ Wess-Zumino-Witten model at level k [49–51]. For the special case of $k = 1$ the dual CFT_2 is known to be the symmetric product orbifold $\mathrm{Sym}^N(\mathrm{T}^4)$ [52–54]. This theory is given by N copies of T^4, containing four free bosons and fermions each, which are identified under permutations.

Moreover, the background is known to be classically integrable for mixed flux, as well as for pure-RR or pure-NSNS flux [55, 56] and the theory is believed to be also integrable at quantum level. The spectrum problem was then studied for pure-RR and mixed flux and the S matrix was fixed from symmetry constraints [57–59]. A qualitative difference to the case of $\mathrm{AdS}_5 \times \mathrm{S}^5$ is, that the particle content of this theory contains massive as well as massless excitations. The scattering processes between the different representations are captured by different blocks in the S matrix. Finally, there are five independent dressing factors for the S matrix [60]. A proposal for these factors for pure-RR flux was made in [61, 62], which however featured some difficulties and led to the new proposal [63]. For pure-NSNS flux the S matrix cannot be fixed by symmetries and a proposal for it was made in [64].

Having worked out the S matrix and its dressing factors for pure-RR flux, the mirror thermodynamic Bethe ansatz equations were derived in [65]. Here, we should also mention, that a quantum spectral curve was proposed for $\mathrm{AdS}_3 \times \mathrm{S}^3 \times \mathrm{T}^4$ in [66, 67]. While the construction of the QSC for $\mathrm{AdS}_5 \times \mathrm{S}^5$ was based on the TBA equations, it is based on symmetry considerations in [66, 67] and it will be interesting to see whether these two approaches yield a consistent description for $\mathrm{AdS}_3 \times \mathrm{S}^3 \times \mathrm{T}^4$.

Outline

This thesis is divided into two parts, which are dedicated to certain aspects of integrability in $\mathrm{AdS}_5/\mathrm{CFT}_4$ and $\mathrm{AdS}_3/\mathrm{CFT}_2$, respectively. Here, we will give a brief outline of the material discussed in the two parts.

Part I: Integrability in $\mathcal{N} = 4$ SYM. In this part we focus on the CFT side of the $\mathrm{AdS}_5/\mathrm{CFT}_4$ duality. In Chapter 2 we review $\mathcal{N} = 4$ SYM theory as well as methods from integrability in order to solve the spectral problem. In particular, we consider higher-rank models and the nested Bethe ansatz in Sec. 2.2, which allows us to construct the respective Bethe eigenstates in a straightforward way. In addition, we introduce marginal deformations and consider the implications of the real β-deformation for the Bethe equations in Sec. 2.3.

Chapter 3 is devoted to applications of the hexagon form factor in $\mathcal{N} = 4$ SYM. We begin by reviewing the hexagon formalism in Sec. 3.1, discussing the evaluation of higher-point functions as well as the inclusion of wrapping corrections. As this formalism was mainly studied for rank-one sectors, we consider its extension to higher-rank sectors in Sec. 3.2. There we study tree-level correlators of operators from the SU(3) and SU(1|2) sectors, respectively. In Sec. 3.3 we ask whether a similar formalism

exists for the β-deformed theory. Here we consider a minimal change of the original hexagon form factor only by dressing it with deformation factors. We use the resulting prescription to compute correlators in the SU(1|2) as well as SU(2) sector and discuss some conceptual difficulties. In Sec. 3.4 we study double excitations, which allow us to also consider excitations which can a priori not be realised in the spin chain picture. We introduce the respective creation amplitudes and work out an example in the SO(6) sector. Moreover, we can use these results to build the Yang-Mills term of the Lagrange operator in Sec. 3.5. Using the concept of the Lagrangian insertion method, which is well established for field theory calculations in $\mathcal{N} = 4$ SYM [68, 69], we propose a way to calculate loop corrections in the hexagon formalism without having to include mirror magnons. We test this proposal by considering a simple but non-trivial example of protected correlators.

Part II: Integrability in $\mathbf{AdS_3}$. In this part we address integrability techniques in $\mathrm{AdS}_3\times\mathrm{S}^3\times\mathrm{T}^4$ string theory. We begin by reviewing important results from the literature in Sec. 4. In particular, we consider the particle content as well as the scattering matrix. Since integrability proved to be a powerful tool also for the calculation of higher-point functions in $\mathrm{AdS}_5/\mathrm{CFT}_4$, we will turn to three-point functions in Sec. 5 and ask whether a hexagon formalism can be devised for $\mathrm{AdS}_3 \times \mathrm{S}^3 \times \mathrm{T}^4$. As only for the background with pure-NSNS flux CFT techniques exist this would be a desirable advance. In fact, in Sec. 5.2 we will bootstrap the one- and two-particle hexagon form factor for backgrounds supported by pure-RR and mixed flux. The form factor is related to the Borsato–Ohlsson-Sax–Sfondrini S matrix [70] and we can extend it to arbitrarily many particles. Further, we find that the dressing phases for the hexagon are related to those of the S matrix in the spectral problem by imposing consistency constraints in Sec. 5.4. Finally, we consider some correlation functions of protected operators in Sec. 5.5 and compare the hexagons predictions with results in the literature [71].

In Chapter 6 we will consider the mirror TBA equations for $\mathrm{AdS}_3 \times \mathrm{S}^3 \times \mathrm{T}^4$ backgrounds with pure-RR flux derived in [65] and study how they can be simplified in the small tension limit. We begin by reviewing the TBA for the simpler example of the Heisenberg XXX spin chain in Sec. 6.1. This allows us to introduce the relevant concepts and ideas before moving to the more involved set of equations at hand in Sec. 6.2. There we will use the contour deformation trick [72] in order to excite massless modes. In Sec. 6.3 we will then study the simplification of the equations in the tensionless limit $h \to 0$. Magnificently, in this limit the massless modes decouple and the resulting equations only contain the Cauchy kernel and corresponding source terms.

In the concluding Chapter 7 the results are summarised and we will discuss several directions for future research. In addition, we added two appendices where some rather technical details are collected for the reader's convenience. In App. A we give details on the evaluation of the hexagon form factor in $\mathcal{N} = 4$ SYM [38] relevant for Part I. Furthermore, App. B lists the S matrices from [63, 65] relevant for the TBA equations in AdS_3 from Part II.

Part I.

Integrability in $\mathcal{N} = 4$ SYM

Chapter 2.

Review of integrability in $\mathcal{N} = 4$ super Yang-Mills theory

In this chapter we will review $\mathcal{N} = 4$ SYM theory and its connection to integrability. We will begin by introducing the maximally supersymmetric $\mathcal{N} = 4$ SYM field theory and discuss its symmetry algebra. In particular, we consider the oscillator picture, which will be helpful later on in the context of double excitations. Further, we will discuss the spectrum problem and the one-loop dilatation operator. Following Minahan and Zarembo [14], the planar one-loop mixing problem in the scalar sector can be mapped to an integrable spin chain. Thus, we will introduce methods from integrability. In particular, we will consider the coordinate Bethe ansatz as well as the nested Bethe ansatz, which plays a crucial role for higher-rank sectors. The concepts introduced here will also be useful later on in this thesis in the context of integrability in $\mathrm{AdS}_3/\mathrm{CFT}_2$. Finally, we discuss marginal deformations of $\mathcal{N} = 4$ SYM and focus in particular on the real β-deformation.

2.1. Field theory

2.1.1. Field content and the Lagrangian

In four-dimensional spacetime $\mathcal{N} = 4$ SYM theory [73, 74] is the unique maximally supersymmetric gauge theory. The matter content of the theory is given by three complex scalar fields $\Phi^{IJ} = -\Phi^{JI}$ as well as four fermions Ψ^I_α and four anti-fermions $\bar{\Psi}_{I\dot{\alpha}}$. The latin indices $I, J = 1, 2, 3, 4$ correspond to the internal flavour symmetry, which is given by the global R-symmetry group $\mathrm{SO}(6) \simeq \mathrm{SU}(4)$. Under this group the bosons and fermions transform in the fundamental representation, while the conjugate fermions transform in the anti-fundamental representation. The $\mathfrak{su}(2)$ spinor indices $\alpha, \dot{\alpha}$ may take the values $1, 2$ or $\dot{1}, \dot{2}$, respectively. Finally, there is the gauge field $\mathcal{A}^\mu$ with the spacetime index taking values $\mu = 0, 1, 2, 3$. We will consider the gauge group $\mathrm{SU}(N)$ with all the fields transforming in its adjoint representation. Furthermore, we can define the covariant derivative $\mathcal{D}^\mu$ and its action on any field $\mathcal{X}$ as

$$\mathcal{D}^\mu = \partial^\mu - ig_{\mathrm{YM}}\mathcal{A}^\mu\,, \qquad \mathcal{D}^\mu\mathcal{X} = (\partial^\mu\mathcal{X}) - ig_{\mathrm{YM}}[\mathcal{A}^\mu, \mathcal{X}]\,, \tag{2.1}$$

where we introduced the dimensionless Yang-Mills coupling constant g_{YM}. Introducing the field strength $\mathcal{F}^{\mu\nu}$ through

$$\mathcal{F}^{\mu\nu} = \frac{i}{g_{\mathrm{YM}}}[\mathcal{D}^\mu, \mathcal{D}^\nu] = \partial^\mu\mathcal{A}^\nu - \partial^\nu\mathcal{A}^\mu - ig_{\mathrm{YM}}[\mathcal{A}^\mu, \mathcal{A}^\nu] \tag{2.2}$$

we can write the Lagrangian of $\mathcal{N}=4$ SYM theory [74]

$$\begin{aligned}\mathcal{L}_{\mathcal{N}=4} = \mathrm{tr}\Big(&-\frac{1}{4}\mathcal{F}^{\mu\nu}\mathcal{F}_{\mu\nu} - \frac{1}{2}(\mathcal{D}^{\mu}\Phi^{IJ})(\mathcal{D}_{\mu}\Phi_{IJ}) + \frac{1}{8}g_{\mathrm{YM}}^2[\Phi^{IJ},\Phi^{KL}][\Phi_{IJ},\Phi_{KL}] \\ &+ \sqrt{2}g_{\mathrm{YM}}\Psi^{I\alpha}[\Phi_{IJ},\Psi^{J}_{\alpha}] + \sqrt{2}g_{\mathrm{YM}}\bar{\Psi}_{I\dot{\alpha}}[\Phi^{IJ},\bar{\Psi}^{\dot{\alpha}}_{J}] + i\bar{\Psi}_{I\dot{\alpha}}\bar{\sigma}_{\mu}^{\dot{\alpha}\alpha}\mathcal{D}^{\mu}\Psi^{I}_{\alpha}\Big)\,,\end{aligned} \tag{2.3}$$

where $(\bar{\sigma}_{\mu})^{\dot{\alpha}\alpha} = (\mathbb{1},\sigma_1,\sigma_2,\sigma_3)^{\dot{\alpha}\alpha}$ denotes the Pauli matrices. Taking the gauge-group trace ensures that we obtain a gauge invariant Lagrangian. Further, the scalar fields are self-dual as under conjugation they obey $\bar{\Phi}^{IJ} = \Phi_{IJ} = \frac{1}{2}\epsilon_{IJKL}\Phi^{KL}$. Similarly, for the anti-fermion we have $\bar{\Psi}^{IJK}_{\dot{\alpha}} = \epsilon^{IJKL}\bar{\Psi}_{L\dot{\alpha}}$ with three antisymmetrized fundamental SU(4) indices.

2.1.2. Gauge group

Let us introduce the generators T^a for the SU(N) gauge group. In the fundamental representation the T^a are given by $N \times N$ hermitian and traceless matrices with $a = 1,\ldots,N^2-1$. Further, the generators obey the commutation relation

$$[T^a, T^b] = i\sqrt{2}f_c^{ab}T^c\,, \tag{2.4}$$

with the structure constant f_c^{ab}. We may choose a diagonal basis, such that

$$\mathrm{tr}\big(T^aT^b\big) = \delta^{ab}\,. \tag{2.5}$$

Going to the adjoint representation, under which all fields of the theory transform, we write the generators as $(T^a)^b_c = -i\sqrt{2}f_c^{ab}$. For SU($N$) we notice the important identity

$$(T^a)^b_c(T^a)^e_f = \delta^b_f\delta^e_c - \frac{1}{N}\delta^b_c\delta^e_f\,, \tag{2.6}$$

where the last terms ensures the tracelessness. The fields are matrix-valued, for instance the complex scalar fields Φ^{IJ} should implicitly be understood as $\Phi^{IJ}_a\,T^a$, with N^2-1 component fields Φ^{IJ}_a.

Planar limit. The *planar limit* or *'t Hooft limit* can be obtained by taking the rank of the SU(N) gauge group to infinity and the coupling g_{YM} to zero, while keeping the 't Hooft coupling $\lambda = g^2_{\mathrm{YM}}N$ finite [6]. The Feynman diagrams can then be classified by the genus of the surface on which they can be drawn without crossing propagators. In the large-N limit diagrams are then suppressed according to their genus. Therefore, taking the planar limit simplifies the theory, as only Feynman diagrams that can be drawn on a sphere contribute. Further, we can rescale the coupling and define

$$g^2 = \frac{\lambda}{16\pi^2}\,, \tag{2.7}$$

which we will mainly use as the coupling throughout this work.

2.1.3. Symmetry algebra

$\mathcal{N}=4$ SYM theory is the maximally supersymmetric gauge theory in $d=4$ dimensions. The theory is conformal and the conformal symmetry algebra is given by $\mathfrak{so}(2,4)\simeq\mathfrak{su}(2,2)$. In addition to the Lorentz transformations $\mathfrak{L}^{\alpha}{}_{\beta}, \dot{\mathfrak{L}}^{\dot\alpha}{}_{\dot\beta}$ and translation $\mathfrak{P}^{\alpha\dot\alpha}$ generating the Poincaré symmetry, the conformal symmetry algebra also contains the dilatation generator $\mathfrak{D}$ as well as the special conformal transformations $\mathfrak{K}_{\alpha\dot\alpha}$. The $\mathfrak{su}(4)$ R-symmetry is generated by the R-charges $\mathfrak{R}^{I}{}_{J}$. The $\mathcal{N}=4$ supersymmetry includes 16 supercharges $\mathfrak{Q}^{\alpha}{}_{I}, \dot{\mathfrak{Q}}^{I\dot\alpha}$. Combining the conformal symmetry algebra with supersymmetry leads to $\mathfrak{su}(2,2|4)$, which also contains the 16 superconformal charges $\mathfrak{S}^{I}{}_{\alpha}, \dot{\mathfrak{S}}^{\dot\alpha I}$. Further, the algebra $\mathfrak{su}(2,2|4)$ contains the central charge $\mathfrak{C}$. The superconformal algebra is then given by the irreducible part $\mathfrak{psu}(2,2|4)$.

For a semi-simple super Lie algebra the Dynkin diagram is not unique. However, the *beauty diagram* given in Fig. 2.1 turns out to be very useful [16]. Composite operators formed from the fundamental fields of $\mathcal{N}=4$ SYM are called *primary states*, if they are annihilated by all the lowering operators, *i.e.* the generators

$$\{\mathfrak{K}_{\alpha\dot\alpha},\ \mathfrak{L}^{\alpha}{}_{\beta}\,\text{for}\,\alpha>\beta,\ \dot{\mathfrak{L}}^{\dot\alpha}{}_{\dot\beta}\,\text{for}\,\dot\alpha>\dot\beta,\ \mathfrak{R}^{I}{}_{J}\,\text{for}\,I>J,\ \mathfrak{S}^{I}{}_{\alpha},\ \dot{\mathfrak{S}}^{\dot\alpha I}\}\,. \tag{2.8}$$

For instance the field $Z\equiv\Phi^{34}$ is a primary field. Acting with the raising operators on primary states yields then descendant operators. Correspondingly, the raising operators are given by

$$\{\mathfrak{P}^{\alpha\dot\alpha},\ \mathfrak{L}^{\alpha}{}_{\beta}\,\text{for}\,\alpha<\beta,\ \dot{\mathfrak{L}}^{\dot\alpha}{}_{\dot\beta}\,\text{for}\,\dot\alpha<\dot\beta,\ \mathfrak{R}^{I}{}_{J}\,\text{for}\,I<J,\ \mathfrak{Q}^{\alpha}{}_{I},\ \dot{\mathfrak{Q}}^{I\dot\alpha}\}\,. \tag{2.9}$$

Finally, the generators of the Cartan subalgebra commute among each other. Their action on primary operators can be used to classify them by their charges. For later convenience let us give here the Cartan charges of the $\mathfrak{su}(4)$ R-symmetry group

$$q_1=\mathfrak{R}^{2}{}_{2}-\mathfrak{R}^{1}{}_{1}\,,\qquad p=\mathfrak{R}^{3}{}_{3}-\mathfrak{R}^{2}{}_{2}\,,\qquad q_2=\mathfrak{R}^{4}{}_{4}-\mathfrak{R}^{3}{}_{3}\,, \tag{2.10}$$

where the eigenvalues $[q_1,p,q_2]$ are the $\mathfrak{su}(4)$ Dynkin labels for a given state. Further, when discussing twists and marginal deformations, it will be useful to introduce the $\mathfrak{so}(6)$ weights $[j_1,j_2,j_3]$ defined as

$$j_1=\frac{q_1+2p+q_2}{2}\,,\qquad j_2=\frac{q_1+q_2}{2}\,,\qquad j_2=\frac{q_1-q_2}{2}\,. \tag{2.11}$$

The charges of the fundamental fields of $\mathcal{N}=4$ SYM are given in Tab. 2.1. Conjugate fields have the opposite charges while the derivatives $\mathcal{D}^{\alpha\dot\alpha}$ are not charged.

	Φ^{34}	Φ^{24}	Φ^{23}	Ψ^{1}_{α}	Ψ^{2}_{α}	Ψ^{3}_{α}	Ψ^{4}_{α}
j_1	1	0	0	$-1/2$	$-1/2$	$+1/2$	$+1/2$
j_2	0	1	0	$-1/2$	$+1/2$	$-1/2$	$+1/2$
j_3	0	0	1	$-1/2$	$+1/2$	$+1/2$	$-1/2$

Table 2.1.: The $\mathfrak{so}(6)$ Cartan charges of the fundamental fields. Conjugate fields carry opposite charges while the derivatives $\mathcal{D}^{\alpha\dot\alpha}$ are not charged.

Moreover, we have the Dynkin labels of the Lorentz algebra $\mathfrak{so}(3,1)\simeq\mathfrak{su}(2)\times\mathfrak{su}(2)$

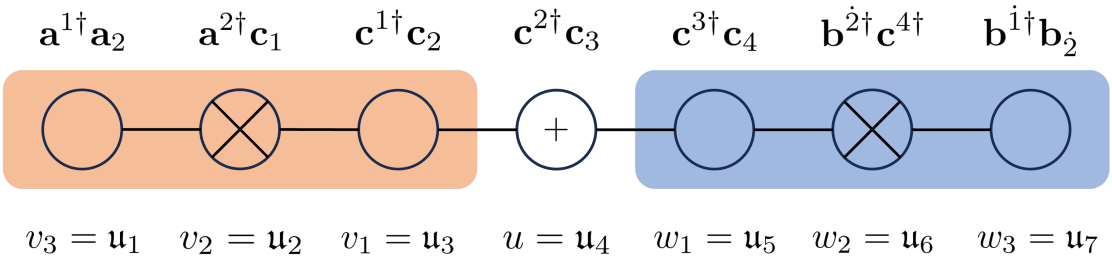

Figure 2.1.: Dynkin diagram in the beauty grading. The momentum carrying node is in the middle and the left (orange) and right (blue) $\mathfrak{su}(2|2)$ wings become apparent. The simple roots are given in the oscillator picture. By acting with the roots we can create excitations.

given through

$$s_1 = \mathfrak{L}^2{}_2 - \mathfrak{L}^1{}_1\,, \qquad s_2 = \dot{\mathfrak{L}}^{\dot{2}}{}_{\dot{2}} - \dot{\mathfrak{L}}^{\dot{1}}{}_{\dot{1}}\,, \tag{2.12}$$

as well as the scaling dimension Δ, which is measured by the dilatation operator $\mathfrak{D}$.

Unitary representations of $\mathfrak{psu}(2,2|4)$ have been classified in [75]. The shortest physical multiplet is the *half-BPS* multiplet with highest weight given by the Dynkin labels $\Delta = p$ and the remaining labels vanish with $s_1 = s_2 = q_1 = q_2 = 0$. In the field theory the highest weight state is composed from the fields $Z = \Phi^{34}$ and hence all the states of the form $\mathrm{tr}\big(Z^L\big)$ are half-BPS states. Moreover, half-BPS states are protected, *i.e.* their scaling dimension does not receive quantum corrections.

The oscillator picture. Another useful concept is the oscillator picture [17, 76, 77] which allows us to realise the elementary fields in terms of oscillators.

We introduce the bosonic creation operators $\mathbf{a}^{\alpha\dagger}, \mathbf{b}^{\dot\alpha\dagger}$ with two-component spinor indices $\alpha, \dot\alpha$ as well as the fermionic creation operators $\mathbf{c}^{I\dagger}$, with flavour indices $I \in \{1\dots4\}$. The commutation operators are given by

$$[\mathbf{a}_\alpha, \mathbf{a}^{\beta\dagger}] = \delta_\alpha^\beta\,, \qquad [\mathbf{b}_{\dot\alpha}, \mathbf{b}^{\dot\beta\dagger}] = \delta_{\dot\alpha}^{\dot\beta}\,, \qquad \{\mathbf{c}_I, \mathbf{c}^{J\dagger}\} = \delta_I^J\,. \tag{2.13}$$

The highest weight state Z is then given by $Z = \mathbf{c}^{3\dagger}\mathbf{c}^{4\dagger}\,|0\rangle$. The remaining fundamental fields can be written in terms of the oscillators as well

$$\begin{aligned}
Z &= \Phi^{34} = \mathbf{c}^{3\dagger}\mathbf{c}^{4\dagger}\,|0\rangle\,, & \bar Z &= \Phi^{12} = \mathbf{c}^{1\dagger}\mathbf{c}^{2\dagger}\,|0\rangle\,,\\
X &= \Phi^{24} = \mathbf{c}^{2\dagger}\mathbf{c}^{4\dagger}\,|0\rangle\,, & \bar X &= \Phi^{13} = \mathbf{c}^{1\dagger}\mathbf{c}^{3\dagger}\,|0\rangle\,,\\
Y &= \Phi^{14} = \mathbf{c}^{1\dagger}\mathbf{c}^{4\dagger}\,|0\rangle\,, & \bar Y &= \Phi^{23} = \mathbf{c}^{2\dagger}\mathbf{c}^{3\dagger}\,|0\rangle\,,\\
\Psi^{\alpha I} &= \mathbf{a}^{\alpha\dagger}\mathbf{c}^{I\dagger}\,|0\rangle\,, & \bar\Psi_I^{\dot\alpha} &= \frac{1}{3!}\epsilon_{JKLI}\mathbf{b}^{\dot\alpha\dagger}\mathbf{c}^{J\dagger}\mathbf{c}^{K\dagger}\mathbf{c}^{L\dagger}\,|0\rangle\,,\\
\mathcal{F}^{\alpha\beta} &= \mathbf{a}^{\alpha\dagger}\mathbf{a}^{\beta\dagger}\,|0\rangle\,, & \bar{\mathcal{F}}^{\dot\alpha\dot\beta} &= \mathbf{b}^{\dot\alpha\dagger}\mathbf{b}^{\dot\beta\dagger}\mathbf{c}^{1\dagger}\mathbf{c}^{2\dagger}\mathbf{c}^{3\dagger}\mathbf{c}^{4\dagger}\,|0\rangle\,,\\
\mathcal{D}^{\alpha\dot\alpha} &= \mathbf{a}^{\alpha\dagger}\mathbf{b}^{\dot\alpha\dagger}\,,
\end{aligned} \tag{2.14}$$

where the covariant derivative $\mathcal{D}^{\alpha\dot\alpha}$ always acts on some other field, as indicated by omitting $|0\rangle$ in the last line.

Moreover, the symmetry generators can be expressed in the oscillator picture, for

instance the positive roots can be written as, *cf.* the Dynkin diagram in Fig. 2.1

$$\begin{aligned}
\mathfrak{L}^1{}_2 &= \mathbf{a}^{1\dagger}\mathbf{a}_2\,, & \dot{\mathfrak{L}}^{\dot{1}}{}_{\dot{2}} &= \mathbf{b}^{\dot{1}\dagger}\mathbf{b}_{\dot{2}}\,,\\
\mathfrak{Q}^2{}_1 &= \mathbf{a}^{2\dagger}\mathbf{c}_1\,, & \dot{\mathfrak{Q}}^{4\dot{2}} &= \mathbf{b}^{\dot{2}\dagger}\mathbf{c}^{4\dagger}\,,\\
\mathfrak{R}^1{}_2 &= \mathbf{c}^{1\dagger}\mathbf{c}_2\,, & \mathfrak{R}^3{}_4 &= \mathbf{c}^{3\dagger}\mathbf{c}_4\,,\\
\mathfrak{R}^2{}_3 &= \mathbf{c}^{2\dagger}\mathbf{c}_3\,.
\end{aligned} \tag{2.15}$$

For physical states the central charge $\mathfrak{C}$ of $\mathfrak{su}(2,2|4)$ needs to vanish. In terms of the oscillators it is given as [17]

$$\mathfrak{C} = 1 - \frac{1}{2}\mathbf{a}^{\alpha\dagger}\mathbf{a}_\alpha + \frac{1}{2}\mathbf{b}^{\dot\alpha\dagger}\mathbf{b}_{\dot\alpha} - \frac{1}{2}\mathbf{c}^{I\dagger}\mathbf{c}_I\,, \tag{2.16}$$

which vanishes for all the fields given in eq. (2.14).

The excitation picture. Since the highest weight state Z is the physical vacuum, it breaks the $\mathfrak{su}(4)$ symmetry. However, it is invariant under an $\mathfrak{su}(2)\times\mathfrak{su}(2)$ subgroup. Therefore, we introduce a more convenient notation by splitting the $\mathfrak{su}(4)$ index $I = 1,2,3,4$ into $a = 1,2$ and $\dot a = \dot 3, \dot 4$ with the oscillators [77]

$$\mathbf{d}^{\dot 3\dagger} = \mathbf{c}_3\,, \qquad \mathbf{d}^{\dot 4\dagger} = \mathbf{c}_4\,, \qquad \mathbf{d}_{\dot 3} = \mathbf{c}^{3\dagger}\,, \qquad \mathbf{d}_{\dot 4} = \mathbf{c}^{4\dagger}\,. \tag{2.17}$$

This notation ensures, that the primary field Z is annihilated by the operators $\mathbf{a}_\alpha, \mathbf{b}_{\dot\alpha}, \mathbf{c}_a, \mathbf{d}_{\dot a}$. If we now group the creation operators as $(\mathbf{a}^{\alpha\dagger}, \mathbf{c}^{a\dagger})$ and $(\mathbf{b}^{\dot\alpha\dagger}, \mathbf{d}^{\dot a\dagger})$, with the annihilation operators respectively, we have manifest $\mathfrak{su}(2|2)\times\mathfrak{su}(2|2)$ symmetry. These two $\mathfrak{su}(2|2)$ correspond to the three left and right nodes in the Dynkin diagram in Fig. 2.1, respectively, which are also referred to as *left* and *right wings*.

We can then write the excitations transforming under $\mathfrak{su}(2|2)\times\mathfrak{su}(2|2)$ as bi-fundamental excitations. In this *excitation picture* we have

$$\begin{aligned}
X &= \phi^2\otimes\dot\phi^{\dot 4}\,, & \bar X &= \phi^1\otimes\dot\phi^{\dot 3}\,,\\
Y &= \phi^1\otimes\dot\phi^{\dot 4}\,, & \bar Y &= \phi^2\otimes\dot\phi^{\dot 3}\,,\\
\Psi^{\alpha\dot a} &= \psi^\alpha\otimes\dot\phi^{\dot a}\,, & \bar\Psi^{a\dot\alpha} &= \phi^a\otimes\dot\psi^{\dot\alpha}\,,\\
\mathcal{D}^{\alpha\dot\alpha} &= \psi^\alpha\otimes\dot\psi^{\dot\alpha}\,,
\end{aligned} \tag{2.18}$$

where $(\phi^1,\phi^2,\psi^1,\psi^2)$ transform in the fundamental representation under the first and $(\dot\phi^{\dot 3},\dot\phi^{\dot 4},\dot\psi^{\dot 1},\dot\psi^{\dot 2})$ under the second copy of $\mathfrak{su}(2|2)$. Moreover, since we can obtain these excitations by acting with lowering generators in the left or right wing in the Dynkin diagram in Fig. 2.1, we will denote them as left or right excitations, respectively. For instance, the middle node creates an excitation $|X\rangle$ from the physical vacuum $|Z\rangle$. Moving one note to the left or right, we obtain a $|Y\rangle$ or $|\bar Y\rangle$, while combining both yields $|\bar X\rangle$. In this way we can construct the excitations in eq. (2.18). Note further, that this picture seems to exclude excitations such as the field strength $\mathcal{F}^{\alpha\beta}, \bar{\mathcal{F}}^{\dot\alpha\dot\beta}$ and the fermions $\Psi^{\alpha 1}, \Psi^{\alpha 2}, \bar\Psi^{\dot\alpha}_{\dot 3}, \bar\Psi^{\dot\alpha}_{\dot 4}$. We will see later, that these can be incorporated by allowing for *double excitations*.

2.1.4. Correlation functions

In this thesis we are mainly interested in the computation of correlation functions of two or three operators. Though we will focus on integrability methods for the evaluation, let us review how to obtain results from field theory. The path integral formalism allows us to lift a field theory to a quantum field theory. Using the path integral a time-ordered correlation function can be written as

$$\langle \mathcal{O}_1(x_1) \dots \mathcal{O}_n(x_n) \rangle = \int \mathcal{D}\xi \; \mathcal{O}_1(x_1) \dots \mathcal{O}_n(x_n) \; e^{iS[\xi]} \tag{2.19}$$

where the action is given by

$$S[\xi] = \int \mathrm{d}^4x \; \mathcal{L}_{\mathcal{N}=4}[\xi] \,, \tag{2.20}$$

with the Lagrangian $\mathcal{L}_{\mathcal{N}=4}$ from eq. (2.3) and the normalisation chosen such that $\int \mathcal{D}\xi \; e^{iS[\xi]} \equiv 1$. Here we use ξ to represent the set of elementary fields of $\mathcal{N}=4$ SYM discussed in Sec. 2.1.1. The integration measure $\mathcal{D}\xi$ formally sums the expression under the path integral over all field configurations weighted by the exponential of the action $S[\xi]$. The *generating functional* is defined as

$$Z[J] \equiv \int \mathcal{D}\xi \exp\left(iS[\xi] + i \int \mathrm{d}^4x \; J_A(x) \xi^A(x) \right) , \tag{2.21}$$

and couples the fields $\xi^A(x)$ to an auxiliary current $J_A(x)$. This yields a convenient way to calculate correlation functions. For instance, the correlation function of n elementary fields can be obtained by taking the functional derivative with respect to the currents

$$\langle \xi^{A_1}(x_1) \dots \xi^{A_n}(x_n) \rangle = \frac{(-i)^n}{Z[0]} \frac{\delta^n Z[J]}{\delta J_{A_1}(x_1) \dots \delta J_{A_n}(x_n)} \bigg|_{J=0} . \tag{2.22}$$

Further, in the perturbative regime the action can be split into $S = S_0 + S_{\text{int}}$, where S_0 is the free action. The interacting part S_{int} is cubic and quartic in the fields. The free generating functional can be obtained from combining the free action with the currents and may then be written as

$$Z_0[J] = e^{\int \mathrm{d}^4x \, \mathrm{d}^4y \; \mathrm{tr}(J_A(x) \, \Pi(x,y) \, J_A(y))} \,, \tag{2.23}$$

where we introduced the free propagator $\Pi(x,y)$, which is given by the inverse of the kinetic term. This allows us to rewrite the correlation function from eq. (2.19) as

$$\langle \mathcal{O}_1[\xi] \dots \mathcal{O}_n[\xi] \rangle = \left(\mathcal{O}_1 \left[\frac{\delta}{\delta J} \right] \dots \mathcal{O}_n \left[\frac{\delta}{\delta J} \right] e^{iS_{\text{int}}\left[\frac{\delta}{\delta J}\right]} Z_0[J] \right) \bigg|_{J=0} . \tag{2.24}$$

This expression can be used to generate Feynman diagrams in perturbation theory by expanding the interacting part in the coupling. A given loop-order in perturbation theory introduces a certain number of interaction vertices S_{int}. The variations $\frac{\delta}{\delta J}$ then introduce propagators, connecting the fields from the local operators $\mathcal{O}_j$ and the interaction vertices S_{int} in all possible ways.

In addition, gauge fixing is required, since gauge invariance allows non-propagating modes of the gauge field. In order to obtain a well defined propagator for the gauge

field a gauge fixing term is introduced, which contains Faddeev-Popov ghosts. These ghosts are auxiliary fermionic fields and must not appear in external states but may do so inside loops coupling to the gauge boson. Furthermore, divergencies appear in perturbative calculations and need to be regularised. This can be achieved using dimensional regularisation. This technique analytically continues the integral to $4-2\epsilon$ dimensions, where ϵ is the regularisation parameter. The divergence of the correlator becomes then a pole at $\epsilon \to 0$.

Moreover, in a conformal field theory, the conformal symmetry constrains correlation functions of local operators. Let us consider a two-point function $\langle \mathcal{O}_1(x_1)\mathcal{O}_2(x_2)\rangle$, where $\mathcal{O}_j$ may be scalar primary operators inserted at the point x_j. Invariance under Poincaré symmetry enforces that the correlator solely depends on the distance between the two operators $|x_1 - x_2|$. Further, requiring invariance under dilatations and special conformal transformations, the form of the correlator is fixed to

$$\langle \mathcal{O}_1(x_1)\mathcal{O}_2(x_2)\rangle = \frac{\delta_{1,2}}{|x_1 - x_2|^{2\Delta}}\,, \tag{2.25}$$

where $\Delta = \Delta_1 = \Delta_2$ is the scaling dimension of the respective operator and we chose a convenient normalisation. Similarly, three-point functions can be constrained to

$$\langle \mathcal{O}_1(x_1)\mathcal{O}_2(x_2)\mathcal{O}_3(x_3)\rangle = \frac{C_{123}}{|x_{12}|^{\Delta_1+\Delta_2-\Delta_3}|x_{23}|^{\Delta_2+\Delta_3-\Delta_1}|x_{31}|^{\Delta_3+\Delta_1-\Delta_2}}\,, \tag{2.26}$$

where the structure constant C_{123} cannot be absorbed into a normalisation but yields physical data on the conformal field theory considered. Moreover, such correlation functions can always be brought to a generic configuration for two and three points by using conformal transformations. We will make use of this later in this thesis and consider a configuration where the three operators are placed on a line at $x_1 = 0$, $x_2 = 1$ and $x_3 = \infty$.

For higher-point functions, the conformal symmetry is not constraining enough to fix the spacetime dependence of the correlation function. For instance, four-point functions depend on the two conformally invariant cross ratios given by

$$u = \frac{x_{12}^2 x_{34}^2}{x_{13}^2 x_{24}^2}\,, \qquad v = \frac{x_{14}^2 x_{23}^2}{x_{13}^2 x_{24}^2}\,. \tag{2.27}$$

However, the dependence of the function on u and v is not fully fixed.

Further, conformal field theories allow for an *operator product expansion* (OPE), which can be used to approximate the product of two sufficiently close operators $\mathcal{O}_j(x), \mathcal{O}_k(y)$ by a linear combination of operators at one of the points, *i.e.*

$$\mathcal{O}_j(x)\,\mathcal{O}_k(y) = \sum_l \tilde{C}_{jk}^l(x-y)\mathcal{O}_l(x)\,. \tag{2.28}$$

The functions $\tilde{C}_{jk}^l(x-y)$ are related to the structure constant C_{jkl}. For a four-point function one obtains

$$\langle \mathcal{O}_j(x_1)\mathcal{O}_k(x_2)\mathcal{O}_l(x_3)\mathcal{O}_m(x_4)\rangle = \sum_{r,s} \tilde{C}_{jk}^r(x_1-x_2)\tilde{C}_{lm}^s(x_3-x_4)\,\langle \mathcal{O}_r(x_1)\mathcal{O}_s(x_3)\rangle\,, \tag{2.29}$$

where we assumed that the pairs x_1, x_2 and x_3, x_4 are sufficiently close. The OPE can

be generalised to higher-point functions straightforwardly. The form of eq. (2.29) then suggests, that the OPE can also be understood as an insertion of a full set of states. Nonetheless, the explicit knowledge of *all* the involved structure constants is necessary for the evaluation, which makes the OPE somewhat impractical.

2.2. The spectral problem and integrability

Classically conformal theories do not necessarily inherit conformal invariance in the quantum theory. Remarkably, $\mathcal{N} = 4$ SYM theory is a (super)conformal theory even at the quantum level, as its β-function is believed to vanish identically [78–80]

$$\beta(g_{\text{YM}}) = \mu \frac{\mathrm{d}g_{\text{YM}}}{\mathrm{d}\mu} \equiv 0\,. \tag{2.30}$$

Since the β-function describes the dependence of the theory on the renormalization scale μ, a non-vanishing β-function is related to the breakdown of scale invariance. The vanishing of the β-function in $\mathcal{N} = 4$ SYM implies, that divergencies and the dependence on the scale μ drop out in the calculation of physical quantities after properly normalising the operators involved.

In general, the classical scaling dimension Δ_0 of local composite operators receives quantum corrections. At weak coupling in the planar limit, the scaling dimension of an operator $\mathcal{O}$ may be written as

$$\Delta = \Delta_0 + \sum_{\ell=1}^{\infty} g^{2\ell} \gamma_\ell\,, \tag{2.31}$$

with g^2 as defined in eq. (2.7). The anomalous dimension γ_ℓ is the quantum correction to Δ at ℓ-th loop order.

The dilatation operator $\mathfrak{D}$ generates dilatations and hence it measures the scaling dimension of a local operator. In the perturbative regime the dilatation operator may be written as

$$\mathfrak{D} = \sum_{n} g^{2\ell} \mathfrak{D}_{2\ell}\,. \tag{2.32}$$

The One-loop Dilatation operator. Let us consider the example of a rank-one sector. We consider the SU(2) sector spanned by two complex scalar fields X and Z. To form gauge invariant operators, the fields have to appear under the trace, such as

$$\operatorname{tr}\big(XZ^{\ell_1}XZ^{\ell_2}\ldots XZ^{\ell_M}\big)\,, \qquad \text{or} \qquad \operatorname{tr}\big(XZ^{\ell_1}XZ^{\ell_2}\big)\operatorname{tr}\big(XZ^{\ell_3}\ldots XZ^{\ell_M}\big)\,. \tag{2.33}$$

We will denote the first example as a single-trace operator, while the latter is an example of multi-trace type. This sector is known to be closed under the action of the dilatation operator and does therefore not mix with operators containing the other types of fields. The one-loop dilatation operator $\mathfrak{D}_2$ can be written as [18]

$$\mathfrak{D}_2 = -\frac{1}{N} : \operatorname{tr}\big([X,Z][\check{X},\check{Z}]\big) :\,, \tag{2.34}$$

where the check indicates a functional derivative of fields as

$$(\check{Z})^b_c \equiv \frac{\delta}{\delta(Z)^c_b} \qquad \text{with} \qquad (\check{Z})^b_c(Z)^d_e = \delta^b_e\delta^d_c - \frac{1}{N}\delta^b_c\delta^d_e\,. \tag{2.35}$$

Of course, the action of the functional derivative $\check{Z}$ on the field X vanishes. The normal-ordering ensures that the functional derivatives do not act on the fields within the colons. Further, we have the joining and splitting rules for SU(N) following with eq. (2.6) as

$$\begin{aligned} \operatorname{tr}\big(\check{Z}A\big)\operatorname{tr}(ZB) &= \operatorname{tr}(AB) - \frac{1}{N}\operatorname{tr}(A)\operatorname{tr}(B)\,, \\ \operatorname{tr}\big(\check{Z}AZB\big) &= \operatorname{tr}(A)\operatorname{tr}(B) - \frac{1}{N}\operatorname{tr}(AB)\,. \end{aligned} \tag{2.36}$$

Similarly, $\check{Z}$ acts on fields Z within A and B. In this thesis we will always consider the planar limit.

Example with $L = 4$. Let us consider a simple example with operators of length four carrying two fields X. Due to the cyclicity of the trace, there are only the two distinct operators $\mathcal{O}^0_4 = \operatorname{tr}(ZZXX)$ and $\mathcal{O}^1_4 = \operatorname{tr}(ZXZX)$. Applying the planar one-loop dilatation operator we find

$$\mathfrak{D}_2\mathcal{O}^0_4 = 2(\mathcal{O}^0_4 - \mathcal{O}^1_4)\,, \qquad \text{and} \qquad \mathfrak{D}_2\mathcal{O}^1_4 = 4(\mathcal{O}^1_4 - \mathcal{O}^0_4)\,. \tag{2.37}$$

Diagonalizing the resulting mixing matrix yields two eigenvectors. The first being $2\mathcal{O}^0_4 + \mathcal{O}^1_4$, which has anomalous dimension $\gamma_1 = 0$. In fact, it can be easily seen, that this is a vacuum descendant, which can be obtained by acting twice with the raising generator $\mathfrak{R}^2_{\dot{3}}$ on the vacuum $\operatorname{tr}(ZZZZ)$. The second eigenvector is $\mathcal{O}^0_4 - \mathcal{O}^1_4$. It has anomalous dimension $\gamma_1 = 6$ and is a primary operator in the $SU(2)$ sector considered here. Such primary operators are also denoted *BMN operators* [13].

2.2.1. Classical integrability

Exactly solvable models are highly constrained by symmetry, allowing to solve for the dynamical variables analytically. Often the reason for the solvability of the model lies in its integrability. The concept of integrability was discovered in the context of classical Hamiltonians, where the requirement is that sufficiently many conserved quantities exist (along the flow of the Hamiltonian). The equations of motion can then be integrated, hence the historically shaped term *integrability*.

The concept of integrability can also be extended to quantum mechanical models. Though there is no universal mathematical definition, there are some features that integrable systems share. We will consider the SU(2) spin chain in great detail in the next section. Let us briefly review classical integrability in this paragraph. A road to construct the conserved quantities is through Lax pairs. In a classical mechanics system of M particles, the phase space is $2M$ dimensional. The Hamiltonian H generates then the time flow of the canonical coordinates q_j and momenta p_j by

$$\dot{q_j} = \frac{\partial H}{\partial p_j}\,, \qquad \dot{p_j} = -\frac{\partial H}{\partial q_j}\,, \tag{2.38}$$

with $j = 1 \dots M$. The Liouville-Arnol'd theorem states then that if there exist M independent quantities that Poisson commute with the Hamiltonain, the phase space reduces to an M dimensional manifold, which is diffeomorphic to the M-torus T^M. Moreover, there exists a canonical transformation to action-angle variables I_j, θ_j such that the equations of motion take the form

$$\dot{I}_j = 0\,, \qquad \dot{\theta}_j = 1\,. \tag{2.39}$$

Sometimes the symmetry of the problem allows to find the set of conserved quantities. An example is the Kepler problem. When describing models with infinitely many degrees of freedom, such as classical field theories, it becomes handy to use the Lax pair formalism. The Lax pair is given by the pair of square matrices L, M satisfying the relation

$$\frac{\mathrm{d}L}{\mathrm{d}t} = [L, M]\,. \tag{2.40}$$

Given a Lax pair, we can easily generate conserved quantities by considering $\mathrm{tr}\big(L^k\big)$. Taking the derivative we have

$$\frac{\mathrm{d}}{\mathrm{d}t}\,\mathrm{tr}\big(L^k\big) = k\,\mathrm{tr}\big(L^{k-1}[M, L]\big) = 0\,, \tag{2.41}$$

which vanish due to the cyclicity of the trace. The Lax pair allows to generate the conserved charges of classical integrable models. In addition, the conserved charges must also Poisson commute with each other. This structure of the underlying Hamiltonian system can be reinstated by introducing the classical R matrix, which also has to satisfy the classical Yang-Baxter equation.

For a more detailed discussion of classical integrability we refer the reader to the books [81, 82] or lecture notes [83, 84].

2.2.2. SU(2) spin chain

An important development was the observation by Minahan and Zarembo [14], that in the planar limit the one-loop mixing problem in the scalar sector of $\mathcal{N} = 4$ SYM can be mapped to an integrable spin chain. More precisely, the mixing matrix can be identified with the spin chain Hamiltonian and the anomalous dimension corresponds to the spin chain energy. There are various approaches to solving the Heisenberg spin chain. In the following we will discuss the coordinate Bethe ansatz for the SU(2) sector. Further, considering higher-rank sectors in Section 2.2.4 we make use of the nested Bethe ansatz.

For completeness, let us also briefly mention the algebraic and the thermodynamic Bethe ansatz, which we will not need here. The algebraic Bethe ansatz ansatz uses the construction of the monodromy and transfer matrix to find the Bethe equations and state. The thermodynamic Bethe ansatz considers the model in a thermodynamic limit. Moreover, it allows to capture finite size or wrapping corrections. We will review and discuss it in more detail in the context of AdS_3 in Sec. 6.

Heisenberg spin chain. Let us introduce the spin chain notation for single-trace operators in the SU(2) sector. The idea is to write the single trace operator containing L fields as a cyclic spin chain of length L. The particle at the i-th site of the spin

chain can have spin up $|\uparrow\rangle$ or down $|\downarrow\rangle$ and therefore generates a local two-dimensional Hilbert space $\mathbb{C}^2$. Hence, the model is defined on $\mathcal{H} = (\mathbb{C}^2)^{\otimes L}$. We will identify the vacuum field Z with $|\downarrow\rangle$ and a BPS operator can therefore be written as

$$\mathrm{tr}\big(Z^L\big) \quad \to \quad |\downarrow \ldots \downarrow\rangle_L \ , \tag{2.42}$$

Correspondingly, the field X will be identified with $|\uparrow\rangle$. Inserting M fields X into a vacuum of $(L-M)$ fields Z, we can write

$$\mathrm{tr}\big(Z^{n_1-1}XZ^{n_2-n_1-1}X\ldots\big) \quad \to \quad |\underbrace{\downarrow\ldots\downarrow}_{n_1-1}\uparrow\underbrace{\downarrow\ldots\downarrow}_{n_1+n_2-1}\uparrow\ldots\rangle_L \equiv |X^{n_1}X^{n_2}\ldots X^{n_M}\rangle_L \ , \tag{2.43}$$

where the labels n_i denote the sites at which the *magnons* are inserted. We will implicitly assume periodic boundary conditions by defining $|\ldots X^{L+1}\rangle_L \equiv |X^1\ldots\rangle_L$.

The planar one-loop dilatation operator from eq. (2.34) acts as

$$H = \sum_{i=1}^{L}\left(\mathbb{1}_{i,i+1} - \mathbb{P}_{i,i+1}\right) = \sum_{i=1}^{L}\frac{1}{2}\left(1 - \vec{\sigma}_i\cdot\vec{\sigma}_{i+1}\right) \ , \tag{2.44}$$

where the permutation operator $\mathbb{P}_{i,i+1}$ exchanges the fields at the sites i and $(i+1)$. It can be identified with the Hamiltonian of the Heisenberg spin chain describing nearest neighbour spin-spin interactions [14], where the operator $\vec{\sigma}_i$ at site i is given by the Pauli matrices $\vec{\sigma}_i = (\sigma_i^1, \sigma_i^2, \sigma_i^3)$. Thus, the spectral problem of finding the anomalous dimensions at one loop is equivalent to finding the energy spectrum of the Heisenberg spin cain. The action of the Hamiltonian on a state is then given by

$$\begin{aligned} &H|X^{n_1}X^{n_2}\ldots\rangle_L \\ &\qquad = \sum_{j=1}^{M}\left(2\,|\ldots X^{n_j}\ldots\rangle_L - |\ldots X^{n_j-1}\ldots\rangle_L - |\ldots X^{n_j+1}\ldots\rangle_L\right) \ , \end{aligned} \tag{2.45}$$

where two magnons cannot occupy the same site. The Bethe ansatz aims at diagonalising the Hamiltonian above.

Coordinate Bethe ansatz. The coordinate state containing M excitations is given by

$$|\Psi(p_1,\ldots,p_M)\rangle_L = \sum_{1\le n1<\cdots<n_M\le L}\psi(n_1,\ldots,n_M)\,|X^{n_1}\ldots X^{n_M}\rangle_L \ . \tag{2.46}$$

Here we have introduced the position space wave function $\psi(n_1,\ldots,n_M)$ depending on the position n_i of the magnons on the chain. The state $|\Psi(p_1,\ldots,p_M)\rangle$ is characterised by the set of momenta $\{p\}$.

For the position space wave function we can use the coordinate Bethe ansatz [15], which reads

$$\psi(n_1,\ldots,n_M) = \sum_{\sigma\in S_M} e^{i\sum_{k=1}^{M}p_{\sigma(k)}n_k}\prod_{\substack{j>k\\ \sigma(j)<\sigma(k)}}\mathcal{A}(p_{\sigma(j)},p_{\sigma(k)})\,, \tag{2.47}$$

where we sum over all permutations σ of M excitations. Here, the amplitude $\mathcal{A}$ is the

scattering matrix and describes the scattering between the magnons, when a particle with momentum $p_{\sigma(j)}$ overtakes a particle with momentum $p_{\sigma(k)}$. The S matrix element takes the form

$$\mathcal{A}(p_j, p_k) = -\frac{e^{ip_j+ip_k} + 1 - 2e^{ip_k}}{e^{ip_j+ip_k} + 1 - 2e^{ip_j}} \,. \tag{2.48}$$

Acting with the Hamiltonian on the state (2.47), yields the energy

$$E(p_1, \ldots, p_M) = \sum_{j=1}^{M} 4 \sin^2\left(\frac{p_j}{2}\right) \,. \tag{2.49}$$

The total energy is then given as the sum of the energies E_j of the individual magnons with momentum p_j. Introducing the *Bethe rapidities* $u_j = \frac{1}{2}\cot\left(\frac{p_j}{2}\right)$ allows us to write the momentum factor, the S matrix and the energy as

$$e^{ip_j} = \frac{u_j + \frac{i}{2}}{u_j - \frac{i}{2}} \,, \qquad \mathcal{A}(u_j, u_k) = \frac{u_j - u_k - i}{u_j - u_k + i} \,, \qquad E(\{u_j\}) = \sum_{j=1}^{M} \frac{1}{u_j^2 + \frac{1}{4}} \,. \tag{2.50}$$

The cyclicity of the trace for gauge-theory operators translates to the invariance of the state from eq. (2.47) under the simultaneous shift $n_j \to n_j + 1$ of all n_j. This leads to the zero-momentum constraint

$$\prod_{j=1}^{M} e^{ip_j} = 1 \,, \tag{2.51}$$

ensuring that the total momentum of the magnons vanishes. Further, we can shift the j-th magnon once around the spin chain, *i.e.* $n_j \to n_j + L$. The wave function picks up a phase e^{ip_jL} and S matrix elements from scattering the j-th magnon with the other $(M-1)$ magnons on the chain. Since this should not change the state, we can write the *Bethe equations*

$$e^{ip_jL} \prod_{k \neq j} \mathcal{A}(u_j, u_k) = 1 \,. \tag{2.52}$$

By solving these constraints, we can obtain solutions for the set of momenta $\{p\}$ and their corresponding Bethe rapidities $\{u\}$. Note that we can also add roots at infinity. The respective magnon carries zero momentum and hence it does not contribute to the energy in eq. (2.50). States with infinite rapidities correspond to *descendant* operators, *i.e.* they can be obtained from primary operators by acting with raising operators.

Substituting the solutions of eqs. (2.52) and (2.51) into the ansatz (2.47), we obtain the conformal eigenoperators, that we would also find from the dilatation operator. The unit norm is obtained by normalising as [85, 86]

$$\frac{|\Psi(\{p_j\})\rangle_L}{\sqrt{L\,\mathcal{G}\,\prod_j (u_j^2 + \frac{1}{4})\,\prod_{j<k} \mathcal{A}(u_j, u_k)}} \,. \tag{2.53}$$

The state does not depend on the ordering of the rapidities as long as the latter is equal in the wave function and the phase factor $\prod \mathcal{A}(u_j, u_k)$. In the last formula, we

introduced the *Gaudin norm*, which is defined as

$$\mathcal{G} = \text{Det } \phi_{jk}\,, \qquad \phi_{jk} = -i\,\frac{\partial \log\left(e^{ip_j L}\prod_{j\neq k}\mathcal{A}(u_j,u_k)\right)}{\partial u_k}\,. \tag{2.54}$$

Cutting Bethe States. In the following we will introduce the method of cutting a Bethe state. Consider a generic spin chain state $|\Psi(\{u\})\rangle_L$ of length L. We now want to cut this state into two shorter subchains of length ℓ and $L-\ell$. Introducing the splitting factor

$$\omega(\alpha,\bar{\alpha};\ell) = \prod_{u_j\in\bar{\alpha}} e^{ip_j\ell}\prod_{\substack{j<k\\ u_k\in\alpha}}\mathcal{A}(u_j,u_k)\,, \tag{2.55}$$

the entangled state can be written as [37]

$$|\Psi(\{u\})\rangle_L = \sum_{\{u\}=\alpha\cup\bar{\alpha}}\omega(\alpha,\bar{\alpha};\ell)\,|\Psi(\alpha)\rangle_\ell\,|\Psi(\bar{\alpha})\rangle_{L-\ell}\,. \tag{2.56}$$

This identity has a quite vivid interpretation: Say we place a magnon with rapidity u_j on the first subchain of length ℓ, it can propagate to the second subchain of length $L-\ell$, picking up the shift factor $e^{ip_j\ell}$. In addition, by propagating it might overtake other magnons with rapidities u_k with $j<k$ sitting on the first subchain. Thus, the scattering phases $\mathcal{A}(u_j,u_k)$ have to be taken into account. For short states, the identity (2.56) can also be checked explicitly.

Two-magnon example. Let us consider the example of an operator of length L carrying two excitations X. The momentum constraint yields $p_2=-p_1$ and written in terms of the rapidities $u_2=-u_1$. The Bethe equation for u_1 is given by

$$\left(\frac{u_1+\frac{i}{2}}{u_1-\frac{i}{2}}\right)^L\frac{u_1-u_2-i}{u_1-u_2+i} = 1\,. \tag{2.57}$$

Solving explicitly for short lengths $L=4,5,6,7$, we find the rapidities and energies listed in Tab. 2.2. Once again, the energies can also be obtained by explicitly diagonalising the planar one-loop dilatation operator.

L	u	E	$\mathcal{G}$
4	$\frac{1}{2\sqrt{3}}$	6	108
5	$\frac{1}{2}$	4	80
6	$\frac{1}{2}\sqrt{1\pm\frac{2}{\sqrt{5}}}$	$5\mp\sqrt{5}$	$75(\sqrt{5}\pm 3)$
7	$\frac{\sqrt{3}}{2}$	2	42
	$\frac{1}{2\sqrt{3}}$	6	378

Table 2.2.: Bethe rapidities u, energies E and Gaudin norm $\mathcal{G}$ for operators in the SU(2) sector with lengths $L=4,\ldots,7$.

We can also write the coordinate Bethe state from eq. (2.46) more explicitly for two

magnons as

$$|\Psi(p_1,p_2)\rangle_L = \sum_{1\leq n1<n_2\leq L} \left(e^{i(p_1n_1+p_2n_2)} + \mathcal{A}(p_1,p_2)e^{i(p_1n_2+p_2n_1)}\right)|X^{n_1}X^{n_2}\rangle_L \ . \tag{2.58}$$

For short lengths we plug in the rapidities from Tab. 2.2 and using the normalisation from eq. (2.53), we will find the normalised Bethe states. Moreover, mapping the spin chain to single trace operators, we can identify them with the eigenstates obtained from directly diagonalising the one-loop dilatation operator.

For short states with few magnons the identity in eq. (2.56) can also be written explicitly. For instance, for a two magnon state in the SU(2) sector it reads

$$\begin{aligned}|\Psi(u_1,u_2)\rangle_L = |\Psi(u_1,u_2)\rangle_\ell \, |\Psi(\{\})\rangle_{L-\ell} + e^{ip_2\ell}\,|\Psi(u_1)\rangle_\ell \, |\Psi(u_2)\rangle_{L-\ell} + \\ e^{ip_1\ell}\mathcal{A}(u_1,u_2)\ |\Psi(u_2)\rangle_\ell \, |\Psi(u_1)\rangle_{L-\ell} + e^{i(p_1+p_2)\ell}\ |\Psi(\{\})\rangle_\ell \, |\Psi(u_1,u_2)\rangle_{L-\ell} \ .\end{aligned} \tag{2.59}$$

Let us address some remarkable points here: Firstly, the energy of a multi-particle state is just the sum of the single-particle energies. Next, the multi-particle scattering factorises into two-particle scattering processes. Since the result must not depend on the order of the two-particle scattering processes, the S matrix needs to obey the *Yang-Baxter equation*. This property is a direct consequence of the integrability of the system and we will come back to it below. Further, the analogy between the planar one-loop dilatation operator and an integrable spin chain Hamiltonian can be extended beyond the scalar sector. The complete one-loop dilatation operator for $\mathcal{N}=4$ SYM is given in [17]. At higher-loop orders, the system is still integrable and can be solved via the asymptotic Bethe ansatz, but the corresponding Hamiltonian describes no longer a nearest-neighbour interaction. At ℓ-th loop order it rather involves the ℓ-th neighbouring magnons. When the loop order and the length of the spin chain are of the same magnitude, the asymptotic Bethe ansatz breaks down, as *wrapping corrections* start to contribute. As the name implies these interactions wrap around the spin chain.

2.2.3. S matrix from symmetries

In the preceding subsection, we constructed the S matrix for the SU(2) sector using the coordinate Bethe ansatz. In Sec. 2.1.3 we saw, that by choosing the vacuum Z, the symmetry is broken to $\mathfrak{psu}(2|2)^{\oplus 2}$ and excitations can be obtained from acting with the lowering operators from either of the two algebras. It turns out, that the full S matrix $\mathbb{S}$, describing the scattering of the magnons, is given by the tensor product of two copies of $\mathfrak{su}(2|2)$ S matrices [19] with an appropriate overall dressing factor

$$\mathbb{S} = \mathcal{S}\otimes\dot{\mathcal{S}}\,, \tag{2.60}$$

where the dot indicates, that the matrix acts on the second copy.

The $\mathfrak{su}(2|2)$ S matrix can be found from the symmetries of the model using the concept of a dynamic spin chain as worked out by Beisert in [19]. Here dynamic refers to length changing effects, as vacuum sites can be inserted or removed. This is indicated by writing $Z^\pm$. These insertions can be shifted over the chain, yielding factors $e^{\mp ip}$ whenever they overtake a magnon with momentum p, *i.e.*

$$|Z^\pm X\rangle = e^{\mp ip}\,|XZ^\pm\rangle \ . \tag{2.61}$$

The S matrix $\mathcal{S}(u_j, u_k)$ scatters the two adjacent magnons of the spin chain with momenta p_j and p_k. The operator can be fixed by the requirement, that it commutes with the $\mathfrak{su}(2|2)$ algebra generators $\mathfrak{J}$, such that

$$[\mathfrak{J}_j + \mathfrak{J}_k, \mathcal{S}(u_j, u_k)] = 0\,, \tag{2.62}$$

where the indices j, k indicate on which particle the generators act, respectively. Since the central charges act diagonally, commutators involving these are automatically satisfied. The bosonic generators $\mathfrak{L}$, $\mathfrak{R}$ fix the form of the S matrix up to ten coefficient functions $\mathcal{A}(u_j, u_k)$ to $\mathcal{L}(u_j, u_k)$. The commutation relation with the fermionic charges $\mathfrak{Q}, \mathfrak{S}$ yield a unique solution up to an undetermined overall phase $S^0(u_j, u_k)$. We refer the reader to [19] for the explicit form.

Additionally, the S matrix has to fulfil the unitarity condition

$$\mathcal{S}(u_k, u_j)\,\mathcal{S}(u_j, u_k) = \mathbb{1}\,, \tag{2.63}$$

ensuring that scattering the same particles twice does not change the state. The physical unitarity condition requires the S matrix to be unitary as a matrix

$$\mathcal{S}(u_j, u_k)^\dagger\,\mathcal{S}(u_j, u_k) = \mathbb{1}\,. \tag{2.64}$$

Finally, the scattering matrix $\mathcal{S}$ does also fulfil the *Yang-Baxter equation*

$$\mathcal{S}_{23}\,\mathcal{S}_{13}\,\mathcal{S}_{12} = \mathcal{S}_{12}\,\mathcal{S}_{13}\,\mathcal{S}_{23}\,, \tag{2.65}$$

where the subscripts indicate the particles the S matrix acts on. Remarkably, the Yang-Baxter equation states that the result of a multi-particle scattering process is independent of the order in which the individual two-particles scattering processes occur. For instance, on the left hand site of eq. (2.65) the particles 1 and 2 are scattered first, whereas on the right hand site we begin by scattering particles 2 and 3.

2.2.4. Higher rank models and the nested Bethe Ansatz

So far, we introduced the coordinate Bethe ansatz for the rank-one SU(2) sector in Sec. 2.2.2. In order to generalise the description to higher-rank cases, let us start by considering an SU(3) model with excitations X and Y on top of the vacuum Z. Though this subsector is not closed at higher loops, it is an illustrative example and we will make use of it for tree-level calculations later in this work.

Using the tensor-product notation from eq. (2.18) for the excitations $X = \phi^2 \otimes \dot{\phi}^{\dot{4}}$ and $Y = \phi^1 \otimes \dot{\phi}^{\dot{4}}$, we can put the excitations on a chain and consider their scattering with the S matrix

$$\mathbb{S}\,|X(u_1)Y(u_2)\rangle = (\mathcal{S}\,|\phi^2(u_1)\phi^1(u_2)\rangle) \otimes (\dot{\mathcal{S}}\,|\dot{\phi}^{\dot{4}}(u_1)\dot{\phi}^{\dot{4}}(u_2)\rangle)\,. \tag{2.66}$$

Since scattering the $\dot{\phi}^{\dot{4}}$ on the right chain leads only to a phase $\mathcal{A}(u_j, u_k)$, we will consider only the left chain and neglect the overall dressing factors in the following. At leading order, *i.e.* neglecting length changing effects, the two excitations can either be transmitted through each other or they are reflected and exchange their flavour

$$\mathcal{S}\,|\phi^2(u_1)\phi^1(u_2)\rangle = T(u_1, u_2)\,|\phi^1(u_2)\phi^2(u_1)\rangle + R(u_1, u_2)\,|\phi^2(u_2)\phi^1(u_1)\rangle\,. \tag{2.67}$$

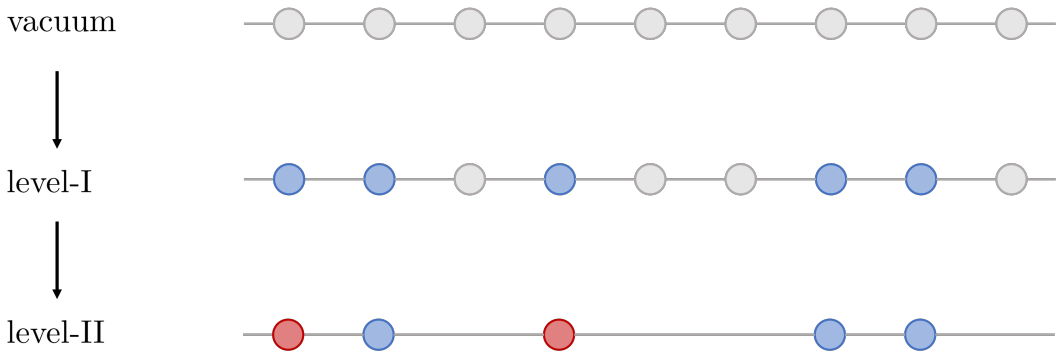

Figure 2.2.: Illustration of the nested Bethe state. We start with a level-I vacuum (grey sites), on which we can place level-I excitations (blue sites). Level-II excitations (red sites) then move over a level-II vacuum built from the level-I excitations.

The coefficients $T(u_1, u_2)$ and $R(u_1, u_2)$ are the transmission and reflection amplitudes, respectively. Using the Beisert S matrix and its elements $\mathcal{A}(u_1, u_2)$ and $\mathcal{B}(u_1, u_2)$ [19], we can easily identify

$$T_{12} = \frac{\mathcal{A}_{12} - \mathcal{B}_{12}}{2} = \frac{u_1 - u_2}{u_1 - u_2 + i}\,, \qquad R_{12} = \frac{\mathcal{A}_{12} + \mathcal{B}_{12}}{2} = \frac{-i}{u_1 - u_2 + i}\,, \tag{2.68}$$

where the indices indicate the rapidities. For instance, we can now place two excitations ordered as $X(u_1)$ and $Y(u_2)$ on the spin chain and let them propagate as in eq. (2.46). This yields

$$\begin{aligned} |\Psi(X_1, Y_2)\rangle_L = &\sum_{n_1<n_2} e^{ip_1 n_1 + ip_2 n_2} \, |X_1^{n_1} Y_2^{n_2}\rangle_L + \\ &\sum_{n_1<n_2} e^{ip_2 n_1 + ip_1 n_2} \left(T_{12} \, |Y_2^{n_1} X_1^{n_2}\rangle_L + R_{12} \, |X_2^{n_1} Y_1^{n_2}\rangle_L\right) . \end{aligned} \tag{2.69}$$

In order to maintain a simple notation, we put the position of the excitation in the superscript, while the subscript indicates the momentum. Obviously, the wave function (2.69) does not lead to a periodic state, since the transmission changes the ordering of the flavours. In order to obtain a periodic state, we need to add a second wave function $|\Psi(Y_1, X_2)\rangle_L$ with the excitations ordered as Y_1, X_2. By introducing the yet to be determined coefficients g_{XY} and g_{YX}, we can write the Bethe state as the sum

$$|\Psi_{XY}(p_1, p_2)\rangle_L = g_{XY} \, |\Psi(X_1, Y_2)\rangle_L + g_{YX} \, |\Psi(Y_1, X_2)\rangle_L \,. \tag{2.70}$$

Similar to the SU(2) case, we could now impose periodicity constraints to obtain a set of Bethe equations, which fix the rapidities as well as the ratio of the coefficients g_{XY}/g_{YX}. The generalisation to higher numbers of magnons is straightforward, though the wave functions become rather bulky.

Nested Bethe ansatz. A means to diagonalise the scattering matrix is the *nested Bethe ansatz* [87]. We will discuss this technique in the following. The reasoning here relies on the oscillator picture introduced in Sec. 2.1.3. Let us start by considering a vacuum consisting of the fields Z only. The action of the operator $\mathfrak{R}^2_{\dot{3}}$ creates a level-I excitation X with rapidity u moving over the chain of vacua Z. These can scatter with

other level-I excitations. Hence, we write

$$\mathcal{S}^{\mathrm{I},0}(u) = e^{ip}\,, \qquad \mathcal{S}^{\mathrm{I},\mathrm{I}}_{jk} \equiv \mathcal{S}^{\mathrm{I},\mathrm{I}}(u_j,u_k) = \mathcal{A}_{jk}\,, \tag{2.71}$$

where the superscripts indicate the level of the excitations involved. This yields the previously discussed SU(2) sector. The factor $\mathcal{S}^{\mathrm{I},0}(u)$ describes the shift of the level-I excitation over the vacuum, *i.e.* level-0 excitations. The scattering of two level-I excitations is given by $\mathcal{S}^{\mathrm{I},\mathrm{I}}_{jk}$.

Suppose we now have a chain of length L with M_1 excitations X. Next, we use $\mathfrak{R}^1{}_2$ to create the excitation Y from the excitations X. The excitation Y then moves over the length M_1 subchain of all the X, *cf.* Fig. 2.2. Thus we associate a secondary rapidity v to this level-II excitation. Again, there is a shift operator as well as a scattering matrix

$$\mathcal{S}^{\mathrm{II},\mathrm{I}}(v,u) = \frac{v-u+\frac{i}{2}}{v-u-\frac{i}{2}}\,, \qquad \mathcal{S}^{\mathrm{II},\mathrm{II}}_{jk} \equiv \mathcal{S}^{\mathrm{II},\mathrm{II}}(v_j,v_k) = \frac{v_j-v_k-i}{v_j-v_k+i}\,. \tag{2.72}$$

Since the factor $\mathcal{S}^{\mathrm{II},\mathrm{I}}(v,u)$ shifts the level-II excitation over the subchain, it is referred to as level-I vacuum. Additionally, there is the *creation amplitude* $f^{\mathrm{II},\mathrm{I}}(v,u)$ for the creation of a Y with rapidity v on top of the excitation X with rapidity u. This amplitude is given by

$$f^{\mathrm{II},\mathrm{I}}(v,u) = \frac{1}{v-u-\frac{i}{2}}\,. \tag{2.73}$$

This feature is inherent to higher-rank sectors. The analogous amplitude corresponding to the creation of a level-I excitation from the vacuum is simply given by one.

The nested structure becomes apparent, when we write the nested Bethe equation. The M_1 level-I magnons carry the rapidities from the set $\{u\}$. On top of the level-I vacuum we have M_2 level-II excitations Y and hence we have (M_1-M_2) excitations X. By demanding that the configuration is identically reproduced by taking any one excitation once around the chain, we find the SU(3) Bethe equations

$$\begin{aligned}
1 &= \prod_{j=1}^{M_1} e^{ip_j}\,,\\
1 &= e^{ip_jL}\prod_{\substack{k=1\\k\neq j}}^{M_1}\frac{u_j-u_k-i}{u_j-u_k+i}\prod_{l=1}^{M_2}\frac{u_j-v_l+\frac{i}{2}}{u_j-v_l-\frac{i}{2}}\,,\\
1 &= \prod_{k=1}^{M_1}\frac{v_j-u_k+\frac{i}{2}}{v_j-u_k-\frac{i}{2}}\prod_{\substack{l=1\\l\neq j}}^{M_2}\frac{v_j-v_l-i}{v_j-v_l+i}\,.
\end{aligned} \tag{2.74}$$

Since the primary rapidities u_j are associated to the e^{ip_j} factors, they are also called momentum-carrying roots. The secondary rapidities v_j are also called auxiliary roots.

Though the construction above focused on the SU(3) sector, its generalisation to other sectors is quite straightforward.

Nested wave function. Let us put the ingredients gathered above together to construct the nested wave function. We will continue with the explicit SU(3) example

for concreteness. We aim to construct the wave function

$$|\Psi_{XY}(\{u\})\rangle_L = \sum_{\substack{1\leq n_1<\cdots<n_{M_1}\leq L\\ 1\leq m_1<\cdots<m_{M_2}\leq M_1}} \psi^{\mathrm{I}}(\{n\},\{m\})\,|X^{n_1}\ldots Y^{n_m}\ldots X^{M_1}\rangle_L\,, \tag{2.75}$$

where the level-I excitations are placed at the positions $\{n\}$ with momentum carrying rapidities $\{u\}$. The level-II excitations move on top of the M_1 level-I excitations and can hence take the positions $\{m\}$ with $1 \leq m_1 < \cdots < m_{M_2} \leq M_1$. For the level-I wave function we can write

$$\psi^{\mathrm{I}}(\{n\},\{m\}) = \sum_{\sigma_{\mathrm{I}}\in S_{M_1}} \prod_{k=1}^{M_1} \left(\mathcal{S}^{\mathrm{I},0}(u_{\sigma_{\mathrm{I}}(k)})\right)^{n_k} \prod_{\substack{j>k\\ \sigma_{\mathrm{I}}(j)<\sigma_{\mathrm{I}}(k)}} \mathcal{S}^{\mathrm{I},\mathrm{I}}(u_{\sigma_{\mathrm{I}}(j)},u_{\sigma_{\mathrm{I}}(k)})\;\psi^{\mathrm{II}}(\{m\})\,, \tag{2.76}$$

where $\psi^{\mathrm{II}}(\{m\})$ is the level-II wave function. The level-II excitations are then described by

$$\psi^{\mathrm{II}}(\{m\}) = \sum_{\sigma_{\mathrm{II}}\in S_{M_2}} \prod_{k=1}^{M_2} f^{\mathrm{II},\mathrm{I}}(v_{\sigma_{\mathrm{II}}(k)},u_{\sigma_{\mathrm{II}}(k)}) \prod_{j=1}^{m_k-1} \mathcal{S}^{\mathrm{II},\mathrm{I}}(v_{\sigma_{\mathrm{II}}(k)},u_{\sigma_{\mathrm{I}}(j)}) \prod_{\substack{l>k\\ \sigma_{\mathrm{II}}(l)<\sigma_{\mathrm{II}}(k)}} \mathcal{S}^{\mathrm{II},\mathrm{II}}(v_{\sigma_{\mathrm{II}}(l)},v_{\sigma_{\mathrm{II}}(k)})\,. \tag{2.77}$$

This emphasises the nested structure. In a similar fashion, we can introduce further levels and write corresponding wave functions.

Two-magnon example. Let us consider a state in the SU(3) sector with two magnons. Using the notation introduced above we can write the level-I state given in eq. (2.46) as

$$|\Psi_X(u_1,u_2)\rangle_L = \sum \psi^{\mathrm{I}}(n_1,n_2)\,|X^{n_1}X^{n_2}\rangle^{\mathrm{I}}_L\,, \tag{2.78}$$

where the level-I wave function is given in eq. (2.47). Since this is simply a state in the SU(2) sector, it is identical with eq. (2.59). We can now consider it as a level-II vacuum $|0\rangle^{\mathrm{II}}$ on which we can place level-II excitations. Adding one excitation Y with auxiliary rapidity v can then write

$$\begin{aligned}|\Psi_{XY}(u_1,u_2)\rangle_L = \sum_{n_1<n_2}\Big(\;& e^{i(p_1n_1+p_2n_2)} f^{\mathrm{II},\mathrm{I}}(v,u_1) && |Y_1^{n_1}X_2^{n_2}\rangle^{\mathrm{I}}_L\\ &+e^{i(p_1n_1+p_2n_2)} f^{\mathrm{II},\mathrm{I}}(v,u_2)\mathcal{S}^{\mathrm{II},\mathrm{I}}(v,u_1) && |X_1^{n_1}Y_2^{n_2}\rangle^{\mathrm{I}}_L\\ &+e^{i(p_1n_2+p_2n_1)} f^{\mathrm{II},\mathrm{I}}(v,u_2) && \mathcal{S}^{\mathrm{I},\mathrm{I}}(u_1,u_2)\quad |Y_2^{n_1}X_1^{n_2}\rangle^{\mathrm{I}}_L\\ &+e^{i(p_1n_2+p_2n_1)} f^{\mathrm{II},\mathrm{I}}(v,u_1)\mathcal{S}^{\mathrm{II},\mathrm{I}}(v,u_2)\mathcal{S}^{\mathrm{I},\mathrm{I}}(u_1,u_2) && |X_2^{n_1}Y_1^{n_2}\rangle^{\mathrm{I}}_L\Big)\,.\end{aligned} \tag{2.79}$$

Solving the Bethe equations (2.74) for these kinds of states with $M_1 = 2$ and $M_2 = 1$, we find for $L = 3, 4, 5$ the set of solutions given in Tab. 2.3.

Similar to the construction in eq. (2.70), we can write the Bethe wave function for

L	u	v	E	$\mathcal{G}$
3	$\frac{1}{2\sqrt{3}}$	0	6	486
4	$\frac{1}{2}$	0	4	256
5	$\frac{1}{2}\sqrt{1\pm\frac{2}{\sqrt{5}}}$	0	$5\mp\sqrt{5}$	$250\left(5\mp 2\sqrt{5}\right)$

Table 2.3.: Set of SU(3) states containing two excitations.

SU(3) states with two excitations. Up to a normalisation it is schematically given by

$$\begin{aligned}|\Psi_{XY}(u_1,u_2)\rangle_L = &\sum_{n_1<n_2}\left(g_{XY}e^{i(p_1n_1+p_2n_2)}+(g_{XY}R_{12}+g_{YX}T_{12})e^{i(p_2n_1+p_1n_2)}\right)|X^{n_1}Y^{n_2}\rangle_L\\ &+\sum_{n_1<n_2}\left(g_{YX}e^{i(p_1n_1+p_2n_2)}+(g_{YX}R_{12}+g_{XY}T_{12})e^{i(p_2n_1+p_1n_2)}\right)|Y^{n_1}X^{n_2}\rangle_L\,.\end{aligned} \tag{2.80}$$

For readability purposes we left the magnon momenta implicit here. The transmission and reflection amplitudes are given in eq. (2.68). By comparing with eq. (2.79), the coefficients g_{XY} and g_{YX} can be easily identified as

$$g_{YX}=f^{\text{II,I}}(v,u_1)\,,\qquad g_{XY}=f^{\text{II,I}}(v,u_2)\mathcal{S}^{\text{II,I}}(v,u_1)\,. \tag{2.81}$$

In the example with $M_1=2$ and $M_2=1$, it is easy to see that $g_{XY}=-g_{YX}$ and hence up to normalisation the state reads

$$|\Psi_{XY}(u_1,u_2)\rangle_L=\sum_{n_1<n_2}\left(e^{i(p_1n_1+p_2n_2)}-e^{i(p_2n_1+p_1n_2)}\right)\left(|X^{n_1}Y^{n_2}\rangle-|Y^{n_1}X^{n_2}\rangle\right)\,. \tag{2.82}$$

It is remarkable that all the information from the auxiliary Bethe roots is hidden in the prefactors g_{XY},g_{YX} in eq. (2.81), while the momentum carrying roots appear more explicitly in the transmission and reflection processes. We will make use of this observation later on.

Higher-rank Bethe equations from Dynkin diagrams. There is also a neat way to obtain the Bethe equations from the Dynkin diagram [16] in Fig. 2.1. For this we associate the momentum carrying Bethe roots $\mathfrak{u}_{4,j}=u_j$ to the middle node. As before, we get the constraint for the vanishing total momentum

$$1=\prod_{j=1}^{M_k}\frac{\mathfrak{u}_{k_j,j}+\frac{i}{2}\delta_{4,k_j}}{\mathfrak{u}_{k_j,j}-\frac{i}{2}\delta_{4,k_j}}\,. \tag{2.83}$$

Further we associate the auxiliary rapidities $\mathfrak{u}_{1,j}=v_{3,j},\mathfrak{u}_{2,j}=v_{2,j},\mathfrak{u}_{3,j}=v_{1,j}$ for the left wing of the beauty diagram in Fig. 2.1 as well as $\mathfrak{u}_{5,j}=w_{1,j},\mathfrak{u}_{6,j}=w_{2,j},\mathfrak{u}_{7,j}=w_{3,j}$ for the right wing. The Bethe equations can then be written in the compact form

$$\left(\frac{\mathfrak{u}_{k_j,j}+\frac{i}{2}\delta_{4,k_j}}{\mathfrak{u}_{k_j,j}-\frac{i}{2}\delta_{4,k_j}}\right)^L=\prod_{\substack{l=1\\l\neq j}}^{M_1}\frac{\mathfrak{u}_{k_j,j}-\mathfrak{u}_{k_l,l}+\frac{i}{2}A_{k_j,k_l}}{\mathfrak{u}_{k_j,j}-\mathfrak{u}_{k_l,l}-\frac{i}{2}A_{k_j,k_l}}\,, \tag{2.84}$$

where A_{k_j,k_l} are the entries of the Cartan matrix corresponding to the Dynkin diagram.

The Gaudin norm can also be generalised to higher-rank sectors. In order to do this, let us introduce $\phi_{\mathfrak{u}_{k,j}}$ as the logarithm of the nested Bethe equations, *i.e.* the Bethe equations can be rewritten as $e^{i\phi_{\mathfrak{u}_{k,j}}} = 1$. The full Gaudin norm $\mathcal{G}$ is then given by the determinant of the matrix

$$\mathcal{G} = \mathrm{Det}\, \frac{\partial\, \phi_{\mathfrak{u}_{k_j,j}}}{\partial\, \mathfrak{u}_{k_l,l}}\,. \tag{2.85}$$

Using the full Gaudin norm in eq. (2.53) generalises the normalisation of states to higher-rank sectors.

In this chapter we considered the beauty diagram. However, it is also possible to generalise to alternative choices of the Dynkin diagram. In that case the δ_{4,k_j} need to be replaced by the Dynkin labels of the spin representation V_{k_j}, *cf.* [16] for a discussion of the beast diagram.

2.3. Marginal deformations

To obtain a better understanding of why $\mathcal{N} = 4$ SYM is integrable, one might consider looking for deformations of the theory that preserve integrability. Here we will consider the exactly marginal deformations of $\mathcal{N} = 4$ SYM theory that preserve $\mathcal{N} = 1$ supersymmetry, which were classified by Leigh and Strassler in [34]. These classes of theories are very interesting to study as they preserve quantum conformal invariance. The deformation can be written using an $\mathcal{N} = 1$ superfield formulation, where the superfields are built out of the $\mathcal{N} = 4$ fields encountered in Sec. 2.1.1 and appear as component fields. For instance, the three complex scalar fields are combined with a fermion into the three chiral superfields $\boldsymbol{\phi}_1, \boldsymbol{\phi}_2, \boldsymbol{\phi}_3$. Further, the remaining gauge field and fermion build the $\mathcal{N} = 1$ vector superfield V. The super Yukawa vertex of the $\mathcal{N} = 4$ SYM Lagrangian in terms of the $\mathcal{N} = 1$ superfields is given by

$$W_{\mathcal{N}=4} = g_{\mathrm{YM}}\, \mathrm{tr}([\boldsymbol{\phi}_1, \boldsymbol{\phi}_2]\boldsymbol{\phi}_3)\,. \tag{2.86}$$

Introducing the two-parameter Leigh-Strassler deformation [34] leads to

$$W_{\mathrm{LS}} = \kappa\, \mathrm{tr}\left(\boldsymbol{\phi}_1\boldsymbol{\phi}_2\boldsymbol{\phi}_3 - q\,\boldsymbol{\phi}_2\boldsymbol{\phi}_1\boldsymbol{\phi}_3 + \frac{h}{3}(\boldsymbol{\phi}_1^3 + \boldsymbol{\phi}_2^3 + \boldsymbol{\phi}_3^3)\right)\,, \tag{2.87}$$

where κ, q and h are complex parameters. Requiring conformal invariance at the quantum level poses a constraint on the parameters. A derivation is given in [88] and for instance at one loop the constraint reads

$$2g_{\mathrm{YM}}^2 = |\kappa|^2 \left(\frac{2}{N^2}|1+q|^2 + \left(1 - \frac{4}{N^2}\right)(1 + |q|^2 + |h|^2)\right)\,. \tag{2.88}$$

While the $\mathcal{N} = 4$ superpotential $W_{\mathcal{N}=4}$ from eq. (2.86) has a global SU(3) × U(1) symmetry, the Leigh-Strassler superpotential (2.87) has in general only U(1) symmetry. It is easy to see, that the undeformed $\mathcal{N} = 4$ SYM theory is recovered by setting $\kappa = g_{\mathrm{YM}}$, $q = 1$ and $h = 0$. For generic values of q and h the theory is not integrable in the planar limit. In fact, integrability yields a strong constraint on the parameters and is only satisfied for special values, *cf.* [89–91].

The *real β-deformed $\mathcal{N}=4$ SYM theory* is integrable [35] and corresponds to the choice $q=e^{i\beta}$ with $\beta\in\mathbb{R}$ and $h=0$. Moreover, taking the planar limit of the real β-deformation, the constraint (2.88) simplifies considerably to $g_{\mathrm{YM}}^2=|\kappa|^2$ and receives no higher-loop corrections [92]. It is natural to ask, what kind of geometry the string dual posses corresponding to the β-deformed theory. The according background was found by Lunin and Maldacena [36] and is obtained by deforming the sphere S^5.

Introducing the non-commutative star-product, the β-deformation can be defined through the action on two fields given by

$$A*B=AB\,e^{\frac{i}{2}(\mathbf{j}(A)\wedge\mathbf{j}(B))}\,, \tag{2.89}$$

where we denote the $\mathfrak{so}(6)$ charges of a field A by the vector $\mathbf{j}(A)=(j_1(A),j_2(A),j_3(A))$. The Cartan charges of the respective fields are given in Tab. 2.1. For two particles of type A,B we define the *charge wedge* as [36]

$$\mathbf{j}(A)\wedge\mathbf{j}(B)=-\beta\sum_{a,b,c=1}^{3}\epsilon_{abc}\,j_a(A)\,j_b(B)\,, \tag{2.90}$$

where we chose the normalisation $\epsilon_{123}=1$.

The Lagrangian of the β-deformed $\mathcal{N}=4$ SYM theory can be obtained as a single-trace deformation from the $\mathcal{N}=1$ superfield formalism by exchanging all the products with $*$-products. Written in terms of the component fields as in eq. (2.3), an additional double-trace deformation is present [93, 94]. However, this double-trace term is suppressed by $1/N$ and does not contribute for long operators in the planar limit. For short operators, such as $\mathrm{tr}(YZ)$, it may be relevant at leading order. We will restrict to sufficiently long operators and the planar limit in the following.

Though one might worry that calculations will become more complicated in the β-deformed theory, they are in fact very similar to calculations in the undeformed theory due to *Filk's theorem* [95]. Evaluating Feynman diagrams, the β-deformation results in decorating the planar amplitudes by a phase factor associated to the external legs [94]. More precisely, this phase factor only depends on the $\mathfrak{so}(6)$ Cartan charges of the incoming and outgoing particles [94, 96].

Moreover, the Bethe equations for the β-deformed theory can be worked out. In [97] it has been observed, that this introduces deformation factors into the Bethe equations as well as the various S matrices of the nested Bethe ansatz. Let us make this more explicit in the following.

2.3.1. The β-deformed SU(2) sector

Considering the β-deformed SU(2) sector, we can work out the differences to Sec. 2.2.2. The commutator in the deformed theory is given by

$$[Y,Z]_\beta=e^{i\beta}YZ-e^{-i\beta}ZY\,. \tag{2.91}$$

The single-trace contribution to the planar one-loop dilatation is obtained by introducing the $*$-product in eq. (2.34). Restricting to operators of length $L>2$, the single trace part is sufficient to find the anomalous dimension. As in the undeformed theory, the

dilatation operator can be mapped to an integrable Hamiltonian [35, 89], acting as

$$\begin{aligned} &H_\beta |X^{n_1} X^{n_2} \dots\rangle_L \\ &\quad = \sum_{j=1}^{M} \left(2\,|\dots X^{n_j}\dots\rangle_L - e^{2i\beta}\,|\dots X^{n_j-1}\dots\rangle_L - e^{-2i\beta}\,|\dots X^{n_j+1}\dots\rangle_L\right) . \end{aligned} \tag{2.92}$$

The coordinate Bethe Ansatz then yields the deformed S-matrix element $\mathcal{A}^\beta(p_j, p_k)$ given by

$$\mathcal{A}^\beta(p_j, p_k) = -\frac{e^{i(p_j+p_k)}e^{2i\beta} + e^{-2i\beta} - 2e^{ip_k}}{e^{i(p_j+p_k)}e^{2i\beta} + e^{-2i\beta} - 2e^{ip_j}} . \tag{2.93}$$

Similarly, the energy is given by

$$E(p_1, \dots, p_M) = \sum_{j=1}^{M} 4\sin^2\left(\frac{p_j + 2\beta}{2}\right) . \tag{2.94}$$

The Bethe equations and cyclicity condition in the SU(2) sector can be directly derived from the β-deformed dilatation operator, *cf.* [89].

The introduction of the shifted momenta via $\tilde{p} = p + 2\beta$ removes the explicit β-dependence from the S-matrix, which then takes the form of the undeformed S-matrix element $A(u_j, u_k)$ of (2.48). This comes at the cost of an explicit β-dependence of the Bethe equations and cyclicity constraint, given by

$$e^{i(\tilde{p}_j - 2\beta)L} \prod_{k\neq j} \frac{\tilde{u}_j - \tilde{u}_k - i}{\tilde{u}_j - \tilde{u}_k + i} = 1 , \qquad \text{and} \qquad \prod_{j=1}^{n_1} e^{i(\tilde{p}_j - 2\beta)} = 1 , \tag{2.95}$$

where we introduced the rapidities $\tilde{u}_j$ via the relation $\tilde{p}_j = 2\,\mathrm{arccot}(2\tilde{u}_j)$. We can solve the Bethe equations (2.95) perturbatively as a small β-expansion. For short lengths $L = 4, 5$ and two magnons, we find the following rapidities $\tilde{u}_\pm$

$$\begin{aligned} L = 4: \quad \tilde{u}_\pm &= \pm\frac{1}{2\sqrt{3}} - \frac{2\beta}{3} \pm \frac{8\beta^2}{9\sqrt{3}} - \frac{16\beta^3}{27} \pm \frac{112\beta^4}{81\sqrt{3}} + O(\beta^5) , \\ L = 5: \quad \tilde{u}_\pm &= \pm\frac{1}{2} - \beta \pm \frac{5\beta^2}{4} - \frac{11\beta^3}{6} \pm \frac{145\beta^4}{48} + O(\beta^5) , \end{aligned} \tag{2.96}$$

where the two signs $(\pm)$ correspond to the rapidities of the two magnons.

As mentioned earlier, in the undeformed theory the Bethe equations allow for so-called vacuum descendants, *i.e.* solutions to the Bethe equations with infinite rapidities. As the energy of such operators vanishes, they are still BPS even though there are magnons on top of the vacuum. In the β-deformed theory however, roots at infinity are no longer a solution due to the presence of the phase $e^{-i\beta L}$ in the deformed Bethe equations. Thus, the deformation lifts the degeneracy of these operators with the vacuum and their roots become proportional to β^{-1} at leading order in a perturbative expansion in β. For instance, we can find the following solutions for operators of short

lenghts with two magnons

$$\begin{aligned}
L=2: \quad \tilde{u}_\pm &= \frac{1\pm i}{4}\frac{1}{\beta}+\frac{-2\pm i}{6}\beta+\frac{-8\pm 7i}{90}\beta^3+O(\beta^5)\,,\\
L=3: \quad \tilde{u}_\pm &= \frac{2\pm i\sqrt{2}}{6}\frac{1}{\beta}+\frac{-8\pm 3i\sqrt{2}}{24}\beta+\left(-\frac{7}{45}\pm\frac{67i}{480\sqrt{2}}\right)\beta^3+O(\beta^5)\,,\\
L=4: \quad \tilde{u}_\pm &= \frac{3\pm i\sqrt{3}}{8}\frac{1}{\beta}+\frac{-3\pm i\sqrt{3}}{9}\beta+\frac{4}{405}(-21\pm 8\sqrt{3}i)\beta^3+O(\beta^5)\,,\\
L=5: \quad \tilde{u}_\pm &= \frac{2\pm i}{5}\frac{1}{\beta}+\frac{-8\pm 5i}{24}\beta+\left(-\frac{23}{90}\pm\frac{211i}{1152}\right)\beta^3+O(\beta^5)\,.
\end{aligned} \tag{2.97}$$

The signs correspond to the two magnons again. Note, that here we also have $L=2$, which is fine as we consider states with two excitations. Obviously, taking the limit $\beta\to 0$ sends the rapidities back to infinity and the operators become protected again as their energy vanishes.

2.4. Chapter summary

In this chapter, we reviewed important results in the field of integrability in $\mathcal{N}=4$ SYM theory. In Sec. 2.1 we considered the field content and the symmetry algebra $\mathfrak{psu}(2,2|4)$ of the model. By fixing the highest weight state $\mathrm{tr}\big(Z^L\big)$ as the vacuum, we obtained the magnon group $\mathfrak{psu}(2|2)^{\oplus 2}$, under which excitations on top of the vacuum transform. Further, we introduced the oscillator picture. Finally, we considered correlators and the constraints from conformal symmetry, which fix two- and three-point functions.

In Sec. 2.2 we reviewed the spectrum problem and one-loop dilatation operator for the closed SU(2) subsector. After briefly introducing classical integrability, we turned to the SU(2) spin chain and saw how the spectrum problem can be equivalently solved by Bethe ansatz techniques. In Sec. 2.2.3 we discussed the construction of the S matrix from symmetry, which scatters the $\mathfrak{su}(2|2)^{\oplus 2}$ excitations. Further, in Sec. 2.2.4 we considered the generalisation of the Bethe ansatz to higher-rank models by means of the nested Bethe ansatz.

Finally, in Sec. 2.3, we turned to marginal deformations of $\mathcal{N}=4$ SYM, which preserve integrability. We focused in particular on the real β-deformation and worked out the corresponding deformed Bethe equations and S matrix for the SU(2) subsector.

Chapter 3.

The hexagon form factor for three-point functions

As discussed in the preceding chapter, methods from quantum integrable systems have played an essential role in the study of the spectrum problem. It is natural to wonder whether these tools can also be used for the calculation of correlation functions involving more than two operators. The introduction of the *hexagon form factors* [38] made three-point functions accessible through integrability. We will review the general idea and the formalism in Sec. 3.1, in order to introduce the tools for calculations. We refer the reader interested in more technical details of the construction to the original literature [38] or to Chapter 5 for the conceptionally similar construction of the hexagon form factor in $\mathrm{AdS}_3/\mathrm{CFT}_2$.

Further, we will consider the calculation of correlation functions involving operators from higher-rank sectors. Here we will use a hybrid formalism to import information from the nested Bethe ansatz into the hexagon-operator formalism. Equipped with these techniques, we give a variety of explicit examples for three-point functions at tree-level, involving operators of short length in the SU(3) and SU(1|2) sector, respectively.

In Sec. 3.3, we will also consider marginal deformations. Our aim is to extend the hexagon formalism to β-deformed $\mathcal{N} = 4$ SYM by introducing additional deformation factors in the evaluation. Though this seems not applicable in general, we will give a set of examples, for which we find agreement with field theory results.

Moreover, in Sec. 3.4 we will introduce the concept of double excitations. This allows us to consider excitations in the hexagon formalism, which are not in the magnon group. Finally, we will use the results from the preceding sections in Sec. 3.5 to construct and insert a Lagrangian into a correlation function evaluated with hexagons. This might offer an adittional way to incorporate loop corrections into the hexagon formalism.

3.1. Review of the hexagon form formalism

In this section we will review the hexagon form factor and its application. For details on the construction for $\mathcal{N} = 4$ SYM we refer the reader to the original literature [38].

The hexagon formalism introduced in [38] allows us to compute three-point functions by summing over a set of *hexagon form factors*. The idea is to cut a three-point function into two hexagonal patches and associate a form factor to those, *cf.* Fig. 3.1. The form factors can be fixed by the symmetry of the three-point function and the form factor axioms [38], *cf.* also [98] and references therein. Considering operators with physical excitations, these can end up on either hexagon after cutting. Hence, one has to sum over all possible partitions of the excitations. Since the operators can be viewed as

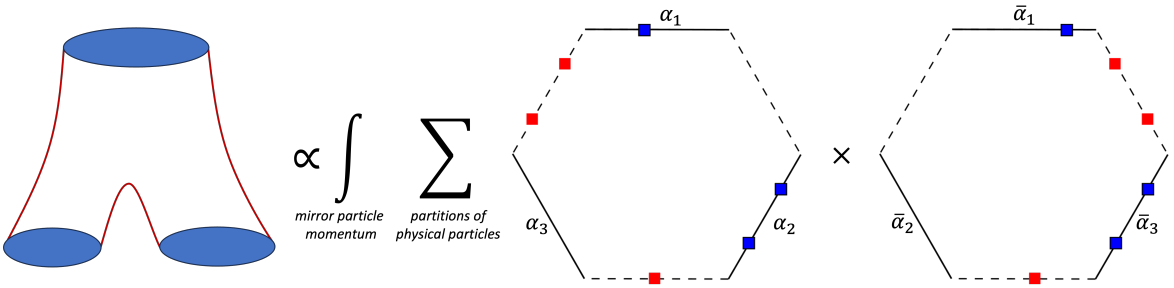

Figure 3.1.: A three-point function can be cut into two hexagonal patches. Since the magnons of the respective operators can end up on either hexagon (blue squares), their partitions need to be summed. To glue the hexagons back together a full set of virtual particles (red squares) needs to be inserted along the cuts.

spin chains carrying magnons, the cutting of these states is governed by the Bethe equations and leads to additional weight factors for the different partitions, *cf.* the discussion in Sec. 2.2.2.

Cutting three-point functions. Consider for instance a planar three-point function involving one non-BPS operators $\mathcal{B}$ and two BPS operators $\mathcal{O}$, given by $\langle \mathcal{B}_{L_1} \mathcal{O}_{L_2} \mathcal{O}_{L_3} \rangle$. By cutting the three-point function, the operator $\mathcal{B}$ of length L_1 is cut into two subchains of lengths $\ell_{12} = \frac{L_1+L_2-L_3}{2}$ and $\ell_{13} = \frac{L_1+L_3-L_2}{2}$. We denote ℓ_{12}, ℓ_{13} as *bridge lengths* as they correspond to the number of propagators between the operators $1, 2$ and $1, 3$ in a tree-level diagram, respectively. After cutting the operator $\mathcal{B}$ its excitations can end up either on the front hexagon, denoted by the set α or on the back hexagon denoted by $\bar{\alpha}$. With two magnons, there are four partitions that need to be summed up with an appropriate splitting factor $\omega(\alpha, \bar{\alpha}, \ell_{1j})$ given in eq. (2.55). We can then evaluate the thee-point function as

$$\langle \mathcal{B}_{L_1} \mathcal{O}_{L_2} \mathcal{O}_{L_3} \rangle = \sqrt{\frac{L_1 L_2 L_3}{\mathcal{G}\mathcal{A}(u_1, u_2)}} \sum_{\alpha \cup \bar{\alpha} = \{u_1, u_2\}} (-1)^{|\bar{\alpha}|} \, \omega(\alpha, \bar{\alpha}, \ell_{1j}) \, \langle \mathfrak{h} | \alpha \rangle \, \langle \mathfrak{h} | \bar{\alpha} \rangle \ . \tag{3.1}$$

The hexagon form factor $\langle \mathbf{h} | \alpha \rangle$ is given by a combination of the matrix elements from the Beisert S matrix [19] and the scalar factor h found in [38]. Further, all the expressions in eq. (3.1) depend on the rapidities of the magnons. As the operators can be viewed as spin chain eigenstates, the corresponding rapidities can be found by using the Bethe ansatz. The factor $\omega(\alpha, \bar{\alpha}, \ell_{1j})$ additionally depends on the bridge-length ℓ_{1j}, which counts the numbers of propagators between the operator $\mathcal{B}_1$ and the BPS operator $\mathcal{O}_j$, as well as on the partition $\{u_1, u_2\} = \alpha \cup \bar{\alpha}$.

Bootstrapping the hexagon. The form factor can be constructed from symmetry. The idea of the bootstrap is, that the three-point function should preserve as much (super)symmetry as possible. To achieve this, the *twisted translation* generator [38] is introduced

$$\mathcal{T} = -i \epsilon_{\alpha\dot{\alpha}} \, \mathfrak{P}^{\alpha\dot{\alpha}} + \epsilon_{a\dot{a}} \, \mathfrak{R}^{a\dot{a}} \, , \tag{3.2}$$

with the translation operator $\mathfrak{P}$ and the internal-space rotation $\mathfrak{R}$ from Sec. 2.1.3. This generator is then used to translate the operators in the generic configuration. It turns out, that the generators commuting with $\mathcal{T}$ form a diagonal $\mathfrak{psu}(2|2)_D$ subalgebra in $\mathfrak{psu}(2|2)^{\oplus 2}$. The hexagon form factor should preserve this diagonal subalgebra and indeed this constraint yields a unique solution for one- and two-particle form factors. Similar to the S matrix the hexagon is fixed up to a scalar phase $h(u_j, u_k)$. For instance, the non-vanishing one-particle form factors are given by

$$\langle \mathbf{h}|Y\rangle = -\langle \mathbf{h}|\bar{Y}\rangle = 1\,, \qquad \text{and} \qquad \langle \mathbf{h}|\mathcal{D}^{1\dot{2}}\rangle = -\langle \mathbf{h}|\mathcal{D}^{2\dot{1}}\rangle = i\,. \tag{3.3}$$

We will evaluate three-point functions with operators inserted along the line $(0,0,t,0)$ at the positions $t = 0, 1, \infty$. In order to do so, we construct the operators at $t = 0$ and then translate them with the help of the twisted-translation operator given in eq. (3.2). As $\mathcal{T}$ contains the lowering operators $\mathfrak{R}^1{}_{\dot{3}}$, $\mathfrak{R}^2{}_{\dot{4}}$ of the internal flavour symmetry $\mathfrak{su}(4)$, it acts on the field Z as [99]

$$\hat{Z}(t) = Z + t\,(Y - \bar{Y}) + t^2\,\bar{Z}\,, \tag{3.4}$$

mixing the spin-chain vacuum Z with the scalars $Y, \bar{Y}$. We will call $\hat{Z}(t)$ the *co-moving vacuum*. At the point $t = 1$ this creates an inhomogeneous superposition of operators, which ensures the matching between hexagon and free field theory results. For the transversal and longitudinal scalars, the twisted translation acts as

$$\begin{aligned} \hat{X}(t) &= X\,, & \hat{\bar{X}}(t) &= \bar{X} \\ \hat{Y}(t) &= Y + t\,\bar{Z}\,, & \hat{\bar{Y}}(t) &= \bar{Y} - t\,\bar{Z}\,. \end{aligned} \tag{3.5}$$

The resulting *effective* propagator for the co-moving vacuum is $\langle \hat{Z}(t_1)\hat{Z}(t_2)\rangle = 1$, and there exist non-vanishing off-diagonal propagators $\langle \hat{Z}(t_1)\hat{Y}(t_2)\rangle$, $\langle \hat{Z}(t_1)\hat{\bar{Y}}(t_2)\rangle$. Therefore, we will denote $\hat{Y}$ and $\hat{\bar{Y}}$ as *longitudinal* scalars, whereas we refer to $\hat{X}$ and $\hat{\bar{X}}$ as *transversal* since these cannot be contracted with $\hat{Z}$. The possibility to contract two operators with fermions is similarly provided by the twisted translation. It acts on the fermions in the magnon group $\Psi^{\dot{I}}$ and $\bar{\Psi}_I$ as

$$\begin{aligned} \hat{\Psi}^{\dot{3}}(t) &= \Psi^{\dot{3}} + t\,\Psi^1\,, & \hat{\bar{\Psi}}_1(t) &= \bar{\Psi}_1 - t\,\bar{\Psi}_{\dot{3}}\,, \\ \hat{\Psi}^{\dot{4}}(t) &= \Psi^{\dot{4}} + t\,\Psi^2\,, & \hat{\bar{\Psi}}_2(t) &= \bar{\Psi}_2 - t\,\bar{\Psi}_{\dot{4}}\,. \end{aligned} \tag{3.6}$$

It is worth noting, that the twisted translation mixes fermions which are in the magnon group with the ones which are not in the magnon group, *i.e.* Ψ^1, Ψ^2 and $\bar{\Psi}_{\dot{3}}, \bar{\Psi}_{\dot{4}}$. Hence the effective fermion propagators like $\langle \hat{\Psi}^4(t_1)\hat{\bar{\Psi}}_2(t_2)\rangle$ are proportional to $1/(t_1 - t_2)^2$, as is the bosonic propagator $\langle \hat{X}(t_1)\hat{\bar{X}}(t_2)\rangle$.

Evaluation of the hexagon form factor. We can evaluate the M-particle hexagon form factor by using the excitation picture from eq. (2.18) and write a generic excitation as $\Xi_p^{A\dot{A}} = \xi_p^A \otimes \dot{\xi}_p^{\dot{A}}$. The evaluation prescription is then given by

$$\begin{aligned} \big\langle \mathbf{h}\big|\Xi_{p_1}^{A_1\dot{A}_1}\Xi_{p_2}^{A_2\dot{A}_2}\ldots\Xi_{p_M}^{A_M\dot{A}_M}\big\rangle \equiv \\ \equiv (-1)^{F_{12\cdots M}}\,\mathbf{K}_{12\cdots M}\Big[\big|\xi_{p_M}^{A_N}\ldots\xi_{p_2}^{A_2}\xi_{p_1}^{A_1}\big\rangle \otimes \dot{\mathcal{S}}_{12\cdots M}\big|\dot{\xi}_{p_1}^{\dot{A}_1}\dot{\xi}_{p_1}^{\dot{A}_1}\ldots\dot{\xi}_{p_M}^{\dot{A}_M}\big\rangle\Big]\,. \end{aligned} \tag{3.7}$$

The sign above is given by

$$F_{12\cdots N} \equiv \sum_{1\leq i<j\leq M} (F_{A_i} + F_{\dot{A}_i}) F_{A_j} \,, \tag{3.8}$$

and stems from moving all the undotted fields to the very left and reordering them. We have $F_{A_j} = 0$ for A_j a boson and $F_{A_j} = 1$ for a fermion. The S matrix $\dot{\mathcal{S}}_{12\cdots M}$ acts on the M dotted fields. The multi-particle scattering factorises into a series of two-particle scattering processes and the Yang-Baxter equation allows to write the self-consistent ansatz from eq. (3.7). Finally, the M-particle contraction operator acts on the expression

$$\mathbf{K}_{12\cdots M} \equiv \mathbf{K}_{p_1} \mathbf{K}_{p_2} \cdots \mathbf{K}_{p_M} \,, \tag{3.9}$$

where the one-particle contraction operator is given by

$$\mathbf{K}_p = h_Y \frac{\partial}{\partial \phi_p^1} \frac{\partial}{\partial \dot{\phi}_p^{\dot{4}}} + h_{\bar{Y}} \frac{\partial}{\partial \phi_p^2} \frac{\partial}{\partial \dot{\phi}_p^{\dot{3}}} + h_{\mathcal{D}^{1\dot{2}}} \frac{\partial}{\partial \psi_p^1} \frac{\partial}{\partial \dot{\psi}_p^{\dot{2}}} + h_{\mathcal{D}^{2\dot{1}}} \frac{\partial}{\partial \psi_p^2} \frac{\partial}{\partial \dot{\psi}_p^{\dot{1}}} \,, \tag{3.10}$$

with the one-particle form factors $h_Y, h_{\bar{Y}}, h_{\mathcal{D}^{1\dot{2}}}, h_{\mathcal{D}^{2\dot{1}}}$ given in eq. (3.3). Note, that in the original work [38] a contraction rule was introduced to contract the left on the right chain. However, this leads to a potential ambiguity for the hexagon formalism in $\mathrm{AdS}_3/\mathrm{CFT}_2$, which will be explained below in Sec. 5. For convenience we will solely use the more general description using the contraction operator [1].

The prescription given in eq. (3.7) can be used when all the excitations are located on the same edge. Evaluating a generic hexagon this is not necessarily the case. A priori the excitations can be on any of the three physical edges of the hexagon. In order to evaluate the form factor, we need to move all the magnons to the same edge. This can be done by crossing transformations [38]. The idea here is to take an incoming particle with momentum p and energy E to an outgoing antiparticle with momentum $-p$ and energy $-E$. We will denote this as a 2γ transformation. The hexagon's scalar phase $h(u_j, u_k)$ is related to the dressing phase of the S matrix and therefore to the Beisert-Eden-Staudacher (BES) phase σ_{BES}. Since the BES phase has a non-trivial monodromy, the h-phase will also inherit it. Details on the parametrisation and the crossing equation for the scalar h-phase are given in Appendix A.

Higher-point functions and non-planar corrections. The hexagon form factor can also be used to calculate higher-point functions. In [45] it was used for the evaluation of planar four-point functions at tree-level involving one BMN operator. For the calculation one has to consider all the graphs arising from Wick contractions and tessellate them in all possible ways into hexagonal patches. For instance, a four-point function contains four hexagons. Finally, one has to sum over the tessellations and, like before, the partitions of excitations. Since different tessellations may correspond to the same diagram if one or several of the edge widths vanish, *i.e.* $\ell_{jk} = 0$, one has to be careful not to overcount. Further, in order to reproduce field theory results, the higher-point functions need to be dressed by space-time factors [41, 42].

Moreover, by studying four-point functions involving two BMN operators, it was found in [42] that the graphs need to be dressed by their corresponding $\mathrm{SU}(N)$ colour factors. This allows us also to include non-planar diagrams, as they contribute at higher order in the $1/N$-expansion in the large N limit. For instance, the $1/N$ correction to a

tree-level two-point function was considered in [42] by tessellating a torus diagram into eight hexagons.

Wrapping corrections. The hexagon formalism described so far reproduces the asymptotic part of a three-point function, *i.e.* it does not include finite size corrections. These can be accounted for by including virtual excitations living on the cut edges, also called *mirror edges* [38]. Summing over a full set of these virtual particles, the two hexagons are *glued* back into a three-point function. The evaluation of these processes is involved, as one has to sum over an infinite set of mirror bound states, evaluate the hexagon and integrate over the mirror rapidity. For more details on calculations of three-point functions including finite size corrections, we refer the reader to the literature [38, 39] and for four-point functions to [41, 42]. Further, in [43, 44] the one-loop correction to a five-point function of BPS operators was studied. Finally, also non-planar correlation functions of four BPS operators were considered in [46].

Fortunately, the finite size corrections are suppressed by the number of propagators. In general, for a bridge length ℓ they will start to contribute at order $g^{2\ell+2}$. Hence for sufficiently large bridge lengths, the asymptotic hexagon does not receive corrections. In this thesis we will restrict to hexagon calculations, where this is the case.

3.2. Higher-rank sectors

The power of the hexagon as a tool for calculations so far was mainly limited to *rank-one sectors*. Such sectors are the $\mathfrak{su}(2)$ containing bosonic excitations, *cf.* for instance refs. [38,42,45] as well as the $\mathfrak{su}(1|1)$ containing fermions, *cf.* ref. [100]. Further, there is the non-compact $\mathfrak{sl}(2)$ sector with Yang-Mills covariant derivatives, where the hexagon was also tested up to three loops, *cf.* refs. [38, 39] and four loops, *cf.* refs. [101–103].

In order to evaluate structure constants in higher-rank sectors, the nested hexagon approach was introduced in [104], where the hexagon operator is to some extent replaced by a wave function of the nested Bethe ansatz[1]. In the following we will take another approach, aiming to use the original hexagon construction, *i.e.* maintaining the matrix picture for the hexagon operator.

3.2.1. The hybrid formalism

In order to use the hexagon formalism for calculations in higher-rank sectors, we need to understand how to cut such states. For rank-one sectors the entangled state was given in eq. (2.56). In the following, let us consider an example in the SU(3) sector to obtain a similar cutting prescription, which we will denote as the *hybrid formalism*.

To cut a state as given in eq. (2.70), we will start with $|\Psi(X_1, Y_2)\rangle_L$ and $|\Psi(Y_1, X_2)\rangle_L$, for which we find

$$\begin{aligned} |\Psi(X_1,Y_2)\rangle_L = &|\Psi(X_1,Y_2)\rangle_{\ell_1}\ |\Psi(\{\})\rangle_{\ell_2} + e^{ip_2\ell_1}\,|\Psi(X_1)\rangle_{\ell_1}\ |\Psi(Y_2)\rangle_{\ell_2} + \\ &e^{ip_1\ell_1}\big[T_{12}\ |\Psi(Y_2)\rangle_{\ell_1}\ |\Psi(X_1)\rangle_{\ell_2} + R_{12}\ |\Psi(X_2)\rangle_{\ell_1}\ |\Psi(Y_1)\rangle_{\ell_2}\big] + \\ &e^{i(p_1+p_2)\ell_1}\ |\Psi(\{\})\rangle_{\ell_1}\ |\Psi(X_1,Y_2)\rangle_{\ell_2}\ , \end{aligned} \tag{3.11}$$

[1] See especially the presentation in appendix F of [104].

as well as

$$\begin{aligned}|\Psi(Y_1,X_2)\rangle_L = &|\Psi(Y_1,X_2)\rangle_{\ell_1}\ |\Psi(\{\})\rangle_{\ell_2} + e^{ip_2\ell_1}\,|\Psi(Y_1)\rangle_{\ell_1}\ |\Psi(X_2)\rangle_{\ell_2} + \\ &e^{ip_1\ell_1}\big[T_{12}\ |\Psi(X_2)\rangle_{\ell_1}\ |\Psi(Y_1)\rangle_{\ell_2} + R_{12}\ |\Psi(Y_2)\rangle_{\ell_1}\ |\Psi(X_1)\rangle_{\ell_2}\big] + \\ &e^{i(p_1+p_2)\ell_1}\ |\Psi(\{\})\rangle_{\ell_1}\ |\Psi(Y_1,X_2)\rangle_{\ell_2}\ ,\end{aligned} \tag{3.12}$$

where $L_1 = \ell_1 + \ell_2$ and T_{12}, R_{12} are the transmission and reflection amplitudes given in eq. (2.68). Equipped with this, we can consider the total wave function $g_{XY}\,|\Psi(X_1,Y_2)\rangle_L + g_{YX}\,|\Psi(Y_1,X_2)\rangle_L$ and find that the transmitted and reflected parts combine in a particular way. More precisely

$$\begin{aligned}|\Psi_{XY}(p_1,p_2)\rangle_L = \ldots + &e^{ip_1\ell_1}\ |\Psi(Y_2)\rangle_{\ell_1}\ |\Psi(X_1)\rangle_{\ell_2}\,[g_{XY}T_{12} + g_{YX}R_{12}] + \\ &e^{ip_1\ell_1}\ |\Psi(X_2)\rangle_{\ell_1}\ |\Psi(Y_1)\rangle_{\ell_2}\,[g_{XY}R_{12} + g_{YX}T_{12}] + \ldots\end{aligned} \tag{3.13}$$

Using the nested S matrix and the creation amplitude from eqs. (2.72) and (2.73), the expressions in the square brackets can be rewritten as

$$\begin{aligned}e^{ip_1\ell_1}\,[g_{XY}T_{12} + g_{YX}R_{12}] &= e^{ip_1\ell_1} f^{\mathrm{II,I}}(v,u_2)\mathcal{S}^{\mathrm{I,I}}(u_1,u_2)\,, \\ e^{ip_1\ell_1}\,[g_{XY}R_{12} + g_{YX}T_{12}] &= e^{ip_1\ell_1} f^{\mathrm{II,I}}(v,u_1)\mathcal{S}^{\mathrm{II,I}}(v,u_2)\mathcal{S}^{\mathrm{I,I}}(u_1,u_2)\,,\end{aligned} \tag{3.14}$$

which is the *splitting factor* we aimed to construct. Again, this has a nice interpretation, as the magnon with rapidity u_1 moves to the second chain, picking up the shift factor $e^{ip_1\ell}$ as well as the level-I S matrix $\mathcal{S}^{\mathrm{I,I}}(u_1,u_2)$. The first line in eq. (3.14) has the magnon Y created on top of u_2 on the first subchain and there is only the creation amplitude $f^{\mathrm{II,I}}(v,u_2)$. In the second line, the magnon is created on top of u_1, hence it needs to move over the subchain of length ℓ_1, thus adding $\mathcal{S}^{\mathrm{II,I}}(v,u_2)$ by overtaking u_2. Finally, there is the creation amplitude $f^{\mathrm{II,I}}(v,u_1)$.

In the following, when cutting higher-rank sector states in this work, we will construct the entangled state in the way described above to obtain the splitting factors. Sorting by inequivalent partitions, we can factor their total splitting amplitudes as in eq. (3.14) in order to minimise the number of terms. For instance, we find eight partitions when cutting a state with two magnons in the SU(3) sector. In comparison, we find four partitions for two-magnon SU(2) states. The added complexity of higher-rank sector states is put into the larger sets of partitions. In this way, we can maintain the operator structure of the hexagon. The hexagon acts on the set of magnons from the respective partition and is evaluated in terms of the momentum carrying rapidities $\{u\}$. The information about the nesting is hidden in the splitting factors, which additionally depend on the auxiliary rapidities $\{v\}$. Due to this use of information from the nested Bethe ansatz for the matrix picture we refer to it as hybrid formalism.

Let us close this discussion with a comment on the literature, where the components of the wave function are often regrouped and ordered by the flavours of the magnons appearing on the chain, *cf.* refs [22,23]. For instance, in our example we could attribute the transmission terms to the other wave functions, respectively. So the terms with T_{12} in eqs. (3.11) and (3.12) are viewed as belonging to the wave functions with the magnons ordered $\{YX\}$ and $\{XY\}$. However, in order to maintain a notion of the entangled state similar to the rank-one sectors we will not adapt this view here.

3.2.2. Correlators in the SU(3) sector

As a first test of our hybrid formalism introduced above, let us consider the calculation of correlators in the scalar SU(3) sector at tree-level. The sector is spanned by the vacuum field Z, the transversal excitation X and the longitudinal excitation Y. Similarly as before, we consider a vacuum built from the fields Z, on which M_1 excitations X and Y are placed. In the nested Bethe ansatz, the scalars X correspond to level-I excitations, and Y to level-II excitations whose number we denote by M_2.[2] We restrict to operators with two excitations, in particular we consider $M_1 = 2$ and $M_2 = 1$, which will be of the form

$$\mathcal{O}_A^L = \mathrm{tr}\Big(\hat{Z}^{L-2}X\hat{Y}\Big)\,, \qquad \mathcal{O}_{\tilde{A}}^L = \mathrm{tr}\Big(\hat{Z}^{L-2}\bar{X}\hat{\bar{Y}}\Big)\,, \qquad \mathcal{O}_{\check{A}}^L = \mathrm{tr}\Big(\hat{Z}^{L-2}\bar{X}\hat{Y}\Big)\,. \tag{3.15}$$

Together with the vacuum operator

$$\mathcal{O}_D^L = \mathrm{tr}\Big(\hat{Z}^L\Big)\,, \tag{3.16}$$

we study the structure constants $\mathcal{C}_{A,\tilde{A},D}^{L_1,L_2,L_3}$ and $\mathcal{C}_{A,\check{A},D}^{L_1,L_2,L_3}$, where the indices refer to the operators considered. For $L = 3, 4, 5$ the solutions to the Bethe equations are given in Tab. 2.3.

We now use the results from Sec. 3.2.1 to cut this state and obtain the splitting factors. Written out explicitly, we find the eight partitions

$$\begin{aligned}
|\Psi_{XY}(p_1,p_2)\rangle_L = &|\Psi(X_1,Y_2)\rangle_{\ell_1}|\Psi(\{\})\rangle_{\ell_2} - |\Psi(Y_1,X_2)\rangle_{\ell_1}|\Psi(\{\})\rangle_{\ell_2} + \\
&e^{ip_2\ell_1}\left(|\Psi(X_1)\rangle_{\ell_1}|\Psi(Y_2)\rangle_{\ell_2} - |\Psi(Y_1)\rangle_{\ell_1}|\Psi(X_2)\rangle_{\ell_2}\right) + \\
&e^{ip_1\ell_1}\left(R_{12}-T_{12}\right)\left(|\Psi(X_2)\rangle_{\ell_1}|\Psi(Y_1)\rangle_{\ell_2} - |\Psi(Y_2)\rangle_{\ell_1}|\Psi(X_1)\rangle_{\ell_2}\right) + \\
&e^{i(p_1+p_2)\ell_1}\left(|\Psi(\{\})\rangle_{\ell_1}|\Psi(X_1,Y_2)\rangle_{\ell_2} - |\Psi(\{\})\rangle_{\ell_1}|\Psi(X_1,Y_2)\rangle_{\ell_2}\right)\,.
\end{aligned} \tag{3.17}$$

Again, the normalisation of the states can be obtained by generalising the Gaudin norm $\mathcal{G}$ in eq. (2.53) to the *full Gaudin determinant* of the SU(3) sector, as defined in eq. (2.85).

We aim to calculate three-point functions involving two of the operators given in (3.15). Since the transversal excitations $X, \bar{X}$ are involved, it is clear, that only hexagons carrying these pairs will be non-vanishing. Moreover, since for coinciding rapidities particle creation poles appear, it is useful to start from a more symmetric partition of the magnons and move them over the same edge in order to factor out the poles. Putting the ingredients together, we reproduce the non-vanishing results obtained from field theory

$$\begin{aligned}
&\mathcal{C}_{A,\tilde{A},D}^{3,3,2} = -\sqrt{2}\,, && \mathcal{C}_{A,\check{A},D}^{4,3,3} = -\sqrt{3}\,, && \mathcal{C}_{A,\check{A},D}^{5\pm,3,2} = \sqrt{5\mp\sqrt{5}}\,, \\
&\mathcal{C}_{A,\tilde{A},D}^{5\pm,3,4} = -\sqrt{2\pm\frac{2}{\sqrt{5}}}\,, && \mathcal{C}_{A,\check{A},D}^{5\pm,4,3} = \sqrt{3\mp\frac{6}{\sqrt{5}}}\,, && \mathcal{C}_{A,\tilde{A},D}^{5\pm,4,3} = \mp\sqrt{3\pm\frac{6}{\sqrt{5}}}\,.
\end{aligned} \tag{3.18}$$

Further, we find a set of vanishing correlation functions, namely $\mathcal{C}_{A,\check{A},D}^{3,3,2}$, $\mathcal{C}_{A,\check{A},D}^{4,3,3}$, $\mathcal{C}_{A,\tilde{A},D}^{4,3,5}$,

[2] We could similarly use Y as level-I excitation with X as level-II excitation, as well as $\bar{Y}$ as level-I excitation and X as level-II excitation.

$\mathcal{C}^{4,3,5}_{A,\dot{A},D}$, $\mathcal{C}^{5\pm,3,2}_{A,\dot{A},D}$, $\mathcal{C}^{5\pm,3,4}_{A,\dot{A},D}$ as expected from field theory calculations.

3.2.3. Correlators in the SU(1|2) sector

Another higher-rank sector we would like to consider here is the SU(1|2) sector, which is also known as the *t-J model*. This model is well-studied in the solid-state literature, and is spanned by one type of bosonic and one type of fermionic excitations. For a comprehensive discussion of this model in the context of AdS/CFT we refer the reader to [22, 23]. This sector is a closed subsector, meaning that there is no mixing with other operators.

In fact, there are two SU(1|2) subsectors, depending on whether we excite the left or right nodes in the Dynkin diagram. For either sector the Bethe equations are given by

$$\begin{aligned} 1 &= \prod_{j=1}^{M_1} e^{ip_j}\,, \\ 1 &= e^{ip_j L} \prod_{\substack{k=1\\k\neq j}}^{M_1} \frac{u_j - u_k - i}{u_j - u_k + i} \prod_{l=1}^{M_2} \frac{u_j - v_l + \frac{i}{2}}{u_j - v_l - \frac{i}{2}}\,, \\ 1 &= \prod_{k=1}^{M_1} \frac{v_j - u_k + \frac{i}{2}}{v_j - u_k - \frac{i}{2}}\,. \end{aligned} \tag{3.19}$$

In this subsection, we will consider the magnon $X = \phi^2 \otimes \dot{\phi}^{\dot{4}}$ as the level-I excitation and the magnon $\Psi^{2\dot{4}} = \psi^2 \otimes \dot{\phi}^{\dot{4}}$ as the level-II excitation. We can now perform a similar construction as in Sec. 2.2.4, where the transmission and reflection amplitudes T_{12}, R_{12} are now given as

$$\mathcal{G}_{12} = \mathcal{L}_{12} = \frac{u_1 - u_2}{u_1 - u_2 + i}\,, \qquad \mathcal{H}_{12} = \mathcal{K}_{12} = \frac{-i}{u_1 - u_2 + i}\,, \tag{3.20}$$

with the elements $\mathcal{G}, \mathcal{H}, \mathcal{K}$ and $\mathcal{L}$ from the S matrix [19]. Thus we can use the Bethe rapidities from Tab. 2.3. Further, also the coefficients $g_{\Psi X}, g_{X\Psi}$ take a similar form as in the SU(3) sector and are given by

$$g_{\Psi X} = f^{\mathrm{II,I}}(v, u_1)\,, \qquad g_{X\Psi} = f^{\mathrm{II,I}}(v, u_2)\mathcal{S}^{\mathrm{II,I}}(v, u_1)\,, \tag{3.21}$$

with the nested S matrix from eq. (2.72).

We define the operators used here as

$$\mathcal{O}^L_B = \mathrm{tr}\Big(\hat{Z}^{L-2} X \hat{\Psi}^{1\dot{3}}\Big)\,, \qquad \mathcal{O}^L_{\bar{B}} = \mathrm{tr}\Big(\hat{Z}^{L-2} \bar{X} \hat{\Psi}^{2\dot{2}}\Big)\,. \tag{3.22}$$

The excitations on the second operator are chosen in such a way, that we can contract the hexagon.

In a similar vein to the SU(3) sector computations, we can avoid particle creation poles by starting from a more symmetric partition. For the set of correlators with

bridge length $\ell_{12}=2$ we find

$$\begin{aligned}
&\mathcal{C}^{3,3,2}_{B,\tilde{B},D}=-\sqrt{2}\,,\quad \mathcal{C}^{4,3,3}_{B,\tilde{B},D}=-\sqrt{3}\,, && \mathcal{C}^{5\pm,3,4}_{B,\check{B},D}=\sqrt{\frac{2}{5}(5\pm\sqrt{5})}\,,\\
&\mathcal{C}^{4,4,4}_{B,\tilde{B},D}=2\,, && \mathcal{C}^{5\pm,4,5}_{B,\check{B},D}=\sqrt{\frac{1}{5}(5\pm\sqrt{5})}\,,
\end{aligned} \tag{3.23}$$

whereas for bridge length $\ell_{12}=3$ the correlators evaluate to

$$\begin{aligned}
&\mathcal{C}^{5\pm,3,2}_{B,\tilde{B},D}=\sqrt{5\mp\sqrt{5}}\,,\quad \mathcal{C}^{4,4,2}_{B,\tilde{B},D}=2\sqrt{2}\,,\quad \mathcal{C}^{5\pm,4,3}_{B,\check{B},D}=\sqrt{\frac{6}{5}(5\pm\sqrt{5})}\,,\\
&\mathcal{C}^{5\pm,5\pm,4}_{B,\tilde{B},D}=3\pm\frac{1}{\sqrt{5}}\,,\quad \mathcal{C}^{5\pm,5\mp,4}_{B,\check{B},D}=\frac{2}{\sqrt{5}}\,.
\end{aligned} \tag{3.24}$$

Finally, for bridge length $\ell_{12}=4$, only correlators with $L_1=L_2=5$ are connected, resulting in

$$\mathcal{C}^{5\pm,5\pm,2}_{B,\tilde{B},D}=3\sqrt{2}\,,\qquad \mathcal{C}^{5\pm,5\mp,2}_{B,\tilde{B},D}=0\,. \tag{3.25}$$

3.3. Marginal deformations

In this section we aim to understand how a β-deformed hexagon approach could be achieved by simply dressing the hexagon amplitudes with deformation factors. We will begin by studying the SU(1|2) sector and will see that some conceptual difficulties arise regarding the co-moving vacuum $\hat{Z}$. Further, we will consider the simplest sectors in which the deformation occurs, namely the SU(2) sector with transversal excitations X, as well as the SU(2) sector with longitudinal excitations Y.

In the following we compute structure constants of operators with two magnons, taken from both the β-deformed transversal and longitudinal SU(2) sector. In particular, we study three-point functions in these sectors where two operators carry two excitations each, while the third is a vacuum operator $\mathcal{O}^L_D=\mathrm{Tr}(\hat{Z}^L)$. For the excited operators we define

$$\mathcal{O}^L_F=\mathrm{tr}\Big(\hat{Z}^{L-2}XX\Big)\,,\qquad \mathcal{O}^L_{\tilde{F}}=\mathrm{tr}\Big(\hat{Z}^{L-2}\bar{X}\bar{X}\Big)\,, \tag{3.26}$$

carrying the transversal excitations X, but also

$$\mathcal{O}^L_G=\mathrm{tr}\Big(\hat{Z}^{L-2}\hat{Y}\hat{Y}\Big)\,,\qquad \mathcal{O}^L_{\tilde{G}}=\mathrm{tr}\Big(\hat{Z}^{L-2}\hat{\bar{Y}}\hat{\bar{Y}}\Big)\,, \tag{3.27}$$

with the longitudinal magnons Y. We also study correlators involving excited operators which correspond to vacuum descendants in the undeformed theory, but acquire non-vanishing anomalous dimension in the deformed case and denote them as $\mathcal{O}'^L_D$. As vacuum descendants these operators can carry either type of excitation. Further, we do not only compute these correlators at tree-level, but also at one-loop order in the deformed hexagon approach and compare then to the respective field-theory results.

Though these results look promising, it is not possible to calculate β-deformed correlators in larger sectors, such as PSU(1, 1|2), of which we considered some examples in [2]. Thus, it would be desirable to obtain a more systematic understanding by constructing the hexagon form factor using a bootstrap approach in deformed theories. However, this is beyond the scope of this thesis.

3.3.1. Correlators in the SU(1|2) sector

By introducing deformation factors into the Bethe equations as in [97], we can obtain the β-deformed Bethe equations. Nonetheless, let us be more general here and introduce real deformation coefficients d_{jk} into the S matrices by defining

$$\tilde{\mathcal{S}}^{\mathrm{II,I}}(\tilde{v}_j, \tilde{u}_k) = e^{i\beta d_{21}} \mathcal{S}^{\mathrm{II,I}}(\tilde{v}_j, \tilde{u}_k)\,. \tag{3.28}$$

The $\mathcal{S}^{\mathrm{I,I}}(\tilde{u}_j, \tilde{u}_k)$ and $\mathcal{S}^{\mathrm{II,II}}(\tilde{v}_j, \tilde{v}_k)$ elements of the nested Bethe ansatz do not receive any additional deformation factors. This follows from the vanishing charge wedge $\mathbf{j}(A) \wedge \mathbf{j}(A)$ for identical flavours. Likewise, the creation amplitude remains unaltered. Further, all momentum factors e^{ip_j} are dressed by a deformation $e^{i\beta d_1}$. In the nesting picture, the entire combination becomes $\tilde{\mathcal{S}}^{\mathrm{I0}}(u_j) = e^{i\beta d_1 + ip_j}$, describing the shift of a level-I excitation over a vacuum site Z. Similarly, we introduce the additional factor

$$\tilde{\mathcal{S}}^{\mathrm{II,0}} = e^{i\beta d_2}\,, \tag{3.29}$$

for moving a level-II magnon over one vacuum site Z. The factor $\tilde{\mathcal{S}}^{\mathrm{II,0}}$ is trivial for the undeformed $\mathcal{N} = 4$ SYM theory.

With these considerations, we can introduce deformations into the Bethe equations from eq. (3.19) in a similar way as in [97]

$$\begin{aligned}
1 &= e^{i\beta(d_1 M_1 + d_2 M_2)} \prod_{j=1}^{M_1} e^{i\tilde{p}_j}\,, \\
1 &= e^{i\tilde{p}_j L}\, e^{i\beta(d_1 L - d_{21} M_2)} \prod_{k\neq j,\, k=1}^{M_1} \mathcal{S}^{\mathrm{I,I}}(\tilde{u}_j, \tilde{u}_k) \prod_{l=1}^{M_2} \frac{1}{\mathcal{S}^{\mathrm{II,I}}(\tilde{v}_l, \tilde{u}_j)}\,, \\
1 &= e^{i\beta(d_2 L + d_{21} M_1)} \prod_{k=1}^{M_1} \mathcal{S}^{\mathrm{II,I}}(\tilde{v}_j, \tilde{u}_k)\,.
\end{aligned} \tag{3.30}$$

We will match the coefficients d_1, d_2 and d_{21} against field theory results to relate them to the β-deformation.

By studying the Bethe states corresponding to operators in the SU(1|2) sector and their anomalous dimensions, we can fix the parameters d in our ansatz. For the left and right SU(1|2) sectors with vacuum Z we find

$$\begin{aligned}
\{X, \Psi^4\}: &\quad d_{12} = -2\beta\,, \quad d_1 = 2\beta\,, \quad d_2 = 0\,, \\
\{\bar{X}, \bar{\Psi}_2\}: &\quad d_{12} = 0\,, \quad d_1 = -2\beta\,, \quad d_2 = 2\beta\,.
\end{aligned} \tag{3.31}$$

We will perform the computation of structure constants in the deformed theory in a perturbative expansion in β. Expanding the Bethe equations up to $\mathcal{O}(\beta^6)$, one can determine $\tilde{u}_j, \tilde{v}_k$ up to the same order. Here we will exclude infinite rapidities for now. For the states in question, the Bethe roots receive corrections at $\mathcal{O}(\beta^1)$. Equipped with these solutions, let us turn to the evaluation of the form factor.

Hexagon calculation. We lack a construction from first principle for a hexagon form factor in the presence of marginal deformations. However, taking into consideration that the deformed spectrum problem can be obtained by dressing the various S matrices

in the nested Bethe ansatz with appropriate factors [97], it seems a natural guess to use a similar procedure for the hexagon amplitudes. A deformed state can be cut by dressing the splitting coefficients from eq. (3.21), *i.e.* deforming $\mathcal{S}^{\text{II,I}}$.

For a correlator of the form $\mathcal{C}_{B,\tilde{B},D}$ there are 16 different partitions of magnons, reading explicitly

$$\begin{aligned}
&\langle \mathbf{h}|\{\Psi\},\{\bar{\Psi}\},\{\}\rangle\,\langle \mathbf{h}|\{X\},\{\},\{\bar{X}\}\rangle\ , && \langle \mathbf{h}|\{\Psi\},\{\},\{\bar{\Psi}\}\rangle\,\langle \mathbf{h}|\{X\},\{\bar{X}\},\{\}\rangle\ ,\\
&\langle \mathbf{h}|\{\Psi,X\},\{\},\{\bar{\Psi},\bar{X}\}\rangle\ , && \langle \mathbf{h}|\{\Psi,X\},\{\},\{\bar{X},\bar{\Psi}\}\rangle\ ,\\
&\langle \mathbf{h}|\{\Psi,X\},\{\bar{\Psi},\bar{X}\},\{\}\rangle\ , && \langle \mathbf{h}|\{\Psi,X\},\{\bar{X},\bar{\Psi}\},\{\}\rangle\ ,\\
&\langle \mathbf{h}|\{X,\Psi\},\{\},\{\bar{\Psi},\bar{X}\}\rangle\ , && \langle \mathbf{h}|\{X,\Psi\},\{\},\{\bar{X},\bar{\Psi}\}\rangle\ ,\\
&\langle \mathbf{h}|\{X,\Psi\},\{\bar{\Psi},\bar{X}\},\{\}\rangle\ , && \langle \mathbf{h}|\{X,\Psi\},\{\bar{X},\bar{\Psi}\},\{\}\rangle\ .
\end{aligned} \tag{3.32}$$

Here we dropped the momenta, such that the first two cases would appear with four different permutations of the momenta, each. Further, we dropped the empty hexagon as $\langle \mathbf{h}|\{\}\rangle = 1$. We now decorate the ten products of form factors in eq. (3.32) by a global deformation factor $e^{i\beta r_j}$, with $j \in 1,\dots,10$ and $r_j \in \mathbb{R}$. As the deformation should be momentum independent, we can now try to fix the ten coefficients r_j. Nonetheless, we still need to take the global deformation factors of the splitting amplitudes into account.

Marginal deformations have the potential to destroy the usual twisted translation $\mathcal{T}$ from eq. (3.2), as $\mathcal{T}$ mixes operators with different R-charges. Hence, it is not clear how to proceed in the presence of the deformation. Since we consider transversal excitations, we can circumvent these issues to some extent by restricting to three-point functions with $\ell_{12} = 2$. In these cases there are no $\langle \hat{Z}(t=0)\hat{Z}(t=1)\rangle$ propagators and the only lines between these operators are the propagators connecting the two transversal excitations. The shifted vacua in the operators at points 1 and 2 are now contracted with the shifted vacuum $\mathcal{O}_D^{L_3}$ at point 3, whose length is therefore fixed to $L_3 = L_1 + L_2 - 4$. Further, the operator $\mathcal{O}_D^{L_3}$ becomes $\text{tr}\big(\bar{Z}^{L_3}\big)$ at $t = \infty$, thus projecting out only the Z of the twisted vacuum $\hat{Z}$ at point 2. Therefore we conclude, that the operator at point 2 is a conformal eigenoperator also in the deformed theory. We are obliged to trust the effective propagator for fermions, however this seems a mild assumption because the fermions are transversal excitations, *i.e.* they do not mix with the vacuum under the twisted translation.

We can also have particle-creation poles in the hexagon computation when we consider degenerate rapidities. In [105] the β-deformation was used to regulate degeneracies in a $1/N$-expansion in the large N limit. In the same spirit, here we will use the deformation parameter β as a regulator for the hexagon amplitudes. The particle-creation singularities of the hexagon amplitudes are seen as first and second order poles in β. Our strategy is to expand in β, demanding that:

- poles cancel,
- the undeformed amplitude is reproduced for $\beta \to 0$,
- the deformed hexagon computation reproduces free field theory results for the deformed Bethe states (up to rescalings of the operators).

The last condition leads to constraints on the parameters r_j. It will be useful to consider the cases with non-degenerate rapidities and degenerate rapidities separately.

All the constraints are homogeneous in the total power of r_j which increases with the order in β. Fortunately, even at higher orders it is still possible to single out linear constraints by factoring out linear combinations.

Using the β-deformed analogues of the correlators given in eqs. (3.23), (3.24) and (3.25), we can fix the parameters and find that certain hexagon form factors need to be dressed by additional deformation factors. Hexagons with two excitations on the 0γ edge receive a factor of $e^{12i\beta}$, while for two excitations on the 2γ edge the hexagon picks up the inverse dressing factor $e^{-12i\beta}$. Finally, for excitations on the 4γ edge there is no additional deformation factor. Further, we find a global phase $e^{-i\beta}$, which is unphysical as it can be removed by changing the normalisation.

Although, for $\ell_{12} = 2$ we can solve for the parameters r_j, we cannot obtain agreement between the hexagon computation and the free field theory allowing for edge-widths $\ell_{12} > 2$. We suspect the cause of this mismatch in propagators of the form $\langle \hat{Z}(t=0)\hat{Z}(t=1)\rangle$. It is worth stressing again, that we assumed no change in the definition of the twisted translation $\mathcal{T}$ in our analysis and used the $\mathcal{N} = 4$ hexagon amplitudes with global deformation factors introduced only.

3.3.2. Correlators in the SU(2) sector

In the following we compute structure constants of operators in the β-deformed SU(2) sector. Here, we can have transversal and longitudinal excitations, whereas in the examples above, we restricted to transversal excitations only. In particular, the three-point functions we consider have operators at $t = 0$ and $t = 1$ carrying two excitations each, while the operator at $t = \infty$ is a vacuum operator $\mathcal{O}_D^L = \mathrm{Tr}(\hat{Z}^L)$. To be able to Wick-contract, we need to insert the conjugate magnons on the second operator.

As mentioned earlier, in the undeformed theory the Bethe equations allow for so-called vacuum descendants, *i.e.* solutions to the Bethe equations with infinite rapidities. As the energy of such operators vanishes, they are still BPS even though they carry magnons on top of the vacuum. However, in the β-deformed theory infinite roots are no longer a solution due to the presence of the phase $e^{-i\beta L}$ in the deformed Bethe equations, *cf.* the discussion in Sec. 2.3.1. This deformation lifts the degeneracy of these operators with the vacuum and their roots become proportional to β^{-1} at leading order in a perturbative expansion in β. A set of examples with $L = 2, \ldots, 5$ is given in eq. (2.97). Taking the limit $\beta \to 0$ sends the rapidities back to infinity and the operators become protected again, *i.e.* their energies vanish. We will indicate these operators as $\mathcal{O}_D'^L$, due to their relation to the vacua.

Again, we restrict here to the calculation of three-point functions with $\ell_{12} = 2$. This is done in order to avoid propagators of the form $\langle \hat{Z}(t=0)\hat{Z}(t=1)\rangle$, as these might need to be altered for the deformed theory.

Tree-level results. Let us now use the hexagon form factor to compute three-point functions. Considering transversal excitations X first, we find that the correlators can be evaluated straightforwardly by using the shift factor $e^{i(\tilde{p}-2\beta)\ell_{12}}$ $(= e^{ip\ell_{12}})$ for the partitions. Independently of whether the twisted translated vacuum is used or not, the corresponding results from field theory calculations give the following results

Correlator	Tree-level structure constant
$\mathcal{C}^{4,2,2}_{G,D',D}$	$-\frac{2}{\sqrt{3}}+\frac{8}{9\sqrt{3}}\beta^2+\frac{112}{81\sqrt{3}}\beta^4+O(\beta^6)$
$\mathcal{C}^{4,3,3}_{G,D',D}$	$-1+\frac{4}{9}\beta^2+\frac{56}{81}\beta^4+O(\beta^6)$
$\mathcal{C}^{4,4,4}_{G,D',D}$	$-\frac{2\sqrt{2}}{3}+\frac{4\sqrt{2}}{27}\beta^2+\frac{28\sqrt{2}}{81}\beta^4+O(\beta^6)$
$\mathcal{C}^{4,5,5}_{G,D',D}$	$-\sqrt{\frac{5}{6}}-\frac{\sqrt{5}}{18\sqrt{6}}\beta^2+\frac{133\sqrt{5}}{648\sqrt{6}}\beta^4+O(\beta^6)$
$\mathcal{C}^{5,2,3}_{G,D',D}$	$-\sqrt{3}+\frac{\sqrt{3}}{2}\beta^2+\frac{23}{8\sqrt{3}}\beta^4+O(\beta^6)$
$\mathcal{C}^{5,3,4}_{G,D',D}$	$-\sqrt{2}+\frac{1}{\sqrt{2}}\beta^2+\frac{23}{12\sqrt{2}}\beta^4+O(\beta^6)$
$\mathcal{C}^{5,4,5}_{G,D',D}$	$-\sqrt{\frac{5}{3}}+\frac{5\sqrt{5}}{18\sqrt{3}}\beta^2+\frac{517\sqrt{5}}{648\sqrt{3}}\beta^4+O(\beta^6)$
$\mathcal{C}^{4,4,4}_{G,G,D}$	$\frac{2}{3}-\frac{16}{27}\beta^2-\frac{64}{81}\beta^4+O(\beta^6)$
$\mathcal{C}^{5,4,5}_{G,G,D}$	$\sqrt{\frac{5}{6}}-\frac{17}{18}\sqrt{\frac{5}{6}}\beta^2-\frac{925\sqrt{5}}{648\sqrt{6}}\beta^4+O(\beta^6)$
$\mathcal{C}^{3,3,2}_{D',D',D}$	$\sqrt{2}+O(\beta^6)$
$\mathcal{C}^{4,3,3}_{D',D',D}$	$\sqrt{2}+\frac{2\sqrt{2}}{9}\beta^2+\frac{22\sqrt{2}}{81}\beta^4+O(\beta^6)$
$\mathcal{C}^{4,4,4}_{D',D',D}$	$\frac{4}{3}+\frac{16}{27}\beta^2+\frac{64}{81}\beta^4+O(\beta^6)$
$\mathcal{C}^{5,4,5}_{D',D',D}$	$\sqrt{\frac{5}{3}}+\frac{13}{18}\sqrt{\frac{5}{3}}\beta^2+\frac{707}{648}\sqrt{\frac{5}{3}}\beta^4+O(\beta^6)$

In order to reproduce these results in the hexagon approach, we need to use the same Bethe equations for the operators at point 1 and 2. Therefore in the hexagon picture it seems like the operators at point 2 are conjugate with respect to operators at point 1, even though in the field theory they are being built on the same vacuum $\hat{Z}$. This seems not obvious and should be investigated in more detail in future work. Despite these conceptual difficulties, our prescription reproduces the correct results. Moreover, we can calculate three-point functions with longitudinal excitations, as well as at one-loop level, as elaborated in the following.

The normalisation of the three-point functions is given in analogy to the undeformed case in eq. (3.1). The exception is, that the rapidities entering in the Gaudin norm $\mathcal{G}$ and the S matrix depend on β now. For instance, the Gaudin norm corresponding to the operators $\mathcal{O}^4_G$ and $\mathcal{O}^5_G$ is given by

$$\begin{aligned}\mathcal{G}_4 &= 108-384\beta^2+\frac{1216}{3}\beta^4-\frac{7168}{45}\beta^6+O(\beta^7)\,,\\ \mathcal{G}_5 &= 80-440\beta^2+\frac{2000}{3}\beta^4-\frac{1586}{9}\beta^6+O(\beta^7)\,,\end{aligned} \tag{3.33}$$

respectively. The Gaudin norm for the descendant operators $\mathcal{O}'^L_D$ starts contributing at order $\mathcal{O}(\beta^4)$, while the hexagons involving a vacuum descendant start contributing at order $\mathcal{O}(\beta^2)$. The normalisation factor (3.1) contains a factor $1/\sqrt{\mathcal{G}}$ and thus the final result is of leading order $\mathcal{O}(1)$. This makes the calculation of correlators to a given order β^k harder, as one has to use the rapidities up to order β^{k+2}.

Considering longitudinal excitations Y, we need to introduce additional deformation factors $e^{2i\beta(d_\alpha-d_{\bar{\alpha}})}$. The parameters d_α depend on the partition α as well as the flavour and are necessary to find agreement with field theory. Then, the splitting factor becomes

$$\omega_l(\alpha,\bar{\alpha})=(-1)^{|\bar{\alpha}|}\prod_{\tilde{u}_i\in\bar{\alpha}}e^{2i\beta(d_\alpha-d_{\bar{\alpha}})}\left(\frac{u_i+\frac{i}{2}}{u_i-\frac{i}{2}}\right)^\ell e^{-2i\beta\ell}\prod_{u_1\in\bar{\alpha}\,,u_2\in\alpha}\frac{u_1-u_2-i}{u_1-u_2+i}\,. \tag{3.34}$$

We can calculate the structure constants with hexagons by using the usual evaluation formula

$$\mathcal{C}^{L_1,L_2,L_3}_{\mathcal{X},\mathcal{X},D} = \mathcal{N} \sum_{\substack{\alpha_1\cup\bar{\alpha}_1=\{u_1,u_2\}\\ \alpha_2\cup\bar{\alpha}_2=\{u_3,u_4\}}} \omega_{l_{12}}(\alpha_1,\bar{\alpha}_1)\omega_{l_{23}}(\alpha_2,\bar{\alpha}_2)\,\langle\mathfrak{h}|\alpha_1,\alpha_2,\{\}\rangle\,\langle\mathfrak{h}|\bar{\alpha}_1,\{\},\bar{\alpha}_2\rangle\ , \quad (3.35)$$

where $\mathcal{X}$ represents any operator from the table above in one of the SU(2) sectors. We find agreement with field theory when setting

$$d_{\{\}} = 0\,, \qquad d_{\{Y\}} = 1\,, \qquad d_{\{Y,Y\}} = 2\,, \qquad d_{\{\bar{Y}\}} = -1\ . \quad (3.36)$$

Further, we can easily include the transversal SU(2) sector by setting

$$d_{\{X\}} = -d_{\{\bar{X}\}}\ . \quad (3.37)$$

The resulting structure constants are the same as in the transversal case listed in the table above.

Asymptotic one-loop corrections. So far, we restricted the calculations to tree-level. Therefore, let us test the proposed formalism at one-loop order, *i.e.* at order g^2 in an expansion of the gauge coupling. There are two ingredients necessary for the hexagon computation, as there is the asymptotic hexagon as well as the contribution of virtual particles placed on the mirror-edges of the hexagon. In general, the contributions of virtual particles are suppressed by the bridge length ℓ and start at order $g^{2\ell+2}$. Thus, at one-loop order the virtual particles can only contribute if they are placed on an edge with width $\ell = 0$. In the weak coupling limit, we can use $x^{\pm}(\tilde{p}_j) = \frac{\tilde{u}_j \pm \frac{i}{2}}{g}$ to leading order in the coupling g. Solving the asymptotic Bethe equations at first loop order, we find one-loop corrections to the tree-level rapidities. For the operators considered above, they are of the form

Operator	One-loop corrections to rapidities $u_\pm$
$\mathcal{O}'^2_D$	$\mp 4i\beta \pm \frac{8i}{3}\beta^3 + O(\beta^5)$
$\mathcal{O}'^3_D$	$\left(2 \mp \frac{3i}{\sqrt{2}}\right)\beta - \left(-\frac{4}{3} \pm \frac{17i}{4\sqrt{2}}\right)\beta^3 + O(\beta^5)$
$\mathcal{O}^4_G$	$\pm\frac{4}{\sqrt{3}} - \frac{8}{3}\beta \mp \frac{16}{3\sqrt{3}}\beta^2 + \frac{64}{27}\beta^3 \pm \frac{64}{81\sqrt{3}}\beta^4 + O(\beta^5)$
$\mathcal{O}'^4_D$	$\frac{8}{9}\left(3 \mp i\sqrt{3}\right)\beta - \frac{64}{81}(3 \mp 2i\sqrt{3})\beta^3 + O(\beta^5)$
$\mathcal{O}^5_G$	$\pm\frac{5}{2} - \beta \mp \frac{15}{4}\beta^2 + \frac{5}{3}\beta^3 \pm \frac{15}{16}\beta^4 + O(\beta^5)$
$\mathcal{O}'^5_D$	$\left(3 \mp \frac{5i}{4}\right)\beta - \left(3 \mp \frac{245i}{96}\right)\beta^3 + O(\beta^5)$

Finally, we need to include the measure factors $\mu(u_k)$ given in [38] for the hexagon calculation. Using the splitting factor from eq. (3.34), we find the results for the one-loop corrections to structure constants as listed in the table below.

For the field-theory computation[3], the results of [106] and [107] for undeformed and β-deformed $\mathcal{N} = 4$ SYM theory were used. There, the one-loop corrections for structure constants of scalar operators are obtained from inserting a Hamiltonian into the respective three-point function. Using these methods, and comparing the hexagon results against the field-theory predictions, we find agreement.

[3]We thank Anne Spiering for providing the data to check against.

Correlator	One-loop corrections to structure constants
$\mathcal{C}^{4,3,3}_{G,D',D}$	$6-\frac{68}{9}\beta^2+O(\beta^4)$
$\mathcal{C}^{4,4,4}_{G,D',D}$	$4\sqrt{2}-\frac{56\sqrt{2}}{27}\beta^2+O(\beta^4)$
$\mathcal{C}^{4,5,5}_{G,D',D}$	$\sqrt{30}-\frac{1}{18}\sqrt{\frac{5}{6}}\beta^2+O(\beta^4)$
$\mathcal{C}^{5,3,4}_{G,D',D}$	$4\sqrt{2}-\frac{5}{\sqrt{2}}\beta^2+O(\beta^4)$
$\mathcal{C}^{5,4,5}_{G,D',D}$	$4\sqrt{\frac{5}{3}}+\frac{\sqrt{15}}{2}\beta^2+O(\beta^4)$
$\mathcal{C}^{4,4,4}_{G,G,D}$	$-8+\frac{512}{27}\beta^2+O(\beta^6)$
$\mathcal{C}^{5,4,5}_{G,G,D}$	$-10\sqrt{\frac{5}{6}}+\frac{137}{6}\sqrt{\frac{5}{6}}\beta^2+\frac{196}{81}\sqrt{\frac{5}{6}}\beta^4+O(\beta^6)$

As mentioned above, for structure constants involving operators $\mathcal{O}'_D$, we need to use rapidities to higher orders in β as their leading order is $\mathcal{O}(\beta^{-1})$. Since this is a more expensive computation, we only include correlators of the form $\mathcal{C}_{G,G,D}$ and $\mathcal{C}_{G,D',D}$, and leave $\mathcal{C}_{D',D',D}$ for future work. However, we do not expect any conceptual difference in the last case. Finally, we should mention, that we disregard the extremal correlation functions (with $L_1 = L_2 + L_3$) at one-loop order. Here the bridge length l_{23} vanishes and wrapping corrections contribute already at one-loop order. It would be interesting to understand how wrapping effects can be systematically included into the hexagon formalism for the β-deformed theory. As wrapping corrections also remain an obstacle in the undeformed case, we restrict the study presented here to asymptotic results.

3.4. Double excitations

At first glance some fields, such as for instance $\bar{Z}$, cannot be realised in the excitation picture. However, allowing for *double excitations*, *i.e.* the possibility of two magnons occupying the same spin chain site, those missing excitations can be realised. This can also be seen from the oscillator picture discussed in Sec. 2.1.3. Let us for instance take an excitation Y as well as a $\bar{Y}$, which can be obtained by acting with lowering operators on the physical vacuum $|Z\rangle$ as

$$|Y\rangle = \mathfrak{R}^1{}_2\,\mathfrak{R}^2{}_{\dot{3}}\,|Z\rangle = \mathbf{c}^{1\dagger}\mathbf{c}_{\dot{3}}\,|Z\rangle\ , \qquad \text{and} \qquad |\bar{Y}\rangle = \mathfrak{R}^{\dot{3}}{}_{\dot{4}}\,\mathfrak{R}^2{}_{\dot{3}}\,|Z\rangle = \mathbf{c}_{\dot{4}}\mathbf{c}^{2\dagger}\,|Z\rangle\ . \quad (3.38)$$

Next, when placing the two excitations at the same site, *i.e.* acting with the four corresponding $\mathfrak{R}$ generators on the same vacuum, we create the double excitation

$$|\,{}^{Y}_{\bar{Y}}\rangle = \mathfrak{R}^1{}_2\,\mathfrak{R}^2{}_{\dot{3}}\,\mathfrak{R}^{\dot{3}}{}_{\dot{4}}\,\mathfrak{R}^2{}_{\dot{3}}\,|Z\rangle = \mathbf{c}^{1\dagger}\mathbf{c}^{2\dagger}\,|0\rangle = |\bar{Z}\rangle\ , \quad (3.39)$$

which we indicate by stacking Y on top of $\bar{Y}$. A similar concept of double excitations was already introduced for the SU(2|2) S matrix in [19]. Introducing an additional creation amplitude, two level-II excitations ψ^1, ψ^2 of the SU(2|2) can be placed at the same site to create ϕ^2. In the following, we aim at building $\mathrm{SU}(2|2)^2$ double excitations and will see, that analogous creation amplitudes need to be introduced. As in the example above, we will combine a left level-II magnon Y and a right level-II magnon $\bar{Y}$ into a double excitation $\bar{Z}$. We will support this idea with the example of the Konishi singlet.

3.4.1. Creation amplitudes for double excitations

In the following we will denote the excitation Y as a *left* level-II excitation as it is obtained from generators in the left $\mathfrak{su}(2|2)$ subalgebra of the Dynkin diagram in Fig. 2.1. Similarly, we have the *right* level-II excitation $\bar{Y}$. In order to highlight this distinction in the nested Bethe ansatz, we will use dotted creation amplitudes for the right excitations, *i.e.* $\dot{f}^{\mathrm{II,I}}(w, u_1)$, and denote the corresponding auxiliary rapidity w. Further, we can build $\bar{X}$ by placing a left and a right level-II excitation on top of *one* level-I excitation. The double excitations we consider here are created, when placing two level-I excitation with rapidity u_1, u_2 at the same site.

Considering a state with a left excitation Y as well as a right excitation $\bar{Y}$, in the nested Bethe ansatz we thus have the two creation amplitudes $f^{\mathrm{II,I}}(v, u_1)\dot{f}^{\mathrm{II,I}}(w, u_2)$ for $|\dots Y \dots \bar{Y} \dots\rangle$. Next, we allow double excitations $\bar{Z}$ to form, by letting both Y and $\bar{Y}$ to occupy the same site. We will indicate this by placing the magnons on top of each other, *e.g.* $|\,{}^{Y}_{\bar{Y}}\rangle$ as in eq. (3.39) or $|\,{}^{\bar{Y}}_{Y}\rangle$ which also yields the double excitation $\bar{Z}$. Each of the auxiliary rapidities v, w sits now on top of the two primary rapidities u_1, u_2. Hence, the double excitation creation amplitude should contain the four corresponding creation amplitudes $f^{\mathrm{II,I}}(v, u_1)f^{\mathrm{II,I}}(v, u_2)\dot{f}^{\mathrm{II,I}}(w, u_1)\dot{f}^{\mathrm{II,I}}(w, u_2)$. However, when comparing with dilatation-operator eigenstates obtained by direct diagonalisation, we find a mismatch of the coefficients using the creation amplitude above. Matching on known eigenstates allows us to fix an additional polynomial factor, such that the double excitation creation amplitude for $\bar{Z}$ reads

$$\hat{f}(u_1, u_2, v, w) = f^{\mathrm{II,I}}(v, u_1)f^{\mathrm{II,I}}(v, u_2)\dot{f}^{\mathrm{II,I}}(w, u_1)\dot{f}^{\mathrm{II,I}}(w, u_2)\,(u_1 - u_2)(u_1 - u_2 - i)\,. \tag{3.40}$$

It is worth noting that $\hat{f}(u_1, u_2, v, w)$ is not symmetric under the exchange of u_1 and u_2. This implies that the level-I rapidities are implicitly ordered, even though they are sitting at the same site. The order is fixed by their initial ordering, when placed on the chain. In our notation this is indicated, as the magnon on top is shifted slightly to the right, *i.e.* $|\,{}^{Y}_{\bar{Y}}\rangle$.

Naturally we can ask, whether we can match the nested ansatz onto a matrix picture including double excitations. We will consider the example of a Konishi operator below and construct the double excitations by introducing extra creation amplitudes in the matrix picture. As the nested Bethe ansatz is supposed to diagonalise the *matrix picture* in which excitations of the four flavours $X, Y, \bar{Y}, \bar{X}$ scatter with the full S matrix, we include the double excitation $\bar{Z}$ and work out the corresponding creation amplitude by comparing with the nested result. In fact, it turns out that there is one universal creation amplitude valid for all types of double excitations, which is given by

$$\hat{e}(u_1, u_2) = -\frac{u_1 - u_2}{u_1 - u_2 - i}\,. \tag{3.41}$$

In the following subsection the derivation will be explicitly shown by way of example for the SO(6) Konishi singlet.

3.4.2. The Konishi singlet

Let us illustrate the concept described above by considering the explicit example of the Konishi singlet at length $L = 2$. Solving the SO(6) Bethe equations for $L = 2$ with two level-I as well as one left and one right level-II excitation we obtain a primary state with

rapidities $u_1 = -u_2 = \frac{1}{2\sqrt{3}}$, $v = w = 0$. It is worth stressing that the equivalence of the nested and matrix picture should take place off shell and without imposing cyclicity on the ket states. Therefore, let us for now keep L arbitrary in the construction and only specify it for the concrete example.

We begin by constructing the nested state as

$$
\begin{aligned}
&|\mathcal{K}^L(u_1,u_2)\rangle = \\
&\sum_{n_1<n_2} \Big(e^{i(p_1 n_1 + p_2 n_2)} f^{\mathrm{II,I}}(v,u_2)\; \dot{f}^{\mathrm{II,I}}(w,u_2)\, \mathcal{S}^{\mathrm{II,I}}(v,u_1)\, \dot{\mathcal{S}}^{\mathrm{II,I}}(w,u_1) && |X_1^{n_1}\bar{X}_2^{n_2}\rangle_L^{\mathrm{I}} \\
&\quad + e^{i(p_1 n_1 + p_2 n_2)} f^{\mathrm{II,I}}(v,u_1)\, \dot{f}^{\mathrm{II,I}}(w,u_1) && |\bar{X}_1^{n_1} X_2^{n_2}\rangle_L^{\mathrm{I}} \\
&\quad + e^{i(p_1 n_2 + p_2 n_1)} f^{\mathrm{II,I}}(v,u_1)\, \dot{f}^{\mathrm{II,I}}(w,u_1)\, \mathcal{S}^{\mathrm{II,I}}(v,u_2)\, \dot{\mathcal{S}}^{\mathrm{II,I}}(w,u_2) \mathcal{S}^{\mathrm{I,I}}(u_1,u_2) && |X_2^{n_1}\bar{X}_1^{n_2}\rangle_L^{\mathrm{I}} \\
&\quad + e^{i(p_1 n_2 + p_2 n_1)} f^{\mathrm{II,I}}(v,u_2)\, \dot{f}^{\mathrm{II,I}}(w,u_2) \mathcal{S}^{\mathrm{I,I}}(u_1,u_2) && |\bar{X}_2^{n_1} X_1^{n_2}\rangle_L^{\mathrm{I}} \\
&\quad + \text{ terms involving } Y \text{ and } \bar{Y} \;\Big) \\
&\quad + \sum_{n_1=n_2} e^{i(p_1+p_2)n_1}\, \hat{f}(u_1,u_2,v,w) && |\bar{Z}^{n_1}\rangle_L^{\mathrm{I}}\,,
\end{aligned}
\tag{3.42}
$$

where we omitted writing the terms involving Y and $\bar{Y}$ for readability. They can be easily added by using the appropriate creation amplitudes. Further, we introduced here the double excitation $\bar{Z}$, which is created with the creation amplitude $\hat{f}(u_1,u_2,v,w)$ from a pair of magnons sitting on top of each other, *i.e.* X and $\bar{X}$ or Y and $\bar{Y}$. By matching on know eigenstates found from the dilatation operator, we find $\hat{f}(u_1,u_2,v,w)$ to be of the form given in eq. (3.40).

Next, let us construct the same state in the matrix picture. Similarly to the higher-rank examples considered in Sec. 3.2 we have the coefficients $g_{X\bar{X}}$, $g_{\bar{X}X}$, $g_{Y\bar{Y}}$, $g_{\bar{Y}Y}$ for the four possible wave functions. These can be fixed as before by comparing the nested and matrix states without double excitations. In the case at hand, we obtain

$$
\begin{aligned}
g_{X\bar{X}} &= f^{\mathrm{II,I}}(v,u_2)\, \dot{f}^{\mathrm{II,I}}(w,u_2)\, \mathcal{S}^{\mathrm{II,I}}(v,u_1)\, \dot{\mathcal{S}}^{\mathrm{II,I}}(w,u_1)\,, \\
g_{\bar{X}X} &= f^{\mathrm{II,I}}(v,u_1)\, \dot{f}^{\mathrm{II,I}}(w,u_1)\,, \\
g_{Y\bar{Y}} &= f^{\mathrm{II,I}}(v,u_1)\, \dot{f}^{\mathrm{II,I}}(w,u_2)\, \dot{\mathcal{S}}^{\mathrm{II,I}}(w,u_1)\,, \\
g_{\bar{Y}Y} &= f^{\mathrm{II,I}}(v,u_2)\, \dot{f}^{\mathrm{II,I}}(w,u_1)\; \mathcal{S}^{\mathrm{II,I}}(v,u_1)\,.
\end{aligned}
\tag{3.43}
$$

Hence we can write the state in the matrix picture as

$$
\begin{aligned}
|\mathcal{K}^L(u_1,u_2)\rangle = g_{X\bar{X}} \Bigg[\sum_{n_1<n_2} \Bigg(& e^{i(p_1 n_1 + p_2 n_2)}\, |X_1^{n_1}\bar{X}_2^{n_2}\rangle_L + \\
& e^{i(p_2 n_1 + p_1 n_2)} \left[\frac{(T_{12})^2}{A_{12}}\, |\bar{X}_2^{n_1} X_1^{n_2}\rangle_L + \frac{(R_{12})^2}{A_{12}}\, |X_2^{n_1}\bar{X}_1^{n_2}\rangle_L \right] + \\
& e^{i(p_2 n_1 + p_1 n_2)} \left[\frac{R_{12}T_{12}}{A_{12}}\, |Y_2^{n_1}\bar{Y}_1^{n_2}\rangle_L + \frac{R_{12}T_{12}}{A_{12}}\, |\bar{Y}_2^{n_1} Y_1^{n_2}\rangle_L \right] \Bigg) + \\
& \sum_{n_1=n_2} e^{i(p_1+p_2)n_1}\; \hat{e}(u_1,u_2)\; |\bar{Z}^{n_1}\rangle_L \Bigg] \\
& + \text{corresponding terms for } g_{\bar{X}X}\,,\; g_{Y\bar{Y}} \text{ and } g_{\bar{Y}Y}\,,
\end{aligned}
\tag{3.44}
$$

where we have used the transmission and reflection amplitudes T_{12} and R_{12} from eq. (2.68). Again we only wrote a part of the full expression for readability. As for the nested case, we introduce the double excitation $\bar{Z}$ with an additional creation amplitude $\hat{e}(u_1, u_2)$. This additional term is equivalent to allowing the two magnons X, $\bar{X}$ to occupy the same site, *i.e.* $n_1 = n_2$, with a corresponding amplitude. Similarly, we have to allow such terms and their creation amplitudes for $\bar{X}, X$ as well as $Y, \bar{Y}$ and $\bar{X}, X$. Demanding the equivalence of the nested and the matrix picture state fixes the creation amplitude to be of the form given in eq. (3.41). In principle, we could have introduced distinguished amplitudes in the different terms. However, it turns out, that they are universal and hence

$$\hat{e}(u_1, u_2) \equiv e_{X\bar{X}} = e_{\bar{X}X} = e_{Y\bar{Y}} = e_{\bar{Y}Y} = -\frac{u_1 - u_2}{u_1 - u_2 - i}\,. \tag{3.45}$$

Coming to our example with $L = 2$, we can explicitly evaluate the nested and the matrix state. Normalising the state accordingly by using eq. (2.53), both descriptions yield the on-shell unit-norm Konishi singlet operator

$$\mathcal{K} = \frac{1}{\sqrt{3}}\,\mathrm{tr}\big(X\bar{X} + Y\bar{Y} + Z\bar{Z}\big)\,. \tag{3.46}$$

The matrix picture prefactors become all equal up to signs and read

$$g_{X\bar{X}} = g_{\bar{X}X} = -g_{Y\bar{Y}} = -g_{\bar{Y}Y} = \frac{(-1)^{1/3}}{4\sqrt{3}}\,. \tag{3.47}$$

Equipped with the operator let us briefly turn to the class of structure constants corresponding to three-point functions

$$\langle \mathcal{K}^{L_1}\,\mathcal{O}^{L_2}\,\mathcal{O}^{L_3}\rangle\ , \tag{3.48}$$

with the two vacua $\mathcal{O}^{L_2}$ and $\mathcal{O}^{L_3}$ of lengths L_2 and L_3. Here the Konishi operator $\mathcal{K}^{L_1}$ has the length L_1 with two level-I excitations and one left and one right level-II excitation, which generalises the $L_1 = 2$ discussion above. The operators $\mathcal{K}^{L_1}$ are the primary states of the multiplets containing the two-magnon BMN operators [13]. Their one-loop anomalous dimensions γ_1 are given as

$$p_1 = -p_2 = \frac{\pi\, n}{L_1 + 1}\,, \qquad \gamma_1 = 8\sin^2(p_1) = 6, 4, 5 \pm \sqrt{5}, \ldots \tag{3.49}$$

where the integer n labels the solutions with $0 < n < L_1 + 1$.

The remaining input needed for using the hexagon form factors for the calculation of the correlator (3.48), is the entangled state for the non-trivial operators $\mathcal{K}^{L_1}$. As in the examples considered in Sec. 3.2, we have four wave functions with initial magnon orderings $\{X_1\bar{X}_2\}, \{\bar{X}_1X_2\}, \{Y_1\bar{Y}_2\}, \{\bar{Y}_1Y_2\}$. Again, each of the wave functions is cut into two parts, the first of which has length $\ell_{12} = (L_1 + L_2 - L_3)/2$. For instance, the

first wave function can be cut as:

$$\begin{aligned}|\Psi(X_1,\bar{X}_2)\rangle_L = |\Psi(X_1,\bar{X}_2)\rangle_\ell\,|\Psi(\{\})\rangle_{\tilde{\ell}} - e^{ip_2\ell}\,|\Psi(X_1)\rangle_\ell\,|\Psi(\bar{X}_2)\rangle_{\tilde{\ell}} - \\ e^{ip_1\ell}\left[\frac{(T_{12})^2}{A_{12}}\,|\Psi(\bar{X}_2)\rangle_\ell\,|\Psi(X_1)\rangle_{\tilde{\ell}} + \frac{(R_{12})^2}{A_{12}}\,|\Psi(X_2)\rangle_\ell\,|\Psi(\bar{X}_1)\rangle_{\tilde{\ell}}\right] - \\ e^{ip_1\ell}\left[\frac{R_{12}T_{12}}{A_{12}}\,|\Psi(\bar{Y}_2)\rangle_\ell\,|\Psi(Y_1)\rangle_{\tilde{\ell}} + \frac{R_{12}T_{12}}{A_{12}}\,|\Psi(Y_2)\rangle_\ell\,|\Psi(\bar{Y}_1)\rangle_{\tilde{\ell}}\right] + \\ e^{i(p_1+p_2)\ell}\,|\Psi(\{\})\rangle_\ell\,|\Psi(X_1,\bar{X}_2)\rangle_{\tilde{\ell}} + \mathcal{O}(g)\,.\end{aligned} \tag{3.50}$$

Here we have introduced the shorthand notation $\ell = \ell_{12}$ and $\tilde{\ell} = L_1 - \ell_{12}$. Also it can be checked explicitly here, that eq. (3.50) is an identity. It is worth emphasising, that these wave functions implicitly include the ket states with the double excitation $\bar{Z}$. So when cutting the state, we need not to take care of those, as they are hidden in the (sub)states.

Like in the SU(3) examples from Sec. 3.2.2, the $\mathcal{C}(u_1,u_2)$ element of the S matrix [19] can scatter two bosons into two fermions, whenever such a process is allowed by the quantum numbers of the state. However, as this would introduce terms depending on the coupling constant, we can omit these processes by restricting to the leading order, indicating possible corrections by $\mathcal{O}(g)$. Moreover, since the SO(6) sector is not closed, the analysis presented here must be limited to tree-level results. In principle, it should be possible to recover the $\mathcal{K}^{L_1}$ states from the higher-loop nested Bethe ansatz of [22, 23], though at the cost of much higher excitation numbers. If we managed to extract the g-coefficients of the matrix ansatz and the level-I rapidities from there, our approach might also allow to reproduce loop effects, both in the spectrum problem and for structure constants. Further sources of a dependence on the coupling would be the introduction of Zhukowsky variables $x^\pm$ [22, 23] replacing the rapidities as well as the BES phase [21], the loop corrections introduced into the rapidities upon solving the nested Bethe equations, and finally gluing corrections [38].

Returning to the correlator from eq. (3.48) at tree-level and taking the normalisation into account, we expect the relation

$$\mathcal{A}_{\text{QFT}} = \left(u^2+\frac{1}{4}\right) L_1\sqrt{L_2L_3}\;\mathcal{A}_{\mathbf{h}}\,, \tag{3.51}$$

between the field theory amplitude $\mathcal{A}_{\text{QFT}}$ and hexagon amplitude $\mathcal{A}_{\mathbf{h}}$. Apart from the momentum carrying rapidities u, the hexagon amplitudes only depend on the quantum number ℓ_{12}. The amplitude for $\ell_{12}=0$ manifestly vanishes, while for $\ell_{12}=1$ we have

$$\mathcal{A}_{\mathbf{h}}^{\ell_{12}=1}(-u,u) = \frac{8\,g_{X\bar{X}}\,u}{(u-\frac{i}{2})(u+\frac{i}{2})^2}\,, \tag{3.52}$$

for the $L_1=2,3$ and the two $L_1=4$ operators this evaluates to

$$L_1=2\,:\,\mathcal{A}_{\mathbf{h}}^{\ell_{12}=1}=\frac{\sqrt{3}}{2}\,,\qquad L_1=3\,:\,\mathcal{A}_{\mathbf{h}}^{\ell_{12}=1}=\frac{\sqrt{2}}{3}\,,\qquad L_1=4\,:\,\mathcal{A}_{\mathbf{h}}^{\ell_{12}=1}=\frac{1}{4}\,. \tag{3.53}$$

A field theory check is very easy in this case, as we simply put the unit-norm $\mathcal{K}^{L_1}$ operator into a three-point function with two unit-norm vacua $\text{tr}\big(Z^{L_2}\big)/\sqrt{L_2}$ and $\text{tr}\big(\bar{Z}^{L_3}\big)/\sqrt{L_3}$. Placing the operators at the points $0,1,\infty$, we can perform the Wick

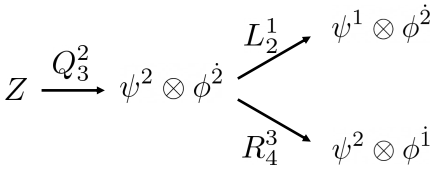

Figure 3.2.: We can generate the fermions needed for the double excitations of the Lagrangian, by acting with the simple roots as in the diagram.

contractions. Restricting to the planar limit, we find

$$\mathcal{A}_{\text{QFT}} \;=\; c_{\bar{Z}}(L_1)\;\sqrt{L_2 L_3} \tag{3.54}$$

for the existing correlators. Here $c_{\bar{Z}}(L_1)$ is the coefficient of the $\text{tr}\big(\bar{Z}Z^{L_1-1}\big)$ term in the operator $\mathcal{K}^{L_1}$. The numbers obtained from eq. (3.54) immediately satisfy eq. (3.51) reproducing the values listed in eq. (3.53).

Beyond $\ell_{12} = 0, 1$, for every Bethe solution the hexagon computations are $\ell_{12} \to L_1 - \ell_{12}$ symmetric. Moreover, these can also be reproduced from Wick contractions, by using the twisted vacua $\hat{Z}$ from eq. (3.4) at points 2 and 3, where the operator at point 2 is placed at the position t along the x_2 axis [38].

3.5. Lagrangian insertion method

The Lagrangian insertion method proved to be a powerful technique for field-theory computations in $\mathcal{N} = 4$ SYM theory [68, 69]. Differentiating a corrleator with respect to the coupling constant inserts an additional Lagrange operator into an n-point function, which has to be integrated. At least for higher-point functions of half-BPS operators, this trick gives a convenient way of constructing higher-loop integrands without the necessity of drawing the Feynman graphs involved [108, 109]. In the hexagon formalism, this may allow to avoid or at least simplify the evaluation of gluing contributions [41, 43, 44]. Further, we may hope that if successful, this procedure can be used to compute non-planar corrections to the spectrum by inserting the Lagrange operator into a two-point function on a tessellation of a torus or possibly higher-genus diagram [42, 46, 47].

The Lagrangian of $\mathcal{N} = 4$ super Yang-Mills theory has the full supersymmetry only on shell, *i.e.* when the equations of motion are satisfied. In the following we will use an on-shell Lagrangian in the form of the chiral Yang-Mills Lagrangian with two higher-order admixtures [110]. These admixtures are given by a Yukawa term at linear order in the coupling constant, and the quartic scalar superpotential at $\mathcal{O}(g^2)$, which ensure that the Lagrangian is protected. In the integrability description [22, 23] admixtures are usually not mentioned as their effects are captured by loop corrections to the rapidities of a given solution of the asymptotic Bethe equations and the dependence of the Zhukowsky variables on the coupling constant.

3.5.1. The on-shell Lagrangian

The $\mathcal{N} = 4$ SYM Lagrangian is given in eq. (2.3). However, for the Lagrangian insertion it is customary to use the on-shell and chiral form. It is obtained from eq. (2.3) by

using the equations of motion and dropping total derivative terms. The result can be found in [110] and reads

$$\mathcal{L} \,=\, \mathrm{tr}\left(-\frac{1}{2}\mathcal{F}_{\alpha\beta}\mathcal{F}^{\alpha\beta} + \sqrt{2}g_{\mathrm{YM}}\,\Psi^{\alpha I}[\Phi_{IJ},\Psi^{J}_{\alpha}] - \frac{1}{8}g^{2}_{\mathrm{YM}}\,[\Phi^{IJ},\Phi^{KL}][\Phi_{IJ},\Phi_{KL}]\right)\,. \tag{3.55}$$

Note that the on-shell Lagrangian involves only the chiral field strength $\mathcal{F}^{\alpha\beta}$. In the integrability picture the admixtures should be captured by the solution of the mixing problem corresponding to the leading-order eigenstate $\mathrm{tr}\big(\mathcal{F}_{\alpha\beta}\mathcal{F}^{\alpha\beta}\big)$. In the following we will construct this highly-excited state and perform a simple but non-trivial test of the proposal with a protected correlation function.

As discussed above, the excitation picture excludes certain fields such as $\bar{Z}$, but also half of the fermionic excitations, namely $\Psi^{1\alpha}, \Psi^{2\alpha}, \bar{\Psi}^{\dot{\alpha}}_{3}, \bar{\Psi}^{\dot{\alpha}}_{4}$, as well as the chiral and antichiral field strengths $\mathcal{F}^{\alpha\beta}, \bar{\mathcal{F}}^{\dot{\alpha}\dot{\beta}}$. However, using the double excitations from above we can realise these types of excitations. As we now aim to recover the Yang-Mills term

$$|\mathcal{F}^{11}\mathcal{F}^{22}\rangle - 2\,|\mathcal{F}^{12}\mathcal{F}^{12}\rangle + |\mathcal{F}^{22}\mathcal{F}^{11}\rangle\,, \tag{3.56}$$

we choose the nested Bethe ansatz corresponding to the diagram in Fig. 3.2. Allowing the double excitations in the same spirit as for $\bar{Z}$, we find, that we can combine two fermions as

$$\begin{aligned}
|\,{}^{\Psi^{1\dot{4}}}_{\Psi^{2\dot{3}}}\rangle &= \mathfrak{L}^{1}{}_{2}\;\mathfrak{Q}^{2}_{\;\dot{3}}\;\mathfrak{R}^{\dot{3}}_{\;\dot{4}}\;\mathfrak{Q}^{2}_{\;\dot{3}}\,|Z\rangle &&= \mathbf{a}^{1\dagger}\mathbf{a}^{2\dagger} = |\mathcal{F}^{12}\rangle\,,\\
|\,{}^{\Psi^{1\dot{4}}}_{\Psi^{1\dot{3}}}\rangle &= \mathfrak{L}^{1}{}_{2}\;\mathfrak{Q}^{2}_{\;\dot{3}}\;\mathfrak{L}^{1}{}_{2}\;\mathfrak{R}^{\dot{3}}_{\;\dot{4}}\;\mathfrak{Q}^{2}_{\;\dot{3}}\,|Z\rangle &&= \mathbf{a}^{1\dagger}\mathbf{a}^{1\dagger} = |\mathcal{F}^{11}\rangle\,,\\
|\,{}^{\Psi^{2\dot{4}}}_{\Psi^{2\dot{3}}}\rangle &= \mathfrak{Q}^{2}_{\;\dot{3}}\;\mathfrak{R}^{\dot{3}}_{\;\dot{4}}\;\mathfrak{Q}^{2}_{\;\dot{3}}\,|Z\rangle &&= \mathbf{a}^{2\dagger}\mathbf{a}^{2\dagger} = |\mathcal{F}^{22}\rangle\,.
\end{aligned} \tag{3.57}$$

The lowering operator $\mathfrak{Q}^{2}_{\;\dot{3}}$ creates the level-I excitation $\Psi^{2\dot{4}}$ from the vacuum Z. The level-I rapidity u moves over the chain as before. However, the S matrix scattering two level-I excitations is given by $\mathcal{S}^{\mathrm{I,I}}(u_1,u_2) = -1$ here, since we consider fermions on the spin chain. We can now create a left or right excitation by acting with $\mathfrak{L}^{1}{}_{2}$ or $\mathfrak{R}^{\dot{3}}_{\;\dot{4}}$, respectively, introducing the corresponding auxiliary rapidities v and w. The Bethe equations are given by

$$\begin{aligned}
1 &= \prod_{j=1}^{M} e^{ip_j}\,,\\
1 &= e^{ip_j}\prod_{\substack{k=1\\k\neq j}}^{M}\mathcal{S}^{\mathrm{I,I}}(u_j,u_k)\prod_{l=1}^{M_L}\mathcal{S}^{\mathrm{I,II}}(u_j,v_l)\prod_{m=1}^{M_R}\dot{\mathcal{S}}^{\mathrm{I,II}}(u_j,w_m)\,,\\
1 &= \prod_{l=1}^{M}\mathcal{S}^{\mathrm{II,I}}(v_j,u_l)\prod_{m=1}^{M_L}\mathcal{S}^{\mathrm{II,II}}(v_j,v_m)\,,\\
1 &= \prod_{l=1}^{M}\dot{\mathcal{S}}^{\mathrm{II,I}}(w_j,u_l)\prod_{m=1}^{M_R}\dot{\mathcal{S}}^{\mathrm{II,II}}(w_j,w_m)\,,
\end{aligned} \tag{3.58}$$

where M is the number of primary roots and M_L, M_R are the numbers of left and right

auxiliary roots, respectively. For the S matrices we have

$$\begin{aligned}\mathcal{S}^{\mathrm{I,II}}(u,y) &= \frac{1}{\dot{\mathcal{S}}^{\mathrm{I,II}}(u,y)} = \frac{y-u+\frac{i}{2}}{y-u-\frac{i}{2}}\,,\\ \mathcal{S}^{\mathrm{II,II}}(y_1,y_2) &= \frac{1}{\dot{\mathcal{S}}^{\mathrm{II,II}}(y_1,y_2)} = \frac{y_1-y_2+i}{y_1-y_2-i}\,,\end{aligned} \tag{3.59}$$

as well as $\mathcal{S}^{\mathrm{II,I}}(y,u) = 1/\mathcal{S}^{\mathrm{I,II}}(u,y)$ and similar for $\dot{\mathcal{S}}^{\mathrm{II,I}}$. It turns out, that the creation amplitudes needed in the nested ansatz take a somewhat different form from the ones in the Konishi example. However, in the matrix picture the creation amplitude is given by the universal $\hat{e}(u_1,u_2)$ from eq. (3.41), sometimes picking up an additional minus sign. Again, explicit examples can be constructed for short lengths $L = 4,5,6$ and compared to eigenstates obtained from the dilatation operator. We spare the technical details here, since we will not need the explicit amplitudes and states in the hexagon computations, as we observed in the preceding section.

Let us come back to the leading-order eigenstate $\mathrm{tr}\big(\mathcal{F}_{\alpha\beta}\mathcal{F}^{\alpha\beta}\big)$. This should be given as an $L = 2$ state and according to eq. (3.57) carry excitations $M = 4$, $M_L = 2$, $M_R = 2$. Moreover, the Lagrangian is a vacuum descendant and hence all the rapidities are infinite. In Sec. 3.3 we introduced twist to regularise the rapidities of vacuum descendants. Similarly, we can introduce twist factors with coefficients $d_0,\ldots,d_3$ in the Bethe equations (3.58). Analogously we will denote the twist as β here, though it should be stressed that it is *not* related to the β-deformation. For the momentum carrying rapidities we find

$$u_1 = \frac{1+i}{\sqrt{2}\beta}\,,\qquad u_2 = \frac{1-i}{\sqrt{2}\beta}\,,\qquad u_3 = -\frac{1+i}{\sqrt{2}\beta}\,,\qquad u_4 = -\frac{1-i}{\sqrt{2}\beta}\,. \tag{3.60}$$

Further, for the auxiliary roots we have

$$v_1 = -v_2 = -\frac{1}{\sqrt[4]{3}\beta}\,,\qquad w_1 = \bar{w}_2 = -\frac{\sqrt{2}+i}{\sqrt[4]{3}\beta}\,, \tag{3.61}$$

and finally there is the constraint $d_3 = -2d_1 = 2\sqrt{2\sqrt{3}}$. As in Sec. 3.3, there will be non-trivial corrections to the rapidities in the odd powers of β only. Expanding the Bethe state incorporating double excitations, using the solution above and normalising appropriately, we obtain the pure Yang-Mills Lagrangian from eq. (3.56).

3.5.2. A simple test of the Lagrangian insertion method

We can absorb a factor of the Yang-Mills coupling g_{YM} into all fields in the $\mathcal{N} = 4$ super Yang-Mills Lagrangian (3.55). The path integral from eq. (2.19) for an n-point function of gauge-invariant composite operators can then be written as

$$\langle\, \mathcal{O}_1 \ldots \mathcal{O}_n \,\rangle = \int D\xi\; e^{\frac{i}{g_{\mathrm{YM}}^2}\int d^4x_0 \mathcal{L}(x_0)}\; \mathcal{O}_1 \ldots \mathcal{O}_n\,. \tag{3.62}$$

Taking the derivative with respect to the coupling yields

$$\frac{\partial}{\partial g_{\mathrm{YM}}^2}\langle\, \mathcal{O}_1 \ldots \mathcal{O}_n \,\rangle = -\frac{i}{g_{\mathrm{YM}}^4}\int d^4x_0\; \langle\, \mathcal{L}(x_0)\; \mathcal{O}_1 \ldots \mathcal{O}_n \,\rangle\;. \tag{3.63}$$

Remarkably, this implies that the one-loop correction to an n-point function can be computed from the Born level of an $(n+1)$-point function in which a Lagrange operator is inserted and integrated over. The right-hand side is indeed a tree-level contribution. This is a consequence of the field rescaling that causes a factor g_{YM}^2 on each propagator. The rescaling can be undone without affecting the functional relation between the two correlation functions.

Since two-point functions of BPS operators are protected [68, 69], we must have

$$\langle\, \mathcal{L}_0\, \mathcal{O}_1^L\, \mathcal{O}_2^L \,\rangle = 0 \tag{3.64}$$

for two spin-chain vacua $\mathcal{O}^L$. In the following we will use this identity as a non-trivial test of our approach.

In the hexagon computation we have to cut the Lagrange operator into two parts. The Bethe state we consider carries the four magnons $\{\Psi^{4\dot{2}}, \Psi^{4\dot{1}}, \Psi^{3\dot{2}}, \Psi^{3\dot{1}}\}$. Apart from the momentum shift $e^{ip\ell}$ that every magnon picks up moving from the first to the second hexagon, the form of the entangled state is independent of the length ℓ. Moreover, as we already saw in Sec. 3.4.2, there is no reference to double excitations as the local structure is hidden inside the cut wave function. We can thus think of a higher length spin chain with four elementary excitations moving on it. Nevertheless, the scattering between the magnons is quite involved, as the $\mathcal{F}_{12}$ and $\mathcal{C}_{12}$ elements of the S matrix can transform a pair of bosons into a pair of fermions and vice versa. As there are no magnons from the two other operators in the three-point function, we only have to partition the four particles over the two hexagons.

Further, the operator $\mathrm{tr}\big(\mathcal{F}_{\alpha\beta}\mathcal{F}^{\alpha\beta}\big)$ is chiral, hence in the excitation picture we have four fermions ψ^α on the left $\mathfrak{su}(2|2)$ chain and four bosons $\dot{\phi}^{\dot{a}}$ on the right $\mathfrak{su}(2|2)$ chain. Recall that the one-particle hexagon form factors are only non-vanishing for $Y, \bar{Y}$ and $\mathcal{D}^{1\dot{2}}, \mathcal{D}^{2\dot{1}}$ as stated in eq. (3.3). Therefore, any non-vanishing contribution to the three-point function in eq. (3.64) must involve at least two $\mathcal{C}(u_j, u_k)$ or $\mathcal{F}(u_j, u_k)$ processes and is thus of order g^2. If fewer of these arise when scattering magnons during the construction of the entangled state, then the missing $\mathcal{C}$ and $\mathcal{F}$ elements must be contributed in the evaluation of the hexagon form factor. We can thus restrict the computation to leading order in the coupling g and the twist β in *all* terms. The effect simplifies the entangled state considerably as the only contributing partitions are

$$\begin{aligned}
\langle \mathcal{L}_0\, \mathcal{O}_1^L\, \mathcal{O}_2^L \rangle = 2\, \Big[&\langle \mathbf{h}| \Psi_1^{2\dot{4}}\, \Psi_2^{2\dot{3}}\, \Psi_3^{1\dot{4}}\, \Psi_4^{1\dot{3}} \rangle + \langle \mathbf{h}| \Psi_1^{2\dot{4}}\, \Psi_4^{1\dot{3}} \rangle\, \langle \mathbf{h}| \Psi_2^{2\dot{3}}\, \Psi_3^{1\dot{4}} \rangle \Big] + \\
\tilde{g}\, \Big[&\langle \mathbf{h}| D_1^{2\dot{1}} \rangle\, \langle \mathbf{h}| \Psi_2^{2\dot{3}}\, \Psi_3^{1\dot{4}}\, D_4^{1\dot{2}} \rangle + \langle \mathbf{h}| D_2^{2\dot{1}} \rangle\, \langle \mathbf{h}| \Psi_1^{2\dot{4}}\, D_3^{1\dot{2}}\, \Psi_4^{1\dot{3}} \rangle + \\
&\langle \mathbf{h}| D_3^{1\dot{2}} \rangle\, \langle \mathbf{h}| \Psi_1^{2\dot{4}}\, D_2^{2\dot{1}}\, \Psi_4^{1\dot{3}} \rangle + \langle \mathbf{h}| D_4^{1\dot{2}} \rangle\, \langle \mathbf{h}| D_1^{2\dot{1}}\, \Psi_2^{2\dot{3}}\, \Psi_3^{1\dot{4}} \rangle + \\
&\langle \mathbf{h}| Y_1 \rangle\, \langle \mathbf{h}| \Psi_2^{2\dot{3}}\, \Psi_3^{1\dot{4}}\, \bar{Y}_4 \rangle + \langle \mathbf{h}| \bar{Y}_2 \rangle\, \langle \mathbf{h}| \Psi_1^{2\dot{4}}\, Y_3\, \Psi_4^{1\dot{3}} \rangle \; + \\
&\langle \mathbf{h}| Y_3 \rangle\; \langle \mathbf{h}| \Psi_1^{2\dot{4}}\, \bar{Y}_2\, \Psi_4^{1\dot{3}} \rangle + \langle \mathbf{h}| \bar{Y}_4 \rangle\, \langle \mathbf{h}| Y_1\, \Psi_2^{2\dot{3}}\, \Psi_3^{1\dot{4}} \rangle \Big] + \\
\tilde{g}^2 \Big[&\langle \mathbf{h}| D_1^{2\dot{1}}\, D_2^{2\dot{1}} \rangle\, \langle \mathbf{h}| D_3^{1\dot{2}}\, D_4^{1\dot{2}} \rangle + \langle \mathbf{h}| D_1^{2\dot{1}}\, \bar{Y}_2 \rangle\, \langle \mathbf{h}| Y_3\, D_4^{1\dot{2}} \rangle + \\
&\langle \mathbf{h}| Y_1\, D_2^{2\dot{1}} \rangle\, \langle \mathbf{h}| D_3^{1\dot{2}}\, \bar{Y}_4 \rangle + \langle \mathbf{h}| Y_1\, \bar{Y}_2 \rangle\, \langle \mathbf{h}| Y_3\, \bar{Y}_4 \rangle \Big] \\
+ \;&\text{permutations of the initial state}\,.
\end{aligned} \tag{3.65}$$

The effective coupling $\tilde{g} = 2\sqrt{2}g\,i\,\beta^2$ arises from the $\mathcal{C}_{12}$ and $\mathcal{F}_{12}$ elements. Inserting the hexagon amplitudes, the expressions in square brackets become

$$\langle\, \mathcal{L}_0\, \mathcal{O}_1^L\, \mathcal{O}_2^L \,\rangle \to 4\,\tilde{g}^2\,(1-2+1) = 0 \tag{3.66}$$

as desired. Curiously, the sign of the individual parts does not flip according to the signature of the permutation when we choose a different initial flavour ordering of the magnons. This already implies that their sum must vanish. Moreover, in eq. (3.65) we also need to sum over the 23 remaining initial orderings of the four fermions and their respective entangled states. The overall order g^2 signals a one-loop computation as expected. The normalisation can be chosen in the usual way. The non-normalised wave function has an overall coefficient $g_{\Psi^{2\dot{4}}\Psi^{2\dot{3}}\Psi^{1\dot{4}}\Psi^{1\dot{3}}} \sim \beta^4$. This will be offset by the root of the full Gaudin determinant when normalising the hexagon amplitude. Alternatively, we can normalise the nested Bethe state to 1, for which we have $g_{\Psi^{2\dot{4}}\Psi^{2\dot{3}}\Psi^{1\dot{4}}\Psi^{1\dot{3}}} = 1/\sqrt{24}$ and therefore the computation stays at $\mathcal{O}(\beta^4)$ as in eq. (3.66). The Korepin factor is given by $\sqrt{\prod(u_i^2+1/4)} \sim 1/\beta^4$ and hence the final result will be of order $\mathcal{O}(\beta^0)$ in accordance with eq. (3.51).

Finally, we evaluated the hexagons in the spin-chain frame, which requires carrying along Z markers [19, 38]. On the other hand, when constructing the entangled state we neglected the appearance of Z markers. This can be justified, as in the case at hand all momentum factors $e^{ip\ell}$ become 1 in the limit $\beta \to 0$. In fact, the edge width as a quantum number in the entangled state drops out. However, considering magnons with non-zero momenta the consequences of length changing will become a subtle issue in the evaluation due to the appearance of Z markers on the spin chain. Nonetheless, this is a first simple but non-trivial check that the Lagrangian insertion might be used in the hexagon formalism.

It would be interesting to study the insertion of $\mathrm{tr}\big(\mathcal{F}_{\alpha\beta}\mathcal{F}^{\alpha\beta}\big)$ into a two-point function of scalar two-excitation BMN operators [13] in order to further test our proposal. However, length-changing effects need to be taken into account, as they introduce shift factors for excitations with non-vanishing momenta.

3.6. Chapter summary

In this chapter we used the hexagon form factor to calculate three-point functions in $\mathcal{N} = 4$ SYM using methods from integrability. In Sec. 3.1 we reviewed the original proposal [38] to cut the correlators into hexagonal patches. Using symmetry constraints, the one- and two-particle form factor can be bootstrapped and generalised to multi-particle states, by using factorised scattering and the Yang-Baxter equation.

In Sec. 3.2 we extended the formalism to higher-rank sectors. In order to obtain this we used a hybrid formalism to extract wave function coefficients g_Ψ from the nested Bethe ansatz. We then used these coefficients to import information on the state into the hexagon calculation, allowing us to preserve the operator structure of the formalism. Further, we gave a set of explicit examples for tree-level correlators in the SU(3) and SU(1|2) sectors, respectively.

In Sec. 3.3 we asked, whether the hexagon formalism can also be amended to calculate correlators in less supersymmetric theories. In particular, we considered β-deformed $\mathcal{N} = 4$ SYM. Interestingly, in the sectors considered, the hexagons of the undeformed theory can be used by simply dressing them with a deformation factor. It is also

necessary to introduce deformation factors in the splitting amplitudes as required by the Bethe equations. Finally, for the evaluation of the form factor the solutions of the deformed Bethe equations are used. Further, we calculated asymptotic one-loop corrections, finding agreement with field theory results. However, this strategy is not compatible with other higher-rank sectors. For instance for the $\mathfrak{psu}(1,1|2)$ sector, it is not possible to evaluate β-deformed correlators introducing global twist factors [2]. In general, it would be interesting to study whether a hexagon can also be bootstrapped for the deformed model.

In addition, we introduced the concept of double excitations in Sec. 3.4. This allowed us to describe excitations, which are not in the magnon group, like for instance $\bar{Z}$. These double excitations come with respective creation amplitudes in the nested and in the matrix picture. In an illustrative example for the Konishi singlet, *cf.* Sec. 3.4.2, we constructed the amplitudes and states explicitly. Moreover, the matrix picture creation amplitude turns out to be general for any kind of double excitation.

Using the results for deformations and double excitations, we constructed the Yang-Mills part $\mathrm{tr}\big(\mathcal{F}_{\alpha\beta}\mathcal{F}^{\alpha\beta}\big)$ of the Lagrange operator as a vacuum descendant in Sec. 3.5. It can be obtained by creating double excitations from fermions. The exact form of the state is not needed in hexagon computations, as its local structure is hidden in the wave function even after cutting the entangled state. We then proposed to use the Lagrangian insertion method to calculate loop corrections to correlation functions by means of the hexagon form factor. This technique has already been proven to be powerful in field-theory computations, *cf.* refs [68, 69]. Finally, we tested our proposal for the simplest possible set-up $\langle \mathcal{L}\mathcal{O}\mathcal{O}\rangle$, *i.e.* a three-point function of two BPS operators $\mathcal{O}$ and the Lagrangian $\mathcal{L}$. As expected, the one-loop correction to the protected two-point function vanishes. However, this provided a first non-trivial check, as different contributions arise in the hexagon evaluation at g^2, which only cancel in the end.

Part II.

Integrability in AdS_3

Chapter 4.

Review of integrability in $\mathrm{AdS}_3 \times \mathrm{S}^3 \times \mathrm{T}^4$

Remarkably, the integrable structures arising in $\mathrm{AdS}_3 \times \mathrm{S}^3 \times \mathrm{T}^4$ are very similar to those in $\mathrm{AdS}_5 \times \mathrm{S}^5$. In the following we will review and highlight certain aspects, that will be important in this part of the thesis. We will consider a type IIB superstring theory on $\mathrm{AdS}_3 \times \mathrm{S}^3 \times \mathrm{T}^4$ background, which is classically integrable [55, 56] and believed to be so as well at quantum level.

One of the main differences to AdS_5 is, that in the case at hand the background can be supported by Ramond-Ramond (RR) and Neveu-Schwarz-Neveu-Schwarz (NSNS) fluxes [59]. The amount of RR flux is measured by $h > 0$ and the NSNS flux by $k \in \mathbb{N}_0$ in units of the radius of AdS_3, respectively. Note that the NSNS flux is quantised. We can distinguish the following three different regimes in the corresponding two-paramter space.

Mixed flux. In this general regime we have $h > 0$ and $k > 0$. Its integrability properties, such as factorised scattering, were studied in refs [57–59]. Further, the dual CFT_2 is not known.

Pure RR. In this case we have $k = 0$ and $h > 0$. When there is no NSNS flux, the background is most similar to case of $\mathrm{AdS}_5 \times \mathrm{S}^5$. Hence, this analogy offered a starting point to study its integrability, see ref. [10] for a review. Also in this case the dual CFT_2 is unknown.

Pure NSNS. This case is obtained for $h = 0$ and $k > 0$. Only for pure NSNS flux a simple worldsheet CFT description exists, which is given by a supersymmetric $\mathfrak{sl}(2, \mathbb{R})$ Wess-Zumino-Witten model at level k [49–51]. For $k = 1$ the dual CFT_2 is given by the symmetric product orbifold of N copies of T^4, namely $\mathrm{Sym}^N(\mathrm{T}^4)$ [52–54].

4.1. Light-cone gauge fixing of the bosonic string

Let us start by motivating how the isometries of the $\mathrm{AdS}_3 \times \mathrm{S}^3 \times \mathrm{T}^4$ superstring theory are broken by the light-cone gauge-fixing procedure. Here we will consider the simpler example of a bosonic non-linear sigma model (NLSM), which will be sufficient to convey the concepts involved. For more details we refer the reader to the review [10].

The NLSM describing the bosonic part of closed strings reads

$$S = -\frac{h}{2}\int_{-\ell/2}^{\ell/2} \mathrm{d}\sigma\ \mathrm{d}\tau\ \sqrt{|\gamma|}\gamma^{\alpha\beta}\ \partial_\alpha X^\mu\ \partial_\beta X^\nu\ G_{\mu\nu}(X)\,, \tag{4.1}$$

where ℓ is the string length and X^μ are the target space coordinates. Further, the worldsheet and target space metrics are given as $\gamma^{\alpha\beta}$ and $G_{\mu\nu}(X)$, respectively. The conjugate momenta are then given through

$$p_\mu = \frac{\delta S}{\delta(\partial_\tau X^\mu)} = -h\ \gamma^{\tau\beta}\ \partial_\beta X^\nu\ G_{\mu\nu}(X)\,. \tag{4.2}$$

Specialising to the background $\mathrm{AdS}_3 \times \mathrm{S}^3 \times \mathrm{T}^4$, we can pick the time-coordinate t in AdS_3 and an angle ϕ parametrising one of the big circles of S^3 and introduce the target space light-cone coordinates

$$X^+ = \frac{\phi + t}{2}\,, \qquad X^- = \phi - t\,. \tag{4.3}$$

The remaining coordinates are transverse coordinates $X^1, \ldots, X^8$. Translations along t and rotations in ϕ are isometries with corresponding conserved Noether charges

$$\mathbf{H}^{\text{t.s.}} = -\int_{-\ell/2}^{\ell/2} \mathrm{d}\sigma\ p_t\,, \qquad \mathbf{J} = +\int_{-\ell/2}^{\ell/2} \mathrm{d}\sigma\ p_\phi\,, \tag{4.4}$$

where p_t and p_ϕ are conjugate momenta. The conserved charges are the target space energy $\mathbf{H}^{\text{t.s.}}$ and the angular momentum $\mathbf{J}$. In terms of the target space light-cone momenta, the conserved charges are given as

$$\int_{-\ell/2}^{\ell/2} \mathrm{d}\sigma\ p_+ = \mathbf{J} - \mathbf{H}^{\text{t.s.}}\,, \qquad \int_{-\ell/2}^{\ell/2} \mathrm{d}\sigma\ p_- = \frac{\mathbf{J} + \mathbf{H}^{\text{t.s.}}}{2}\,. \tag{4.5}$$

The NSLM action is invariant under Weyl rescalings and diffeomorphisms. However, these redundancies need to be removed by choosing a specific gauge in order to study the physical degrees of freedom. For a more detailed discussion of gauge-fixing in the context of AdS/CFT we refer the reader to [10, 111]. The uniform light-cone gauge is then obtained by fixing

$$X^+ = \tau\,, \qquad p_- = 1\,. \tag{4.6}$$

From the second condition we find

$$\frac{\mathbf{J} + \mathbf{H}^{\text{t.s.}}}{2} = \int_{-\ell/2}^{\ell/2} \mathrm{d}\sigma\ p_- = \ell\,. \tag{4.7}$$

Hence, the worldsheet size ℓ is fixed by the charges of the state after gauge fixing, *i.e.* the energy $\mathbf{H}^{\text{t.s.}}$ and the angular momentum $\mathbf{J}$ of the state.

Further, the gauge fixing conditions imply that the worldsheet light-cone Hamiltonian is related to the target-space energy and angular momentum through

$$\mathbf{H}^{\text{l.c.}} = \mathbf{H}^{\text{t.s.}} - \mathbf{J}\,. \tag{4.8}$$

Diagonalising the light-cone Hamiltonian $\mathbf{H}^{\text{l.c.}}$ yields the spectrum of the theory.

After fixing the light-cone gauge, not all the charges generated by the isometries will be conserved. In fact, all the conserved charges must commute with the worldsheet Hamiltonian $\mathbf{H}^{\text{l.c.}}$. We will study the symmetry in more detail in the following section.

4.2. The Superalgebra

The superisometries of the $\text{AdS}_3 \times \text{S}^3 \times \text{T}^4$ metric are given by *two* copies of the superalgebra $\mathfrak{psu}(1,1|2)$. We will use the notation

$$\mathfrak{psu}(1,1|2)_L \oplus \mathfrak{psu}(1,1|2)_R\,, \tag{4.9}$$

where we denote the copies as *left* and *right* as indicated by the subscripts. Each of these superalgebras contains bosonic subalgebras given by a non-compact $\mathfrak{su}(1,1)$ and a compact $\mathfrak{su}(2)$ algebra. These subalgebras can be thought of as the isometries from AdS_3 and S^3. Further, there are eight fermionic supercharges for each of the two copies.

Considering $\mathfrak{psu}(1,1|2)_L$, let us denote the three $\mathfrak{su}(1,1)$ generators by $\mathbf{L}_m$ with $m = \pm, 0$, as well as the three $\mathfrak{su}(2)$ (R-symmetry) generators $\mathbf{J}_\alpha$ with $\alpha = \pm, 3$. Additionally, we have eight supercharges $\mathbf{Q}_{m\alpha a}$, where the indices can take values $\alpha = \pm, a = \pm, m = \pm$. Of course, the right copy $\mathfrak{psu}(1,1|2)_R$ contains similar generators, which we will indicate by tilde, *i.e.* $\widetilde{\mathbf{L}}_m, \widetilde{\mathbf{J}}_\alpha, \widetilde{\mathbf{Q}}_{m\alpha a}$. Further, the supercharges carry the index $a = \pm$ and transform in the fundamental representation of an $\mathfrak{su}(2)_\bullet$ automorphism. In fact, this automorphism is a subalgebra of $\mathfrak{so}(4)_{\mathbf{T}^4}$ and can be seen geometrically [60].

Using the raising and lowering operators, the commutation relations of the algebra $\mathfrak{psu}(1,1|2)$ are given by

$$\begin{aligned}
&[\mathbf{L}_0, \mathbf{L}_\pm] = \pm\mathbf{L}_\pm\,, && [\mathbf{L}_+, \mathbf{L}_-] = 2\mathbf{L}_0\,,\\
&[\mathbf{J}_3, \mathbf{J}_\pm] = \pm\mathbf{J}_\pm\,, && [\mathbf{J}_+, \mathbf{J}_-] = 2\mathbf{J}_3\,,\\
&[\mathbf{L}_0, \mathbf{Q}_{\pm\alpha A}] = \pm\frac{1}{2}\mathbf{Q}_{\pm\alpha A}\,, && [\mathbf{L}_\pm, \mathbf{Q}_{\mp\alpha A}] = \mathbf{Q}_{\pm\alpha A}\,,\\
&[\mathbf{J}_3, \mathbf{Q}_{a\pm A}] = \pm\frac{1}{2}\mathbf{Q}_{a\pm A}\,, && [\mathbf{J}_\pm, \mathbf{Q}_{a\mp A}] = \mathbf{Q}_{a\pm A}\,,\\
&\{\mathbf{Q}_{\pm+A}, \mathbf{Q}_{\pm+B}\} = \pm\epsilon_{AB}\mathbf{L}_\pm\,, && \{\mathbf{Q}_{+\pm A}, \mathbf{Q}_{-\pm B}\} = \mp\epsilon_{AB}\mathbf{J}_\pm\,,
\end{aligned} \tag{4.10}$$

and finally

$$\{\mathbf{Q}_{+\pm A}, \mathbf{Q}_{-\mp B}\} = \epsilon_{AB}\big(-\mathbf{L}_0 \pm \mathbf{J}_3\big)\,. \tag{4.11}$$

For later convenience, it is also useful to construct a matrix realisation in terms of 4×4 supermatrices

$$\mathcal{M} = \left(\begin{array}{c|c} m & \theta \\ \hline \eta & n \end{array}\right), \tag{4.12}$$

where the 2×2 blocks m, n have bosonic grading, while θ, η are fermionic. Using the hermiticity condition

$$\mathcal{M}^\dagger + H^{-1}\mathcal{M}H = 0\,, \qquad \text{with} \qquad H = H^{-1} = \text{diag}(1,-1,1,1)\,, \tag{4.13}$$

leads to the subalgebra $\mathfrak{u}(1,1|2)$. Imposing the vanishing of the supertrace

$$\mathrm{str}\mathcal{M} \equiv \mathrm{tr}\, m - \mathrm{tr}\, n = 0\,, \tag{4.14}$$

defines the matrix algebra $\mathfrak{su}(1,1|2)$. This algebra also contains the central element $\mathbb{1} = \mathrm{diag}(1,1,1,1)$. To obtain $\mathfrak{psu}(1,1|2)$ one would have to form the quotient of $\mathfrak{su}(1,1|2)$ over the $\mathfrak{u}(1)$-factor. However, $\mathfrak{psu}(1,1|2)$ has no matrix realisation. This can be seen by imposing $\mathrm{tr}\,\mathcal{M} = 0$, which removes $\mathbb{1}$. For a generic fermionic element $\mathcal{M}_f$ of $\mathfrak{su}(1,1|2)$, which automatically satisfies $\mathrm{tr}\,\mathcal{M}_f = 0$, we find

$$\mathrm{tr}(\{\mathcal{M}_f, \mathcal{M}_f\}) = -2\,\mathrm{tr}\Big(\mathcal{M}_f H^{-1} \mathcal{M}_f^\dagger H\Big) < 0\,, \tag{4.15}$$

where we used the hermiticity condition (4.13).

The following explicit $\mathfrak{su}(1,1|2)$ matrix realisation for the complexified algebra will be useful later on

$$\mathbf{L}_0 = \frac{1}{2}\left(\begin{array}{cc|cc} -1 & 0 & 0 & 0 \\ 0 & 1 & 0 & 0 \\ \hline 0 & 0 & 0 & 0 \\ 0 & 0 & 0 & 0 \end{array}\right), \quad \mathbf{L}_+ = \left(\begin{array}{cc|cc} 0 & 0 & 0 & 0 \\ 1 & 0 & 0 & 0 \\ \hline 0 & 0 & 0 & 0 \\ 0 & 0 & 0 & 0 \end{array}\right), \quad \mathbf{L}_- = \left(\begin{array}{cc|cc} 0 & 1 & 0 & 0 \\ 0 & 0 & 0 & 0 \\ \hline 0 & 0 & 0 & 0 \\ 0 & 0 & 0 & 0 \end{array}\right), \tag{4.16}$$

$$\mathbf{J}_3 = \frac{1}{2}\left(\begin{array}{cc|cc} 0 & 0 & 0 & 0 \\ 0 & 0 & 0 & 0 \\ \hline 0 & 0 & 1 & 0 \\ 0 & 0 & 0 & -1 \end{array}\right), \quad \mathbf{J}_+ = \left(\begin{array}{cc|cc} 0 & 0 & 0 & 0 \\ 0 & 0 & 0 & 0 \\ \hline 0 & 0 & 0 & 1 \\ 0 & 0 & 0 & 0 \end{array}\right), \quad \mathbf{J}_- = \left(\begin{array}{cc|cc} 0 & 0 & 0 & 0 \\ 0 & 0 & 0 & 0 \\ \hline 0 & 0 & 0 & 0 \\ 0 & 0 & 1 & 0 \end{array}\right), \tag{4.17}$$

$$\mathbf{Q}_{--1} = \left(\begin{array}{cc|cc} 0 & 0 & 0 & 0 \\ 0 & 0 & 0 & 0 \\ \hline 0 & 0 & 0 & 0 \\ 0 & -1 & 0 & 0 \end{array}\right), \qquad \mathbf{Q}_{++2} = \left(\begin{array}{cc|cc} 0 & 0 & 0 & 0 \\ 0 & 0 & 0 & 1 \\ \hline 0 & 0 & 0 & 0 \\ 0 & 0 & 0 & 0 \end{array}\right), \tag{4.18}$$

$$\mathbf{Q}_{++1} = \left(\begin{array}{cc|cc} 0 & 0 & 0 & 0 \\ 0 & 0 & 0 & 0 \\ \hline 1 & 0 & 0 & 0 \\ 0 & 0 & 0 & 0 \end{array}\right), \qquad \mathbf{Q}_{--2} = \left(\begin{array}{cc|cc} 0 & 0 & -1 & 0 \\ 0 & 0 & 0 & 0 \\ \hline 0 & 0 & 0 & 0 \\ 0 & 0 & 0 & 0 \end{array}\right), \tag{4.19}$$

$$\mathbf{Q}_{+-1} = \left(\begin{array}{cc|cc} 0 & 0 & 0 & 0 \\ 0 & 0 & 0 & 0 \\ \hline 0 & 0 & 0 & 0 \\ 1 & 0 & 0 & 0 \end{array}\right), \qquad \mathbf{Q}_{-+2} = \left(\begin{array}{cc|cc} 0 & 0 & 0 & 1 \\ 0 & 0 & 0 & 0 \\ \hline 0 & 0 & 0 & 0 \\ 0 & 0 & 0 & 0 \end{array}\right), \tag{4.20}$$

$$\mathbf{Q}_{-+1} = \left(\begin{array}{cc|cc} 0 & 0 & 0 & 0 \\ 0 & 0 & 0 & 0 \\ \hline 0 & -1 & 0 & 0 \\ 0 & 0 & 0 & 0 \end{array}\right), \qquad \mathbf{Q}_{+-2} = \left(\begin{array}{cc|cc} 0 & 0 & 0 & 0 \\ 0 & 0 & -1 & 0 \\ \hline 0 & 0 & 0 & 0 \\ 0 & 0 & 0 & 0 \end{array}\right). \tag{4.21}$$

When checking the commutation relations, the equalities in eq. (4.10) hold up to a multiple of the identity $\mathbb{1}$.

Next, the Weyl-Cartan basis of the algebra takes the following form

$$[\mathfrak{h}_i, \mathfrak{h}_j] = 0\,, \qquad [\mathfrak{e}_i, \mathfrak{f}_j] = \delta_{ij}\mathfrak{h}_j, \qquad [\mathfrak{h}_i, \mathfrak{e}_j] = A_{ij}\mathfrak{e}_j, \quad [\mathfrak{h}_i, \mathfrak{f}_j] = -A_{ij}\mathfrak{f}_j, \tag{4.22}$$

with the roots given by

$$\begin{aligned} \mathfrak{h}_1 &= -\mathbf{L}_0 - \mathbf{J}_3, & \mathfrak{e}_1 &= +\mathbf{Q}_{+-1} & \mathfrak{f}_1 &= +\mathbf{Q}_{-+2}, \\ \mathfrak{h}_2 &= 2\mathbf{J}_3, & \mathfrak{e}_2 &= +\mathbf{J}_+ & \mathfrak{f}_2 &= +\mathbf{J}_-, \\ \mathfrak{h}_3 &= -\mathbf{L}_0 - \mathbf{J}_3, & \mathfrak{e}_3 &= +\mathbf{Q}_{+-2} & \mathfrak{f}_3 &= -\mathbf{Q}_{-+1}\,, \end{aligned} \tag{4.23}$$

and the Cartan matrix

$$A = \begin{pmatrix} 0 & -1 & 0 \\ -1 & +2 & -1 \\ 0 & -1 & 0 \end{pmatrix}. \tag{4.24}$$

BPS condition and left Hamiltonian. In this notation, the BPS condition for the algebra is

$$-\mathbf{L}_0 - \mathbf{J}_3 \geq 0\,. \tag{4.25}$$

This positive-semidefinite operator of the left algebra can be used to define the *left Hamiltonian*. Indeed it can be shown that this is the contribution of left charges to the light-cone Hamiltonian $\mathbf{H}^{\text{l.c.}}$ from eq. (4.8) [60, 112]

$$\mathbf{H} \equiv -\mathbf{L}_0 - \mathbf{J}_3\,. \tag{4.26}$$

The supercharges commuting with the left Hamiltonian $\mathbf{H}$ are

$$\begin{aligned} \mathbf{Q}^1 &\equiv \mathfrak{f}_1 = +\mathbf{Q}_{-+2}, & \mathbf{Q}^2 &\equiv \mathfrak{f}_3 = -\mathbf{Q}_{-+1}, \\ \mathbf{S}_1 &\equiv \mathfrak{e}_1 = +\mathbf{Q}_{+-1}, & \mathbf{S}_2 &\equiv \mathfrak{e}_3 = +\mathbf{Q}_{+-2}. \end{aligned} \tag{4.27}$$

It is easy to see, that they form the algebra $\mathfrak{psu}(1|1)^{\oplus 2} \oplus \mathfrak{u}(1)$

$$\left\{\mathbf{Q}^A, \mathbf{S}_B\right\} = \delta^A{}_B\, \mathbf{H} \geq 0\,. \tag{4.28}$$

Moreover, the charges satisfy the Hermiticity conditions

$$\begin{aligned} (\mathbf{Q}_{+-1})^\dagger &= +\mathbf{Q}_{-+2}\,, & (\mathbf{Q}_{-+2})^\dagger &= +\mathbf{Q}_{+-1}\,, \\ (\mathbf{Q}_{-+1})^\dagger &= -\mathbf{Q}_{+-2}\,, & (\mathbf{Q}_{+-2})^\dagger &= -\mathbf{Q}_{-+1}\,, \end{aligned} \tag{4.29}$$

or written equivalently

$$(\mathbf{Q}^A)^\dagger = \mathbf{S}_A\,, \qquad (\mathbf{S}_A)^\dagger = \mathbf{Q}^A\,. \tag{4.30}$$

Weyl-Cartan basis and Hamiltonian for the right algebra. Let us also consider the second copy of $\mathfrak{psu}(1,1|2)_R$. The matrix representation is identical to the one given in eqs. (4.16) to (4.21). It will however be convenient to pick a slightly different Weyl-Cartan basis. In terms of the generators, we choose

$$\begin{aligned} \tilde{\mathfrak{h}}_1 &= +\widetilde{\mathbf{L}}_0 + \widetilde{\mathbf{J}}_3, & \tilde{\mathfrak{e}}_1 &= +\widetilde{\mathbf{Q}}_{-+1} & \tilde{\mathfrak{f}}_1 &= +\widetilde{\mathbf{Q}}_{+-2}, \\ \tilde{\mathfrak{h}}_2 &= -2\widetilde{\mathbf{L}}_0, & \tilde{\mathfrak{e}}_2 &= +\widetilde{\mathbf{L}}_+ & \tilde{\mathfrak{f}}_2 &= -\widetilde{\mathbf{L}}_-, \\ \tilde{\mathfrak{h}}_3 &= +\widetilde{\mathbf{L}}_0 + \widetilde{\mathbf{J}}_3, & \tilde{\mathfrak{e}}_3 &= +\widetilde{\mathbf{Q}}_{-+2} & \tilde{\mathfrak{f}}_3 &= -\widetilde{\mathbf{Q}}_{+-1}\,, \end{aligned} \tag{4.31}$$

with the Cartan matrix

$$\widetilde{A} = \begin{pmatrix} 0 & +1 & 0 \\ +1 & -2 & +1 \\ 0 & +1 & 0 \end{pmatrix} . \tag{4.32}$$

Since the algebra (4.9) is factorised, we can choose the positive roots in either copy of the algebra independently. In order to consider off-shell states the symmetry needs to be extended by two central charges, which vanish on-shell. These two central charges will couple the left and right algebras [61] and hence our choice of positive roots will prove convenient.

In a similar manner, we define the right contribution to the light-cone Hamiltonian

$$\widetilde{\mathbf{H}} \equiv -\widetilde{\mathbf{L}}_0 - \widetilde{\mathbf{J}}_3 \geq 0 \,, \tag{4.33}$$

and find the charges commuting with $\widetilde{\mathbf{H}}$ as

$$\begin{aligned} \widetilde{\mathbf{Q}}_1 &\equiv +\mathfrak{e}_1 = +\widetilde{\mathbf{Q}}_{-+1}, \qquad & \widetilde{\mathbf{Q}}_2 &\equiv +\mathfrak{e}_3 = +\widetilde{\mathbf{Q}}_{-+2}, \\ \widetilde{\mathbf{S}}^1 &\equiv -\mathfrak{f}_1 = -\widetilde{\mathbf{Q}}_{+-2}, \qquad & \widetilde{\mathbf{S}}^2 &\equiv -\mathfrak{f}_3 = +\widetilde{\mathbf{Q}}_{+-1}, \end{aligned} \tag{4.34}$$

so that

$$\{\widetilde{\mathbf{Q}}_A, \widetilde{\mathbf{S}}^B\} = \delta_A{}^B \, \widetilde{\mathbf{H}} \geq 0 \,. \tag{4.35}$$

Like before we have the Hermiticity conditions given through

$$(\widetilde{\mathbf{Q}}^A)^\dagger = \widetilde{\mathbf{S}}_A, \qquad (\widetilde{\mathbf{S}}_A)^\dagger = \widetilde{\mathbf{Q}}^A. \tag{4.36}$$

4.3. Centrally extended off-shell symmetry algebra

Similar to $\mathrm{AdS}_5/\mathrm{CFT}_4$ [19, 113], the algebra relevant for integrability features a *central extension* to the superisometry algebra. This central extension annihilates all physical states. However, it acts nontrivially on the individual worldsheet excitations that make up a physical state. Referring to the spin-chain language, it acts on the magnons that form the Bethe state. The construction in the context of $\mathrm{AdS}_5/\mathrm{CFT}_4$ is reviewed in [8, 111].

In the following we are interested in the central extension of the symmetries commuting with $\mathbf{H}$ and $\widetilde{\mathbf{H}}$ and will use the results from [112]. In our notation, the algebra is

$$\left\{\mathbf{Q}^A, \mathbf{S}_B\right\} = \mathbf{H}\, \delta^A{}_B \,, \qquad \left\{\widetilde{\mathbf{Q}}_A, \widetilde{\mathbf{S}}^B\right\} = \widetilde{\mathbf{H}}\, \delta_A{}^B \,. \tag{4.37}$$

Introducing two central charges $\mathbf{P}$ and $\mathbf{K}$ we have

$$\left\{\mathbf{Q}^A, \widetilde{\mathbf{Q}}_B\right\} = \mathbf{P}\, \delta^A{}_B \,, \qquad \left\{\mathbf{S}_A \,, \widetilde{\mathbf{S}}^B\right\} = \mathbf{K}\, \delta_A{}^B \,, \tag{4.38}$$

where the Hermiticity conditions discussed above imply that for a unitary representation $\mathbf{K}^\dagger = \mathbf{P}$ and $\mathbf{P}^\dagger = \mathbf{K}$. This central extension is also the reason for our different choices of simple roots in eq. (4.27) and eq. (4.34). Since $\mathbf{K}$ is central and if $\mathbf{Q}^A$ is a *negative* root, then $\widetilde{\mathbf{Q}}_A$ needs to be a *positive* root, and similarly for $\widetilde{\mathbf{S}}^A$ and $\mathbf{S}_A$.

Factorisation of the centrally extended algebra. The algebra we have is $\mathfrak{psu}(1|1)^{\oplus 4}$ centrally extended. This algebra has a factorised structure, which we

can see by introducing the following $\mathfrak{psu}(1|1)^{\oplus 2}$ centrally extended algebra

$$\Big\{\mathbf{q},\,\mathbf{s}\Big\}=\mathbf{H},\quad \Big\{\widetilde{\mathbf{q}},\widetilde{\mathbf{s}}\Big\}=\widetilde{\mathbf{H}}\,,\qquad \Big\{\mathbf{q},\,\widetilde{\mathbf{q}}\Big\}=\mathbf{P},\quad \Big\{\mathbf{s},\widetilde{\mathbf{s}}\Big\}=\mathbf{K}\,. \tag{4.39}$$

We can then obtain the larger algebra by setting

$$\mathbf{Q}^1\equiv\mathbf{q}\otimes\mathbf{1}\,,\quad \mathbf{Q}^2\equiv\mathbf{\Sigma}\otimes\mathbf{q},\qquad \mathbf{S}_1\equiv\mathbf{s}\otimes\mathbf{1}\,,\quad \mathbf{S}_2\equiv\mathbf{\Sigma}\otimes\mathbf{s}\,, \tag{4.40}$$

where $\mathbf{\Sigma}$ is the graded identity, $\mathbf{\Sigma}=\delta_{ij}(-1)^{F_j}$ and

$$\widetilde{\mathbf{Q}}_1\equiv\widetilde{\mathbf{q}}\otimes\mathbf{1}\,,\quad \widetilde{\mathbf{Q}}_2\equiv\mathbf{\Sigma}\otimes\widetilde{\mathbf{q}},\qquad \widetilde{\mathbf{S}}^1\equiv\widetilde{\mathbf{s}}\otimes\mathbf{1}\,,\quad \widetilde{\mathbf{S}}^2\equiv\mathbf{\Sigma}\otimes\widetilde{\mathbf{s}}\,. \tag{4.41}$$

Note that the indices are lowered for the second copy. To show that this gives the same $\mathfrak{psu}(1|1)^{\oplus 4}$ centrally extended as above, we use that on any supercharge we have

$$\mathbf{\Sigma}\,\mathbf{q}\,\mathbf{\Sigma}=-\mathbf{q}\,. \tag{4.42}$$

Indices are raised and lowered with the Levi-Civita symbol with $\varepsilon^{12}=-\varepsilon_{12}=1$.

Let us note, that $\mathfrak{psu}(1|1)^{\oplus 4}$ centrally extended plays a role similar to $\mathfrak{su}(2|2)^{\oplus 2}$ in $\mathrm{AdS}_5/\mathrm{CFT}_4$. The factorisation is quite useful to simplify computations. For instance it is sufficient to work out a $\mathfrak{su}(2|2)$-invariant S matrix [19] which served as a building block of the full $\mathfrak{su}(2|2)^{\oplus 2}$-invariant S matrix, *cf.* Sec. 2.2.3. Similarly, the algebra in eq. (4.39) plays the role that $\mathfrak{su}(2|2)$ plays for $\mathrm{AdS}_5/\mathrm{CFT}_4$.

4.4. Short representations of the light-cone symmetry algebra

We have identified the algebra $\mathfrak{psu}(1|1)^{\oplus 4}$, which commutes with the left and right Hamiltonians $\mathbf{H}$ and $\widetilde{\mathbf{H}}$, as well as its central extension. We will now construct its short representation. Worldsheet excitations will transform in these representations [60, 61]. It is convenient to start from the smaller algebra (4.39).

We are interested in the short representations of the smaller algebra (4.39). Let us denote the highest weight state as $|\phi\rangle$, and let us say that $\mathbf{q}$ is a lowering operator. Then $\mathbf{s}$ is a raising operator and it follows that we must have $\mathbf{s}\,|\phi\rangle=0$. From the commutation relation involving $\mathbf{P}$, we see that $\widetilde{\mathbf{q}}$ must also act as a raising operator on $\mathbf{q}\,|\phi\rangle$. Assuming that $\widetilde{\mathbf{q}}\,|\phi\rangle=0$ and $\widetilde{\mathbf{s}}(\mathbf{q}\,|\phi\rangle)=0$, we obtain a short representation, so that no new states are generated and the representation is two-dimensional. In that case we can write

$$\begin{aligned}0&=\big[\widetilde{\mathbf{s}}\widetilde{\mathbf{q}}\mathbf{q}-\widetilde{\mathbf{s}}\widetilde{\mathbf{q}}\mathbf{q}\big]\,|\phi\rangle=\big[(\widetilde{\mathbf{s}}\widetilde{\mathbf{q}}+\widetilde{\mathbf{q}}\widetilde{\mathbf{s}})\mathbf{q}-\widetilde{\mathbf{q}}\widetilde{\mathbf{s}}\mathbf{q}-\widetilde{\mathbf{s}}(\widetilde{\mathbf{q}}\mathbf{q}+\mathbf{q}\widetilde{\mathbf{q}})\big]\,|\phi\rangle\\&=\big[\widetilde{\mathbf{H}}\mathbf{q}-\widetilde{\mathbf{q}}\widetilde{\mathbf{s}}\mathbf{q}-\widetilde{\mathbf{s}}\mathbf{P}\big]\,|\phi\rangle=\big[\widetilde{\mathbf{H}}\mathbf{q}-\widetilde{\mathbf{s}}\mathbf{P}\big]\,|\phi\rangle\ .\end{aligned} \tag{4.43}$$

Taking the anticommutator of this expression with $\mathbf{s}$ we can find a condition which depends only on the central charges. Since the central charges act diagonally, this condition holds for the whole representation and reads

$$\mathbf{H}\,\widetilde{\mathbf{H}}=\mathbf{P}\,\mathbf{K}\,. \tag{4.44}$$

Note, that if for instance $\mathbf{P} = 0$ it must be either $\mathbf{H} = 0$ or $\widetilde{\mathbf{H}} = 0$, *i.e.* the representation is chiral. In conclusion, the only short representations (besides singlets) are two dimensional, they consist of one boson and one fermion, and we indicate them as $(\mathbf{1}|\mathbf{1})$.

A short representation with highest weight state $|\phi\rangle$ is parametrised by the eigenvalues of the central charges given by $P, K, H, \widetilde{H}$, respectively. The shortening condition (4.44) implies that, if the representation is unitary,

$$P\,K \geq 0\,. \tag{4.45}$$

For this reason for unitary representations we introduce the notation

$$\mathbf{C} \equiv \mathbf{P}\,, \qquad \mathbf{C}^\dagger \equiv \mathbf{K}\,. \tag{4.46}$$

The representation has the form

$$\mathbf{q}\,|\phi\rangle = a\,|\varphi\rangle, \quad \mathbf{s}\,|\varphi\rangle = a^*\,|\phi\rangle, \quad \widetilde{\mathbf{s}}\,|\phi\rangle = b^*\,|\varphi\rangle, \quad \widetilde{\mathbf{q}}\,|\varphi\rangle = b\,|\phi\rangle\,, \tag{4.47}$$

where $a, b \in \mathbb{C}$ are called the *representation parameters*. Note that we chose this representation as

$$|\phi\rangle = \text{highest-weight state}\,, \qquad |\varphi\rangle = \text{lowest-weight state}\,, \tag{4.48}$$

where $|\phi\rangle$ and $|\varphi\rangle$ must have opposite statistics. We can now obtain two distinct types of representations by choosing $|\phi\rangle$ to be a boson or a fermion, *i.e.* we have

$$\phi \to \phi^{\mathrm{B}} \equiv \text{Boson}\,, \qquad \varphi \to \varphi^{\mathrm{F}} \equiv \text{Fermion}\,, \tag{4.49}$$

or viceversa

$$\phi \to \phi^{\mathrm{F}} \equiv \text{Fermion}\,, \qquad \varphi \to \varphi^{\mathrm{B}} \equiv \text{Boson}. \tag{4.50}$$

Finally the central charges can be expressed in terms of the representation parameters as

$$\begin{aligned} \mathbf{C} &= C\,\mathbf{1} = ab\,\mathbf{1}, \qquad & \mathbf{C}^\dagger &= C^*\,\mathbf{1} = (ab)^*\,\mathbf{1}, \\ \mathbf{H} &= H\,\mathbf{1} = |a|^2\,\mathbf{1}, \qquad & \widetilde{\mathbf{H}} &= \widetilde{H}\,\mathbf{1} = |b|^2\,\mathbf{1}. \end{aligned} \tag{4.51}$$

Moreover, a, b can be rewritten as a functions of $(C, H, \widetilde{H})$.

Physical values of the central charges. The central charges can be written in terms of the coupling constants and the momentum p of the magnon [112] as

$$C = +i\frac{h}{2}\,(e^{ip} - 1)e^{2i\xi}\,, \qquad C^* = -i\frac{h}{2}\,(e^{-ip} - 1)e^{-2i\xi}\,, \tag{4.52}$$

where the representation coefficient ξ is related to an automorphism of the algebra. As we will see below ξ is important to establish the coproduct of the algebra, since it labels the representation. Further, ξ can also be interpreted as arising from the fields' boundary conditions [111]. The central charges vanish for physical states, *i.e.* when $p = 0 \mod 2\pi$. As stated above, the parameter h is a property of the background and measures the amount of Ramond-Ramond flux. In what follows, we will be interested

in the *most-symmetric coproduct* [112], chosen as

$$C = C^* = -h \sin(p/2)\,. \tag{4.53}$$

Combining the left and right Hamiltonians $\mathbf{H}$ and $\widetilde{\mathbf{H}}$, we obtain

$$\begin{aligned} \mathbf{E} &\equiv \mathbf{H}^{\text{l.c.}} = \mathbf{H} + \widetilde{\mathbf{H}} = -\mathbf{L}_0 - \widetilde{\mathbf{L}}_0 - \mathbf{J}_3 - \widetilde{\mathbf{J}}_3 \geq 0\,, \\ \mathbf{M} &\equiv \mathbf{H} - \widetilde{\mathbf{H}} = -\mathbf{L}_0 + \widetilde{\mathbf{L}}_0 - \mathbf{J}_3 + \widetilde{\mathbf{J}}_3\,. \end{aligned} \tag{4.54}$$

The eigenvalues of $\mathbf{M}$ should be quantised in integers for physical states. Considering a bosonsic state this can easily be seen as the AdS_3 and S^3 spins are integer. For fermionic states, both spins are half-integer, so that the total spin in $\mathbf{M}$ is integer again. It turns out that it takes the following eigenvalues [58, 59]

$$M = |a|^2 + |b|^2 = \frac{k}{2\pi} p + m\,, \qquad m \in \mathbb{Z}\,. \tag{4.55}$$

Again, $k = 1, 2, 3, \ldots$ is a property of the string background and measures the amount of NSNS flux, which is quantised. Further, we can use the shortening condition (4.44) to express the last central charge $\mathbf{E}$ as

$$E^2 = M^2 + |C|^2\,, \qquad E = \sqrt{\left(m + \frac{k}{2\pi} p\right)^2 + h^2 \sin^2 \frac{p}{2}}\,. \tag{4.56}$$

In this dispersion relation, we see that m plays the role of a mass. Therefore it is convenient to introduce the following nomenclature:

> **Massless representation:** $m = 0$. Here we have that $E = 0$ at $p = 0$ for any value of h and k.
>
> **Left representation:** $m = +1, +2, \ldots$. At $p = 0$ we have that $E = m$ and $M = m$, which implies $H = m > 0$ and $\widetilde{H} = 0$, hence the name *left*.
>
> **Right representation:** $m = -1, -2, \ldots$. At $p = 0$ we have that $E = -m$ and $M = m$, which implies $H = 0$ and $\widetilde{H} = -m > 0$, hence the name *right*.

Further, the case $|m| = 1$ corresponds to fundamental massive particles. These can then form bound states, which have masses $|m| = 2, 3, \ldots$ [58, 61].

4.5. Particle content of the theory

In order to describe the particle content of the theory, let us consider the irreducible representations of $\mathfrak{psu}(1|1)^{\oplus 2}$ centrally extended. In fact, four irreducible representations will be important in what follows. We denote them by

$$\rho_{\text{L}} = (\phi^{\text{B}}_{\text{L}} | \varphi^{\text{F}}_{\text{L}})\,, \qquad \rho_{\text{R}} = (\phi^{\text{F}}_{\text{R}} | \varphi^{\text{B}}_{\text{R}})\,, \qquad \rho_{\circ} = (\phi^{\text{B}}_{\circ} | \varphi^{\text{F}}_{\circ})\,, \qquad \rho'_{\circ} = (\phi^{\text{F}}_{\circ} | \varphi^{\text{B}}_{\circ})\,, \tag{4.57}$$

where the first state is always the highest-weight state,

$$|\phi^*_*\rangle = \text{highest-weight state}\,, \qquad |\varphi^*_*\rangle = \text{lowest-weight state}\,. \tag{4.58}$$

Here ρ_{L} and ρ_{R} are the left and right representation, respectively. Further, we have two massless representations $\rho_{\circ}$ and $\rho'_{\circ}$. The representations take the same form up to relabelling the representation coefficients. Written out explicitly, this yields

$$\begin{aligned}
&\mathbf{q}\,|\phi^{\mathrm{B}}_{\mathrm{L}}\rangle = a_{\mathrm{L}}\,|\varphi^{\mathrm{F}}_{\mathrm{L}}\rangle, \quad \mathbf{s}\,|\varphi^{\mathrm{F}}_{\mathrm{L}}\rangle = a^*_{\mathrm{L}}\,|\phi^{\mathrm{B}}_{\mathrm{L}}\rangle, \quad \widetilde{\mathbf{s}}\,|\phi^{\mathrm{B}}_{\mathrm{L}}\rangle = b^*_{\mathrm{L}}\,|\varphi^{\mathrm{F}}_{\mathrm{L}}\rangle, \quad \widetilde{\mathbf{q}}\,|\varphi^{\mathrm{F}}_{\mathrm{L}}\rangle = b_{\mathrm{L}}\,|\phi^{\mathrm{B}}_{\mathrm{L}}\rangle\,,\\
&\mathbf{q}\,|\phi^{\mathrm{F}}_{\mathrm{R}}\rangle = a_{\mathrm{R}}\,|\varphi^{\mathrm{B}}_{\mathrm{R}}\rangle, \quad \mathbf{s}\,|\varphi^{\mathrm{B}}_{\mathrm{R}}\rangle = a^*_{\mathrm{R}}\,|\phi^{\mathrm{F}}_{\mathrm{R}}\rangle, \quad \widetilde{\mathbf{s}}\,|\phi^{\mathrm{F}}_{\mathrm{R}}\rangle = b^*_{\mathrm{R}}\,|\varphi^{\mathrm{B}}_{\mathrm{R}}\rangle, \quad \widetilde{\mathbf{q}}\,|\varphi^{\mathrm{B}}_{\mathrm{R}}\rangle = b_{\mathrm{R}}\,|\phi^{\mathrm{F}}_{\mathrm{R}}\rangle\,,\\
&\mathbf{q}\,|\phi^{\mathrm{B}}_{\circ}\rangle = a_{\circ}\,|\varphi^{\mathrm{F}}_{\circ}\rangle, \quad \mathbf{s}\,|\varphi^{\mathrm{F}}_{\circ}\rangle = a^*_{\circ}\,|\phi^{\mathrm{B}}_{\circ}\rangle, \quad \widetilde{\mathbf{s}}\,|\phi^{\mathrm{B}}_{\circ}\rangle = b^*_{\circ}\,|\varphi^{\mathrm{F}}_{\circ}\rangle, \quad \widetilde{\mathbf{q}}\,|\varphi^{\mathrm{F}}_{\circ}\rangle = b_{\circ}\,|\phi^{\mathrm{B}}_{\circ}\rangle\,,\\
&\mathbf{q}\,|\phi^{\mathrm{F}}_{\circ}\rangle = a_{\circ}\,|\varphi^{\mathrm{B}}_{\circ}\rangle, \quad \mathbf{s}\,|\varphi^{\mathrm{B}}_{\circ}\rangle = a^*_{\circ}\,|\phi^{\mathrm{F}}_{\circ}\rangle, \quad \widetilde{\mathbf{s}}\,|\phi^{\mathrm{F}}_{\circ}\rangle = b^*_{\circ}\,|\varphi^{\mathrm{B}}_{\circ}\rangle, \quad \widetilde{\mathbf{q}}\,|\varphi^{\mathrm{B}}_{\circ}\rangle = b_{\circ}\,|\phi^{\mathrm{F}}_{\circ}\rangle\,.
\end{aligned} \tag{4.59}$$

Similarly to AdS_5, the explicit form of the representation coefficients a_*, b_* can be given in terms of Zhukovski variables. In order to do this, let us introduce the different sets of Zhukovsky variables given by

$$\begin{aligned}
&a_{\mathrm{L}} = e^{i\xi}\eta_{\mathrm{L},p}\,, \quad b_{\mathrm{L}} = -e^{i\xi}\frac{e^{-ip/2}}{x^-_{\mathrm{L},p}}\eta_{\mathrm{L},p}\,, \qquad a^*_{\mathrm{L}} = e^{-i\xi}e^{-ip/2}\eta_{\mathrm{L},p}\,, \quad b^*_{\mathrm{L}} = -e^{-i\xi}\frac{1}{x^+_{\mathrm{L},p}}\eta_{\mathrm{L},p},\\
&b_{\mathrm{R}} = e^{i\xi}\eta_{\mathrm{R},p}\,, \quad a_{\mathrm{R}} = -e^{i\xi}\frac{e^{-ip/2}}{x^-_{\mathrm{R},p}}\eta_{\mathrm{R},p}\,, \qquad b^*_{\mathrm{R}} = e^{-i\xi}e^{-ip/2}\eta_{\mathrm{R},p}\,, \quad a^*_{\mathrm{R}} = -e^{-i\xi}\frac{1}{x^+_{\mathrm{R},p}}\eta_{\mathrm{R},p},\\
&a_{\circ} = e^{i\xi}\eta_{\circ,p}\,, \quad b_{\circ} = -e^{i\xi}\frac{e^{-ip/2}}{x^-_{\circ,p}}\eta_{\circ,p}\,, \qquad a^*_{\circ} = e^{-i\xi}e^{-ip/2}\eta_{\circ,p}\,, \quad b^*_{\circ} = -e^{-i\xi}\frac{1}{x^+_{\circ,p}}\eta_{\circ,p}\,,
\end{aligned} \tag{4.60}$$

where the parameter η is always of the form

$$\eta_{*,p} = e^{ip/4}\sqrt{\frac{ih}{2}(x^-_{*,p} - x^+_{*,p})}\,, \tag{4.61}$$

with the star symbols indicating the respective representation $\mathrm{L}, \mathrm{R}, \circ$. Moreover, the Zhukovsky variables satisfy the shortening conditions

$$\begin{aligned}
x^+_{\mathrm{L},p} + \frac{1}{x^+_{\mathrm{L},p}} - x^-_{\mathrm{L},p} - \frac{1}{x^-_{\mathrm{L},p}} &= \frac{2i\left(1+\frac{k}{2\pi}p\right)}{h}\,,\\
x^+_{\mathrm{R},p} + \frac{1}{x^+_{\mathrm{R},p}} - x^-_{\mathrm{R},p} - \frac{1}{x^-_{\mathrm{R},p}} &= \frac{2i\left(1-\frac{k}{2\pi}p\right)}{h}\,,\\
x^+_{\circ,p} + \frac{1}{x^+_{\circ,p}} - x^-_{\circ,p} - \frac{1}{x^-_{\circ,p}} &= \frac{2i\left(0+\frac{k}{2\pi}p\right)}{h}\,,
\end{aligned} \tag{4.62}$$

and can be parametrised as follows

$$\begin{aligned}
x^{\pm}_{\mathrm{L},p} &= \frac{e^{\pm ip/2}}{2h\,\sin\left(\frac{p}{2}\right)}\left(\left(1+\tfrac{k}{2\pi}p\right) + \sqrt{\left(1+\tfrac{k}{2\pi}p\right)^2 + 4h^2\sin^2\left(\tfrac{p}{2}\right)}\right),\\
x^{\pm}_{\mathrm{R},p} &= \frac{e^{\pm ip/2}}{2h\,\sin\left(\frac{p}{2}\right)}\left(\left(1-\tfrac{k}{2\pi}p\right) + \sqrt{\left(1-\tfrac{k}{2\pi}p\right)^2 + 4h^2\sin^2\left(\tfrac{p}{2}\right)}\right),\\
x^{\pm}_{\circ,p} &= \frac{e^{\pm ip/2}}{2h\,\sin\left(\frac{p}{2}\right)}\left(\left(0+\tfrac{k}{2\pi}p\right) + \sqrt{\left(0+\tfrac{k}{2\pi}p\right)^2 + 4h^2\sin^2\left(\tfrac{p}{2}\right)}\right).
\end{aligned} \tag{4.63}$$

It is easy to check, that this parametrisation satisfies the shortening condition in

	AdS_3 Bosons	S^3 Bosons	T^4 Bosons	Fermions
Left, $m = +1$	$Z(p)$	$Y(p)$		$\Psi^A(p)$
Right $m = -1$	$\tilde{Z}(p)$	$\tilde{Y}(p)$		$\tilde{\Psi}^A(p)$
Massless $m = 0$			$T^{A\dot{A}}(p)$	$\chi^{\dot{A}}(p),\ \tilde{\chi}^{\dot{A}}(p)$

Table 4.1.: The fundamental excitations of $AdS_3 \times S^3 \times T^4$ are eight bosons and eight fermions. We arranged them here according to their representation as well as their geometrical interpretation.

eq. (4.62) as well as

$$x^+_{*,p} - \frac{1}{x^+_{*,p}} - x^-_{*,p} + \frac{1}{x^-_{*,p}} = \frac{2i\,E}{h}\,. \tag{4.64}$$

Naively one might expect that the left and right representation are simply related by sending $m \to -m$. However, the parametrisation of the representation coefficients and of the Zhukovski variables in eq. (4.63) is genuinely different. For physical particles the Zhukovski variables are chosen to lie outside of the unit disk, *i.e.* $|x^\pm_{*,p}| \geq 1$ and hence the different parametrisation [70, 114].

In addition, for the massless representation we used the limit

$$a_\circ = \lim_{m\to 0} a_{\rm L}\,, \qquad b_\circ = \lim_{m\to 0} b_{\rm L}\,, \qquad x^\pm_{\circ,p} = \lim_{m\to 0} x^\pm_{{\rm L},p}\,. \tag{4.65}$$

Similarly, we could have used the right representation instead. This results in flipping the sign of p in (4.63) and exchanging $a_\circ \leftrightarrow b_\circ$ in (4.60). This does not change the central charges and hence the two representations obtained in the two limits must be isomorphic. This may be seen through a change of basis, *e.g.* rescaling only the lowest-weight state we have

$$|\varphi\rangle \ \to\ \sigma_p\,|\varphi\rangle\,, \tag{4.66}$$

where we introduced the momentum dependent sign factor

$$\sigma_p \equiv \Big[\frac{a_{\rm L}}{a_{\rm R}}\Big]_{m\to 0} = -{\rm sgn}\Big[\sin p/2\Big]\,. \tag{4.67}$$

Moreover, the following identity will be useful

$$\lim_{m\to 0}\big(x^\pm_{\rm L}(p)\,x^\mp_{\rm R}(p)\big) = 1\,. \tag{4.68}$$

This is valid for any k. For the massless parametrisation we have that $x^+_\circ(p) = 1/x^-_\circ(p)$, which is valid at $k = 0$.

The fundamental particle content of the theory is summarised in Tab. 4.1. It can be arranged in representations constructed out of the $\rho_\pm$, ρ_0, ρ_0' representations discussed above. We want to use these short, two-dimensional representations ρ to construct the representations ϱ of $\mathfrak{psu}(1|1)^{\oplus 4}$ centrally extended. To achieve this, we can for instance set $\varrho = \rho_\pm \otimes \rho_\pm$, or $\varrho = \rho_0 \otimes \rho_0$. However, to obtain a valid representation the two $\mathfrak{psu}(1|1)^{\oplus 2}$ representations appearing in the tensor product need to have the same central charge. Hence, a representation of the form *e.g.* $\varrho = \rho_\pm \otimes \rho_\mp$ or $\varrho = \rho_\pm \otimes \rho_0$

would not be a representation of the centrally extended $\mathfrak{psu}(1|1)^{\oplus 4}$ algebra.

The left representation. To construct the left representation with $M = +1$ we consider

$$\varrho_+ = \rho_+ \otimes \rho_+ \,. \tag{4.69}$$

We define the following states

$$\begin{gathered} |Y(p)\rangle = |\phi^{\mathrm{B}}_{\mathrm{L}}(p) \otimes \phi^{\mathrm{B}}_{\mathrm{L}}(p)\rangle \,, \\ |\Psi^1(p)\rangle = |\varphi^{\mathrm{F}}_{\mathrm{L}}(p) \otimes \phi^{\mathrm{B}}_{\mathrm{L}}(p)\rangle \,, \qquad |\Psi^2\rangle = |\phi^{\mathrm{B}}_{\mathrm{L}}(p) \otimes \varphi^{\mathrm{F}}_{\mathrm{L}}(p)\rangle \,, \\ |Z(p)\rangle = |\varphi^{\mathrm{F}}_{\mathrm{L}}(p) \otimes \varphi^{\mathrm{F}}_{\mathrm{L}}(p)\rangle \,. \end{gathered} \tag{4.70}$$

From this definition we can see that the supercharges act in the following way

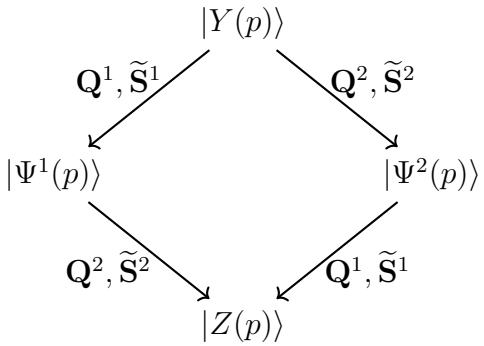

(4.71)

In the figure only the lowering operators are indicated to maintain readability. Further, the states $|\Psi^1(p)\rangle, |\Psi^2(p)\rangle$ transform as a $\mathfrak{su}_\bullet$ doublet. By using the definitions of Sec. 4.3 we find the action of the supercharges as

$$\begin{aligned} \mathbf{Q}^A|Y(p)\rangle &= a_{\mathrm{L}}(p)\,|\Psi^A(p)\rangle \,, & \mathbf{Q}^A|\Psi^B(p)\rangle &= \varepsilon^{AB} a_{\mathrm{L}}(p)\,|Z(p)\rangle \,, \\ \mathbf{S}_A|\Psi^B(p)\rangle &= \delta_A{}^B\, a^*_{\mathrm{L}}(p)\,|Y(p)\rangle \,, & \mathbf{S}_A|Z(p)\rangle &= -\,\varepsilon_{AB}\, a^*_{\mathrm{L}}(p)\,|\Psi^B(p)\rangle \,, \\ \widetilde{\mathbf{S}}^A|Y(p)\rangle &= b^*_{\mathrm{L}}(p)\,|\Psi^A(p)\rangle \,, & \widetilde{\mathbf{S}}^A|\Psi^B(p)\rangle &= \varepsilon^{AB} b^*_{\mathrm{L}}(p)\,|Z(p)\rangle \,, \\ \widetilde{\mathbf{Q}}_A|\Psi^B(p)\rangle &= \delta_A{}^B\, b_{\mathrm{L}}(p)\,|Y(p)\rangle \,, & \widetilde{\mathbf{Q}}_A|Z(p)\rangle &= -\,\varepsilon_{AB}\, b_{\mathrm{L}}(p)\,|\Psi^B(p)\rangle \,, \end{aligned} \tag{4.72}$$

where only the non-vanishing actions are listed. Recall our convention $\varepsilon^{12} = -\varepsilon_{12} = +1$.

The right representation. For the right representation we have

$$\varrho_- = \rho_- \otimes \rho_- \,, \tag{4.73}$$

and $M = -1$. As before we define

$$\begin{gathered} |\tilde{Z}(p)\rangle = |\phi^{\mathrm{F}}_{\mathrm{R}}(p) \otimes \phi^{\mathrm{F}}_{\mathrm{R}}(p)\rangle \,, \\ |\tilde{\Psi}^1(p)\rangle = |\varphi^{\mathrm{B}}_{\mathrm{R}}(p) \otimes \phi^{\mathrm{F}}_{\mathrm{R}}(p)\,, \qquad |\tilde{\Psi}^2(p)\rangle = -|\phi^{\mathrm{F}}_{\mathrm{R}}(p) \otimes \varphi^{\mathrm{B}}_{\mathrm{R}}(p)\rangle \,, \\ |\tilde{Y}(p)\rangle = |\varphi^{\mathrm{B}}_{\mathrm{R}}(p) \otimes \varphi^{\mathrm{B}}_{\mathrm{R}}(p)\rangle \,, \end{gathered} \tag{4.74}$$

where the minus sign stems from the definitions of the right supercharges, which are canonically defined with lower $\mathfrak{su}(2)_\bullet$ indices, *cf.* eq. (4.41). Again, the states $|\tilde{\Psi}^1(p)\rangle, |\tilde{\Psi}^2(p)\rangle$ transform as a doublet under $\mathfrak{su}_\bullet$. Acting with the lowering operators,

we can arrange the representation as above

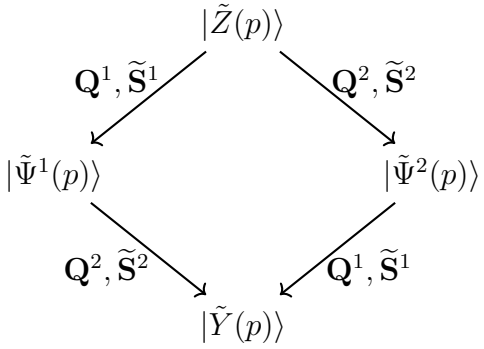

(4.75)

where the representation takes the form

$$\begin{aligned}
\mathbf{Q}^A|\tilde{Z}(p)\rangle &= a_{\mathrm{R}}(p)\,|\tilde{\Psi}^A(p)\rangle\,, & \mathbf{Q}^A|\tilde{\Psi}^B(p)\rangle &= -\,\varepsilon^{AB} a_{\mathrm{R}}(p)\,|\tilde{Y}(p)\rangle\,,\\
\mathbf{S}_A|\tilde{\Psi}^B(p)\rangle &= \delta_A{}^B\, a^*_{\mathrm{R}}(p)\,|\tilde{Z}(p)\rangle\,, & \mathbf{S}_A|\tilde{Y}(p)\rangle &= \varepsilon_{AB}\, a^*_{\mathrm{R}}(p)\,|\tilde{\Psi}^B(p)\rangle\,,\\
\widetilde{\mathbf{S}}^A|\tilde{Z}(p)\rangle &= b^*_{\mathrm{R}}(p)\,|\tilde{\Psi}^A(p)\rangle\,, & \widetilde{\mathbf{S}}^A|\tilde{\Psi}^B(p)\rangle &= -\,\varepsilon^{AB} b^*_{\mathrm{R}}(p)\,|\tilde{Y}(p)\rangle\,,\\
\widetilde{\mathbf{Q}}_A|\tilde{\Psi}^B(p)\rangle &= \delta_A{}^B\, b_{\mathrm{R}}(p)\,|\tilde{Z}(p)\rangle\,, & \widetilde{\mathbf{Q}}_A|\tilde{Y}(p)\rangle &= \varepsilon_{AB}\, b_{\mathrm{R}}(p)\,|\tilde{\Psi}^B(p)\rangle\,.
\end{aligned} \tag{4.76}$$

Notice that there is a discrete *left-right symmetry* [59, 70] when swapping the particles

$$|Y\rangle \leftrightarrow |\tilde{Y}\rangle\,, \qquad |\Psi^A\rangle \leftrightarrow |\tilde{\Psi}_A\rangle\,, \qquad |Z\rangle \leftrightarrow |\tilde{Z}\rangle\,. \tag{4.77}$$

The massless representations. There are two massless representations with $M = 0$, which carry a charge under the $\mathfrak{su}(2)_\circ$ algebra, that commutes with all symmetries introduced. As noted above, this $\mathfrak{su}(2)_\circ$ emerges from the decomposition of $\mathfrak{so}(4)_{\mathrm{T}^4}$. For the massless representations we write

$$\varrho_0^{\dot{A}} = \big(\rho_0 \otimes \rho_0'\big) \oplus \big(\rho_0' \otimes \rho_0\big)\,, \qquad \dot{A} = 1, 2\,, \tag{4.78}$$

imposing that the two modules $\rho_0 \otimes \rho_0'$ and $\rho_0' \otimes \rho_0$ must also transform as a doublet under $\mathfrak{su}(2)_\circ$. This is fine since the $\mathfrak{su}(2)_\circ$ commutes with $\mathfrak{psu}(1|1)^{\oplus 4}$ centrally extended. In fact, as in ref. [115], the same representation $\rho_0 \otimes \rho_0'$ can be used for both $\dot{A} = 1$ and $\dot{A} = 2$. This amounts to a change of basis. However, it will be useful later on to consider two distinct representations. Hence, we have eight states

$$\begin{gathered}
|\chi^{\dot{1}}(p)\rangle = |\phi_0^{\mathrm{B}}(p) \otimes \phi_0^{\mathrm{F}}(p)\rangle\,,\\
|T^{\dot{1}1}(p)\rangle = |\varphi_0^{\mathrm{F}}(p) \otimes \phi_0^{\mathrm{F}}(p)\rangle\,, \qquad |T^{\dot{1}2}(p)\rangle = |\phi_0^{\mathrm{B}}(p) \otimes \varphi_0^{\mathrm{B}}(p)\rangle\,,\\
|\tilde{\chi}^{\dot{1}}(p)\rangle = |\varphi_0^{\mathrm{F}}(p) \otimes \varphi_0^{\mathrm{B}}(p)\rangle\,,
\end{gathered} \tag{4.79}$$

and

$$\begin{gathered}
|\chi^{\dot{2}}(p)\rangle = i|\phi_0^{\mathrm{F}}(p) \otimes \phi_0^{\mathrm{B}}(p)\rangle\,,\\
|T^{\dot{2}1}(p)\rangle = i|\varphi_0^{\mathrm{B}}(p) \otimes \phi_0^{\mathrm{B}}(p)\rangle\,, \qquad |T^{\dot{2}2}(p)\rangle = -i|\phi_0^{\mathrm{F}}(p) \otimes \varphi_0^{\mathrm{F}}(p)\rangle\,,\\
|\tilde{\chi}^{\dot{2}}(p)\rangle = -i|\varphi_0^{\mathrm{B}}(p) \otimes \varphi_0^{\mathrm{F}}(p)\rangle\,.
\end{gathered} \tag{4.80}$$

Note that we have also introduced an overall i in the latter representation. Again, this will be convenient later on, as it simplifies the notation. Of course, it can also be addressed by introducing a suitable normalisation later on. As for the massive representations, we see that the lowering operators act in the same way on either of the massless representation

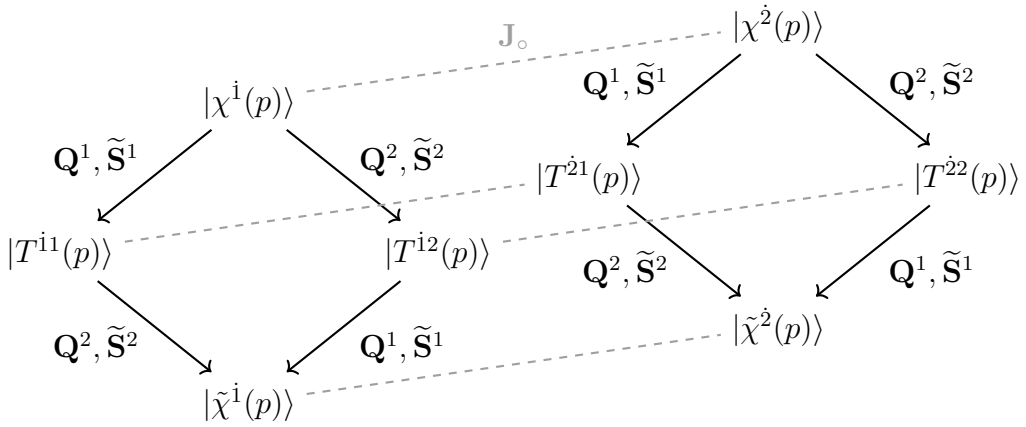

(4.81)

Here, we also indicated the $\mathfrak{su}(2)_\circ$ symmetry. Regardless of the value of the index $\dot A = 1, 2$ the representation takes the form

$$
\begin{aligned}
\mathbf{Q}^A|\chi^{\dot A}(p)\rangle &= a_\circ(p)\,|T^{\dot A A}(p)\rangle\,, & \mathbf{Q}^A|T^{\dot A B}(p)\rangle &= \varepsilon^{AB} a_\circ(p)\,|\tilde\chi^{\dot A}(p)\rangle\,,\\
\mathbf{S}_A|T^{\dot A B}(p)\rangle &= \delta_A{}^B\, a_\circ^*(p)\,|\chi^{\dot A}(p)\rangle\,, & \mathbf{S}_A|\tilde\chi^{\dot A}(p)\rangle &= -\,\varepsilon_{AB}\, a_\circ^*(p)\,|T^{\dot A B}(p)\rangle\,,\\
\widetilde{\mathbf{S}}^A|\chi^{\dot A}(p)\rangle &= b_\circ^*(p)\,|T^{\dot A A}(p)\rangle\,, & \widetilde{\mathbf{S}}^A|T^{\dot A B}(p)\rangle &= \varepsilon^{AB} b_\circ^*(p)\,|\tilde\chi^{\dot A}(p)\rangle\,,\\
\widetilde{\mathbf{Q}}_A|T^{\dot A B}(p)\rangle &= \delta_A{}^B\, b_\circ(p)\,|\chi^{\dot A}(p)\rangle\,, & \widetilde{\mathbf{Q}}_A|\tilde\chi(p)\rangle &= -\,\varepsilon_{AB}\, b_\circ(p)\,|T^{\dot A B}(p)\rangle\,.
\end{aligned}
\tag{4.82}
$$

Multi-particle representation. Since we would like to consider multi-particle states it is useful to understand the multi-particle representation. For instance the S matrix considered in the next section is an operator acting on two-particle states. Let us start by considering a two-particle state obtained through the tensor product of two one-particle representations, *i.e.* $|\Xi_1(p_1)\Xi_2(p_2)\rangle = \Xi_1(p_1)\otimes\Xi_2(p_2)$ with Ξ_j a particle in one of the representations considered above. The action of a generic bosonic generator $\mathfrak{J}$ is then given by the *trivial coproduct* through

$$\Delta(\mathfrak{J}) = \mathfrak{J}\otimes\mathbf{1} + \mathbf{1}\otimes\mathfrak{J}\,. \tag{4.83}$$

Thus, the generator acts on the first and second particle in the state, respectively. When considering the central charge $\mathbf{C}$, we expect it to depend on the total momentum of the two-particle state. From eq. (4.52) it follows that

$$\Delta(\mathbf{C})\,|\Xi_1(p_1)\Xi_2(p_2)\rangle = -i\frac{h}{2}(e^{i(p_1+p_2)}-1)e^{2i\xi}\,|\Xi_1(p_1)\Xi_2(p_2)\rangle\ . \tag{4.84}$$

In order to obtain the most symmetric coproduct from eq. (4.53) we need to choose $\xi = -\frac{p_1+p_2}{4}$. Using the definition of the coproduct from eq. (4.83), we obtain

$$\Delta(\mathbf{C})\,|\Xi_1(p_1)\Xi_2(p_2)\rangle = -i\frac{h}{2}\left((e^{ip_1}-1)e^{2i\xi_1} + (e^{ip_2}-1)e^{2i\xi_2}\right)|\Xi_1(p_1)\Xi_2(p_2)\rangle \tag{4.85}$$

This reproduces the expression of the central charge in eq. (4.84) for

$$\xi_1 = -\frac{p_1+p_2}{4} \quad \xi_2 = -\frac{-p_1+p_2}{4} \qquad \text{or} \qquad \xi_1 = -\frac{p_1-p_2}{4} \quad \xi_2 = -\frac{p_1+p_2}{4}\,. \tag{4.86}$$

Denoting the four dimensional space spanned by one excitation as $\mathcal{V}$, we can label the representation by $\mathcal{V}(p_j,\xi_j)$. The central charge acts on the two-particle state then as

$$\Delta(\mathbf{C})(p_1,p_2) = \mathbf{C}(p_1,\xi_1)\otimes\mathbf{1} + \mathbf{1}\otimes\mathbf{C}(p_2,\xi_2)\,. \tag{4.87}$$

For the supercharges we can write corresponding expressions. Here we have to take the graded identity $\mathbf{\Sigma}$ into account, leading to

$$\Delta(\mathbf{Q})(p_1,p_2) = \mathbf{Q}(p_1,\xi_1)\otimes\mathbf{1} + \mathbf{\Sigma}\otimes\mathbf{Q}(p_2,\xi_2)\,, \tag{4.88}$$

and similarly for $\widetilde{\mathbf{Q}},\mathbf{S},\widetilde{\mathbf{S}}$.

Instead of using the trivial coproduct and keeping track of the ξ_j, we can also modify the coproduct itself, introducing the *braided coproduct* Δ_B. More explicitly, we can write for the two-particle representation

$$\begin{aligned}\Delta_B(\mathbf{Q})(p_1,p_2) &= \mathbf{Q}(p_1)\otimes\mathbf{1} + e^{\frac{i}{2}p_1}\mathbf{\Sigma}\otimes\mathbf{Q}(p_2)\,,\\ \Delta_B(\mathbf{S})(p_1,p_2) &= \mathbf{S}(p_1)\otimes\mathbf{1} + e^{-\frac{i}{2}p_1}\mathbf{\Sigma}\otimes\mathbf{S}(p_2)\,,\end{aligned} \tag{4.89}$$

where all the ξ_j are set to be equal. The appearance of the non-trivial coproduct is a hint towards the mathematical structure of a *Hopf algebra*, which plays an important role in AdS/CFT and integrable models, *cf.* [116, 117].

We can also generalise the above to multi-particle states. This can be achieved by repeatedly applying the twisted coproduct. In terms of the ξ_j we have

$$\xi_1 = -\frac{p_1+\cdots+p_n}{4}\,, \quad \xi_2-\xi_1 = \frac{p_1}{2}\,, \quad \ldots \quad \xi_n-\xi_{n-1} = \frac{p_{n-1}}{2}\,, \tag{4.90}$$

which is the generalisation of the first solution from eq. (4.86). Analogously, the second choice can be generalised.

4.6. Scattering matrix

The construction of the S matrix of $\mathrm{AdS}_3\times\mathrm{S}^3\times\mathrm{T}^4$ closely resembles the construction in $\mathrm{AdS}_5\times\mathrm{S}^5$. The full $\mathfrak{psu}(1|1)^{\oplus 4}$ S matrix can be obtained by taking the graded tensor product [112] of two copies of the $\mathfrak{psu}(1|1)^{\oplus 2}$ S matrix of [70],

$$\mathbf{S} = S\hat{\otimes}\acute{S}, \tag{4.91}$$

which can be defined in terms of the S matrix elements $\mathcal{M}$ by

$$(\mathcal{M}\hat{\otimes}\acute{\mathcal{M}})^{I\acute{I},J\acute{J}}_{K\acute{K},L\acute{L}} = (-1)^{F_{\acute{K}}F_L+F_J F_{\acute{I}}}\mathcal{M}^{IJ}_{KL}\acute{\mathcal{M}}^{\acute{I}\acute{J}}_{\acute{K}\acute{L}}. \tag{4.92}$$

Up to the dressing factors, the $\mathfrak{psu}(1|1)^{\oplus 2}$ S matrix can be bootstrapped by demanding it to commute with the symmetry generators [112]. The action of the S matrix on a two-particle representation is then given by

$$\mathbf{S} \;:\quad \mathcal{V}(p_1,\xi_1)\otimes\mathcal{V}(p_2,\xi_2)\to\mathcal{V}(p_2,\xi_2)\otimes\mathcal{V}(p_1,\xi_1)\,, \tag{4.93}$$

where the action of the S matrix exchanges the first and second set from eq. (4.86).

However, comparing the constructions, there are two main differences. Firstly, here we have $\mathfrak{psu}(1|1)^{\oplus 2}$ centrally extended rather than the centrally extended $\mathfrak{su}(2|2)$ algebra. Secondly, instead of dealing with a single irreducible representation we now have *four* irreducible representations. In $\mathrm{AdS}_5\times\mathrm{S}^5$ we have four-dimensional representations of $\mathfrak{su}(2|2)$ leading to $4^2=16$ dimensional representations of $\mathfrak{su}(2|2)^{\oplus 2}$. Here we start from two-dimensional representations instead. As a result of having four irreducible representations, the S matrix will consist of sixteen blocks with as many dressing factors. Fortunately unitarity and symmetries reduce the number of independent dressing factors to four.

In the following we will introduce the scattering matrices between $\mathfrak{psu}(1|1)^{\oplus 2}$ centrally extended representations that play a role in the next chapter. It can be checked explicitly that this S Matrix also fulfils the unitarity conditions and the Yang-Baxter equation, *cf.* Sec. 2.2.3.

Left-left scattering. The scattering matrix for particles in the ρ_{L} representation of $\mathfrak{psu}(1|1)^{\oplus 2}$ centrally extended is given by

$$\begin{aligned}
S|\phi^{\mathrm{B}}_{\mathrm{L},p}\phi^{\mathrm{B}}_{\mathrm{L},q}\rangle &= A^{\mathrm{LL}}_{pq}\,|\phi^{\mathrm{B}}_{\mathrm{L},q}\phi^{\mathrm{B}}_{\mathrm{L},p}\rangle, & S|\phi^{\mathrm{B}}_{\mathrm{L},p}\varphi^{\mathrm{F}}_{\mathrm{L},q}\rangle &= B^{\mathrm{LL}}_{pq}|\varphi^{\mathrm{F}}_{\mathrm{L},q}\phi^{\mathrm{B}}_{\mathrm{L},p}\rangle + C^{\mathrm{LL}}_{pq}|\phi^{\mathrm{B}}_{\mathrm{L},q}\varphi^{\mathrm{F}}_{\mathrm{L},p}\rangle,\\
S|\varphi^{\mathrm{F}}_{\mathrm{L},p}\varphi^{\mathrm{F}}_{\mathrm{L},q}\rangle &= F^{\mathrm{LL}}_{pq}\,|\varphi^{\mathrm{F}}_{\mathrm{L},q}\varphi^{\mathrm{F}}_{\mathrm{L},p}\rangle, & S|\varphi^{\mathrm{F}}_{\mathrm{L},p}\phi^{\mathrm{B}}_{\mathrm{L},q}\rangle &= D^{\mathrm{LL}}_{pq}|\phi^{\mathrm{B}}_{\mathrm{L},q}\varphi^{\mathrm{F}}_{\mathrm{L},p}\rangle + E^{\mathrm{LL}}_{pq}|\varphi^{\mathrm{F}}_{\mathrm{L},q}\phi^{\mathrm{B}}_{\mathrm{L},p}\rangle,
\end{aligned} \tag{4.94}$$

where the matrix elements are determined up to an overall prefactor $\Sigma^{\mathrm{LL}}_{pq}$,

$$\begin{aligned}
A^{\mathrm{LL}}_{pq} &= \Sigma^{\mathrm{LL}}_{pq}\,, & B^{\mathrm{LL}}_{pq} &= \Sigma^{\mathrm{LL}}_{pq}e^{-\frac{i}{2}p}\frac{x^+_{\mathrm{L},p}-x^+_{\mathrm{L},q}}{x^-_{\mathrm{L},p}-x^+_{\mathrm{L},q}}\,,\\
C^{\mathrm{LL}}_{pq} &= \Sigma^{\mathrm{LL}}_{pq}e^{-\frac{i}{2}p}e^{+\frac{i}{2}q}\frac{x^-_{\mathrm{L},q}-x^+_{\mathrm{L},q}}{x^-_{\mathrm{L},p}-x^+_{\mathrm{L},q}}\frac{\eta_{\mathrm{L},p}}{\eta_{\mathrm{L},q}}\,, & D^{\mathrm{LL}}_{pq} &= \Sigma^{\mathrm{LL}}_{pq}e^{+\frac{i}{2}q}\frac{x^-_{\mathrm{L},p}-x^-_{\mathrm{L},q}}{x^-_{\mathrm{L},p}-x^+_{\mathrm{L},q}}\,,\\
E^{\mathrm{LL}}_{pq} &= C_{pq}\,, & F^{\mathrm{LL}}_{pq} &= -\Sigma^{\mathrm{LL}}_{pq}e^{-\frac{i}{2}p}e^{+\frac{i}{2}q}\frac{x^+_{\mathrm{L},p}-x^-_{\mathrm{L},q}}{x^-_{\mathrm{L},p}-x^+_{\mathrm{L},q}}\,.
\end{aligned} \tag{4.95}$$

We include a minus sign in F^{LL}_{pq} to account for the fermion permutation. Therefore, in the free theory the S matrix reduces to the graded permutation operator.

Right-right scattering. For the scattering matrix of particles in the ρ_{R} representation

$$\begin{aligned}
S|\varphi^{\mathrm{B}}_{\mathrm{R},p}\varphi^{\mathrm{B}}_{\mathrm{R},q}\rangle &= A^{\mathrm{RR}}_{pq}\,|\varphi^{\mathrm{B}}_{\mathrm{R},q}\varphi^{\mathrm{B}}_{\mathrm{R},p}\rangle, & S|\varphi^{\mathrm{B}}_{\mathrm{R},p}\phi^{\mathrm{F}}_{\mathrm{R},q}\rangle &= B^{\mathrm{RR}}_{pq}|\phi^{\mathrm{F}}_{\mathrm{R},q}\varphi^{\mathrm{B}}_{\mathrm{R},p}\rangle + C^{\mathrm{RR}}_{pq}|\varphi^{\mathrm{B}}_{\mathrm{R},q}\phi^{\mathrm{F}}_{\mathrm{R},p}\rangle,\\
S|\phi^{\mathrm{F}}_{\mathrm{R},p}\phi^{\mathrm{F}}_{\mathrm{R},q}\rangle &= F^{\mathrm{RR}}_{pq}\,|\phi^{\mathrm{F}}_{\mathrm{R},q}\phi^{\mathrm{F}}_{\mathrm{R},p}\rangle, & S|\phi^{\mathrm{F}}_{\mathrm{R},p}\varphi^{\mathrm{B}}_{\mathrm{R},q}\rangle &= D^{\mathrm{RR}}_{pq}|\varphi^{\mathrm{B}}_{\mathrm{R},q}\phi^{\mathrm{F}}_{\mathrm{R},p}\rangle + E^{\mathrm{RR}}_{pq}|\phi^{\mathrm{F}}_{\mathrm{R},q}\varphi^{\mathrm{B}}_{\mathrm{R},p}\rangle,
\end{aligned} \tag{4.96}$$

with

$$
\begin{aligned}
A^{\mathrm{RR}}_{pq} &= \Sigma^{\mathrm{RR}}_{pq}\,, & B^{\mathrm{RR}}_{pq} &= \Sigma^{\mathrm{RR}}_{pq} e^{-\frac{i}{2}p}\frac{x^+_{\mathrm{R},p}-x^+_{\mathrm{R},q}}{x^-_{\mathrm{R},p}-x^+_{\mathrm{R},q}}\,,\\
C^{\mathrm{RR}}_{pq} &= \Sigma^{\mathrm{RR}}_{pq} e^{-\frac{i}{2}p}e^{+\frac{i}{2}q}\frac{x^-_{\mathrm{R},q}-x^+_{\mathrm{R},q}}{x^-_{\mathrm{R},p}-x^+_{\mathrm{R},q}}\frac{\eta_{\mathrm{R},p}}{\eta_{\mathrm{R},q}}\,, & D^{\mathrm{RR}}_{pq} &= \Sigma^{\mathrm{RR}}_{pq} e^{+\frac{i}{2}q}\frac{x^-_{\mathrm{R},p}-x^-_{\mathrm{R},q}}{x^-_{\mathrm{R},p}-x^+_{\mathrm{R},q}}\,,\\
E^{\mathrm{RR}}_{pq} &= C_{pq}\,, & F^{\mathrm{RR}}_{pq} &= -\Sigma^{\mathrm{RR}}_{pq} e^{-\frac{i}{2}p}e^{+\frac{i}{2}q}\frac{x^+_{\mathrm{R},p}-x^-_{\mathrm{R},q}}{x^-_{\mathrm{R},p}-x^+_{\mathrm{R},q}}\,.
\end{aligned}
\tag{4.97}
$$

Left-right scattering. Scattering particles in the left and right representation, we have

$$
\begin{aligned}
S|\phi^{\mathrm{B}}_{\mathrm{L},p}\varphi^{\mathrm{B}}_{\mathrm{R},q}\rangle &= A^{\mathrm{LR}}_{pq}|\varphi^{\mathrm{B}}_{\mathrm{R},q}\phi^{\mathrm{B}}_{\mathrm{L},p}\rangle + B^{\mathrm{LR}}_{pq}|\phi^{\mathrm{F}}_{\mathrm{R},q}\varphi^{\mathrm{F}}_{\mathrm{L},p}\rangle, & S|\phi^{\mathrm{B}}_{\mathrm{L},p}\phi^{\mathrm{F}}_{\mathrm{R},q}\rangle &= C^{\mathrm{LR}}_{pq}\,|\phi^{\mathrm{F}}_{\mathrm{R},q}\phi^{\mathrm{B}}_{\mathrm{L},p}\rangle,\\
S|\varphi^{\mathrm{F}}_{\mathrm{L},p}\phi^{\mathrm{F}}_{\mathrm{R},q}\rangle &= E^{\mathrm{LR}}_{pq}|\phi^{\mathrm{F}}_{\mathrm{R},q}\varphi^{\mathrm{F}}_{\mathrm{L},p}\rangle + F^{\mathrm{LR}}_{pq}|\varphi^{\mathrm{B}}_{\mathrm{R},q}\phi^{\mathrm{B}}_{\mathrm{L},p}\rangle, & S|\varphi^{\mathrm{F}}_{\mathrm{L},p}\varphi^{\mathrm{B}}_{\mathrm{R},q}\rangle &= D^{\mathrm{LR}}_{pq}\,|\varphi^{\mathrm{B}}_{\mathrm{R},q}\varphi^{\mathrm{F}}_{\mathrm{L},p}\rangle,
\end{aligned}
\tag{4.98}
$$

with

$$
\begin{aligned}
A^{\mathrm{LR}}_{pq} &= \Sigma^{\mathrm{LR}}_{pq} e^{-\frac{i}{2}p}\frac{1-x^+_{\mathrm{L},p}x^-_{\mathrm{R},q}}{1-x^-_{\mathrm{L},p}x^-_{\mathrm{R},q}}\,, & B^{\mathrm{LR}}_{pq} &= \Sigma^{\mathrm{LR}}_{pq} e^{-\frac{i}{2}p}e^{-\frac{i}{2}q}\frac{2i}{h}\frac{\eta_{\mathrm{L},p}\eta_{\mathrm{R},q}}{1-x^-_{\mathrm{L},p}x^-_{\mathrm{R},q}}\,,\\
C^{\mathrm{LR}}_{pq} &= \Sigma^{\mathrm{LR}}_{pq}\,, & D^{\mathrm{LR}}_{pq} &= \Sigma^{\mathrm{LR}}_{pq} e^{-\frac{i}{2}p}e^{-\frac{i}{2}q}\frac{1-x^+_{\mathrm{L},p}x^+_{\mathrm{R},q}}{1-x^-_{\mathrm{L},p}x^-_{\mathrm{R},q}}\,,\\
E^{\mathrm{LR}}_{pq} &= -\Sigma^{\mathrm{LR}}_{pq} e^{-\frac{i}{2}q}\frac{1-x^-_{\mathrm{L},p}x^+_{\mathrm{R},q}}{1-x^-_{\mathrm{L},p}x^-_{\mathrm{R},q}}\,, & F^{\mathrm{LR}}_{pq} &= -B^{\mathrm{LR}}_{pq}\,.
\end{aligned}
\tag{4.99}
$$

Right-left scattering. The right-left S matrix is related to the left-right one by unitarity. It reads

$$
\begin{aligned}
S|\varphi^{\mathrm{B}}_{\mathrm{R},p}\phi^{\mathrm{B}}_{\mathrm{L},q}\rangle &= A^{\mathrm{RL}}_{pq}|\phi^{\mathrm{B}}_{\mathrm{L},q}\varphi^{\mathrm{B}}_{\mathrm{R},p}\rangle + B^{\mathrm{RL}}_{pq}|\varphi^{\mathrm{F}}_{\mathrm{L},q}\phi^{\mathrm{F}}_{\mathrm{R},p}\rangle, & S|\varphi^{\mathrm{B}}_{\mathrm{R},p}\varphi^{\mathrm{F}}_{\mathrm{L},q}\rangle &= C^{\mathrm{RL}}_{pq}\,|\varphi^{\mathrm{F}}_{\mathrm{L},q}\varphi^{\mathrm{B}}_{\mathrm{R},p}\rangle,\\
S|\phi^{\mathrm{F}}_{\mathrm{R},p}\varphi^{\mathrm{F}}_{\mathrm{L},q}\rangle &= E^{\mathrm{RL}}_{pq}|\varphi^{\mathrm{F}}_{\mathrm{L},q}\phi^{\mathrm{F}}_{\mathrm{R},p}\rangle + F^{\mathrm{RL}}_{pq}|\phi^{\mathrm{B}}_{\mathrm{L},q}\varphi^{\mathrm{B}}_{\mathrm{R},p}\rangle, & S|\phi^{\mathrm{F}}_{\mathrm{R},p}\phi^{\mathrm{B}}_{\mathrm{L},q}\rangle &= D^{\mathrm{RL}}_{pq}\,|\phi^{\mathrm{B}}_{\mathrm{L},q}\phi^{\mathrm{F}}_{\mathrm{R},p}\rangle,
\end{aligned}
\tag{4.100}
$$

with

$$
\begin{aligned}
A^{\mathrm{RL}}_{pq} &= \Sigma^{\mathrm{RL}}_{pq} e^{+\frac{i}{2}q}\frac{1-x^+_{\mathrm{R},p}x^-_{\mathrm{L},q}}{1-x^+_{\mathrm{R},p}x^+_{\mathrm{L},q}}\,, & B^{\mathrm{RL}}_{pq} &= \Sigma^{\mathrm{RL}}_{pq}\frac{2i}{h}\frac{\eta_{\mathrm{R},p}\eta_{\mathrm{L},q}}{1-x^+_{\mathrm{R},p}x^+_{\mathrm{L},q}}\,,\\
C^{\mathrm{RL}}_{pq} &= \Sigma^{\mathrm{RL}}_{pq} e^{+\frac{i}{2}p}e^{+\frac{i}{2}q}\frac{1-x^-_{\mathrm{R},p}x^-_{\mathrm{L},q}}{1-x^+_{\mathrm{R},p}x^+_{\mathrm{L},q}}\,, & D^{\mathrm{RL}}_{pq} &= \Sigma^{\mathrm{RL}}_{pq}\,,\\
E^{\mathrm{RL}}_{pq} &= -\Sigma^{\mathrm{RL}}_{pq} e^{+\frac{i}{2}p}\frac{1-x^-_{\mathrm{R},p}x^+_{\mathrm{L},q}}{1-x^+_{\mathrm{R},p}x^+_{\mathrm{L},q}}\,, & F^{\mathrm{RL}}_{pq} &= -B^{\mathrm{RL}}_{pq}\,.
\end{aligned}
\tag{4.101}
$$

Massless scattering. The massless representation coefficients may be obtained either from ρ_{L} or ρ_{R} by taking the $m \to 0$ limit. Similarly, the relevant matrix part from the scattering matrix elements can be constructed from the limit. We choose to obtain the massless S-matrix elements from the left-left scattering. Additional caution is needed when it comes to the statistics of the excitations, since in massless representations we may encounter fermionic highest-weight states. This leads to different signs, which we

spell out here, starting by recalling the standard scattering matrix

$$\begin{aligned} S|\phi^{\rm B}_{{\rm o},p}\phi^{\rm B}_{{\rm o},q}\rangle &= A^{\rm LL}_{pq}\,|\phi^{\rm B}_{{\rm o},q}\phi^{\rm B}_{{\rm o},p}\rangle, \qquad S|\phi^{\rm B}_{{\rm o},p}\varphi^{\rm F}_{{\rm o},q}\rangle = B^{\rm LL}_{pq}|\varphi^{\rm F}_{{\rm o},q}\phi^{\rm B}_{{\rm o},p}\rangle + C^{\rm LL}_{pq}|\phi^{\rm B}_{{\rm o},q}\varphi^{\rm F}_{{\rm o},p}\rangle, \\ S|\varphi^{\rm F}_{{\rm o},p}\varphi^{\rm F}_{{\rm o},q}\rangle &= F^{\rm LL}_{pq}\,|\varphi^{\rm F}_{{\rm o},q}\varphi^{\rm F}_{{\rm o},p}\rangle, \qquad S|\varphi^{\rm F}_{{\rm o},p}\phi^{\rm B}_{{\rm o},q}\rangle = D^{\rm LL}_{pq}|\phi^{\rm B}_{{\rm o},q}\varphi^{\rm F}_{{\rm o},p}\rangle + E^{\rm LL}_{pq}|\varphi^{\rm F}_{{\rm o},q}\phi^{\rm B}_{{\rm o},p}\rangle. \end{aligned} \tag{4.102}$$

When both particles are in the $\tilde{\rho}_{\rm L}$ representation we have, instead

$$\begin{aligned} S|\varphi^{\rm B}_{{\rm o},p}\varphi^{\rm B}_{{\rm o},q}\rangle &= -F^{\rm LL}_{pq}\,|\varphi^{\rm B}_{{\rm o},q}\varphi^{\rm B}_{{\rm o},p}\rangle, \qquad S|\varphi^{\rm B}_{{\rm o},p}\phi^{\rm F}_{{\rm o},q}\rangle = D^{\rm LL}_{pq}|\phi^{\rm F}_{{\rm o},q}\varphi^{\rm B}_{{\rm o},p}\rangle - E^{\rm LL}_{pq}|\varphi^{\rm B}_{{\rm o},q}\phi^{\rm F}_{{\rm o},p}\rangle, \\ S|\phi^{\rm F}_{{\rm o},p}\phi^{\rm F}_{{\rm o},q}\rangle &= -A^{\rm LL}_{pq}\,|\phi^{\rm F}_{{\rm o},q}\phi^{\rm F}_{{\rm o},p}\rangle, \qquad S|\phi^{\rm F}_{{\rm o},p}\varphi^{\rm B}_{{\rm o},q}\rangle = B^{\rm LL}_{pq}|\varphi^{\rm B}_{{\rm o},q}\phi^{\rm F}_{{\rm o},p}\rangle - C^{\rm LL}_{pq}|\phi^{\rm F}_{{\rm o},q}\varphi^{\rm B}_{{\rm o},p}\rangle. \end{aligned} \tag{4.103}$$

In analogy with the above, we could have also defined $A^{\tilde{\rm L}\tilde{\rm L}} \equiv -F^{\rm LL}$, $B^{\tilde{\rm L}\tilde{\rm L}} \equiv D^{\rm LL}$, $C^{\tilde{\rm L}\tilde{\rm L}} \equiv -E^{\rm LL}$, $D^{\tilde{\rm L}\tilde{\rm L}} \equiv B^{\rm LL}$, $E^{\tilde{\rm L}\tilde{\rm L}} \equiv -C^{\rm LL}$, and $F^{\tilde{\rm L}\tilde{\rm L}} \equiv -A^{\rm LL}$. Similarly, in the mixed case we have

$$\begin{aligned} S|\phi^{\rm B}_{{\rm o},p}\varphi^{\rm B}_{{\rm o},q}\rangle &= \;\; B^{\rm LL}_{pq}|\varphi^{\rm B}_{{\rm o},q}\phi^{\rm B}_{{\rm o},p}\rangle - C^{\rm LL}_{pq}|\phi^{\rm F}_{{\rm o},q}\varphi^{\rm F}_{{\rm o},p}\rangle, \qquad S|\phi^{\rm B}_{{\rm o},p}\phi^{\rm F}_{{\rm o},q}\rangle = \;\; A^{\rm LL}_{pq}\,|\phi^{\rm F}_{{\rm o},q}\phi^{\rm B}_{{\rm o},p}\rangle, \\ S|\varphi^{\rm F}_{{\rm o},p}\phi^{\rm F}_{{\rm o},q}\rangle &= -D^{\rm LL}_{pq}|\phi^{\rm F}_{{\rm o},q}\varphi^{\rm F}_{{\rm o},p}\rangle + E^{\rm LL}_{pq}|\varphi^{\rm B}_{{\rm o},q}\phi^{\rm B}_{{\rm o},p}\rangle, \qquad S|\varphi^{\rm F}_{{\rm o},p}\varphi^{\rm B}_{{\rm o},q}\rangle = -F^{\rm LL}_{pq}\,|\varphi^{\rm B}_{{\rm o},q}\varphi^{\rm F}_{{\rm o},p}\rangle, \end{aligned} \tag{4.104}$$

and finally

$$\begin{aligned} S|\varphi^{\rm B}_{{\rm o},p}\phi^{\rm B}_{{\rm o},q}\rangle &= \;\; D^{\rm LL}_{pq}|\phi^{\rm B}_{{\rm o},q}\varphi^{\rm B}_{{\rm o},p}\rangle + E^{\rm LL}_{pq}|\varphi^{\rm F}_{{\rm o},q}\phi^{\rm F}_{{\rm o},p}\rangle, \qquad S|\varphi^{\rm B}_{{\rm o},p}\varphi^{\rm F}_{{\rm o},q}\rangle = -F^{\rm LL}_{pq}\,|\varphi^{\rm F}_{{\rm o},q}\varphi^{\rm B}_{{\rm o},p}\rangle, \\ S|\phi^{\rm F}_{{\rm o},p}\varphi^{\rm F}_{{\rm o},q}\rangle &= -B^{\rm LL}_{pq}|\varphi^{\rm F}_{{\rm o},q}\phi^{\rm F}_{{\rm o},p}\rangle - C^{\rm LL}_{pq}|\phi^{\rm B}_{{\rm o},q}\varphi^{\rm B}_{{\rm o},p}\rangle, \qquad S|\phi^{\rm F}_{{\rm o},p}\phi^{\rm B}_{{\rm o},q}\rangle = \;\; A^{\rm LL}_{pq}\,|\phi^{\rm B}_{{\rm o},q}\phi^{\rm F}_{{\rm o},p}\rangle. \end{aligned} \tag{4.105}$$

Mixed-mass scattering. When considering the massless limit of the representation parameters only for one of the variables, we obtain the mixed-mass S matrix. Again, we have to be cautious regarding the various signs that may arise due to the grading of the highest weight state. Below we list those related to the $\rho'_0 \otimes \rho_-$ and $\rho_- \otimes \rho'_0$ representations, since the ones related to $\rho'_0 \otimes \rho_+$ and $\rho_+ \otimes \rho'_0$ are the same as the ones given in eqs. (4.105) and (4.104), respectively. We have

$$\begin{aligned} S|\varphi^{\rm B}_{{\rm R},p}\varphi^{\rm B}_{{\rm o},q}\rangle &= +C^{\rm Ro}_{pq}\,|\varphi^{\rm B}_{{\rm o},q}\varphi^{\rm B}_{{\rm R},p}\rangle, \qquad S|\varphi^{\rm B}_{{\rm R},p}\phi^{\rm F}_{{\rm o},q}\rangle = +A^{\rm Ro}_{pq}|\phi^{\rm F}_{{\rm o},q}\varphi^{\rm B}_{{\rm R},p}\rangle - B^{\rm Ro}_{pq}|\varphi^{\rm B}_{{\rm o},q}\phi^{\rm F}_{{\rm R},p}\rangle, \\ S|\phi^{\rm F}_{{\rm R},p}\phi^{\rm F}_{{\rm o},q}\rangle &= -D^{\rm Ro}_{pq}|\phi^{\rm F}_{{\rm o},q}\phi^{\rm F}_{{\rm R},p}\rangle, \qquad S|\phi^{\rm F}_{{\rm R},p}\varphi^{\rm B}_{{\rm o},q}\rangle = -E^{\rm Ro}_{pq}|\varphi^{\rm B}_{{\rm o},q}\phi^{\rm F}_{{\rm R},p}\rangle + F^{\rm Ro}_{pq}|\phi^{\rm F}_{{\rm o},q}\varphi^{\rm B}_{{\rm R},p}\rangle, \end{aligned} \tag{4.106}$$

and

$$\begin{aligned} S|\varphi^{\rm B}_{{\rm o},p}\varphi^{\rm B}_{{\rm R},q}\rangle &= +D^{\rm oR}_{pq}\,|\varphi^{\rm B}_{{\rm R},q}\varphi^{\rm B}_{{\rm o},p}\rangle, \qquad S|\varphi^{\rm B}_{{\rm o},p}\phi^{\rm F}_{{\rm R},q}\rangle = -E^{\rm oR}_{pq}|\phi^{\rm F}_{{\rm R},q}\varphi^{\rm B}_{{\rm o},p}\rangle - F^{\rm oR}_{pq}|\varphi^{\rm B}_{{\rm R},q}\phi^{\rm F}_{{\rm o},p}\rangle, \\ S|\phi^{\rm F}_{{\rm o},p}\phi^{\rm F}_{{\rm R},q}\rangle &= -C^{\rm oR}_{pq}\,|\phi^{\rm F}_{{\rm R},q}\phi^{\rm F}_{{\rm o},p}\rangle, \qquad S|\phi^{\rm F}_{{\rm o},p}\varphi^{\rm B}_{{\rm R},q}\rangle = +A^{\rm oR}_{pq}|\varphi^{\rm B}_{{\rm R},q}\phi^{\rm F}_{{\rm o},p}\rangle + B^{\rm oR}_{pq}|\phi^{\rm F}_{{\rm R},q}\varphi^{\rm B}_{{\rm o},p}\rangle. \end{aligned} \tag{4.107}$$

4.7. Dressing factors and the crossing equation

In a relativistic theory we can go from the s- to the t-channel by crossing some of the particles involved. The crossing symmetry allows us to replace an incoming particle by an outgoing antiparticle or vice versa. Analogously, in what follows it will be useful to consider particles whose momentum is analytically continued to the crossed region, *i.e.*

$$p \to -p\,, \qquad E(p) \to -E(p)\,. \tag{4.108}$$

Following the notation of ref. [38] we indicate the crossed momentum as $p^{2\gamma}$. This is justified by the fact that p^{γ} represents the continuation of momentum to the *mirror* region [26] which loosely speaking can be considered as *half crossing*. We will give details on this continuation to the mirror theory in Sec. 6.2, where we need it for the thermodynamic Bethe ansatz equations in the pure RR sector. For a more detailed discussion of the mirror and crossed regions we refer the readers to [111] and, in the context of $\mathrm{AdS}_3 \times \mathrm{S}^3 \times \mathrm{T}^4$, to [59, 61, 62].

Parametrisation after crossing. Under the crossing transformation we have [59]

$$x^{\pm}_{\mathrm{L}}(p^{2\gamma}) = \frac{1}{x^{\pm}_{\mathrm{R}}(p)}\,, \qquad x^{\pm}_{\mathrm{R}}(p^{2\gamma}) = \frac{1}{x^{\pm}_{\mathrm{L}}(p)}\,. \tag{4.109}$$

Hence, the Zhukovsky variables and any rational function thereof map to themselves under a 4γ-shift. Instead, the functions $\eta_{\mathrm{L}}(p)$ and $\eta_{\mathrm{R}}(p)$ behave as it follows,

$$\eta_{\mathrm{L}}(p^{\pm 2\gamma}) = \frac{\pm i}{x^{+}_{\mathrm{R}}(p)}\eta_{\mathrm{R}}(p)\,, \qquad \eta_{\mathrm{R}}(p^{\pm 2\gamma}) = \frac{\pm i}{x^{+}_{\mathrm{L}}(p)}\eta_{\mathrm{L}}(p)\,. \tag{4.110}$$

Crossing for massless modes is essentially given by the $m \to 0$ limit of the massive case and by recalling the identity (4.68). We have

$$x^{\pm}_{\circ}(p^{2\gamma}) = x^{\mp}_{\circ}(p)\,, \qquad \eta_{\circ}(p^{\pm 2\gamma}) = \mp i\sigma_p\, e^{-ip/2}\eta_{\circ}(p)\,. \tag{4.111}$$

Charge conjugation matrix. So far, we considered states with $E > 0$ (*cf.* eq. (4.56)) which are related to unitary representations. However, we can obtain another representation by transforming all the charges and supercharges $\mathbf{J} \to -\mathbf{J}^{\mathrm{st}}$, where st is the supertransposition defined on a matrix as $M^{\mathrm{st}}_{jk} = (-1)^{(F_j+1)F_k}M_{kj}$. This flips the signs of the central charges [111], *i.e.* this representation has $E < 0$. Introducing the charge conjugation matrix $\mathcal{C}$ allows to relate the crossing symmetry with the supertransposition.

For the supercharges the charge conjugation matrix $\mathcal{C}$ satisfies [10]

$$e^{+\frac{i}{2}(4\xi+p)}[\mathbf{q}(\bar{p})]^{\mathrm{st}} = -\mathcal{C}\,\mathbf{q}(p)\mathcal{C}^{-1}\,, \qquad e^{-\frac{i}{2}(4\xi+p)}[\mathbf{s}(\bar{p})]^{\mathrm{st}} = -\mathcal{C}\,\mathbf{s}(p)\mathcal{C}^{-1}\,, \tag{4.112}$$

and similarly for $\widetilde{\mathbf{q}}, \widetilde{\mathbf{s}}$. From the respective anticommutators we get

$$e^{+i(4\xi+p)}[\mathbf{C}(\bar{p})]^{\mathrm{st}} = -\mathcal{C}\,\mathbf{C}(p)\mathcal{C}^{-1}\,, \qquad e^{-i(4\xi+p)}[\mathbf{C}^{\dagger}(\bar{p})]^{\mathrm{st}} = -\mathcal{C}\,\mathbf{C}^{\dagger}(p)\mathcal{C}^{-1}\,, \tag{4.113}$$

while

$$\mathbf{H}(\bar{p}) = -\mathcal{C}\,\mathbf{H}(p)\mathcal{C}^{-1}\,, \qquad \widetilde{\mathbf{H}}(\bar{p}) = -\mathcal{C}\,\widetilde{\mathbf{H}}(p)\mathcal{C}^{-1}\,. \tag{4.114}$$

In the last formula the supertransposition is omitted because the charges are bosonic, and moreover they are diagonal. Considering the four representations of $\mathfrak{psu}(1|1)^{\oplus 2}$ in the basis

$$(\phi^{\mathrm{B}}_{\mathrm{L}}, \varphi^{\mathrm{F}}_{\mathrm{L}},\ \phi^{\mathrm{F}}_{\mathrm{R}}, \varphi^{\mathrm{B}}_{\mathrm{R}},\ \phi^{\mathrm{B}}_{\circ}, \varphi^{\mathrm{F}}_{\circ},\ \phi^{\mathrm{F}}_{\circ}, \varphi^{\mathrm{B}}_{\circ})\,, \tag{4.115}$$

the charge conjugation matrix is given by

$$\mathcal{C} = \begin{pmatrix} 0 & 0 & 0 & 1 & & & & \\ 0 & 0 & i & 0 & & & & \\ 0 & i & 0 & 0 & & & & \\ 1 & 0 & 0 & 0 & & & & \\ & & & & 0 & 0 & 0 & 1 \\ & & & & 0 & 0 & i\sigma & 0 \\ & & & & 0 & i\sigma & 0 & 0 \\ & & & & 1 & 0 & 0 & 0 \end{pmatrix}, \qquad \sigma = -\mathrm{sgn}\big[\sin p/2\big]\,. \tag{4.116}$$

Crossing equation. Coming back to representations of $\mathfrak{psu}(1|1)^{\oplus 4}$ c.e., we will denote the crossing matrix for the larger algebra by $\mathcal{C}$ in the following. The crossing equation is then given by [10, 111]

$$\mathcal{C}_{(1)}\mathbf{S}^{\mathrm{t}_1}(p^{2\gamma},q)\mathcal{C}^{\dagger}_{(1)} = \mathbf{S}^{-1}(p,q)\,, \tag{4.117}$$

where $\mathcal{C}_{(1)} = \mathcal{C}\otimes\mathbf{1}$ with the charge conjugation matrix $\mathcal{C}$. The superscript t_1 indicates the transposition of the S-matrix with respect to the first space. Transposing in the second space leads to a similar crossing equation

$$\mathcal{C}_{(2)}\mathbf{S}^{\mathrm{t}_2}(p,q^{-2\gamma})\mathcal{C}^{\dagger}_{(2)} = \mathbf{S}^{-1}(p,q)\,, \tag{4.118}$$

where the charge conjugation $\mathcal{C}_{(2)} = \mathbf{1}\otimes\mathcal{C}$ acts on the second space, correspondingly.

Another way to obtain the crossing equation is by scattering a *Beisert singlet* $|\mathbf{1}_{12}\rangle$ [19]. The singlet is annihilated by all the central charges. Hence it can be realised as a particle-antiparticle pair where the two excitations have momenta p_1 and $p_2 = p_1^{2\gamma}$. The scattering of the singlet with any excitation Ξ should be trivial, *i.e.*

$$\mathbf{S}(p_1,p_3)\mathbf{S}(p_1^{2\gamma},p_3)\,|\mathbf{1}_{12}\Xi_3\rangle = |\Xi_3\mathbf{1}_{12}\rangle\ . \tag{4.119}$$

For eq. (4.117) or equivalently eq. (4.119) to hold, the prefactors Σ^{**}_{pq} introduced in the S matrix elements need to satisfy the crossing equations. Further they must obey unitarity constraints and need to have the correct analytic structure to give a sensible S-matrix for the full $\mathfrak{psu}(1|1)^{\oplus 4}$ c.e. S matrix. It is possible to rewrite the prefactors Σ^{**}_{pq} in the form [61, 62]

$$\begin{aligned}
\big(\Sigma^{\mathrm{LL}}_{pq}\big)^2 &= \big(\Sigma^{\mathrm{RR}}_{pq}\big)^2 = \frac{e^{i(p-q)}}{\sigma^{**}(p,q)^2}\,\frac{x^-_{*,p}-x^+_{*,q}}{x^+_{*,p}-x^-_{*,q}}\,\frac{1-\frac{1}{x^-_{*,p}x^+_{*,q}}}{1-\frac{1}{x^+_{*,p}x^-_{*,q}}}\,,\\
\big(\Sigma^{\mathrm{LR}}_{pq}\big)^2 &= \frac{e^{ip}}{\sigma^{\mathrm{LR}}(p,q)^2}\,\frac{1-x^-_{\mathrm{L},p}x^-_{\mathrm{R},q}}{1-x^+_{\mathrm{L},p}x^+_{\mathrm{R},q}}\,\frac{1-\frac{1}{x^-_{\mathrm{L},p}x^+_{\mathrm{R},q}}}{1-\frac{1}{x^+_{\mathrm{L},p}x^-_{\mathrm{R},q}}}\,,\\
\big(\Sigma^{\mathrm{RL}}_{pq}\big)^2 &= \frac{e^{-iq}}{\sigma^{\mathrm{RL}}(p,q)^2}\,\frac{1-x^+_{\mathrm{R},p}x^+_{\mathrm{L},q}}{1-x^-_{\mathrm{R},p}x^-_{\mathrm{L},q}}\,\frac{1-\frac{1}{x^-_{\mathrm{R},p}x^+_{\mathrm{L},q}}}{1-\frac{1}{x^+_{\mathrm{R},p}x^-_{\mathrm{L},q}}}\,,
\end{aligned} \tag{4.120}$$

and for the massless case

$$\left(\Sigma^{\circ\circ}_{pq}\right)^2 = -\frac{e^{\frac{i}{2}(p-q)}}{\sigma^{\circ\circ}(p,q)^2}\frac{x^-_{\circ,p}-x^+_{\circ,q}}{x^+_{\circ,p}-x^-_{\circ,q}}\,. \tag{4.121}$$

Moreover, for the mixed-mass cases we have

$$\begin{aligned}
\Sigma^{\bullet\circ}_{\mathrm{Lo}}(p,q)^2 &= e^{+i\frac{p}{2}}\frac{x^-_{\mathrm{L},p}-x^+_{\circ,q}}{x^+_{\mathrm{L},p}-x^+_{\circ,q}}\zeta(p,q)\frac{1}{\sigma^{\bullet\circ}_{\mathrm{Lo}}(p,q)^2}\,,\\
\Sigma^{\circ\bullet}_{\mathrm{oL}}(p,q)^2 &= e^{-i\frac{q}{2}}\frac{x^-_{\circ,p}-x^+_{\mathrm{L},q}}{x^-_{\circ,p}-x^-_{\mathrm{L},q}}\zeta(p,q)\frac{1}{\sigma^{\circ\bullet}_{\mathrm{oL}}(p,q)^2}\,,\\
\Sigma^{\bullet\circ}_{\mathrm{Ro}}(p,q)^2 &= e^{-i(\frac{p}{2}+q)}\frac{(1-x^-_{\mathrm{R},p}x^+_{\circ,q})(1-x^+_{\mathrm{R},p}x^+_{\circ,q})}{(1-x^-_{\mathrm{R},p}x^-_{\circ,q})^2}\tilde{\zeta}(p,q)\frac{1}{\sigma^{\bullet\circ}_{\mathrm{Ro}}(p,q)^2}\,,\\
\Sigma^{\circ\bullet}_{\mathrm{oR}}(p,q)^2 &= e^{+i(p+\frac{q}{2})}\frac{(1-x^-_{\circ,p}x^+_{\mathrm{R},q})(1-x^-_{\circ,p}x^-_{\mathrm{R},q})}{(1-x^+_{\circ,p}x^+_{\mathrm{R},q})^2}\tilde{\zeta}(p,q)\frac{1}{\sigma^{\circ\bullet}_{\mathrm{oR}}(p,q)^2}\,,
\end{aligned} \tag{4.122}$$

where we introduced the functions

$$\begin{aligned}
\zeta(p,q) &= \sqrt{\frac{x^-_{*,p}-x^-_{*,q}}{x^+_{*,p}-x^-_{*,q}}\frac{x^+_{*,p}-x^+_{*,q}}{x^-_{*,p}-x^+_{*,q}}}\,,\\
\tilde{\zeta}(p,q) &= \sqrt{\frac{1-x^+_{*,p}x^+_{*,q}}{1-x^+_{*,p}x^-_{*,q}}\frac{1-x^-_{*,p}x^-_{*,q}}{1-x^-_{*,p}x^+_{*,q}}}.
\end{aligned} \tag{4.123}$$

All of the above formulae are written in terms of some functions σ^{**} which have branch cuts on the Zhukovski plane. The transformations of the Zhukovski variables are given above. Using these expressions, we can find from eq. (4.117) and eq. (4.118) the *crossing equations* for the functions σ^{**} given by

$$\begin{aligned}
&\sigma^{\mathrm{LL}}(p^{+2\gamma},q)^2\sigma^{\mathrm{RL}}(p,q)^2 = g^{\mathrm{RL}}(p,q)\,, && \sigma^{\mathrm{LL}}(p,q)^2\sigma^{\mathrm{RL}}(p^{+2\gamma},q)^2 = \tilde{g}^{\mathrm{LL}}(p,q)\,,\\
&\sigma^{\mathrm{RR}}(p^{+2\gamma},q)^2\sigma^{\mathrm{LR}}(p,q)^2 = g^{\mathrm{LR}}(p,q)\,, && \sigma^{\mathrm{RR}}(p,q)^2\sigma^{\mathrm{LR}}(p^{2\gamma},q)^2 = \tilde{g}^{\mathrm{RR}}(p,q)\,,\\
&\sigma^{\mathrm{LL}}(p,q^{-2\gamma})^2\sigma^{\mathrm{LR}}(p,q)^2 = \frac{1}{\tilde{g}^{\mathrm{LL}}(q^{2\gamma},p)}\,, && \sigma^{\mathrm{LL}}(p,q)^2\sigma^{\mathrm{LR}}(p,q^{-2\gamma})^2 = \frac{1}{g^{\mathrm{RL}}(q^{2\gamma},p)}\,,\\
&\sigma^{\mathrm{RR}}(p,q^{-2\gamma})^2\sigma^{\mathrm{RL}}(p,q)^2 = \frac{1}{\tilde{g}^{\mathrm{RR}}(q^{2\gamma},p)}\,, && \sigma^{\mathrm{RR}}(p,q)^2\sigma^{\mathrm{RL}}(p,q^{-2\gamma})^2 = \frac{1}{g^{\mathrm{LR}}(q^{2\gamma},p)}\,,
\end{aligned} \tag{4.124}$$

where the rational functions $g(p,q)$ and $\tilde{g}(p,q)$ were introduced as

$$\begin{aligned}
g^{**}(p,q) &= e^{-2iq}\frac{\left(1-\frac{1}{x^+_{*,p}x^+_{*,q}}\right)\left(1-\frac{1}{x^-_{*,p}x^-_{*,q}}\right)}{\left(1-\frac{1}{x^+_{*,p}x^-_{*,q}}\right)^2}\frac{x^-_{*,p}-x^+_{*,q}}{x^+_{*,p}-x^-_{*,q}}\,,\\
\tilde{g}^{**}(p,q) &= e^{-2iq}\frac{(x^-_{*,p}-x^+_{*,q})^2}{(x^+_{*,p}-x^+_{*,q})(x^-_{*,p}-x^-_{*,q})}\frac{1-\frac{1}{x^-_{*,p}x^+_{*,q}}}{1-\frac{1}{x^+_{*,p}x^-_{*,q}}}\,.
\end{aligned} \tag{4.125}$$

Similarly, for the massless phase we have that

$$\sigma^{\circ\circ}(p^{2\gamma},q)^2\sigma^{\circ\circ}(p,q)^2=\frac{x^+_{\circ,p}-x^-_{\circ,q}}{x^+_{\circ,p}-x^+_{\circ,q}}\frac{x^-_{\circ,p}-x^+_{\circ,q}}{x^-_{\circ,p}-x^-_{\circ,q}}\,, \tag{4.126}$$

and for the mixed-mass phases,

$$\begin{aligned}\sigma^{\bullet\circ}_{\mathrm{Ro}}(p^{2\gamma},q)^2\sigma^{\bullet\circ}_{\mathrm{Lo}}(p,q)^2&=\frac{x^-_{\mathrm{L},p}-x^+_{\circ,q}}{x^+_{\mathrm{L},p}-x^+_{\circ,q}}\frac{x^+_{\mathrm{L},p}-x^-_{\circ,q}}{x^-_{\mathrm{L},p}-x^-_{\circ,q}}&&=\sigma^{\circ\bullet}_{\mathrm{oL}}(q^{2\gamma},p)^2\sigma^{\circ\bullet}_{\mathrm{oL}}(q,p)^2\,,\\ \sigma^{\bullet\circ}_{\mathrm{Lo}}(p^{2\gamma},q)^2\sigma^{\bullet\circ}_{\mathrm{Ro}}(p,q)^2&=\frac{1-\frac{1}{x^+_{\mathrm{R},p}x^+_{\circ,q}}}{1-\frac{1}{x^+_{\mathrm{R},p}x^-_{\circ,q}}}\frac{1-\frac{1}{x^-_{\mathrm{R},p}x^-_{\circ,q}}}{1-\frac{1}{x^-_{\mathrm{R},p}x^+_{\circ,q}}}&&=\sigma^{\circ\bullet}_{\mathrm{oR}}(q^{2\gamma},p)^2\sigma^{\circ\bullet}_{\mathrm{oR}}(q,p)^2\,.\end{aligned} \tag{4.127}$$

For the detailed description of the cuts of the dressing factors σ^{**} we refer the reader to the review [10] and the original literature [61–63]. In the following Chapter 5 on hexagon form factors we will not use the explicit form of the dressing factors, but merely their properties under crossing and unitarity. However, for the thermodynamic Bethe ansatz in Chapter 6 we will need the dressing factors more explicitly.

4.8. Chapter summary

In this chapter we reviewed a selection of important results of integrability in $\mathrm{AdS}_3\times\mathrm{S}^3\times\mathrm{T}^4$ string theory. In Sec. 4.1 we fixed the light-cone Hamiltonian and proceeded in Sec. 4.2 to study the symmetry algebra $\mathfrak{psu}(1,1|2)_L\oplus\mathfrak{psu}(1,1|2)_R$ of the theory. After light-cone fixing, the algebra factorises to $\mathfrak{psu}(1|1)^{\oplus4}$, the central extension of which was considered in Sec. 4.3. It is worth emphasising again, that this symmetry algebra plays a similar role in $\mathrm{AdS}_3/\mathrm{CFT}_2$ as $\mathfrak{su}(2|2)^{\oplus2}$ plays in $\mathrm{AdS}_5/\mathrm{CFT}_4$. In Sec. 4.4 short representations were considered in order to describe the particle content of the theory in Sec. 4.5. There we considered the different representations, namely left, right and massless, as well as multi-particles representations. Further, we explicitly gave the $\mathfrak{psu}(1|1)^{\oplus2}$ S matrix of [70] in Sec. 4.6 for later convenience. The S matrix consists of blocks capturing the scattering between the different representations and can be found from the symmetry up to an overall dressing phase. Finally, in Sec. 4.7, we considered crossing symmetry and worked out the crossing equations, which the dressing phases of the S matrix need to obey.

Chapter 5.

Hexagon form factors in AdS_3

In Sec. 3.1 we reviewed the hexagon proposal for $AdS_5 \times S^5$ superstrings. The goal is to construct three- [38] and higher-point functions [41, 45] of generic operators by using integrability techniques. This follows a similar idea as in the spectral problem. There, one goes from a closed string to a decompactified worldsheet on which the S matrix may be defined [111]. Similarly, one wants to consider such a decompactification for three-point functions by cutting it into two hexagonal patches. As described in Sec. 3.1 the respective patches contain pieces of each of the three closed-string states, see Fig. 5.1. In the case of $AdS_5 \times S^5$, it was possible [38] to bootstrap the form factors of generic operators by starting from the light-cone gauge symmetries that helped determine the S matrix. It is therefore natural to ask whether a similar construction may be applied to the setup we have at hand in $AdS_3 \times S^3 \times T^4$. In this section we will perform the bootstrap construction and use further constraints to propose a self-consistent multi-particle hexagon form factor. We will further perform a simple test, calculating a protected three-point function and comparing to known results.

5.1. The supertranslation operator and the hexagon subalgebra

In the following we will consider three-point functions in $AdS_3 \times S^3 \times T^4$ with the generic configuration, where one operator is placed at the origin $t = 0$, the second at $t = 1$ and the third is sent to infinity $t = \infty$. Recall that in the case of a two-point function and the S matrix the original $\mathfrak{psu}(1,1|2)^{\oplus 2}$ supersymmetry was broken to $\mathfrak{psu}(1|1)^{\oplus 4}$ by gauge fixing. In the dual CFT this comes from picking a reference two-point function involving one half-BPS operator $O(0)$ and its conjugate $O^\dagger(\infty)$. Similarly, in the case of three-point functions we can ask, what the maximal amount of preserved supersymmetry is. Let us use a similar construction to that of ref. [118].

We begin by choosing a reference half-BPS scalar operator $O(0)$ at $t = 0$. It follows from Sec. 4.2 that this operator is a highest-weight state with

$$-\mathbf{L}_0 = \mathbf{J}^3 = j\,, \qquad -\widetilde{\mathbf{L}}_0 = \widetilde{\mathbf{J}}^3 = j\,. \tag{5.1}$$

We are now interested in constructing translated operators $O(t)$. In terms of generators a translation is given by

$$\mathbf{T} = i\mathbf{L}_- + i\widetilde{\mathbf{L}}_-\,, \tag{5.2}$$

where the $\mathbf{L}_-$ and $\widetilde{\mathbf{L}}_-$ are the left and right lowering operators of the $\mathfrak{psu}(1,1|2)^{\oplus 2}$ algebra. For the three-point function, we are interested in constructing *three* translated operators in a way, that preserves as much (super)symmetry as possible. As it turns

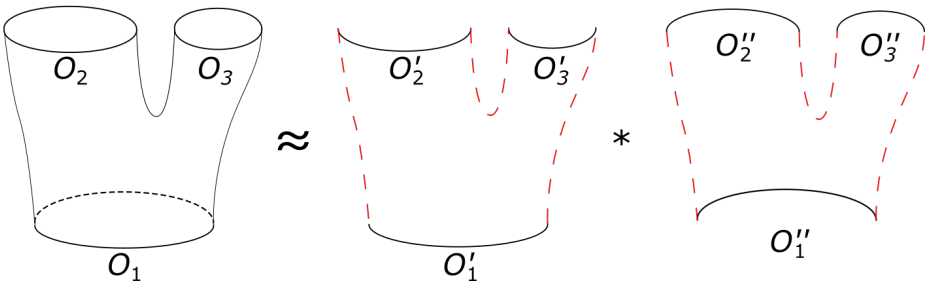

Figure 5.1.: A three-point function can be cut into two hexagons, containing pieces of the three closed-string states.

out, this requires combining the translation with an R-symmetry rotation [38,118]. Let us introduce the supertranslation generator as

$$\mathbf{T}_\kappa = i\mathbf{L}_- + i\widetilde{\mathbf{L}}_- + \kappa\,\mathbf{J}_- + \kappa\,\widetilde{\mathbf{J}}_-\,, \tag{5.3}$$

where $\kappa \in \mathbb{C}$ is some free constant, which will be determined below. We may introduce distinct κ and $\tilde{\kappa}$ for the left and right part of the algebra. Fortunately, we will be able to carry out the bootstrap procedure with a single $\kappa = \tilde{\kappa}$. The twisted translation generator $\mathbf{T}_\kappa$ allows us to construct a one parameter family of operators $O_{t,\kappa}$ sitting at position t starting from $O(0)$, namely

$$O_{t,\kappa} = e^{t\,\mathbf{T}_\kappa}\,O(0)\,e^{-t\,\mathbf{T}_\kappa}\,. \tag{5.4}$$

At the same time, we have that the operator is t-rotated in R-symmetry space. For instance, sending the operator to infinity yields $O_{t=\infty,\kappa} = O^\dagger(\infty)$.

Similarly to picking a two-point function in the spectrum problem, also here we expect some of the $\mathfrak{psu}(1|1)^{\oplus 4}$ centrally extended symmetry described in Sec. 4.3 to be broken. We can construct four supercharges $\mathcal{Q}_1, \mathcal{Q}_2$ and $\widetilde{\mathcal{Q}}_1, \widetilde{\mathcal{Q}}_2$ in $\mathfrak{psu}(1|1)^{\oplus 4}$ with which the supertranslation generator $\mathbf{T}_\kappa$ from eq. (5.3) commutes. The explicit form of these charges is given by

$$\begin{aligned}\mathcal{Q}_A &= \mathbf{S}_A - \frac{i}{\kappa}\,\epsilon_{AB}\,\mathbf{Q}^B,\\ \widetilde{\mathcal{Q}}_A &= \widetilde{\mathbf{Q}}_A - i\kappa\,\epsilon_{AB}\,\widetilde{\mathbf{S}}^B\,.\end{aligned} \tag{5.5}$$

Further, the anticommutation relations can be worked out as

$$\{\mathcal{Q}_A, \mathcal{Q}_A\} = 0, \qquad \{\mathcal{Q}_1, \mathcal{Q}_2\} = -\frac{i}{\kappa}\Big(\{\mathbf{S}_1, \epsilon_{21}\mathbf{Q}^1\} + \{\epsilon_{12}\mathbf{Q}^2, \mathbf{S}_2\}\Big) = 0\,, \tag{5.6}$$

using the relations from Sec. 4.3. Finally, we have

$$\big\{\mathcal{Q}_A, \widetilde{\mathcal{Q}}_B\big\} = -i\kappa\{\mathbf{S}_A, \epsilon_{BC}\widetilde{\mathbf{S}}^C\} - \frac{i}{\kappa}\{\epsilon_{AC}\mathbf{Q}^C, \widetilde{\mathbf{Q}}_B\} = -\frac{i}{\kappa}\epsilon_{AB}\Big(\mathbf{P} - \kappa^2\mathbf{K}\Big)\,, \tag{5.7}$$

where $\mathbf{P}$ and $\mathbf{K}$ are the central extensions of the $\mathfrak{psu}(1|1)^{\oplus 4}$ algebra which are not in $\mathfrak{psu}(1,1|2)^{\oplus 2}$.

For a unitary representation of the $\mathfrak{psu}(1|1)^{\oplus 4}$ algebra the central charges $\mathbf{P}$ and $\mathbf{K}$

should be hermitian conjugate to each other. Further it is possible and convenient to take them to be real, *cf.* eq. (4.53) in Sec. 4.3. Introducing the central charge

$$\mathcal{C} \equiv -\frac{i}{\kappa}\Big(\mathbf{P} - \kappa^2 \mathbf{K}\Big)\,, \tag{5.8}$$

we have that on a multi-excitation state involving momenta $p_1, \dots p_N$,

$$\mathcal{C}\,|p_1, \dots p_N\rangle = \frac{(\kappa^2-1)h}{i\kappa}\,\sin\left(\frac{p_1 + \dots + p_N}{2}\right)\,|p_1, \dots p_N\rangle\,. \tag{5.9}$$

From the definition in eq. (5.5) and their commutation relations, we see, that the charges commuting with the supertranslation generator $\mathbf{T}_\kappa$ from eq. (5.3) form a diagonal $\mathfrak{psu}(1|1)^{\oplus 2}_D$ subalgebra of the centrally extended $\mathfrak{psu}(1|1)^{\oplus 4}$. In the following we will refer to this diagonal $\mathfrak{psu}(1|1)^{\oplus 2}_D$ as the *hexagon subalgebra*.

5.2. Bootstrap principle

For a three-point functions we need to consider three images of the half-BPS operator $O(0)$. Without loss of generality we may take the images under the superstranslation with $t = 0$, $t' = 1$ and $t'' = \infty$, owing to conformal symmetry. The first operator, sitting at $t = 0$, will be $O(0)$, and is the highest-weight state in its R-symmetry multiplet. The third operator will be $O_{t=\infty,\kappa} = O^\dagger(\infty)$, sitting at $t = \infty$ and being the *lowest* weight state in the R-symmetry multiplet. The second operator will be sitting at $t = 1$ and it will be neither the highest- nor the lowest-weight state in the R-symmetry multiplet. The symmetry algebra preserved by this configuration is generated by the four supercharges $\mathcal{Q}_A$ and $\widetilde{\mathcal{Q}}_A$, *i.e.* the hexagon subalgebra. Following [38] we shall assume that this is also the symmetry preserved by the *hexagon operator* $\mathbf{h}$. Indicating the form factor of the operator $\mathbf{h}$ with *any* state Ψ as $\langle \mathbf{h}|\Psi\rangle$, it follows that

$$\langle \mathbf{h}|\mathcal{Q}_A|\Psi\rangle = 0\,, \qquad \langle \mathbf{h}|\widetilde{\mathcal{Q}}_A|\Psi\rangle = 0\,, \tag{5.10}$$

where the supercharges $\mathcal{Q}_A, \widetilde{\mathcal{Q}}_A$ act on the state. Similarly, also anticommutators of these charges annihilate the form factor

$$\langle \mathbf{h}|\mathcal{C}|\Psi\rangle = 0\,. \tag{5.11}$$

The bootstrap condition (5.11) takes a particular simple form, since the central charge $\mathcal{C}$ acts diagonally and independently on the particles' flavour. From eq. (5.9) it follows, whenever the Ramond-Ramond coupling $h \neq 0$, $\mathcal{C}$ only annihilates physical states, *i.e.* on-shell. This is also the case for $\mathbf{P}$ and $\mathbf{K}$ in the spectral problem. However, by setting $\kappa^2 = 1$ eq. (5.11) is also fulfilled for off-shell states. Let us recall that κ is a free parameter in eq. (5.3) and we can choose its value most suitable for the bootstrap procedure. Following the reasoning of [38], we must require $\kappa^2 = 1$. Otherwise, the hexagon form factor in eq. (5.10) would annihilate all non-physical states, which would be too strong a requirement. Similarly to the S matrix, we want to define an off-shell object that acts on just a subset of excitations of a physical state. Therefore, we will set

$$\kappa = 1\,. \tag{5.12}$$

Acting with the charges in eq. (5.10) on the ket yields a set of linear constraints on the hexagon form factor. We will now use these constraints to bootstrap the one- and two-particle form factor.

In the following we will use the bootstrap principle of eq. (5.10) to fix the matrix part of the hexagon form factor up to an overall phase factor. We will explicitly consider the case where $|\Psi\rangle$ is a single-particle state, as well as two-particle states. Unfortunately, the symmetry is not constraining enough to fix multi-particle states. However, using factorized scattering and the Yang-Baxter equation, we will propose a self-consistent ansatz for multi-particle states.

5.2.1. One-particle states

We will use the representation of the $\mathfrak{psu}(1|1)^{\oplus 4}$ c.e. excitations of the theory in terms of tensor products of excitations in $\mathfrak{psu}(1|1)^{\oplus 2}$ c.e. as discussed in Sec. 4.5. For instance, we can represent the massive left representation as $|Y\rangle = |\phi_{\mathrm{L}}^{\mathrm{B}} \otimes \phi_{\mathrm{L}}^{\mathrm{B}}\rangle$, $|\Psi^1\rangle = |\varphi_{\mathrm{L}}^{\mathrm{F}} \otimes \phi_{\mathrm{L}}^{\mathrm{B}}\rangle$, $|\Psi^2\rangle = |\phi_{\mathrm{L}}^{\mathrm{B}} \otimes \varphi_{\mathrm{L}}^{\mathrm{F}}\rangle$ and $|Z\rangle = |\varphi_{\mathrm{L}}^{\mathrm{F}} \otimes \varphi_{\mathrm{L}}^{\mathrm{F}}\rangle$. To act on these excitations, it is useful to rewrite the supercharges of the hexagon subalgebra given in eq. (5.5) in terms of the same decomposition,

$$\begin{aligned} \mathcal{Q}_1 &= \mathbf{s} \otimes \mathbf{1} + i\,\Sigma \otimes \mathbf{q}, \qquad & \mathcal{Q}_2 &= \Sigma \otimes \mathbf{s} - i\,\mathbf{q} \otimes \mathbf{1}, \\ \widetilde{\mathcal{Q}}_1 &= \widetilde{\mathbf{q}} \otimes \mathbf{1} + i\,\Sigma \otimes \widetilde{\mathbf{s}}, \qquad & \widetilde{\mathcal{Q}}_2 &= \Sigma \otimes \widetilde{\mathbf{q}} - i\,\widetilde{\mathbf{s}} \otimes \mathbf{1}, \end{aligned} \tag{5.13}$$

where Σ is again the fermion sign operator. Imposing the bootstrap equation (5.10) we get relations of the form

$$\langle \mathbf{h}|\mathcal{Q}_1|Y(p)\rangle = 0 \quad \Rightarrow \quad \langle \mathbf{h}|\Psi^2(p)\rangle = 0\,, \tag{5.14}$$

which yields that the one-particle form factor $\langle \mathbf{h}|\Psi^2(p)\rangle$ has to vanish. Similarly, it is easy to find that $\langle \mathbf{h}|\Psi^1(p)\rangle = 0$. This is also expected from the $\mathfrak{su}(2)_\bullet$ symmetry. We note, that we have more bootstrap equations than undetermined one-particle form factors. However, they all lead to one single relation

$$\langle \mathbf{h}|Y(p)\rangle = i\,\frac{a_{\mathrm{L}}(p)}{a_{\mathrm{L}}(p)^*}\,\langle \mathbf{h}|Z(p)\rangle = i\,\langle \mathbf{h}|Z(p)\rangle\,, \tag{5.15}$$

where $a_{\mathrm{L}}(p)$ is the representation coefficient introduced in Sec. 4.4. Since the equations we are imposing are linear, we are not able to fix the overall normalisation of the form factor. For the other representations, the bootstrap principle yields analogous results

$$\begin{aligned} \langle \mathbf{h}|Y_p\rangle &= i\,\langle \mathbf{h}|Z_p\rangle, \qquad & \langle \mathbf{h}|\tilde{Z}_p\rangle &= -i\,\langle \mathbf{h}|\tilde{Y}_p\rangle, \\ \langle \mathbf{h}|\chi_p^{\dot{1}}\rangle &= i\,\langle \mathbf{h}|\tilde{\chi}_p^{\dot{1}}\rangle, \qquad & \langle \mathbf{h}|\chi_p^{\dot{2}}\rangle &= \quad i\,\langle \mathbf{h}|\tilde{\chi}_p^{\dot{2}}\rangle, \end{aligned} \tag{5.16}$$

while the remaining form factors vanish,

$$\langle \mathbf{h}|\Psi_p^A\rangle = 0\,, \qquad \langle \mathbf{h}|\widetilde{\Psi}_p^A\rangle = 0\,, \qquad \langle \mathbf{h}|\widetilde{T}_p^{A\dot{A}}\rangle = 0\,. \tag{5.17}$$

Without loss of generality, we normalise the form factor so that

$$\begin{aligned} \langle \mathbf{h}|Y_p\rangle &= 1\,, & \langle \mathbf{h}|Z_p\rangle &= -i\,, & \langle \mathbf{h}|\tilde{Y}_p\rangle &= 1\,, & \langle \mathbf{h}|\tilde{Z}_p\rangle &= -i\,, \\ \langle \mathbf{h}|\chi_p^{\dot{1}}\rangle &= 1\,, & \langle \mathbf{h}|\tilde{\chi}_p^{\dot{1}}\rangle &= -i\,, & \langle \mathbf{h}|\chi_p^{\dot{2}}\rangle &= 1\,, & \langle \mathbf{h}|\tilde{\chi}_p^{\dot{2}}\rangle &= -i\,. \end{aligned} \tag{5.18}$$

Only highest and lowest weight one-particle form factors are non-vanishing. This leads in the massless case to one-particle form factors involving fermions. Note that our choice in eq. (5.18) also ensures left-right symmetry for the massive as well as $\mathfrak{su}(2)_\circ$ symmetry for the massless one-particle form factors.

5.2.2. Two-particle states

We can determine the hexagon form factor for two-particle states by explicitly evaluating the bootstrap constraint from eq. (5.10). At this point it is worth recalling that the hexagon subalgebra that we are exploiting is a *diagonal* $\mathfrak{psu}(1|1)^{\oplus 2}_D$ subalgebra in $\mathfrak{psu}(1|1)^{\oplus 4}$. We will see, that the two-particle form-factor may be expressed in terms of the Borsato–Ohlsson-Sax–Sfondrini S matrix [70]. This does not come as a surprise as the scattering matrix was also bootstrapped from two short $\mathfrak{psu}(1|1)^{\oplus 2}$ representations. The analogous also happens in $\mathrm{AdS}_5 \times \mathrm{S}^5$, where the hexagon subalgebra is a diagonal $\mathfrak{psu}(2|2)_D$ and relates the hexagon to the Beisert S matrix [19], *cf.* also Sec. 3.1. A solution of all bootstrap equations for the two-particle form factor may be written explicitly in terms of the S-matrix elements of Sec. 4.6. Note that, as expected, we are unable to fix the overall prefactor for each choice of irreducible representations. We will denote the prefactors as $h(p,q)$ and study their properties in Sec. 5.4.

Form factor for two massive excitations. Solving the bootstrap conditions (5.10) explicitly, we have to distinguish, whether the two exitations are left or right. When they are both left we have

$$\begin{aligned} \langle \mathbf{h}|Y_pY_q\rangle &= +A^{\mathrm{LL}}_{pq}, & \langle \mathbf{h}|Z_pZ_q\rangle &= +F^{\mathrm{LL}}_{pq}, \\ \langle \mathbf{h}|Y_pZ_q\rangle &= -iB^{\mathrm{LL}}_{pq}, & \langle \mathbf{h}|Z_pY_q\rangle &= -iD^{\mathrm{LL}}_{pq}, \\ \langle \mathbf{h}|\Psi^2_p\Psi^1_q\rangle &= +iC^{\mathrm{LL}}_{pq}, & \langle \mathbf{h}|\Psi^1_p\Psi^2_q\rangle &= -iC^{\mathrm{LL}}_{pq}. \end{aligned} \tag{5.19}$$

When both particles are right we get

$$\begin{aligned} \langle \mathbf{h}|\tilde{Y}_p\tilde{Y}_q\rangle &= +A^{\mathrm{RR}}_{pq}, & \langle \mathbf{h}|\tilde{Z}_p\tilde{Z}_q\rangle &= +F^{\mathrm{RR}}_{pq}, \\ \langle \mathbf{h}|\tilde{Y}_p\tilde{Z}_q\rangle &= -iB^{\mathrm{RR}}_{pq}, & \langle \mathbf{h}|\tilde{Z}_p\tilde{Y}_q\rangle &= -iD^{\mathrm{RR}}_{pq}, \\ \langle \mathbf{h}|\tilde{\Psi}^1_p\tilde{\Psi}^2_q\rangle &= -iC^{\mathrm{RR}}_{pq}, & \langle \mathbf{h}|\tilde{\Psi}^2_p\tilde{\Psi}^1_q\rangle &= +iC^{\mathrm{RR}}_{p,q}. \end{aligned} \tag{5.20}$$

In the case of mixed chirality, we find for the left–right form factors

$$\begin{aligned} \langle \mathbf{h}|Y_p\tilde{Y}_q\rangle &= +A^{\mathrm{LR}}_{pq}, & \langle \mathbf{h}|\Psi^1_p\tilde{\Psi}^2_q\rangle &= -F^{\mathrm{LR}}_{pq}, \\ \langle \mathbf{h}|\Psi^2_p\tilde{\Psi}^1_q\rangle &= -B^{\mathrm{LR}}_{pq}, & \langle \mathbf{h}|Z_p\tilde{Y}_q\rangle &= -iD^{\mathrm{LR}}_{pq}, \\ \langle \mathbf{h}|Y_p\tilde{Z}_q\rangle &= -iC^{\mathrm{LR}}_{pq}, & \langle \mathbf{h}|Z_p\tilde{Z}_q\rangle &= +E^{\mathrm{LR}}_{pq}. \end{aligned} \tag{5.21}$$

Finally, for right–left we have

$$\begin{aligned}
\langle \mathbf{h}|\tilde{Y}_p Y_q\rangle &= +A^{\mathrm{RL}}_{pq}, & \langle \mathbf{h}|\tilde{\Psi}^2_p \Psi^1_q\rangle &= -F^{\mathrm{RL}}_{pq},\\
\langle \mathbf{h}|\tilde{\Psi}^1_p \Psi^2_q\rangle &= -B^{\mathrm{RL}}_{pq}, & \langle \mathbf{h}|\tilde{Z}_p Y_q\rangle &= -iD^{\mathrm{RL}}_{pq},\\
\langle \mathbf{h}|\tilde{Y}_p Z_q\rangle &= -iC^{\mathrm{RL}}_{pq}, & \langle \mathbf{h}|\tilde{Z}_p Z_q\rangle &= +E^{\mathrm{RL}}_{pq}.
\end{aligned} \tag{5.22}$$

One massless and one massive particle. In this case we have left and right massive particles and massless particles carrying the $\mathfrak{su}(2)_\circ$ charge. Further, we have to distinguish their order, *i.e.* massive–massless or massless–massive. Fortunately, it turns out that the hexagon form factor is blind to the $\mathfrak{su}(2)_\circ$ charge, which allows us to write the formulae in a more compact way. This is not surprising, as the hexagon subalgebra which we are using here commutes with $\mathfrak{su}(2)_\circ$.

In the case of one left-massive particle and one massless particle we obtain

$$\begin{aligned}
\langle \mathbf{h}|Y_p \chi^{\dot{A}}_q\rangle &= +A^{\mathrm{Lo}}_{pq}\,, & \langle \mathbf{h}|Z_p \tilde{\chi}^{\dot{A}}_q\rangle &= +F^{\mathrm{Lo}}_{pq}\,,\\
\langle \mathbf{h}|Y_p \tilde{\chi}^{\dot{A}}_q\rangle &= -iB^{\mathrm{Lo}}_{pq}\,, & \langle \mathbf{h}|Z_p \chi^{\dot{A}}_q\rangle &= -iD^{\mathrm{Lo}}_{pq}\,,\\
\langle \mathbf{h}|\Psi^2_p T^{\dot{A}1}_q\rangle &= +iC^{\mathrm{Lo}}_{pq}\,, & \langle \mathbf{h}|\Psi^1_p T^{\dot{A}2}_q\rangle &= -iC^{\mathrm{Lo}}_{pq}\,.
\end{aligned} \tag{5.23}$$

Similarly, for one right-massive particle and one massless particle we have

$$\begin{aligned}
\langle \mathbf{h}|\tilde{Y}_p \chi^{\dot{A}}_q\rangle &= +A^{\mathrm{Ro}}_{pq}\,, & \langle \mathbf{h}|\tilde{\Psi}^2_p T^{\dot{A}1}_q\rangle &= -F^{\mathrm{Ro}}_{pq}\,,\\
\langle \mathbf{h}|\tilde{\Psi}^1_p T^{\dot{A}2}_q\rangle &= -B^{\mathrm{Ro}}_{pq}\,, & \langle \mathbf{h}|\tilde{Z}_p \chi^{\dot{A}}_q\rangle &= -iD^{\mathrm{Ro}}_{pq}\,,\\
\langle \mathbf{h}|\tilde{Y}_p \tilde{\chi}^{\dot{A}}_q\rangle &= -iC^{\mathrm{Ro}}_{pq}\,, & \langle \mathbf{h}|\tilde{Z}_p \tilde{\chi}^{\dot{A}}_q\rangle &= +E^{\mathrm{Ro}}_{pq}\,.
\end{aligned} \tag{5.24}$$

Let us also list the mixed-mass form factors when particles are in the reversed order,

$$\begin{aligned}
\langle \mathbf{h}|\chi^{\dot{A}}_p Y_q\rangle &= +A^{\mathrm{oL}}_{pq}\,, & \langle \mathbf{h}|\tilde{\chi}^{\dot{A}}_p Z_q\rangle &= +F^{\mathrm{oL}}_{pq}\,,\\
\langle \mathbf{h}|\chi^{\dot{A}}_p Z_q\rangle &= -iB^{\mathrm{oL}}_{pq}\,, & \langle \mathbf{h}|\tilde{\chi}^{\dot{A}}_p Y_q\rangle &= -iD^{\mathrm{oL}}_{pq}\,,\\
\langle \mathbf{h}|T^{\dot{A}2}_p \Psi^1_q\rangle &= -iC^{\mathrm{oL}}_{pq}\,, & \langle \mathbf{h}|T^{\dot{A}1}_p \Psi^2_q\rangle &= +iC^{\mathrm{oL}}_{pq}\,,
\end{aligned} \tag{5.25}$$

and finally

$$\begin{aligned}
\langle \mathbf{h}|\chi^{\dot{A}}_p \tilde{Y}_q\rangle &= +A^{\mathrm{oR}}_{pq}\,, & \langle \mathbf{h}|T^{\dot{A}1}_p \tilde{\Psi}^2_q\rangle &= +F^{\mathrm{oR}}_{pq}\,,\\
\langle \mathbf{h}|T^{\dot{A}2}_p \tilde{\Psi}^1_q\rangle &= +B^{\mathrm{oR}}_{pq}\,, & \langle \mathbf{h}|\tilde{\chi}^{\dot{A}}_p \tilde{Y}_q\rangle &= -iD^{\mathrm{oR}}_{pq}\,,\\
\langle \mathbf{h}|\chi^{\dot{A}}_p \tilde{Z}_q\rangle &= -iC^{\mathrm{oR}}_{pq}\,, & \langle \mathbf{h}|\tilde{\chi}^{\dot{A}}_p \tilde{Z}_q\rangle &= +E^{\mathrm{oR}}_{pq}\,.
\end{aligned} \tag{5.26}$$

Two massless particles. The massless two-particle form factor is again blind to the $\mathfrak{su}(2)_\circ$, which allows us to compactly write

$$\begin{aligned}
\langle \mathbf{h}|\chi^{\dot{A}}_p \chi^{\dot{B}}_q\rangle &= +A^{\mathrm{oo}}_{pq}, & \langle \mathbf{h}|\tilde{\chi}^{\dot{A}}_p \tilde{\chi}^{\dot{B}}_q\rangle &= +F^{\mathrm{oo}}_{pq},\\
\langle \mathbf{h}|\chi^{\dot{A}}_p \tilde{\chi}^{\dot{B}}_q\rangle &= -iB^{\mathrm{oo}}_{pq}, & \langle \mathbf{h}|\tilde{\chi}^{\dot{A}}_p \chi^{\dot{B}}_q\rangle &= -iD^{\mathrm{oo}}_{pq},\\
\langle \mathbf{h}|T^{\dot{A}1} T^{\dot{B}2}\rangle &= +iC^{\mathrm{oo}}_{pq}, & \langle \mathbf{h}|T^{\dot{A}2} T^{\dot{B}1}\rangle &= -iC^{\mathrm{oo}}_{pq}.
\end{aligned} \tag{5.27}$$

Let us stress here again that the eqs. (5.10) we have imposed are linear. The results obtained above for the different blocks, *i.e.* left–left, left–right, *etc.*, are only determined

up to an overall factor. Hence, multiplying each block by an arbitrary function, yields new solutions. Similarly, in the S matrix bootstrap the matrix elements are fixed up to the prefactors $\Sigma^{\mathrm{LL}}_{p,q}$, $\Sigma^{\mathrm{LR}}_{p,q}$, *etc.* Hence, additional constraints are necessary for finding these phase factors. We shall use further constraints later to determine the hexagon prefactors $h(p,q)$, see Sec. 5.4.

The possibility of writing the formulae in such a compact way is already a sign of the symmetry structure underlying the form factor. We shall further investigate this in the next section.

5.2.3. General form of the two-particle hexagon form factor

We found, that the two-particle hexagon form factors are related to S matrix elements. It seems therefore natural to ask, whether we can summarize it in a way that encompasses the different representations. To obtain this, let us denote a generic $\mathfrak{psu}(1|1)^{\oplus 4}$ excitation in the tensor product form of Sec. 4.3 as

$$\Xi^{a\acute{a}} \equiv \xi^a \otimes \acute{\xi}^{\acute{a}}\,, \tag{5.28}$$

where the prime denotes the second entry of the tensor product. Here ξ^a and $\acute{\xi}^{\acute{a}}$ could transform under any of the representations which we encountered in Sec. 4.5, *i.e.* $\rho_\pm$, ρ_0 or ρ_0'. The information of the representation is hidden in the indices a and $\acute{a}$ for sake of readability. Then, we can relate the two-particle hexagon form factor to the S matrix as

$$\begin{aligned}\langle \mathbf{h}|\Xi^{a\acute{a}}_p \Xi^{b\acute{b}}_q\rangle &= \mathbf{K}_p\mathbf{K}_q(-1)^{(F_a+F_{\acute{a}})F_b}\Big[|\xi^b_q\xi^a_p\rangle \otimes \mathbf{S}|\acute{\xi}^{\acute{a}}_p\acute{\xi}^{\acute{b}}_q\rangle\Big]\\ &= (-1)^{(F_a+F_{\acute{a}})F_b}\, S^{\acute{a}\acute{b}}_{\acute{d}\acute{c}}(p,q)\mathbf{K}_p\mathbf{K}_q\Big[|\xi^b_q\xi^a_p\rangle \otimes |\acute{\xi}^{\acute{d}}_q\acute{\xi}^{\acute{c}}_p\rangle\Big],\end{aligned} \tag{5.29}$$

where we have introduced the *contraction operator*

$$\begin{aligned}\mathbf{K}_p \equiv &\Big(h_Y \frac{\partial}{\partial\acute{\phi}^{\mathrm{B}}_{\mathrm{L}}(p)}\frac{\partial}{\partial\phi^{\mathrm{B}}_{\mathrm{L}}(p)} + h_Z \frac{\partial}{\partial\acute{\varphi}^{\mathrm{F}}_{\mathrm{L}}(p)}\frac{\partial}{\partial\varphi^{\mathrm{F}}_{\mathrm{L}}(p)}\Big)\\ &+\Big(h_{\tilde{Y}} \frac{\partial}{\partial\acute{\varphi}^{\mathrm{B}}_{\mathrm{R}}(p)}\frac{\partial}{\partial\varphi^{\mathrm{B}}_{\mathrm{R}}(p)} + h_{\tilde{Z}} \frac{\partial}{\partial\acute{\phi}^{\mathrm{F}}_{\mathrm{R}}(p)}\frac{\partial}{\partial\phi^{\mathrm{F}}_{\mathrm{R}}(p)}\Big)\\ &+\Big(h_{\chi^1} \frac{\partial}{\partial\acute{\phi}^{\mathrm{F}}_{\mathrm{o}}(p)}\frac{\partial}{\partial\phi^{\mathrm{B}}_{\mathrm{o}}(p)} + h_{\tilde{\chi}^1} \frac{\partial}{\partial\acute{\varphi}^{\mathrm{B}}_{\mathrm{o}}(p)}\frac{\partial}{\partial\varphi^{\mathrm{F}}_{\mathrm{o}}(p)}\Big)\\ &+\Big(h_{\chi^2} \frac{\partial}{\partial\acute{\phi}^{\mathrm{B}}_{\mathrm{o}}(p)}\frac{\partial}{\partial\phi^{\mathrm{F}}_{\mathrm{o}}(p)} + h_{\tilde{\chi}^2} \frac{\partial}{\partial\acute{\varphi}^{\mathrm{F}}_{\mathrm{o}}(p)}\frac{\partial}{\partial\varphi^{\mathrm{B}}_{\mathrm{o}}(p)}\Big)\,.\end{aligned} \tag{5.30}$$

Here we also introduced the short-hand notation for the one-particle hexagon form factors of eq. (5.18) as $h_Y = \langle \mathbf{h}|Y\rangle$, *etc.*

Let us elaborate on this notation, as in the first equality in eq. (5.29) we rearrange the excitations and group them with respect to their corresponding factor of the diagonal symmetry algebra. This reordering leads to picking up appropriate fermion signs. Hence we define

$$F_a = \begin{cases} 0 & \text{if } \xi^a \text{ is a boson}\\ 1 & \text{if } \xi^a \text{ is a fermion}\end{cases} \qquad \text{and} \quad F_{\acute{a}} = \begin{cases} 0 & \text{if } \acute{\xi}^{\acute{a}} \text{ is a boson}\\ 1 & \text{if } \acute{\xi}^{\acute{a}} \text{ is a fermion}\end{cases} \tag{5.31}$$

We then scatter the primed particles by using the $\mathfrak{psu}(1|1)^{\oplus 2}_{\text{c.e.}}$ S matrix. Depending on the indices $\acute{a}$, $\acute{b}$, we have to use the S matrix in the appropriate representation, *e.g.* the respective blocks for $\rho_{\text{L}} \otimes \rho_{\text{L}}$, $\rho_{\text{L}} \otimes \rho'_{\text{o}}$, *etc.* This yields the relative S matrix elements, which now additionally contain a prefactor $h^{\acute{a}\acute{b}}(p,q)$, that explicitly depends on the representation. Finally, we act with the contraction operator. From eq. (5.30) we see that $\mathbf{K}_p$ simply picks out the one-particle states with a non-trivial hexagon form factor and assigns them the respective value, *i.e.* $\mathbf{K}_p|\Xi^{a\acute{a}}(p)\rangle = \langle \mathbf{h}|\Xi^{a\acute{a}}\rangle$. While such an operator is not necessary in $\text{AdS}_5 \times \text{S}^5$, it becomes important here. The reason is that one-particle hexagon form factors in the massless representations are non-vanishing for particles with fermionic statistics. This creates a potential ambiguity for massless particles whenever we want to contract multi-particle states. Indeed, by introducing the contraction operator this can be circumvented as the commutator $[\mathbf{K}_p, \mathbf{K}_q]$ does not vanish for massless particles due to the statistics. The graded differential operator $\mathbf{K}_p$ will make it easier to properly account for signs from the statistics. Acting with the contraction operator in eq. (5.29) and keeping track of the statistics we can perfectly reproduce the results which we listed above.

It is worth stressing that this prescription can also be applied to the hexagon in $\text{AdS}_5 \times \text{S}^5$, *cf.* the discussion in Sec. 3.1, which is compatible with the original proposal [38].

5.2.4. Many-particle states

In principle we can also impose eq. (5.10) for three- and higher-particle states. While the symmetry is constraining enough to fix the form factor completely for two-particle states (up to the scalar prefactor for each choice of representations), it is not sufficient to fix the coefficients for a higher number of particles. Therefore, let us utilise the result that the two-particle solution can be written in terms of a factorised S matrix [70, 115]. Then the Yang-Baxter equation allows us to write a self-consistent ansatz which is guaranteed to satisfy all symmetry requirements. This follows the approach in ref. [38] for the proposal of a multi-particle hexagon in $\text{AdS}_5 \times \text{S}^5$. We set

$$\begin{aligned}\big\langle \mathbf{h}\big|\Xi^{a_1\acute{a}_1}_{p_1}\Xi^{a_2\acute{a}_2}_{p_2}\dots\Xi^{a_N\acute{a}_N}_{p_N}\big\rangle \equiv \\ \equiv (-1)^{F_{12\cdots N}}\,\mathbf{K}_{12\cdots N}\Big[\big|\xi^{a_N}_{p_N}\dots\xi^{a_2}_{p_2}\xi^{a_1}_{p_1}\big\rangle \otimes \mathbf{S}_{12\cdots N}\big|\acute{\xi}^{\acute{a}_1}_{p_1}\acute{\xi}^{\acute{a}_1}_{p_1}\dots\acute{\xi}^{\acute{a}_N}_{p_N}\big\rangle\Big]\,,\end{aligned} \tag{5.32}$$

where

$$F_{12\cdots N} \equiv \sum_{1\le i<j\le N}(F_{a_i}+F_{\acute{a}_i})F_{a_j}\,, \qquad \mathbf{K}_{12\cdots N} \equiv \mathbf{K}_{p_1}\mathbf{K}_{p_2}\cdots\mathbf{K}_{p_N}\,, \tag{5.33}$$

and $\mathbf{S}_{12\cdots N}$ is the N-particle S matrix, which factorizes and hence the Yang-Baxter equation can be used. Again, it is worth remarking that the contraction operator $\mathbf{K}$ can also be amended to the case of $\text{AdS}_5 \times \text{S}^5$ and, despite the apparent difference from the original proposal of [38], it is perfectly equivalent to that.

5.3. Representations of the hexagon algebra and crossing

Let us consider more closely the structure of the hexagon subalgebra, which is given by $\mathfrak{psu}(1|1)^{\oplus 2}_{D}$ without any central extension. As stated above, this emerges as a sort of

diagonal subalgebra of $\mathfrak{psu}(1|1)^{\oplus 4}$ c.e., see for instance eq. (5.5). Further, we found that the two-particle hexagon form factor from Sec. 5.2.2 is related to the Borsato–Ohlsson-Sax–Sfondrini $\mathfrak{psu}(1|1)^{\oplus 2}$ c.e. S matrix [70, 115]. We would now like to take a closer look at the tensor product decomposition of these representations. For this we will use that the $\mathrm{AdS}_3 \times \mathrm{S}^3 \times \mathrm{T}^4$ symmetries and representations can be factorised as described in Sec. 4.3. Using the short hand notation introduced above, we can again indicate a $\mathfrak{psu}(1|1)^{\oplus 4}$ state as $\Xi^{a\acute{a}}$ and a generic $\mathfrak{psu}(1|1)^{\oplus 2}$ state as either ξ^a or $\acute{\xi}^{\acute{a}}$ depending on its embedding in the $(\mathfrak{psu}(1|1)^{\oplus 2})^{\otimes 2}$ decomposition. Let us now recall the form of the generators of the hexagon subalgebra $\mathcal{Q}_A$, $\widetilde{\mathcal{Q}}_A$ in terms of this factorisation given in eq. (5.13). Rewriting the charges $\mathcal{Q}_2$ and $\widetilde{\mathcal{Q}}_2$ slightly by multiplying with i for later convenience, we obtain

$$\begin{aligned} \mathcal{Q}_1 &= \mathbf{s} \otimes \mathbf{1} + i\,\Sigma \otimes \mathbf{q}, & i\mathcal{Q}_2 &= \mathbf{q} \otimes \mathbf{1} + i\,\Sigma \otimes \mathbf{s}, \\ \widetilde{\mathcal{Q}}_1 &= \widetilde{\mathbf{q}} \otimes \mathbf{1} + i\,\Sigma \otimes \widetilde{\mathbf{s}}, & i\widetilde{\mathcal{Q}}_2 &= \widetilde{\mathbf{s}} \otimes \mathbf{1} + i\,\Sigma \otimes \widetilde{\mathbf{q}}\,. \end{aligned} \tag{5.34}$$

Of course, this way of writing is completely equivalent. But in fact, it will be easier to consider the representations of the algebra generated by $\mathcal{Q}_1,\ \widetilde{\mathcal{Q}}_1,\ i\mathcal{Q}_2, i\widetilde{\mathcal{Q}}_2$. Similarly, a generic $\mathfrak{psu}(1|1)^{\oplus 2}$ state ξ^a or $\acute{\xi}^{\acute{a}}$ can then be written in the factorized form as

$$|\xi\rangle \equiv \xi \otimes 1\,, \qquad |\acute{\xi}\rangle \equiv 1 \otimes \acute{\xi}\,. \tag{5.35}$$

Massive representations. Let us consider the action of the generators generators (5.34) on massive excitations. We first consider states of the type $|\psi\rangle = \psi \otimes 1$ where $\psi \in \rho_{\mathrm{L}}$ or $\psi \in \rho_{\mathrm{R}}$ is a massive $\mathfrak{psu}(1|1)^{\oplus 2}$ excitation. In the notation of eq. (5.35) we have

$$\begin{aligned} \mathcal{Q}_1\,|\varphi^{\mathrm{F}}_{\mathrm{L}}\rangle &= a^*_{\mathrm{L}}\,|\phi^{\mathrm{B}}_{\mathrm{L}}\rangle\,, & \mathcal{Q}_1\,|\varphi^{\mathrm{B}}_{\mathrm{R}}\rangle &= a^*_{\mathrm{R}}\,|\phi^{\mathrm{F}}_{\mathrm{R}}\rangle\,, \\ i\mathcal{Q}_2\,|\phi^{\mathrm{B}}_{\mathrm{L}}\rangle &= a_{\mathrm{L}}\,|\varphi^{\mathrm{F}}_{\mathrm{L}}\rangle\,, & i\mathcal{Q}_2\,|\phi^{\mathrm{F}}_{\mathrm{R}}\rangle &= a_{\mathrm{R}}\,|\varphi^{\mathrm{B}}_{\mathrm{R}}\rangle\,, \\ \widetilde{\mathcal{Q}}_1\,|\varphi^{\mathrm{F}}_{\mathrm{L}}\rangle &= b_{\mathrm{L}}\,|\phi^{\mathrm{B}}_{\mathrm{L}}\rangle\,, & \widetilde{\mathcal{Q}}_1\,|\varphi^{\mathrm{B}}_{\mathrm{R}}\rangle &= b_{\mathrm{R}}\,|\phi^{\mathrm{F}}_{\mathrm{R}}\rangle\,, \\ i\widetilde{\mathcal{Q}}_2\,|\phi^{\mathrm{B}}_{\mathrm{L}}\rangle &= b^*_{\mathrm{L}}\,|\varphi^{\mathrm{F}}_{\mathrm{L}}\rangle\,, & i\widetilde{\mathcal{Q}}_2\,|\phi^{\mathrm{F}}_{\mathrm{R}}\rangle &= b^*_{\mathrm{R}}\,|\varphi^{\mathrm{B}}_{\mathrm{R}}\rangle\,. \end{aligned} \tag{5.36}$$

Comparing with the $\mathfrak{psu}(1|1)^{\oplus 2}$ c.e. representations reviewed in Sec. 4.2, we see that these are precisely ρ_{L} and ρ_{R}. Of course, this can be easily seen from eq. (5.34), as the action of the charges in the first space is given by $\mathbf{q}$, $\widetilde{\mathbf{q}}$, $\mathbf{s}$ and $\widetilde{\mathbf{s}}$. Considering instead excitations of the form $|\acute{\psi}\rangle = 1 \otimes \psi$, the action looks less trivial. Here we find

$$\begin{aligned} \mathcal{Q}_1\,|\acute{\phi}^{\mathrm{F}}_{\mathrm{R}}\rangle &= ia_{\mathrm{R}}\,|\acute{\varphi}^{\mathrm{B}}_{\mathrm{R}}\rangle\,, & \mathcal{Q}_1\,|\acute{\phi}^{\mathrm{B}}_{\mathrm{L}}\rangle &= ia_{\mathrm{L}}\,|\acute{\varphi}^{\mathrm{F}}_{\mathrm{L}}\rangle\,, \\ i\mathcal{Q}_2\,|\acute{\varphi}^{\mathrm{B}}_{\mathrm{R}}\rangle &= ia^*_{\mathrm{R}}\,|\acute{\phi}^{\mathrm{F}}_{\mathrm{R}}\rangle\,, & i\mathcal{Q}_2\,|\acute{\varphi}^{\mathrm{F}}_{\mathrm{L}}\rangle &= ia^*_{\mathrm{L}}\,|\acute{\phi}^{\mathrm{B}}_{\mathrm{L}}\rangle\,, \\ \widetilde{\mathcal{Q}}_1\,|\acute{\phi}^{\mathrm{F}}_{\mathrm{R}}\rangle &= ib^*_{\mathrm{R}}\,|\acute{\varphi}^{\mathrm{B}}_{\mathrm{R}}\rangle\,, & \widetilde{\mathcal{Q}}_1\,|\acute{\phi}^{\mathrm{B}}_{\mathrm{L}}\rangle &= ib^*_{\mathrm{L}}\,|\acute{\varphi}^{\mathrm{F}}_{\mathrm{L}}\rangle\,, \\ i\widetilde{\mathcal{Q}}_2\,|\acute{\varphi}^{\mathrm{B}}_{\mathrm{R}}\rangle &= ib_{\mathrm{R}}\,|\acute{\phi}^{\mathrm{F}}_{\mathrm{R}}\rangle\,, & i\widetilde{\mathcal{Q}}_2\,|\acute{\varphi}^{\mathrm{F}}_{\mathrm{L}}\rangle &= ib_{\mathrm{L}}\,|\acute{\phi}^{\mathrm{B}}_{\mathrm{L}}\rangle\,. \end{aligned} \tag{5.37}$$

By using the definition of the crossing transformation from Sec. 4.7, we notice that the representations of eq. (5.37) are actually the analytic continuation of those in eq. (5.36). For instance, we find

$$a^*_{\mathrm{L}}(p^{\pm 2\gamma}) = \mp i a_{\mathrm{R}}(p) \qquad \text{and} \qquad b_{\mathrm{L}}(p^{\pm 2\gamma}) = \mp i b^*_{\mathrm{R}}(p)\,, \tag{5.38}$$

where we denote crossing and anti-crossing of a particle of momentum p by $p^{2\gamma}$ and $p^{-2\gamma}$, respectively. Because of this identifications $|\acute{\phi}^{\mathrm{F}}_{\mathrm{R}}\rangle$ and $|\acute{\varphi}^{\mathrm{B}}_{\mathrm{R}}\rangle$ transform as the analytic

continuation of ρ_{L}, while $\acute{\phi}^{\mathrm{B}}_{\mathrm{L}}$ and $\acute{\varphi}^{\mathrm{F}}_{\mathrm{L}}$ transform as the analytic continuation of ρ_{R}. More explicitly, we can identify

$$\begin{aligned} |\acute{\phi}^{\mathrm{B}}_{\mathrm{L}}(p)\rangle &= |\varphi^{\mathrm{B}}_{\mathrm{R}}(p^{-2\gamma})\rangle\ , & |\acute{\varphi}^{\mathrm{F}}_{\mathrm{L}}(p)\rangle &= |\phi^{\mathrm{F}}_{\mathrm{R}}(p^{-2\gamma})\rangle\ , \\ |\acute{\phi}^{\mathrm{F}}_{\mathrm{R}}(p)\rangle &= |\varphi^{\mathrm{F}}_{\mathrm{L}}(p^{-2\gamma})\rangle\ , & |\acute{\varphi}^{\mathrm{B}}_{\mathrm{R}}(p)\rangle &= |\phi^{\mathrm{B}}_{\mathrm{L}}(p^{-2\gamma})\rangle\ . \end{aligned} \tag{5.39}$$

Let us emphasise that the $\mathfrak{psu}(1|1)^{\oplus 2}$ c.e. representations are not invariant under 4γ-shifts, but instead they pick up some minus sign [10]. This is due to the fact that the representation parameter $\eta_*(p)$ from eq. (4.61) is not 4γ-periodic since it is not a meromorphic function of the Zhukovski variables, *cf.* Sec. 4.7. In practice this means that fermions pick up a minus sign after a 4γ transformation,

$$\begin{aligned} \phi^{\mathrm{B}}_{\mathrm{L}}(p^{2\gamma}) &= +\phi^{\mathrm{B}}_{\mathrm{L}}(p^{-2\gamma})\,, & \varphi^{\mathrm{F}}_{\mathrm{L}}(p^{2\gamma}) &= -\varphi^{\mathrm{F}}_{\mathrm{L}}(p^{-2\gamma})\,, \\ \varphi^{\mathrm{B}}_{\mathrm{R}}(p^{2\gamma}) &= +\varphi^{\mathrm{B}}_{\mathrm{R}}(p^{-2\gamma})\,, & \phi^{\mathrm{F}}_{\mathrm{R}}(p^{2\gamma}) &= -\phi^{\mathrm{F}}_{\mathrm{R}}(p^{-2\gamma})\,. \end{aligned} \tag{5.40}$$

Such monodromies are well known from the study of the S matrix in $\mathrm{AdS}_5 \times \mathrm{S}^5$ [111].

These considerations allow us now to consider the true massive excitations of $\mathrm{AdS}_3 \times \mathrm{S}^3 \times \mathrm{T}^4$, *i.e.* those that lie in the $\varrho_{\mathrm{L}} = \rho_{\mathrm{L}} \otimes \rho_{\mathrm{L}}$ and $\varrho_{\mathrm{R}} = \rho_{\mathrm{R}} \otimes \rho_{\mathrm{R}}$ representations. Of course, we could act straightforwardly with the diagonal generators from eq. (5.34) on this representation. However, having seen that we can identify this diagonal algebra as the Borsato–Ohlsson-Sax–Sfondrini $\mathfrak{psu}(1|1)^{\oplus 2}$ c.e. let us use the representations as the tensor products $\rho_{\mathrm{L}} \otimes \rho_{\mathrm{R}}^{-2\gamma}$ and $\rho_{\mathrm{R}} \otimes \rho_{\mathrm{L}}^{-2\gamma}$. More specifically, we write

$$\begin{aligned} Y_p &= \phi^{\mathrm{B}}_{\mathrm{L},p}\, \varphi^{\mathrm{B}}_{\mathrm{R},p^{-2\gamma}}\,, & \tilde{Z}_p &= \phi^{\mathrm{F}}_{\mathrm{R},p}\, \varphi^{\mathrm{F}}_{\mathrm{L},p^{-2\gamma}}\,, \\ \Psi^1_p &= \varphi^{\mathrm{F}}_{\mathrm{L},p}\, \varphi^{\mathrm{B}}_{\mathrm{R},p^{-2\gamma}}\,, & \tilde{\Psi}^1_p &= \varphi^{\mathrm{B}}_{\mathrm{R},p}\, \varphi^{\mathrm{F}}_{\mathrm{L},p^{-2\gamma}}\,, \\ \Psi^2_p &= \phi^{\mathrm{B}}_{\mathrm{L},p}\, \phi^{\mathrm{F}}_{\mathrm{R},p^{-2\gamma}}\,, & \tilde{\Psi}^2_p &= \phi^{\mathrm{F}}_{\mathrm{R},p}\, \phi^{\mathrm{B}}_{\mathrm{L},p^{-2\gamma}}\,, \\ Z_p &= \varphi^{\mathrm{F}}_{\mathrm{L},p}\, \phi^{\mathrm{F}}_{\mathrm{R},p^{-2\gamma}}\,, & \tilde{Y}_p &= \varphi^{\mathrm{B}}_{\mathrm{R},p}\, \phi^{\mathrm{B}}_{\mathrm{L},p^{-2\gamma}}\,. \end{aligned} \tag{5.41}$$

Using these identifications, we find the crossing rules for the physical particles. For the left representation these read

$$\begin{aligned} Y_p = \phi^{\mathrm{B}}_{\mathrm{L},p}\, \varphi^{\mathrm{B}}_{\mathrm{R},p^{-2\gamma}} \quad &\xrightarrow{2\gamma} \quad Y_{p^{2\gamma}} = \phi^{\mathrm{B}}_{\mathrm{L},p^{2\gamma}}\, \varphi^{\mathrm{B}}_{\mathrm{R},p} = +\varphi^{\mathrm{B}}_{\mathrm{R},p}\, \phi^{\mathrm{B}}_{\mathrm{L},p^{-2\gamma}} = +\tilde{Y}_p\,, \\ \Psi^1_p = \varphi^{\mathrm{F}}_{\mathrm{L},p}\, \varphi^{\mathrm{B}}_{\mathrm{R},p^{-2\gamma}} \quad &\xrightarrow{2\gamma} \quad \Psi^1_{p^{2\gamma}} = \varphi^{\mathrm{F}}_{\mathrm{L},p^{2\gamma}}\, \varphi^{\mathrm{B}}_{\mathrm{R},p} = -\varphi^{\mathrm{B}}_{\mathrm{R},p}\, \varphi^{\mathrm{F}}_{\mathrm{L},p^{-2\gamma}} = -\tilde{\Psi}^1_p\,, \\ \Psi^2_p = \phi^{\mathrm{B}}_{\mathrm{L},p}\, \phi^{\mathrm{F}}_{\mathrm{R},p^{-2\gamma}} \quad &\xrightarrow{2\gamma} \quad \Psi^2_{p^{2\gamma}} = \phi^{\mathrm{B}}_{\mathrm{L},p^{2\gamma}}\, \phi^{\mathrm{F}}_{\mathrm{R},p} = +\phi^{\mathrm{F}}_{\mathrm{R},p}\, \phi^{\mathrm{B}}_{\mathrm{L},p^{-2\gamma}} = -\tilde{\Psi}^2_p\,, \\ Z_p = \varphi^{\mathrm{F}}_{\mathrm{L},p}\phi^{\mathrm{F}}_{\mathrm{R},p^{-2\gamma}} \quad &\xrightarrow{2\gamma} \quad Z_{p^{2\gamma}} = \varphi^{\mathrm{F}}_{\mathrm{L},p^{2\gamma}}\, \phi^{\mathrm{F}}_{\mathrm{R},p} = +\phi^{\mathrm{F}}_{\mathrm{R},p}\, \varphi^{\mathrm{F}}_{\mathrm{L},p^{-2\gamma}} = +\tilde{Z}_p\,. \end{aligned} \tag{5.42}$$

Note that we used the automorphism from eq. (5.40) that relates 4γ-shifted representations. This yields an additional minus signs in the second and last line. For the right representation we find similar crossing rules

$$\tilde{Z}_{p^{2\gamma}} = Z_p\,, \qquad \tilde{\Psi}^1_{p^{2\gamma}} = \Psi^1_p\,, \qquad \tilde{\Psi}^2_{p^{2\gamma}} = \Psi^2_p\,, \qquad \tilde{Y}_{p^{2\gamma}} = Y_p\,. \tag{5.43}$$

Let us emphasise, that these signs differ from the ones found in eq. (5.42).

Massless representations. A similar reasoning can be applied to the massless representations of Sec. 4.4. We can obtain the massless representations by taking the

limit $m \to 0$ of either the right or the left representation [62]. In particular we can write

$$\begin{aligned} \mathcal{Q}_1 |\varphi_{\circ}^{\mathrm{F}}\rangle &= a_{\circ}^* |\phi_{\circ}^{\mathrm{B}}\rangle \,, & \mathcal{Q}_1 |\varphi_{\circ}^{\mathrm{B}}\rangle &= a_{\circ}^* |\phi_{\circ}^{\mathrm{F}}\rangle \,, \\ i\mathcal{Q}_2 |\phi_{\circ}^{\mathrm{B}}\rangle &= a_{\circ} |\varphi_{\circ}^{\mathrm{F}}\rangle \,, & i\mathcal{Q}_2 |\phi_{\circ}^{\mathrm{F}}\rangle &= a_{\circ} |\varphi_{\circ}^{\mathrm{B}}\rangle \,, \\ \widetilde{\mathcal{Q}}_1 |\varphi_{\circ}^{\mathrm{F}}\rangle &= b_{\circ} |\phi_{\circ}^{\mathrm{B}}\rangle \,, & \widetilde{\mathcal{Q}}_1 |\varphi_{\circ}^{\mathrm{B}}\rangle &= b_{\circ} |\phi_{\circ}^{\mathrm{F}}\rangle \,, \\ i\widetilde{\mathcal{Q}}_2 |\phi_{\circ}^{\mathrm{B}}\rangle &= b_{\circ}^* |\varphi_{\circ}^{\mathrm{F}}\rangle \,, & i\widetilde{\mathcal{Q}}_2 |\phi_{\circ}^{\mathrm{F}}\rangle &= b_{\circ}^* |\varphi_{\circ}^{\mathrm{B}}\rangle \,, \end{aligned} \tag{5.44}$$

while for massless excitations of the form $|\acute{\psi}\rangle = 1 \otimes \psi$, we have

$$\begin{aligned} \mathcal{Q}_1 |\acute{\phi}_{\circ}^{\mathrm{F}}\rangle &= ia_{\circ} |\acute{\varphi}_{\circ}^{\mathrm{B}}\rangle \,, & \mathcal{Q}_1 |\acute{\phi}_{\circ}^{\mathrm{B}}\rangle &= ia_{\circ} |\acute{\varphi}_{\circ}^{\mathrm{F}}\rangle \,, \\ i\mathcal{Q}_2 |\acute{\varphi}_{\circ}^{\mathrm{B}}\rangle &= ia_{\circ}^* |\acute{\phi}_{\circ}^{\mathrm{F}}\rangle \,, & i\mathcal{Q}_2 |\acute{\varphi}_{\circ}^{\mathrm{F}}\rangle &= ia_{\circ}^* |\acute{\phi}_{\circ}^{\mathrm{B}}\rangle \,, \\ \widetilde{\mathcal{Q}}_1 |\acute{\phi}_{\circ}^{\mathrm{F}}\rangle &= ib_{\circ}^* |\acute{\varphi}_{\circ}^{\mathrm{B}}\rangle \,, & \widetilde{\mathcal{Q}}_1 |\acute{\phi}_{\circ}^{\mathrm{B}}\rangle &= ib_{\circ}^* |\acute{\varphi}_{\circ}^{\mathrm{F}}\rangle \,, \\ i\widetilde{\mathcal{Q}}_2 |\acute{\varphi}_{\circ}^{\mathrm{B}}\rangle &= ib_{\circ} |\acute{\phi}_{\circ}^{\mathrm{F}}\rangle \,, & i\widetilde{\mathcal{Q}}_2 |\acute{\varphi}_{\circ}^{\mathrm{F}}\rangle &= ib_{\circ} |\acute{\phi}_{\circ}^{\mathrm{B}}\rangle \,. \end{aligned} \tag{5.45}$$

Analogously to the massive case, we can then identify

$$\begin{aligned} \acute{\phi}_{\circ}^{\mathrm{B}}(p) &= -\sigma_p \, \varphi_{\circ}^{\mathrm{F}}(p^{-2\gamma}) \,, & \acute{\varphi}_{\circ}^{\mathrm{B}}(p) &= -\sigma_p \, \phi_{\circ}^{\mathrm{F}}(p^{-2\gamma}) \,, \\ \acute{\phi}_{\circ}^{\mathrm{F}}(p) &= \varphi_{\circ}^{\mathrm{B}}(p^{-2\gamma}) \,, & \acute{\varphi}_{\circ}^{\mathrm{F}}(p) &= \phi_{\circ}^{\mathrm{B}}(p^{-2\gamma}) \,. \end{aligned} \tag{5.46}$$

We should highlight an important difference here. In the massive case, crossing linked the left to the right representation. By taking the $m \to 0$ limit we have that the left and right representation are isomorphic. Thus we can link the massless representation to itself, but we need to keep track of the sign $\sigma(p) = -\mathrm{sgn}[\sin(p/2)]$ appearing in the isomorphism. In fact, we have $\sigma(p^{-2\gamma})$ appearing in eq. (5.46), but this can be simplified to $-\sigma(p)$, due to the fact that the momentum p changes sign under $\pm 2\gamma$ crossing. Another difference to the massive case is that the massless representation parameter $\eta_{\circ}(p)$ given in eq. (4.61) is 4γ-periodic, *cf.* Sec. 4.7. Hence, in the massless case we do not pick up a minus sign for the fermions after 4γ,

$$\begin{aligned} \phi_{\circ}^{\mathrm{B}}(p^{2\gamma}) &= +\phi_{\circ}^{\mathrm{B}}(p^{-2\gamma}) \,, & \varphi_{\circ}^{\mathrm{F}}(p^{2\gamma}) &= +\varphi_{\circ}^{\mathrm{F}}(p^{-2\gamma}) \,, \\ \varphi_{\circ}^{\mathrm{B}}(p^{2\gamma}) &= +\varphi_{\circ}^{\mathrm{B}}(p^{-2\gamma}) \,, & \phi_{\circ}^{\mathrm{F}}(p^{2\gamma}) &= +\phi_{\circ}^{\mathrm{F}}(p^{-2\gamma}) \,. \end{aligned} \tag{5.47}$$

Therefore we can write

$$\begin{aligned} \chi_p^{\dot{1}} &= \phi_{\circ,p}^{\mathrm{B}} \, \varphi_{\circ,p^{-2\gamma}}^{\mathrm{B}} \,, & \chi_p^{\dot{2}} &= -i\sigma_p \phi_{\circ,p}^{\mathrm{F}} \, \varphi_{\circ,p^{-2\gamma}}^{\mathrm{F}} \,, \\ T_p^{\dot{1}1} &= \varphi_{\circ,p}^{\mathrm{F}} \, \varphi_{\circ,p^{-2\gamma}}^{\mathrm{B}} \,, & T_p^{\dot{2}1} &= -i\sigma_p \varphi_{\circ,p}^{\mathrm{B}} \, \varphi_{\circ,p^{-2\gamma}}^{\mathrm{F}} \,, \\ T_p^{\dot{1}2} &= -\sigma_p \phi_{\circ,p}^{\mathrm{B}} \, \phi_{\circ,p^{-2\gamma}}^{\mathrm{F}} \,, & T_p^{\dot{2}2} &= -i\phi_{\circ,p}^{\mathrm{F}} \, \phi_{\circ,p^{-2\gamma}}^{\mathrm{B}} \,, \\ \tilde{\chi}_p^{\dot{1}} &= -\sigma_p \varphi_{\circ,p}^{\mathrm{F}} \, \phi_{\circ,p^{-2\gamma}}^{\mathrm{F}} \,, & \tilde{\chi}_p^{\dot{2}} &= -i\varphi_{\circ,p}^{\mathrm{B}} \, \phi_{\circ,p^{-2\gamma}}^{\mathrm{B}} \,. \end{aligned} \tag{5.48}$$

Using these identifications, the crossing rules for the physical particles are given by

$$\begin{aligned} \chi_p^{\dot{1}} = \phi_{\circ,p}^{\mathrm{B}} \, \varphi_{\circ,p^{-2\gamma}}^{\mathrm{B}} \quad &\xrightarrow{2\gamma} \quad \chi_{p^{2\gamma}}^{\dot{1}} = \phi_{\circ,p^{2\gamma}}^{\mathrm{B}} \, \varphi_{\circ,p}^{\mathrm{B}} = i\tilde{\chi}_p^{\dot{2}} \,, \\ T_p^{\dot{1}1} = \varphi_{\circ,p}^{\mathrm{F}} \, \varphi_{\circ,p^{-2\gamma}}^{\mathrm{B}} \quad &\xrightarrow{2\gamma} \quad T_{p^{2\gamma}}^{\dot{1}1} = \varphi_{\circ,p^{2\gamma}}^{\mathrm{F}} \, \varphi_{\circ,p}^{\mathrm{B}} = i\sigma_p T_p^{\dot{2}1} \,, \\ T_p^{\dot{1}2} = -\sigma_p \phi_{\circ,p}^{\mathrm{B}} \, \phi_{\circ,p^{-2\gamma}}^{\mathrm{F}} \quad &\xrightarrow{2\gamma} \quad T_{p^{2\gamma}}^{\dot{1}2} = -\sigma_{p^{2\gamma}} \phi_{\circ,p^{2\gamma}}^{\mathrm{B}} \, \phi_{\circ,p}^{\mathrm{F}} = i\sigma_p T_p^{\dot{2}2} \,, \\ \tilde{\chi}_p^{\dot{1}} = -\sigma_p \varphi_{\circ,p}^{\mathrm{F}} \phi_{\circ,p^{-2\gamma}}^{\mathrm{F}} \quad &\xrightarrow{2\gamma} \quad \tilde{\chi}_{p^{2\gamma}}^{\dot{1}} = -\sigma_{p^{2\gamma}} \varphi_{\circ,p^{2\gamma}}^{\mathrm{F}} \, \phi_{\circ,p}^{\mathrm{F}} = -i\chi_p^{\dot{2}} \,. \end{aligned} \tag{5.49}$$

Similarly, we find

$$\chi^{\dot{2}}_{p^{2\gamma}} = i\tilde{\chi}^{\dot{1}}_{p}\,, \qquad T^{\dot{2}\dot{1}}_{p^{2\gamma}} = i\sigma_p T^{\dot{1}1}_{p}\,, \qquad T^{\dot{2}\dot{2}}_{p^{2\gamma}} = i\sigma_p T^{\dot{1}2}_{p}\,, \qquad \tilde{\chi}^{\dot{2}}_{p^{2\gamma}} = -i\chi^{\dot{1}}_{p}\,. \tag{5.50}$$

In this construction we explicitly used two different representations for $\dot{A} = 1, 2$ to construct the crossing rules. This is essential to understand the rules for the massless tensor-product representation in a similar vein as crossing in the massive case. However, we should stress, that these two massless representations are isomorphic and that the hexagon is blind to the $\mathfrak{su}(2)_\circ$ index. Therefore we can sweep aside the explicit form of the representations and instead use the resulting effective crossing rules

$$\chi^{\dot{A}}_{p^{2\gamma}} = i\tilde{\chi}^{\dot{A}}_{p}\,, \qquad T^{\dot{A}1}_{p^{2\gamma}} = i\sigma_p T^{\dot{A}1}_{p}\,, \qquad T^{\dot{A}2}_{p^{2\gamma}} = i\sigma_p T^{\dot{A}2}_{p}\,, \qquad \tilde{\chi}^{\dot{A}}_{p^{2\gamma}} = -i\chi^{\dot{A}}_{p}\,. \tag{5.51}$$

5.4. The scalar factors

The symmetry given by the hexagon subalgebra allowed us to fix the two-particle hexagon form factor for the various combinations of particles. Since the conditions imposed lead to linear equations, there is still the freedom of a scalar factor $h(p,q)$ for each pair of irreducible representations. This is similar to the role that the dressing phase $\Sigma(p,q)$ plays in the S matrix. For instance, in the case of two left representations we have the dressing phase $\Sigma^{\text{LL}}(p,q)$ in the S matrix and the prefactor $h^{\text{LL}}(p,q)$ in the hexagon. Choosing the normalisation of the massive–massive form factors in a convenient way

$$\begin{aligned} \langle \mathbf{h}|Y_p Y_q\rangle &= h^{\text{LL}}(p,q)\,, & \langle \mathbf{h}|\tilde{Y}_p \tilde{Y}_q\rangle &= h^{\text{RR}}(p,q)\,, \\ \langle \mathbf{h}|Y_p \tilde{Z}_q\rangle &= h^{\text{LR}}(p,q)\,, & \langle \mathbf{h}|\tilde{Z}_p Y_q\rangle &= h^{\text{RL}}(p,q)\,, \end{aligned} \tag{5.52}$$

allows us to use the S matrix elements given in Sec. 4.6 up to simply replacing Σ with h. Further, by imposing left-right symmetry [70], we can halve the number of independent scalar factors like in [61]. We set

$$h^{\bullet\bullet}(p,q) \equiv h^{\text{LL}}(p,q) = h^{\text{RR}}(p,q)\,, \tag{5.53}$$

which ensures that $\langle \mathbf{h}|Y_p Y_q\rangle = \langle \mathbf{h}|\tilde{Y}_p \tilde{Y}_q\rangle$, and so on. Further, setting

$$\tilde{h}^{\bullet\bullet}(p,q) \equiv h^{\text{LR}}(p,q) = e^{\frac{i}{2}(p+q)}\frac{1 - x^-_{\text{R},p}x^-_{\text{L},q}}{1 - x^+_{\text{R},p}x^+_{\text{L},q}} h^{\text{RL}}(p,q)\,, \tag{5.54}$$

ensures that $\langle \mathbf{h}|Y_p \tilde{Z}_q\rangle = \langle \mathbf{h}|\tilde{Y}_p Z_q\rangle$, *etc.* For massless particles, we assume the prefactors to be blind regarding the $\mathfrak{su}(2)_\circ$ structure like it is the case for the prefactors of the S matrix [60, 63, 115]. In this case, we have a single massless dressing factor, which appears as

$$\langle \mathbf{h}|\chi^{\dot{A}}_p \chi^{\dot{B}}_q\rangle = h^{\circ\circ}(p,q)\,. \tag{5.55}$$

Finally, we have processes that involve one massive and one massless particle. Using again $\mathfrak{su}(2)_\circ$ as well as left-right symmetry, we obtain two dressing factors

$$\langle \mathbf{h}|Y_p \chi^{\dot{A}}_q\rangle = \langle \mathbf{h}|\tilde{Y}_p \chi^{\dot{A}}_q\rangle = h^{\bullet\circ}(p,q)\,, \qquad \langle \mathbf{h}|\chi^{\dot{A}}_p Y_q\rangle = \langle \mathbf{h}|\chi^{\dot{A}}_p \tilde{Y}_q\rangle = h^{\circ\bullet}(p,q)\,. \tag{5.56}$$

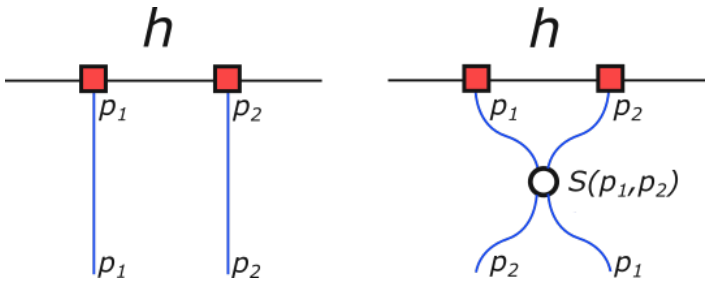

Figure 5.2.: The Watson equation allows us to relate the form factor and its dressing phase $h(p,q)$ to the full S matrix of the theory, complete with dressing factors $\mathbf{S}^{\mathrm{AdS}_3\times\mathrm{S}^3\times\mathrm{T}^4}(p,q)$.

In the following we will further constrain these five prefactors, allowing us to propose a solution. There are three physical constraints we shall impose: The first is the Watson equation, which relates the form factor to the full S matrix of the theory [38, 119, 120]. Further the decoupling condition states that a singlet should decouple from the form factor [19, 38]. This yields a crossing equations for the scalar prefactors. Thirdly, we impose a cyclicity condition for excitations on the form factor.

5.4.1. The Watson equation

The Watson equation relates the original $\mathfrak{psu}(1|1)^{\oplus 4}$ S matrix and the hexagon form factor, see Fig. 5.2. It states that we may scatter a pair of particles in the form factor using the S matrix,

$$\langle \mathbf{h}|\Xi^{a_1\dot{a}_1}_{p_1}\cdots\Xi^{a_j\dot{a}_j}_{p_j}\Xi^{a_{j+1}\dot{a}_{j+1}}_{p_{j+1}}\cdots\rangle = \langle \mathbf{h}|\mathbf{S}^{\mathrm{AdS}_3\times\mathrm{S}^3\times\mathrm{T}^4}_{j,j+1}|\Xi^{a_1\dot{a}_1}_{p_1}\cdots\Xi^{a_j\dot{a}_j}_{p_j}\Xi^{a_{j+1}\dot{a}_{j+1}}_{p_{j+1}}\cdots\rangle\,. \tag{5.57}$$

Importantly, here $\mathbf{S}^{\mathrm{AdS}_3\times\mathrm{S}^3\times\mathrm{T}^4}$ is the full $\mathfrak{psu}(1|1)^{\oplus 4}$ S matrix of [115] including the corresponding dressing factors. Exploiting the factorisation of the multi-particle ansatz, we can restrict to the two-particle form factor to impose this constraint. The resulting expression is a matrix equation. Using the explicit evaluation of the form factors and matrix elements, it boils down to only one non-trivial relation per phase factor h^{**}. Nonetheless, the evaluation of the whole matrix equation yields an important check to ensure that the form factor and the $\mathfrak{psu}(1|1)^{\oplus 4}$ S matrix are compatible, *i.e.* written in the same basis. We find the following conditions

$$\begin{aligned}
\frac{h^{\bullet\bullet}(p,q)}{h^{\bullet\bullet}(q,p)} &= \left[\Sigma^{\bullet\bullet}(p,q)\right]^2, \qquad \frac{\tilde{h}^{\bullet\bullet}(p,q)}{\tilde{h}^{\bullet\bullet}(q,p)} = \left[\tilde{\Sigma}^{\bullet\bullet}(p,q)\right]^2, \\
\frac{h^{\circ\circ}(p,q)}{h^{\circ\circ}(q,p)} &= -\left[\Sigma^{\circ\circ}(p,q)\right]^2, \\
\frac{h^{\bullet\circ}_*(p,q)}{h^{\circ\bullet}_*(q,p)} &= \left[\Sigma^{\bullet\circ}_*(p,q)\right]^2, \qquad \frac{h^{\circ\bullet}_*(p,q)}{h^{\bullet\circ}_*(q,p)} = \left[\Sigma^{\circ\bullet}_*(p,q)\right]^2,
\end{aligned} \tag{5.58}$$

where the asterisk in the subscript stands for either L or R. Though surprising at first glance, the minus sign appearing for massless excitations can be explained by recalling that we are scattering fermions, when looking at highest-weight states. To sum up, these conditions resemble the antisymmetry conditions for Σ that are imposed by braiding unitarity.

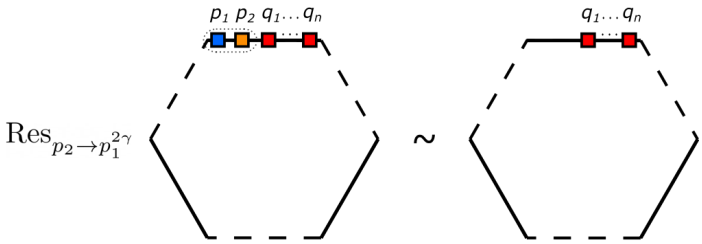

Figure 5.3.: The decoupling condition states that a particle-antiparticle pair decouples from the form factor. In the figure these are the particles with momenta p_1 and p_2, with the latter in the crossed channel. The form factor features a simple pole and its residue is given by the form factor of the remaining particles $q_1, \dots, q_n$. This condition yields crossing equations for the scalar prefactors.

5.4.2. Decoupling condition and crossing

The decoupling condition states that, whenever two particles form a singlet, they decouple from the form factor. More precisely, the singlet must be annihilated by the momentum and energy operators, which means that $p_1 + p_2 = 0$ and $E(p_1) + E(p_2) = 0$. In order to have this, the momenta of the particles p_1 and p_2 cannot both be physical and one of the momenta has to be crossed, *i.e.* $p_1 = p_2^{\pm 2\gamma}$.

Then, when the momenta satisfy this condition, the form factor has a pole. Its residue is given by

$$\mathrm{Res}_{p_2 \to p_1^{2\gamma}} \langle \mathbf{h} | \Xi_{p_1}^{a_1 \acute{a}_1} \Xi_{p_2}^{a_2 \acute{a}_2} \cdots \Xi_{p_N}^{a_N \acute{a}_N} \rangle = C^{a_1 \acute{a}_1, a_2 \acute{a}_2} \langle \mathbf{h} | \Xi_{p_3}^{a_3 \acute{a}_3} \cdots \Xi_{p_N}^{a_N \acute{a}_N} \rangle \,, \tag{5.59}$$

where the factor $C^{a_1 \acute{a}_1, a_2 \acute{a}_2}$ projects onto the singlet representation and must be independent of $p_3, \dots p_N$. Using that the evaluation of the multi-particle hexagon form factor factorises from eq. (5.32), we find that this becomes the requirement, that for the $\mathfrak{psu}(1|1)^{\oplus 2}$ S matrix scattering processes with the singlet are trivial. More precisely, the process of scattering the singlet with a particle of momentum p_3 reads

$$\mathbf{S}_{12}\mathbf{S}_{23}\Big(C_{\acute{a}_1,\acute{a}_2} |\acute{\xi}^{\acute{a}_1}(p_1)\acute{\xi}^{\acute{a}_2}(p_1^{2\gamma})\acute{\xi}^{\acute{a}_3}(p_3)\rangle\Big) = C_{\acute{a}_1,\acute{a}_2}\, |\acute{\xi}^{\acute{a}_3}(p_3)\acute{\xi}^{\acute{a}_1}(p_1)\acute{\xi}^{\acute{a}_2}(p_1^{2\gamma})\rangle \,, \tag{5.60}$$

where the scattering phase on the right-hand side is precisely equal to one. This is precisely the crossing equation (4.119) for the $\mathfrak{psu}(1|1)^{\oplus 2}$ S matrix as derived in ref. [70]. The relationship between the projectors $C_{\acute{a}_1,\acute{a}_2}$ for $\mathfrak{psu}(1|1)^{\oplus 2}$ and $C_{a_1\acute{a}_1,a_2\acute{a}_2}$ for the $\mathfrak{psu}(1|1)^{\oplus 4}$ was discussed in ref. [112]. Therefore, the decoupling condition for the hexagon form factors boils down to the crossing equation of the $\mathfrak{psu}(1|1)^{\oplus 2}$ S matrix, which is now normalised in terms of the prefactors $h(p,q)$. This yields the following crossing equations for the hexagon prefactors in the massive sector,

$$\begin{aligned} h^{\bullet\bullet}(p,q)\tilde{h}^{\bullet\bullet}(p^{2\gamma},q) &= h^{\bullet\bullet}(p,q)\tilde{h}^{\bullet\bullet}(p,q^{-2\gamma}) = \left[e^{-\frac{i}{2}p}\frac{x^+_{*,p} - x^-_{*,q}}{x^-_{*,p} - x^-_{*,q}}\right]^{-1}, \\ h^{\bullet\bullet}(p^{2\gamma},q)\tilde{h}^{\bullet\bullet}(p,q) &= h^{\bullet\bullet}(p,q^{-2\gamma})\tilde{h}^{\bullet\bullet}(p,q) = \left[e^{-\frac{i}{2}p}\frac{1 - x^+_{*,p}x^+_{*,q}}{1 - x^-_{*,p}x^+_{*,q}}\right]^{-1}. \end{aligned} \tag{5.61}$$

Much like in the case of the $\mathfrak{psu}(1|1)^{\oplus 2}$ S matrix also the prefactors $h(p,q)$ have non-

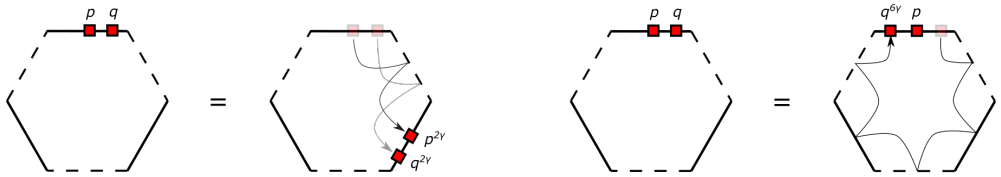

Figure 5.4.: Cyclic invariance is a further consistency condition for the hexagon construction. Left: Cyclically relabeling the edges of the hexagon amounts to "moving" all excitations by 2γ in the sense of Sec. 5.3. Right: We can also move a particle by 6γ to obtain a different ordering of momenta.

trivial double crossing equations. For instance, by crossing in the first line p by 2γ and dividing it by the second line we have

$$\frac{\tilde{h}^{\bullet\bullet}(p^{4\gamma},q)}{\tilde{h}^{\bullet\bullet}(p,q)} = \frac{1-x^+_{*,p}x^+_{*,q}}{1-x^-_{*,p}x^+_{*,q}}\frac{1-x^-_{*,p}x^-_{*,q}}{1-x^+_{*,p}x^-_{*,q}}\,, \tag{5.62}$$

i.e. a non-trivial monodromy. Similarly, by crossing the second line by 2γ and dividing by the first we find $h^{\bullet\bullet}(p^{4\gamma},q) \neq h^{\bullet\bullet}(p,q)$. The crossing equations in the massless sector read

$$\begin{aligned} h^{\circ\circ}(p,q)h^{\circ\circ}(p^{2\gamma},q) &= \left[e^{\frac{i}{2}q}\frac{x^+_{\mathrm{o},p}-x^-_{\mathrm{o},q}}{x^+_{\mathrm{o},p}-x^+_{\mathrm{o},q}}\right]^{-1}\,, \\ h^{\circ\circ}(p,q)h^{\circ\circ}(p,q^{-2\gamma}) &= \left[e^{-\frac{i}{2}p}\frac{x^+_{\mathrm{o},p}-x^-_{\mathrm{o},q}}{x^-_{\mathrm{o},p}-x^-_{\mathrm{o},q}}\right]^{-1}\,. \end{aligned} \tag{5.63}$$

Finally, in the mixed-mass sector we have

$$\begin{aligned} h^{\bullet\circ}_{\mathrm{Ro}}(p^{2\gamma},q)h^{\bullet\circ}_{\mathrm{Lo}}(p,q) &= e^{-i\frac{q}{2}}\frac{x^+_{\mathrm{L},p}-x^+_{\mathrm{o},q}}{x^+_{\mathrm{L},p}-x^-_{\mathrm{o},q}}\,, \\ h^{\circ\bullet}_{\mathrm{oL}}(p^{2\gamma},q)h^{\circ\bullet}_{\mathrm{oL}}(p,q) &= e^{-i\frac{q}{2}}\frac{x^+_{\mathrm{o},p}-x^+_{\mathrm{L},q}}{x^+_{\mathrm{o},p}-x^-_{\mathrm{L},q}}\,, \\ h^{\bullet\circ}_{\mathrm{Lo}}(p^{2\gamma},q)h^{\bullet\circ}_{\mathrm{Ro}}(p,q) &= e^{-i\frac{q}{2}}\frac{1-x^-_{\mathrm{R},p}x^+_{\mathrm{o},q}}{1-x^-_{\mathrm{R},p}x^-_{\mathrm{o},q}}\,, \\ h^{\circ\bullet}_{\mathrm{oR}}(p^{2\gamma},q)h^{\circ\bullet}_{\mathrm{oR}}(p,q) &= e^{+i\frac{q}{2}}\frac{1-x^+_{\mathrm{o},p}x^-_{\mathrm{R},q}}{1-x^+_{\mathrm{o},p}x^+_{\mathrm{R},q}}\,. \end{aligned} \tag{5.64}$$

5.4.3. Cyclic invariance

The last set of conditions we impose is cyclic invariance. This is also observed in [38], though there it is not used to constrain the scalar factor. Let us use the fact that none of the three operators appearing in the three-point function should play a special role. In the hexagon formalism, it is postulated that bringing an excitation from one edge to another amounts to a 2γ crossing transformation [38]. Hence we should have that the scalar factor and the matrix part of the S matrix remain invariant under a 2γ-shift of all momenta. In particular, for the massive–massive case this means

$$h^{\bullet\bullet}(p,q) = h^{\bullet\bullet}(p^{2\gamma},q^{2\gamma})\,, \tag{5.65}$$

see Fig. 5.4 left. This, as well as the similar conditions for the other sectors, is actually a consequence of the crossing equations above. This can be seen from the first equality in eq. (5.61). Similar conditions hold for other processes, where we also have to use the monodromies of the matrix part of the $\mathfrak{psu}(1|1)^{\oplus 2}$ S matrix [70, 111].

Moreover, we can study the case where we pick a two-particle process and cycle only the second particle all around the hexagon, see Fig. 5.4 right. In the case of the massive-left representation, this gives for the highest-weight states

$$\langle \mathbf{h}|Y(p)Y(q)\rangle = \langle \mathbf{h}|\tilde{Y}(q^{6\gamma})Y(p)\rangle\,, \tag{5.66}$$

where we used eqs. (5.42) and (5.43). An explicit evaluation yields

$$h^{\bullet\bullet}(p,q) = e^{-iq/2}\frac{x^-_{\mathrm{L}}(p) - x^+_{\mathrm{L}}(q)}{x^-_{\mathrm{L}}(p) - x^-_{\mathrm{L}}(q)}\,\tilde{h}^{\bullet\bullet}(q^{6\gamma},p)\,. \tag{5.67}$$

We can further simplify this expression by using the monodromy condition from eq. (5.62) and the crossing equation (5.61) itself, resulting in

$$h^{\bullet\bullet}(p,q)h^{\bullet\bullet}(q,p) = \frac{x^+_{\mathrm{L}}(p) - x^+_{\mathrm{L}}(q)}{x^-_{\mathrm{L}}(p) - x^+_{\mathrm{L}}(q)}\frac{x^-_{\mathrm{L}}(p) - x^-_{\mathrm{L}}(q)}{x^+_{\mathrm{L}}(p) - x^-_{\mathrm{L}}(q)}\,. \tag{5.68}$$

Finally, combining this equation with the Watson equation (5.58) one can fix $h^{\bullet\bullet}(p,q)$ up to an overall sign.

Similarly, $\tilde{h}^{\bullet\bullet}(p,q)$ should remain invariant under 2γ-shifts

$$\tilde{h}^{\bullet\bullet}(p,q) = \tilde{h}^{\bullet\bullet}(p^{2\gamma},q^{2\gamma})\,. \tag{5.69}$$

The highest-weight state form-factor leads to

$$\langle \mathbf{h}|Y(p)\tilde{Z}(q)\rangle = \langle \mathbf{h}|Z(q^{6\gamma})Y(p)\rangle\,, \tag{5.70}$$

which can be written explicitly as

$$\tilde{h}^{\bullet\bullet}(p,q) = e^{ip/2}\frac{1 - x^-_{\mathrm{L}}(p)x^-_{\mathrm{R}}(q)}{1 - x^+_{\mathrm{L}}(p)x^-_{\mathrm{R}}(q)}\,h^{\bullet\bullet}(q^{6\gamma},p)\,. \tag{5.71}$$

Using the crossing equations, this leads to

$$\tilde{h}^{\bullet\bullet}(p,q)\tilde{h}^{\bullet\bullet}(q,p) = \frac{1 - x^+_{\mathrm{L}}(p)x^-_{\mathrm{R}}(q)}{1 - x^-_{\mathrm{L}}(p)x^-_{\mathrm{R}}(q)}\frac{1 - x^-_{\mathrm{L}}(p)x^+_{\mathrm{R}}(q)}{1 - x^+_{\mathrm{L}}(p)x^+_{\mathrm{R}}(q)}\,. \tag{5.72}$$

This condition takes care of all cyclicity requirements on the hexagon for massive particles.

In the massless case we have

$$\langle \mathbf{h}|\chi(p)\chi(q)\rangle = i\langle \mathbf{h}|\tilde{\chi}(q^{6\gamma})\chi(p)\rangle\,, \tag{5.73}$$

which reads explicitly

$$h^{\circ\circ}(p,q) = e^{ip/2}\frac{x^-_{\circ}(p) - x^+_{\circ}(q)}{x^+_{\circ}(p) - x^+_{\circ}(q)}\,h^{\circ\circ}(q^{6\gamma},p)\,. \tag{5.74}$$

Using the crossing equation for $h^{\circ\circ}(p,q)$ leads to

$$h^{\circ\circ}(p,q)h^{\circ\circ}(q,p) = \frac{x_{\circ}^{+}(p) - x_{\circ}^{+}(q)}{x_{\circ}^{+}(p) - x_{\circ}^{-}(q)} \frac{x_{\circ}^{-}(p) - x_{\circ}^{-}(q)}{x_{\circ}^{-}(p) - x_{\circ}^{+}(q)} \,. \tag{5.75}$$

It is interesting to note a peculiar observation. When cycling a massless boson around the hexagon, we sometimes pick up an overall minus sign. This is not surprising as for an odd number of massless particles, the hexagon has fermionic statistics. As a result, when cycling a massless boson around an object with an overall fermion statistic, we must account for an additional minus sign.

For the remaining mixed–mass dressing factors, we obtain similar equations, namely

$$h_{\mathrm{L}\circ}^{\bullet\circ}(p,q)h_{\circ\mathrm{L}}^{\circ\bullet}(q,p) = \frac{x_{\mathrm{L}}^{+}(p) - x_{\circ}^{+}(q)}{x_{\mathrm{L}}^{-}(p) - x_{\circ}^{+}(q)} \frac{x_{\mathrm{L}}^{-}(p) - x_{\circ}^{-}(q)}{x_{\mathrm{L}}^{+}(p) - x_{\circ}^{-}(q)} \,, \tag{5.76}$$

and

$$h_{\mathrm{R}\circ}^{\bullet\circ}(p,q)h_{\circ\mathrm{R}}^{\circ\bullet}(q,p) = \frac{1 - x_{\mathrm{R}}^{-}(p)x_{\circ}^{+}(q)}{1 - x_{\mathrm{R}}^{+}(p)x_{\circ}^{+}(q)} \frac{1 - x_{\mathrm{R}}^{+}(p)x_{\circ}^{-}(q)}{1 - x_{\mathrm{R}}^{-}(p)x_{\circ}^{-}(q)} \,. \tag{5.77}$$

Once again, we observe, that when cycling a massless boson around an object with fermionic statistics, we pick up a minus sign.

5.4.4. Solution for the scalar factors

We can now put together the conditions we encountered to write down a solution for the square of the various dressing factors $h^{**}(p,q)$. For instance, for the massive–massive sector we can simply multiply eq. (5.58) by eq. (5.68). Taking the square root of the resulting expression, we may write

$$\begin{aligned} h^{\bullet\bullet}(p,q) &= \frac{e^{i(p+q)/2}}{\sigma^{\bullet\bullet}(p,q)} \sqrt{\frac{[x_{*}^{+}(p) - x_{*}^{+}(q)][x_{*}^{-}(p) - x_{*}^{-}(q)]}{[x_{*}^{+}(p) - x_{*}^{-}(q)]^2}} \sqrt{\frac{1 - \frac{1}{x_{*}^{-}(p)x_{*}^{+}(p)}}{1 - \frac{1}{x_{*}^{+}(p)x_{*}^{-}(p)}}} \,, \\ \tilde{h}^{\bullet\bullet}(p,q) &= \frac{e^{-i\frac{q}{2}}}{\tilde{\sigma}^{\bullet\bullet}(p,q)} \frac{1 - \frac{1}{x_{*}^{-}(p)x_{*}^{+}(q)}}{1 - \frac{1}{x_{*}^{+}(p)x_{*}^{+}(q)}} \,, \end{aligned} \tag{5.78}$$

where we have chosen the branches so that in the BMN limit (schematically given by $k = 0$, $p \sim p/h$, and $h \to \infty$) the prefactor reduces to plus one. The non-trivial monodromy of the prefactor is due to $\sigma^{\bullet\bullet}(p,q)$, which is known for pure-Ramond-Ramond backgrounds and was proposed in ref. [61, 63].

Similarly, in the massless sector we find

$$h^{\circ\circ}(p,q) = \frac{e^{i(p-q)/4}}{\sigma^{\circ\circ}(p,q)} \sqrt{\frac{[x_{\circ}^{+}(p) - x_{\circ}^{+}(q)][x_{\circ}^{-}(p) - x_{\circ}^{-}(q)]}{[x_{\circ}^{+}(p) - x_{\circ}^{-}(q)]^2}} \,. \tag{5.79}$$

In the mixed-mass sector we find the prefactors

$$
\begin{aligned}
h^{\bullet\circ}_{\mathrm{L_o}}(p,q) &= e^{+i\frac{p}{4}}\sqrt{\frac{x^-_{\mathrm{L}}(p)-x^+_{\mathrm{o}}(q)}{x^-_{\mathrm{L}}(p)-x^-_{\mathrm{o}}(q)}\zeta(p,q)}\frac{1}{\sigma^{\bullet\circ}_{\mathrm{L_o}}(p,q)}\,,\\
h^{\circ\bullet}_{\mathrm{o_L}}(p,q) &= e^{-i\frac{q}{4}}\sqrt{\frac{x^+_{\mathrm{o}}(p)-x^+_{\mathrm{L}}(q)}{x^+_{\mathrm{o}}(p)-x^-_{\mathrm{L}}(q)}\zeta(p,q)}\frac{1}{\sigma^{\circ\bullet}_{\mathrm{o_L}}(p,q)}\,,\\
h^{\bullet\circ}_{\mathrm{R_o}}(p,q) &= e^{-i(\frac{p}{4}+\frac{q}{2})}\sqrt{\frac{[1-x^-_{\mathrm{R}}(p)x^+_{\mathrm{o}}(q)][1-x^+_{\mathrm{R}}(p)x^+_{\mathrm{o}}(q)]}{[1-x^-_{\mathrm{R}}(p)x^-_{\mathrm{o}}(q)]^2}\tilde{\zeta}(p,q)}\frac{1}{\sigma^{\bullet\circ}_{\mathrm{R_o}}(p,q)}\,,\\
h^{\circ\bullet}_{\mathrm{o_R}}(p,q) &= e^{+i(\frac{p}{2}+\frac{q}{4})}\sqrt{\frac{[1-x^-_{\mathrm{o}}(p)x^+_{\mathrm{R}}(q)][1-x^-_{\mathrm{o}}(p)x^-_{\mathrm{R}}(q)]}{[1-x^+_{\mathrm{o}}(p)x^+_{\mathrm{R}}(q)]^2}\tilde{\zeta}(p,q)}\frac{1}{\sigma^{\circ\bullet}_{\mathrm{o_R}}(p,q)}\,,
\end{aligned}
\tag{5.80}
$$

where again we use the functions introduced in Sec. 4.7 as

$$
\begin{aligned}
\zeta(p,q) &= \sqrt{\frac{x^-_{*,p}-x^-_{*,q}}{x^+_{*,p}-x^-_{*,q}}\frac{x^+_{*,p}-x^+_{*,q}}{x^-_{*,p}-x^+_{*,q}}}\,,\\
\tilde{\zeta}(p,q) &= \sqrt{\frac{1-x^+_{*,p}x^+_{*,q}}{1-x^+_{*,p}x^-_{*,q}}\frac{1-x^-_{*,p}x^-_{*,q}}{1-x^-_{*,p}x^+_{*,q}}}\,,
\end{aligned}
\tag{5.81}
$$

for a more compact notation of the prefactors.

5.5. An explicit check with protected three-point functions

In order to test the proposed hexagon form factor, let us compute some explicit result and compare it with the literature. Let us do so by considering a simple, but non-trivial example of three-point functions involving only protected half-BPS operators, which are themselves protected by supersymmetry [121]. For generic operators, *e.g.* non-protected, we would only be able to carry out such a comparison in the case of pure-NS-NS backgrounds.

5.5.1. Definition of the correlation functions

In $\mathrm{AdS}_5/\mathrm{CFT}_4$ the highest weight state in a half-BPS supermultiplet is the BMN vacuum $|0\rangle$ not carrying any excitations, which corresponds to the single trace operator $\mathrm{tr}\big(Z^L\big)$, *cf.* Sec. 2.1.3. These states are annihilated by half of the supersymmetry generators. For each value J of the R-charge we have exactly one BPS operator. However, in comparison with $\mathrm{AdS}_5/\mathrm{CFT}_4$ we have only half of the amount of supersymmetry in $\mathrm{AdS}_3/\mathrm{CFT}_2$. Therefore, the half-BPS states are less restricted and there is a total of 16 multiplets.

Structure of protected operators. Let us describe the multiplets in more detail. First of all, we have two $\mathfrak{su}(2)$ corresponding to left and right orbital quantum numbers, which we indicate by $(J,\tilde{J})$. These are the eigenvalues of the highest-weight state in the BPS representation under $(\mathbf{J}_3,\widetilde{\mathbf{J}}_3)$, respectively. For BPS states we must have

Magnon	$\mathbf{J}^3$	$\widetilde{\mathbf{J}}^3$
$\lim_{p\to 0^+} \lvert\chi^1(p)\rangle$	$-\frac{1}{2}$	0
$\lim_{p\to 0^-} \lvert\chi^2(p)\rangle$	0	$+\frac{1}{2}$
$\lim_{p\to 0^+} \lvert\tilde{\chi}^1(p)\rangle$	$+\frac{1}{2}$	0
$\lim_{p\to 0^-} \lvert\tilde{\chi}^2(p)\rangle$	0	$-\frac{1}{2}$

Table 5.1.: The fermions $|\chi^{\dot{A}}(p)\rangle$ have $\mathfrak{su}(2)$ spin $-1/2$ under $(\mathbf{J}^3 - \widetilde{\mathbf{J}}^3)$, while $|\tilde{\chi}^{\dot{A}}(p)\rangle$ have $+1/2$. Since they are massless, it follows from eq. (4.54) that the $\mathfrak{su}(1,1)$ spin is $(-\mathbf{L}_0 + \widetilde{\mathbf{L}}_0)$. Further, the particles are chiral depending on the sign of $\sin(p/2)$, *cf.* eq. (4.56). Hence, we propose this identification of the massless modes.

$-\mathbf{L}_0 = \mathbf{J}_3$ and $-\widetilde{\mathbf{L}}_0 = \widetilde{\mathbf{J}}_3$. For every positive integer value j there is the following diamond of BPS multiplets

$$\begin{array}{ccccc} & & \left(\frac{j-1}{2},\frac{j-1}{2}\right) & & \\ & \left(\frac{j}{2},\frac{j-1}{2}\right)^{\dot{A}} & & \left(\frac{j-1}{2},\frac{j}{2}\right)^{\dot{A}} & \\ \left(\frac{j+1}{2},\frac{j-1}{2}\right) & & \left(\frac{j}{2},\frac{j}{2}\right)^{\dot{A}\dot{B}} & & \left(\frac{j-1}{2},\frac{j+1}{2}\right) \\ & \left(\frac{j+1}{2},\frac{j}{2}\right)^{\dot{A}} & & \left(\frac{j}{2},\frac{j+1}{2}\right)^{\dot{A}} & \\ & & \left(\frac{j+1}{2},\frac{j+1}{2}\right) & & \end{array} \tag{5.82}$$

indicated here by the charge of their highest-weight states. The dotted indices indicate that some of these states transform in an $\mathfrak{su}(2)_\circ$ representations. Moreover, these multiplets may be identified with those arising in the dual CFT from the symmetric-product orbifold $\mathrm{Sym}^N \mathrm{T}^4$. Using the notation of ref. [71], the diamond can be written as

$$\begin{array}{ccccc} & & \mathbb{V}_j^{--} & & \\ & \mathbb{V}_j^{\dot{A}-} & & \mathbb{V}_j^{-\dot{A}} & \\ \mathbb{V}_j^{+-} & & \mathbb{V}_j^{\dot{A}\dot{B}} & & \mathbb{V}_j^{-+} \\ & \mathbb{V}_j^{+\dot{A}} & & \mathbb{V}_j^{\dot{A}+} & \\ & & \mathbb{V}_j^{++} & & \end{array} \tag{5.83}$$

where the subscript index j in $\mathbb{V}_j^{**}$ denotes the length of the permutation cycle of the operator.

Coming back to the language of integrability that we have been using so far, we have the BMN vacuum $|0\rangle$, featuring no particles at all. We can now add massless fermions $\chi^{\dot{A}}(p)$ and $\tilde{\chi}^{\dot{A}}(p)$ at zero momentum [122], which neither contribute to the mass nor the energy. The zero-modes which we can use have charges under $(\mathbf{J}_3, \widetilde{\mathbf{J}}_3)$ as in Tab. 5.1 [123] and yield the 16 states owing to Pauli's principle. Of course, we could also add zero-modes of *massive* states, however, these are vacuum descendants, which can be obtained from acting with charges. This is similar to the discussion in Sec. 2.2.2, where we considered zero momentum (or infinite rapidity) excitations to describe

vacuum descendants in the context of $\mathrm{AdS}_5/\mathrm{CFT}_4$. Here, it is worth stressing, that the zero-modes of $\chi^{\dot{A}}(p)$ and $\tilde{\chi}^{\dot{A}}(p)$ yield genuinely new $\mathfrak{psu}(1,1|2)^{\oplus 2}$ multiplets. Based on Tab. 5.1, the highest-weight states can be identified with the following insertion of fermions

$$\begin{array}{ccccc} & & |\chi^1\tilde{\chi}^2\rangle & & \\ & \big(|\chi^1\tilde{\chi}^1\tilde{\chi}^2\rangle, |\tilde{\chi}^2\rangle\big) & & \big(|\chi^1\rangle, |\chi^1\chi^2\tilde{\chi}^2\rangle\big) & \\ |\tilde{\chi}^1\tilde{\chi}^2\rangle & & |0\rangle \oplus \big(|\chi^1\tilde{\chi}^1\rangle, |\chi^1\tilde{\chi}^1\chi^2\tilde{\chi}^2\rangle, |\chi^2\tilde{\chi}^2\rangle\big) & & |\chi^1\chi^2\rangle \\ & \big(|\tilde{\chi}^1\rangle, |\chi^2\tilde{\chi}^1\tilde{\chi}^2\rangle\big) & & \big(|\chi^1\chi^2\tilde{\chi}^1\rangle, |\chi^2\rangle\big) & \\ & & |\chi^2\tilde{\chi}^1\rangle & & \end{array} \tag{5.84}$$

It should be emphasised that the number of magnons, *i.e.* the length of the operators, is not a quantum number, and it is not preserved by the $\mathfrak{su}(2)_\circ$ action.

From the above we see that most of the half-BPS multiplets can mix among themselves, as there are several multiplets with the exact same charge. Consider for instance, the states $\mathbb{V}^{--}_{j+1}$, $\varepsilon_{\dot{A}\dot{B}}\mathbb{V}^{\dot{A}\dot{B}}_{j}$ and $\mathbb{V}^{++}_{j-1}$ which all have the same charges. Therefore, we cannot distinguish the multiples just by their quantum numbers. In principle they could all mix with $|0\rangle, |\chi^2\tilde{\chi}^1\rangle$ and $|\chi^1\tilde{\chi}^2\rangle$. Fortunately, the multiplets $\mathbb{V}^{+-}_{j}$ and $\mathbb{V}^{-+}_{j}$ do not mix. Hence it will be convenient to consider them in the following.

The correlation functions. We are interested in three-point functions constructed out of operators in the multiplets $\mathbb{V}^{+-}_{j}$ and $\mathbb{V}^{-+}_{j}$ for appropriate values of j. Therefore, we can either have three-point functions involving all operators from the same type of multiplets or those involving two operators from one type of multiplet and the third from the other. Hence there are two categories of correlators we can consider, since the other combinations follow from exchanging the left and right algebra. These correlation functions are well-known in the literature [71, 124, 125]. In particular, we consider the result as written in ref. [71]. Recall from Sec. 5.1 that in our construction we want one of the operators to be the highest-weight state, one to be the lowest-weight state, and one to have vanishing $\mathfrak{su}(2)$ quantum number.

The result of [71] reads for the correlation functions in question

$$\begin{aligned} \langle \mathbb{V}^{-+}_{j_1}\mathbb{V}^{-+}_{j_2}\mathbb{V}^{-+}_{j_3}\rangle &= -\frac{1}{4\sqrt{N}} D_{J_1J_2J_3} D_{\tilde{J}_1\tilde{J}_2\tilde{J}_3} \frac{(j_1+j_2+j_3-1)(j_1+j_2+j_3+1)}{\sqrt{j_1j_2j_3}}\,, \\ \langle \mathbb{V}^{-+}_{j_1}\mathbb{V}^{-+}_{j_2}\mathbb{V}^{+-}_{j_3}\rangle &= -\frac{1}{4\sqrt{N}} D_{J_1J_2J_3} D_{\tilde{J}_1\tilde{J}_2\tilde{J}_3} \frac{(j_1+j_2-j_3-1)(j_1+j_2-j_3+1)}{\sqrt{j_1j_2j_3}}\,, \end{aligned} \tag{5.85}$$

where in the first line $J_k = j_k + 1$ and $\bar{J}_k = j_k - 1$. In the second line the same holds but for operator 3, for which instead $J_3 = j_3 - 1$ and $\bar{J}_3 = j_3 + 1$. The factors $D_{J_1J_2J_3}$ and $D_{\tilde{J}_1\tilde{J}_2\tilde{J}_3}$ depend also on the $\mathfrak{su}(2)$ charges, *i.e.* on the $\mathbf{J}^3$ and $\widetilde{\mathbf{J}}^3$ charges of the operators, respectively. Recall that we have that operator 1 is a highest-weight state, operator 3 is a lowest weight state, and operator 2 has vanishing orbital quantum numbers. All in all, for our configuration of states they are simply given by

$$D_{J_1J_2J_3} = (-1)^{J_2+2J_3}\frac{J_2!}{\sqrt{(2J_2)!}}\,. \tag{5.86}$$

The prefactor $1/\sqrt{N}$ is an overall normalisation common to all three-point functions and is related to the number of copies N in the symmetric product orbifold CFT $\mathrm{Sym}^N(\mathrm{T}^4)$.

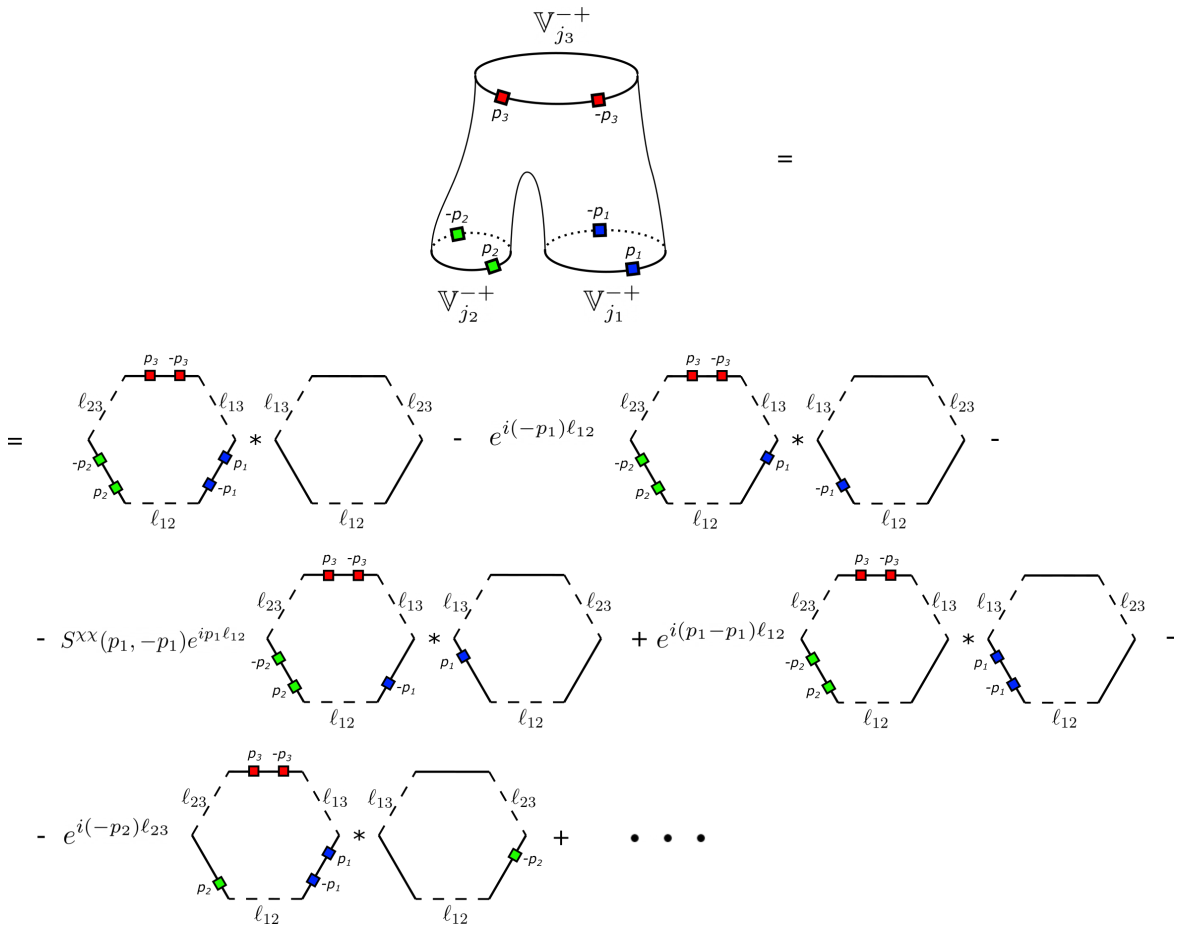

Figure 5.5.: The three-point function is cut into two hexagons, one corresponding to the *front* and one to the *back*. We need to sum over all possible ways of distributing each pair of particles over the two patches, for a total of $(2^2)^3 = 64$ possibilities, weighted as in eq. (5.91). Schematically some of the terms are presented. The first $2^2 = 4$ terms correspond to distributing $\{p_1, -p_1\}$ (in blue), and one term relative to moving $\{p_2, -p_2\}$ (in green).

For the three-point function to be non-vanishing, we will specialise eq. (5.85) to the case $J_3 = J_1$, $\tilde{J}_3 = \tilde{J}_1$.

5.5.2. Hexagon computation

Similarly to the calculation of three-point functions in AdS_5/CFT_4 in Sec. 3.1, we now aim to use the formalism developed in order to reproduce the result (5.85). In principle the integrability machinery is suitable for computing non-protected correlation functions. However, the example considered here is merely intended as a relatively simple check of our proposal.

We are interested in the operators related to $\mathbb{V}^{-+}_j$ and $\mathbb{V}^{+-}_j$, which we identified as

$$\mathbb{V}^{-+}_j \sim \lim_{p\to 0^+}\lim_{q\to 0^-} |\tilde{\chi}^1(p)\tilde{\chi}^2(q)\rangle\,, \qquad \mathbb{V}^{-+}_j \sim \lim_{p\to 0^+}\lim_{q\to 0^-} |\chi^1(p)\chi^2(q)\rangle\,. \tag{5.87}$$

These are constructed over a vacuum of total R-charge j. We need to be careful

describing the zero-momentum magnons considered above. As we have seen in Sec. 3.3 in the context of vacuum descendants in $\mathrm{AdS}_5/\mathrm{CFT}_4$, zero-momentum magnons may lead to singularities in the $p, q \to 0$ limit. There we used the β-deformation as a regulator. It is not surprising that also here singularities appear, given that the dispersion relation from eq. (4.56) is singular at that point. It turns out that the resulting expressions may be simplified, when we take the limit on the two momenta symmetrically,

$$\mathbb{V}_j^{+-} \sim \lim_{p\to 0^+} |\tilde{\chi}^1(p)\tilde{\chi}^2(-p)\rangle\,, \qquad \mathbb{V}_j^{-+} \sim \lim_{p\to 0^+} |\chi^1(p)\chi^2(-p)\rangle\,. \tag{5.88}$$

We are interested in inserting three such operators on the three distinguished edges of the hexagon, which we have labeled with 0γ, 2γ and 4γ. Hence we have to consider the following sets of excitations

$$\langle \mathbb{V}_{j_1}^{-+}\mathbb{V}_{j_2}^{-+}\mathbb{V}_{j_3}^{-+}\rangle \sim \Big(\{\chi^1(p_1),\chi^2(-p_1)\},\,\{\chi^1(p_2),\chi^2(-p_2)\},\,\{\chi^1(p_3),\chi^2(-p_3)\}\Big)\,. \tag{5.89}$$

Here and from now on, we leave the momenta p_j generic and take the limit later. Similarly, we have

$$\langle \mathbb{V}_{j_1}^{-+}\mathbb{V}_{j_2}^{-+}\mathbb{V}_{j_3}^{+-}\rangle \sim \Big(\{\chi^1(p_1),\chi^2(-p_1)\},\,\{\chi^1(p_2),\chi^2(-p_2)\},\,\{\tilde{\chi}^1(p_3),\tilde{\chi}^2(-p_3)\}\Big)\,. \tag{5.90}$$

The hexagon prescription [38] requires us to partition the three sets of excitations identified above in all possible ways over the two hexagonal patches of the worldsheet, see Fig. 5.5. Let us begin with the setting in eq. (5.89). There we have three sets $X_1 = \{\chi^1(p_1),\chi^2(-p_1)\}$, $X_2 = \{\chi^1(p_2),\chi^2(-p_2)\}$ and $X_3 = \{\chi^1(p_3),\chi^2(-p_3)\}$. Accordingly, we sum over all partitions of the form $X_j = \alpha_j \cup \bar{\alpha}_j$ obtaining

$$\Big(\prod_{j=1}^{3}\sum_{X_j=\alpha_j\cup\bar{\alpha}_j}(-1)^{\bar{\alpha}_j}\omega_{\alpha_j,\bar{\alpha}_j}\Big)\langle \mathbf{h}|\alpha_1^{4\gamma}\alpha_2^{2\gamma}\alpha_3^{0\gamma}\rangle\,\langle \mathbf{h}|\bar{\alpha}_2^{4\gamma}\bar{\alpha}_1^{2\gamma}\bar{\alpha}_3^{0\gamma}\rangle\,. \tag{5.91}$$

Further, we also indicated how the particles have to be analytically continued on the various edges. Following the rules devised in Sec. 5.3, a 2γ-shift results in a flavour change, *e.g.* $\chi^1(p^{2\gamma}) = i\tilde{\chi}^2(p)$. Finally, the sum is weighted by the splitting factor $\omega_{\alpha,\bar{\alpha}}$, which takes as similar form as in $\mathrm{AdS}_5/\mathrm{CFT}_4$, namely

$$\omega_{\alpha,\bar{\alpha}} = \prod_{p_j\in\bar{\alpha}} e^{ip_j\ell_{12}}\prod_{\substack{j<k\\ p_k\in\alpha}} S^{\chi\chi}(p_j,p_k)\,. \tag{5.92}$$

In the small-p limit the expression further simplifies as $S^{\chi\chi}(p,-p)\to 1$. The *bridge length* ℓ_{12} [38] we have introduced here is given by

$$\ell_{12} = \frac{j_1+j_2-j_3}{2}\,, \qquad \ell_{23} = \frac{j_2+j_3-j_1}{2}\,, \qquad \ell_{13} = \frac{j_1+j_3-j_2}{2}\,. \tag{5.93}$$

Similar formulae hold for the weight factors for the other partitions, up to cycling the indices $1, 2$ and 3. Finally, there might be additional signs which should be assigned to a given partition, especially when the permuted particles are fermionic [38, 100]. Unfortunately, these rules still lack a systematic understanding. In our case we will

impose that the signs satisfy all relevant self-consistency and symmetry conditions, at which point we will be able to obtain the result and match the existing literature.

Limit procedure and evaluation. As we have mentioned, the limit $p_j \to 0$ requires a careful treatment as we encounter two types of singular behaviour. The first one arises because of possible singularities at $p = 0$, while the second occurs when a pair of momenta approaches each other, *i.e.* $p_j = p_k$. As discussed in Sec. 5.3 in the context of crossing, a particle-antiparticle pair results in a pole, which is what happens in our setup when for instance $p_2 \to p_1$. Finally, we require that the hexagon formalism does not depend on the details of how we construct the external states. For instance, it should not depend on the ordering of the particles within each state. This is indeed the case, but only as long as the particles in each state satisfy the Bethe equations. In other words, in order to have a consistent formalism we need to require p_1, p_2 and p_3 to obey the Bethe equations. Fortunately, these are very simple in our setup, as we are interested in a limit where particles behave as free, *i.e.* $S^{\chi\chi}(p,-p) = S^{\tilde{\chi}\tilde{\chi}}(p,-p) = 1$. Still, they impose three non-trivial conditions on the momenta,

$$e^{ip_k j_k} = 1 \qquad \Rightarrow \qquad p_k = \frac{2\pi\nu_k}{j_k}\,, \quad \nu_k \in \mathbb{Z}\,, \qquad k = 1,2,3\,. \tag{5.94}$$

This discrete structure of the momenta requires care when taking the coincident-momenta limit. We can introduce a small $\varepsilon > 0$ and three real numbers ϵ_k and redefine

$$j_k \to \frac{j_k}{1+\varepsilon\,\epsilon_k}\,, \qquad p_k \to p_k(1+\varepsilon\,\epsilon_k)\,, \tag{5.95}$$

which leaves the Bethe equations (5.94) unchanged. In this way, we can get the coincident-momenta limit by setting

$$p_1 = p_2 = p_3\,, \qquad \text{and} \qquad \varepsilon \to 0\,. \tag{5.96}$$

Since the limit should be independent from ϵ_1, ϵ_2 and ϵ_3, this yields an additional check of the construction.

To perform the computation it will be useful to consider an additional limit. As already stated, the structure constants for the three-point correlation functions of protected operators are themselves protected [126]. Hence, the result is independent of the values of h and k. Moreover, we can see from eq. (4.63) that the kinematics for massless particles only depends on the ratio h/k. Hence it is convenient to take the limit $h/k \to 0$ with k arbitrary. The upshot is that, in this way, we may rewrite all the ingredients necessary for the computation in terms of the new variables

$$y^{\pm}(p) \equiv e^{\pm i\frac{p}{2}}\,\frac{\sin\left(\frac{p}{2}\right)}{\frac{p}{2}}\,, \tag{5.97}$$

which play the role of the Zhukovsky variables $x^{\pm}_{\circ}$. In terms of these, we can easily rewrite the various S-matrix elements necessary for the hexagon computation, including the relevant scalar factor.

Turning to the computation of the hexagon form factors for the two correlators of interest in eqs. (5.89) and (5.90), we can expect a singularity when any pair of momenta

approach. This yields, that the most singular part of (5.89) should go like

$$\frac{1}{\varepsilon^6}\frac{1}{(\epsilon_1-\epsilon_2)^2(\epsilon_2-\epsilon_3)^2(\epsilon_1-\epsilon_3)^2}\,. \tag{5.98}$$

Further, for the correlator of eq. (5.90) the decoupling condition yields only a pole for operators one and two, since the third operator is different. Therefore we expect the most singular part to go like

$$\frac{1}{\varepsilon^2}\frac{1}{(\epsilon_1-\epsilon_2)^2}\,. \tag{5.99}$$

At first glance this mismatch seems to be an issue, given that both correlators should eventually give a finite result, possibly up to an overall factor. Evaluating the partitions carefully, the term which would naively be the most divergent as in eq. (5.98) eventually goes like $\mathcal{O}(\varepsilon^{-2})$, *i.e.* exactly like eq. (5.99). Finally, in the limit $p \to 0$ we find for the correlator from eq. (5.89) the result

$$4\big(j_1+j_2+j_3-1\big)\big(j_1+j_2+j_3+1\big)p^2+\dots\,, \tag{5.100}$$

as expected from eq. (5.85). In a similar way we can compute the hexagon form factor for the correlator (5.90). In this case, the result in the $p \to 0$ limit is

$$-4\,(1-2\,\ell_{12})(1-2\,\ell_{12})\,p^2+\dots\,, \tag{5.101}$$

which again matches with eq. (5.85). In particular, if we disregard the overall normalisations, we find that the ratio of the two families of correlation functions matches for arbitrary j_1, j_2 and j_3.

To conclude this discussion, we note that our result only relied on the *asymptotic* part of the hexagon, without accounting for wrapping effects. This can be done in the hexagon formalism order by order [38–40, 103] by considering Lüscher-type corrections. The computation above was redone in [127], taking wrapping corrections explicitly into account. However, our result matches those in the literature nonetheless. This is because we are dealing with half-BPS states, which are composed of zero-momentum excitations only. The argument was first noted in the context of the computation of the spectrum for the very same operators in refs. [122, 128]. The transfer matrix appearing in the computation of wrapping effects only involves zero-momentum excitations and as such it gets precisely the same and opposite corrections for fermionic and bosonic mirror particles, leading to a complete cancellation of wrapping effects.

5.6. Chapter summary

In this chapter we constructed the hexagon form factor for $\mathrm{AdS}_3 \times \mathrm{S}^3 \times \mathrm{T}^4$ and performed a first test with protected three-point functions. To achieve this, we used the supertranslation operator $\mathcal{T}$ in Sec. 5.1 to find the hexagon subalgebra. This subalgebra turns out to be a diagonal $\mathfrak{psu}(1|1)^{\oplus 2}_D$ subalgebra of the centrally extended $\mathfrak{psu}(1|1)^{\oplus 4}$ symmetry algebra of the gauge fixed theory.

In Sec. 5.2 we then used the bootstrap principle to find the one- and two-particle hexagon form factors. The latter are given in terms of the Borsato–Ohlsson-Sax–Sfondrini S matrix [70], up to overall prefactors $h^{**}(p,q)$, which depend on the representation. Building on these results, we gave a rule for the evaluation of general

two-particle hexagon form factors by scattering with the $\mathfrak{psu}(1|1)^{\oplus 2}$ S matrix and contracting the resulting state. Moreover, we needed to introduce contraction operators, resolving a potential ambiguity, due to the non-vanishing one-particle form factor for massless fermions. We were then able to propose a generalisation of the evaluation rule to many-particle states, by using factorised scattering and the Yang-Baxter equation.

Further, we considered the representation of the hexagon subalgebra in Sec. 5.3. This also allowed us to work out the crossing rules for physical particles. These are necessary in order to evaluate a general hexagon with excitations on all physical edges, as the crossing rules can be used to move all excitations to the same edge.

In Sec. 5.4 we then focussed on the scalar prefactors $h^{**}(p,q)$. In fact, by imposing some constraints, these can be further fixed. The first constraint is the Watson equation, relating the hexagon phases $h^{**}(p,q)$ to the dressing phases $\Sigma^{**}(p,q)$ of the full $\mathfrak{psu}(1|1)^{\oplus 4}$ S matrix. Next, we have the decoupling condition, stating that, whenever a particle-antiparticle pair appears, it decouples from the form factor. This condition yields crossing equations for the scalar prefactors $h^{**}(p,q)$. Finally, there is the cyclicity constraint, demanding that the form factor should yield the same result, even if we bring one excitation once around the hexagon by a 6γ crossing transformation. Combining these three constraints, the solutions for the different $h^{**}(p,q)$ can be written in terms of rational functions and the dressing phases $\sigma^{**}(p,q)$ for the respective representations.

Finally, in Sec. 5.5, we considered a protected three-point function. The three operators we considered carry two massless fermionic excitations at zero momentum each. In order to perform the hexagon calculation, which has possible singularities at $p = 0$, we considered finite momenta by slightly deforming the Bethe equations and taking the zero momentum limit in the end. In this way we were able to reproduce the results for the correlation functions as written in ref. [71], providing a first successful check of the hexagon form factor in $\mathrm{AdS}_3/\mathrm{CFT}_2$.

Chapter 6.

Thermodynamic Bethe Ansatz for pure Ramond-Ramond flux

The thermodynamic Bethe ansatz (TBA) can be applied to integrable models in a thermodynamic setting. In the context of the integrable spin chains discussed in Sec. 2.2, the Bethe ansatz allowed us to find the momenta or equivalently rapidities of spin chain excitations. In the thermodynamic limit, we consider large chains aiming to describe the particle and hole distributions in the thermodynamic equilibrium. Considering an integrable field theory, the TBA then allows to compute the free energy in large volume. Moreover, by going to the mirror theory, the exact ground state energies can be computed for states of finite length [25]. This can be viewed as putting the field theory on a cylinder of finite size, where the mirror TBA then captures corrections from virtual particles travelling around the cylinder. These corrections are also called Lüscher like or wrapping corrections [129]. Further, by analytic continuation of the mirror TBA, the energies of excited states can be captured [72].

In this chapter, we will review the thermodynamic Bethe ansatz for the simple model of the Heisenberg XXX spin chain and work out the corresponding TBA equations. Once we have introduced the concept and notation, we will consider the mirror TBA equations for pure Ramond-Ramond flux in $\mathrm{AdS}_3 \times \mathrm{S}^3 \times \mathrm{T}^4$ which were derived in [65]. We are especially interested in the excited TBA equations with pairs of massless modes excited only. As it turns out, the resulting equations can be simplified significantly in the small-tension limit $h \to 0$.

6.1. Review of the Thermodynamic Bethe Ansatz

Before considering the TBA equations for $\mathrm{AdS}_3 \times \mathrm{S}^3 \times \mathrm{T}^4$, let us begin by reviewing the basic ideas. We refer the reader to refs. [26, 130–132] for a more detailed discussion, especially in the context of $\mathrm{AdS}_5/\mathrm{CFT}_4$.

In order to familiarise with the TBA, we will start out with the simpler example of the Heisenberg XXX spin chain as in the review [131]. This model was already discussed in Sec. 2.2.2. Recall the Bethe equations for M particles, which read

$$e^{ip_j L} \prod_{k \neq j}^{M} \frac{u_j - u_k - i}{u_j - u_k + i} = 1 \,, \tag{6.1}$$

where L is the length of the spin chain. We now want to consider the thermodynamic limit, which corresponds to taking the volume and the number of particles to be large, while keeping their ratio fixed. In doing so, the number of complex solutions for the

Bethe equations grows very fast. However, in the large volume limit $L \to \infty$ states with complex momenta $\mathrm{Im}(p_1) > 0$ lead to $e^{ip_1 L} \to 0$. The only way to satisfy the Bethe equation (6.1) for p_1 is, if there is a pole in the S matrix. For instance we can choose $u_2 = u_1 + i$ and pulling the S matrix involving u_1 and u_2 out of the product, we get

$$e^{ip_1 L} \frac{u_1 - u_2 - i}{u_1 - u_2 + i} \prod_{k \neq 1,2}^{M} \frac{u_1 - u_k - i}{u_1 - u_k + i} = 1 \,. \tag{6.2}$$

Of course, now one might worry that we have created an issue for the Bethe equation involving p_2. By multiplying the eq. (6.2) by the analogous equation for p_2, we obtain

$$e^{i(p_1+p_2)L} \prod_{k \neq 1,2}^{M} \frac{u_1 - u_k - i}{u_1 - u_k + i} \, \frac{u_2 - u_k - i}{u_2 - u_k + i} = 1 \,. \tag{6.3}$$

We immediately see that this equation is fine, if $\mathrm{Im}(p_1 + p_2) = 0$, in which case we have the Bethe roots $u_1 = u - \frac{i}{2}$ and $u_2 = u + \frac{i}{2}$ for some $u \in \mathbb{R}$. However, if $\mathrm{Im}(p_1 + p_2) > 0$ we need to have another pole at $u_3 = u_2 + i$ for instance. For real total momentum, we would then have the solution $u_1 = u - i$, $u_2 = u$ and $u_3 = u + i$.

It is easy to see how to continue this procedure. The solutions constructed in this way are called *Bethe strings*, as they form a sort of string in the complex rapidity plane around the real rapidity u. In general the rapidities u_j^Q of a Bethe string of length Q are given by

$$u_j^Q = u - i \, \frac{Q + 1 - 2j}{2} \,, \tag{6.4}$$

with $u \in \mathbb{R}$ being the center of the string and $j = 1, \ldots, Q$. It is worth stressing, that these string solutions are only solutions of the Bethe equations for $L \to \infty$. The *string hypothesis* is the assumption, that all solutions relevant in the thermodynamic limit are Bethe strings. For instance, in the example considered at hand, solutions which are not of this form can be found, *cf.* refs. [133–135]. However, it turns out that for low magnon densities it is sufficient to consider only the contribution of Bethe string configurations, as the free energy is captured correctly [136].

Further, Bethe strings can be viewed as bound states, as their energy amounts to less than the sum of energies of two individual magnons with real momenta. In particular, the energy of a Q-string is given by

$$E_Q(u) = \sum_{j=1}^{Q} \frac{1}{(u_j^Q)^2 + \frac{1}{4}} = \frac{4Q}{4u^2 + Q^2} \,, \tag{6.5}$$

and the Q-string momentum is also given as the sum over the individual momenta, which simplifies to

$$p_Q(u) = \sum_{j=1}^{Q} -i \log\left(\frac{u_j^Q + \frac{i}{2}}{u_j^Q - \frac{i}{2}} \right) = -i \log\left(\frac{u + i\frac{Q}{2}}{u - i\frac{Q}{2}} \right) . \tag{6.6}$$

To obtain the equations above we used $u_j^Q + \frac{i}{2} = u_{j+1}^Q - \frac{i}{2}$ in order to cancel most of the numerators and denominators.

The interpretation of the Q-strings as bound states is also indicated by the pole

structure of the two-particle S matrix. Moreover, for a given string of length Q, we can simplify the products of S matrices and define

$$S^{Q1}(u-u_k) \equiv \prod_{j=1}^{Q} \frac{u_j^Q - u_k - i}{u_j^Q - u_k + i} = \frac{u-u_k-\frac{Q+1}{2}i}{u-u_k+\frac{Q+1}{2}i}\,\frac{u-u_k-\frac{Q-1}{2}i}{u-u_k+\frac{Q-1}{2}i}\,. \tag{6.7}$$

This is quite remarkable as the resulting S matrix depends only on the center rapidity u of the sting and the second magnons rapidity u_k. The combination of scattering processes into a bound state scattering matrix is also called *fusion* of the corresponding scattering amplitudes, *cf.* the discussion in the review [130]. The Bethe equations for a magnon with rapidity u_k can then be written as

$$e^{ip_k L} \prod_{Q=1}^{\infty} \prod_{j\neq k}^{M_Q} S^{1Q}(u_k - u^{Q_j}) = 1\,, \tag{6.8}$$

where M_Q is the number of bound states of length Q, such that the total number of magnons M is given by

$$\sum_{Q=1}^{\infty} Q M_Q = M\,. \tag{6.9}$$

In a similar fashion, we can fuse products of S matrices S^{1Q} to construct an object that describes the scattering between P-strings with center u and Q-strings with center u', namely $S^{PQ}(u-u')$. The corresponding Bethe equations become

$$e^{ip^{Q_j} L} \prod_{Q_k=1}^{\infty} \prod_{j\neq k}^{M_{Q_j}} S^{Q_j Q_k}(u_j - u_k) = 1\,, \tag{6.10}$$

where u_j is the center of the j-th Bethe string of length Q.

Free energy. The partition functions allows to describe the thermodynamical system and is given by

$$Z = \sum_k \langle \psi_k | e^{-\beta H} | \psi_k \rangle = e^{-\beta F}\,, \tag{6.11}$$

where F ist the free energy and $\beta = 1/T$ is the inverse temperature. In order to obtain the partition function, we need to find the free energy per site f, which is given by

$$f = e - Ts\,, \tag{6.12}$$

with e and s being the energy and the entropy per site, respectively. The entropy is defined as the logarithm of the number of possible states. In the following it will be useful to introduce the densities ρ, defined as

$$\begin{aligned} L\rho(u)\Delta u &= \text{ number of magnons with rapidity in } [u, u+\Delta u] \equiv n\,, \\ L\bar{\rho}(u)\Delta u &= \text{ number of holes with rapidity in } [u, u+\Delta u] \equiv \bar{n}\,, \end{aligned} \tag{6.13}$$

where *holes* are understood as sites, which are not occupied by a magnon. Further, we can introduce the total density of states $\rho_t = \rho + \bar{\rho}$ and number of sites $n_t = n + \bar{n}$.

The entropy is then given as the logarithm of the number of possible distributions of n particles over the n_t vacant sites

$$\Delta S = \log\left(\frac{(L\rho_t(u)\Delta u)!}{(L\rho(u)\Delta u)!(L\bar{\rho}(u)\Delta u)!}\right). \tag{6.14}$$

Using Stirlings formula $\log n! \approx n\log n + \mathcal{O}(\log n)$ in the large L limit, eq. (6.14) yields

$$\Delta S = L\Delta u\left(\rho_t \log\rho_t - \rho\log\rho - \bar{\rho}\log\bar{\rho}\right). \tag{6.15}$$

Finally, for the entropy per site we have

$$s = \int_{-\infty}^{\infty} \mathrm{d}u\left(\rho_t \log\rho_t - \rho\log\rho - \bar{\rho}\log\bar{\rho}\right). \tag{6.16}$$

TBA equations. Let us consider the Bethe equations in logarithmic form. Thus, eq. (6.10) becomes

$$p^{Q_j}L - i\sum_{Q_k=1}^{\infty}\sum_{j\neq k}^{M_{Q_j}} \log\big(S^{Q_jQ_k}(u_j-u_k)\big) = -2\pi m_j^{Q_j}, \tag{6.17}$$

here $m_j^{Q_j}$ is an integer labelling the solutions. Introducing the counting function $c^{Q_j}(u) = m_j^{Q_j}/L$, we can further write

$$-\frac{p^Q}{2\pi} - \frac{1}{2\pi i}\sum_{Q'=1}^{\infty}\int_{-\infty}^{\infty}\mathrm{d}u' \log\Big(S^{QQ'}(u-u')\Big)\rho(u') = c^Q(u), \tag{6.18}$$

where we used $\frac{1}{L} = \frac{\Delta u'}{L\Delta u'} = \frac{\rho(u')}{n}\Delta u'$ and took the large L limit to obtain the integration over u'. The counting function allows to move between different Bethe solutions. Taking for instance a state with labels $m_j^{Q_j}$, then the rapidities of the corresponding particles are given by $Lc^Q(u_j) = m_j^{Q_j}$. On the other hand, holes can be captured by the rapidities satisfying $Lc^Q(u_k) = m_k^{Q_k}$ with $m_k^{Q_k} \neq m_j^{Q_j}$. Hence, taking the derivative of the counting functional with respect to the rapidity u yields the total density of states

$$\frac{\mathrm{d}c^Q(u)}{\mathrm{d}u} = \rho_t^Q(u) = \rho^Q(u) + \bar{\rho}^Q(u). \tag{6.19}$$

Differentiating eq. (6.18) with respect to u, the Bethe equation becomes

$$-\frac{1}{2\pi}\frac{\mathrm{d}p^Q}{\mathrm{d}u} - \sum_{Q'=1}^{\infty}\int_{-\infty}^{\infty}\mathrm{d}u' K^{QQ'}(u-u')\rho^Q(u') = \rho^Q(u) + \bar{\rho}^Q(u). \tag{6.20}$$

The function $K^{QQ'}(u-u')$ introduced above is referred to as *kernel* and is given through

$$K^{QQ'}(u-u') = \frac{1}{2\pi i}\frac{\mathrm{d}}{\mathrm{d}u}\log\Big(S^{QQ'}(u-u')\Big). \tag{6.21}$$

Let us come back to the free energy per site, which can be written in terms of the

densities as

$$f = \sum_{Q=1}^{\infty} \int_{-\infty}^{\infty} \mathrm{d}u \left(E^Q \rho^Q - T \left(\rho^Q \log\left(\frac{\rho_t^Q}{\rho^Q}\right) + \bar{\rho}^Q \log\left(\frac{\rho_t^Q}{\bar{\rho}^Q}\right)\right)\right) . \tag{6.22}$$

In the thermodynamic equilibrium the free energy becomes stationary and we have $\delta f = 0$. The variation here is done with respect to ρ and $\bar{\rho}$. In the same manner, we also variate eq. (6.20). Solving for $\delta\bar{\rho}$ and substituting the result into $\delta f = 0$, we find the *thermodynamic Bethe ansatz equations* as

$$\log\left(\frac{\bar{\rho}^Q}{\rho^Q}\right) = \frac{E^Q}{T} + \sum_{Q'} \log\left(1 + \frac{\rho^{Q'}}{\bar{\rho}^{Q'}}\right) \star K^{Q'Q}(u) . \tag{6.23}$$

We also introduced the *convolution* here, which is defined for the functions $g(u)$ and $h(u)$ as

$$g \star h(u) = \int_{-\infty}^{\infty} \mathrm{d}u' g(u') h(u' - u) . \tag{6.24}$$

Finally, we can define the *Y-functions* as the ratio of the densities

$$Y_{Q'} = \frac{\rho^{Q'}}{\bar{\rho}^{Q'}} . \tag{6.25}$$

This allows us to rewrite the TBA equations as well as the free energy $E_0 = Lf$ as

$$\begin{aligned} -\log(Y_Q) &= \frac{E^Q}{T} + \sum_{Q'} \log(1 + Y_{Q'}) \star K^{Q'Q}(u) , \\ E_0 &= \frac{LT}{2\pi} \sum_{Q} \int_{-\infty}^{\infty} \mathrm{d}u \frac{\mathrm{d}p^Q}{\mathrm{d}u} \log(1 + Y_Q) . \end{aligned} \tag{6.26}$$

As usual, we will not write the explicit sum over Q', but leave it implicit as the index appears as a sub- and superscript.

The mirror theory. The thermodynamic Bethe equations given above describe the system in the large volume limit at finite temperature T. However, by going to the *mirror model* they also allow us to study the theory in finite volume at vanishing temperature [25]. To make this more precise, let us start by considering the ground state energy E_0. At low temperature $\beta = 1/T \to \infty$, E_0 is the leading contribution to the partition function

$$Z(\beta, L) = \sum_k e^{-\beta E_k(L)} \approx e^{-\beta E_0(L)} + \dots , \tag{6.27}$$

where the dots indicate terms exponentially suppressed in β. The model can be analytically continued to the *mirror model*. In the mirror theory the role of space and time have been interchanged, which can be achieved by a double Wick rotation [26], sending $\tau \to \tilde{\sigma} = i\tau$ and $\sigma \to \tilde{\tau} = i\sigma$. The mirror energy and the mirror momentum,

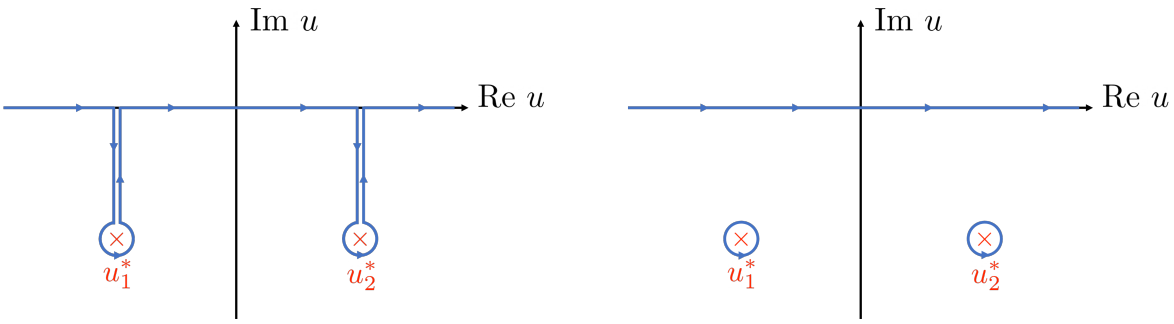

Figure 6.1.: The excited TBA equations can be obtained by deforming the integration contour in such a way, that it includes singularities of the integrand located at u_j^*. This corresponds to integrating over the original domain and picking up the corresponding residues, which are called *source terms* in this context.

are related to the momentum and the energy through

$$\tilde{E} = -ip\,, \qquad \tilde{p} = -iE\,, \tag{6.28}$$

where the tildes denote the mirror quantities. The partition function $Z(\beta, L)$ can now be evaluated by using the partition function of the mirror theory

$$Z(\beta, L) = \tilde{Z}(L, \beta) = \sum_k e^{-L\tilde{E}_k(\beta)}\,. \tag{6.29}$$

Hence, the mirror model computes the partition function at temperature $1/L$ and volume $R = \beta$. Note that the mirror volume is canonically denoted as R. For further details on the double Wick rotation and the analytical continuation to the mirror theory, we refer the reader to ref. [26] and the reviews [130, 132].

The mirror model allows us to work in the infinite volume limit $R \to \infty$, where factorised scattering and the asymptotic Bethe ansatz is valid. On the other hand, we have the finite temperature $1/L$, which can be dealt with by using the TBA for the mirror model. Hence by analytically continuing the thermodynamic Bethe equations from eq. (6.26) to the mirror region, we obtain the mirror TBA equations and ground state energy $E_0(L) = L\tilde{f}$ for a ground state of length L as

$$\begin{aligned} -\log(Y_Q(u)) &= L\tilde{E}^Q(u) + \left(\log(1+Y_{Q'}) \star K^{Q'Q}\right)(u)\,, \\ E_0(L) &= -\frac{1}{2\pi}\int_{-\infty}^{\infty} \mathrm{d}u \frac{\mathrm{d}\tilde{p}^Q}{\mathrm{d}u}\log(1+Y_Q)\,. \end{aligned} \tag{6.30}$$

For readability, the dependence on u in the first line is usually not written explicitly.

Excited TBA. Let us suppose that we can analytically continue in some parameter to reach all excited states. The appearance of the excited states can be understood as picking up residues. To see this, let us consider eq. (6.30) and suppose that by analytically continuing in the rapidity u, we can reach singularities $Y_Q(u_j^*) = -1$, which are located at the rapidities u_j^*. We can then deform the integration contour of the convolution in such a way that it also includes u_j^*, see Fig. 6.1. We will denote the deformed contour by C'. For instance, we can write the energy as

$$
\begin{aligned}
E(L) &= \frac{1}{2\pi}\int_{C'} \mathrm{d}u\ \tilde{p}^{Q}(u)\frac{Y'_Q(u)}{1+Y_Q(u)} \\
&= \frac{1}{2\pi}\int_{-\infty}^{\infty} \mathrm{d}u\ \tilde{p}^{Q}(u)\frac{Y'_Q(u)}{1+Y_Q(u)} + i\sum_j \operatorname*{Res}_{u=u_j^*} \tilde{p}^{Q}(u)\frac{Y'_Q(u)}{1+Y_Q(u)}\,,
\end{aligned}
\tag{6.31}
$$

where we used partial integration and that $Y'_Q(u)$ is the derivative of $Y_Q(u)$ with respect to u. Subsequently, the residue can then be evaluated to $\tilde{p}^{Q}(u_*)$. Further, the same contour deformation can be used in the TBA equation for the Y-functions, resulting in contributions of the form $\log\big(S^{Q'Q}(u_j^*,u)\big)$. The terms $\log\big(S^{Q'Q}\big)$ and $i\tilde{p}$, that we picked up through the contour deformation are called *driving terms*. We can then write the excited TBA equations as well as the energy as

$$
\begin{aligned}
-\log(Y_Q)(u) &= L\tilde{E}^{Q}(u) + \Big(\log(1+Y_{Q'})\star K^{Q'Q}\Big)(u) - \sum_j \log\Big(S^{Q'Q}(u_j^*,u)\Big)\,, \\
E(L) &= -\frac{1}{2\pi}\int_{-\infty}^{\infty}\mathrm{d}u\frac{\mathrm{d}\tilde{p}^{Q}}{\mathrm{d}u}\log(1+Y_Q(u)) + i\sum_j \tilde{p}(u_j^*)\,.
\end{aligned}
\tag{6.32}
$$

By substituting $i\tilde{p}(u_j^*) = E(u_j^*)$ in the equation above, we see the rapidities u_j^* contribute to the energy. Solving these equations at large L and neglecting the corrections from the convolutions, it turns out, that the positions of the singularities u_j^* are solutions to the asymptotic Bethe equations, *i.e.* in our example

$$
-1 = e^{ip_j^* L}\prod_k S^{Q'Q}(u_j^*,u_k^*)\,. \tag{6.33}
$$

Note that, unlike the case studied in Sec. 2.2.2, here we did include $S^{Q'Q}(u_j^*,u_j^*) = -1$ and thus we also have -1 on the left-hand side. In eq. (6.30), we use the rapidity u for the parametrisation of the mirror region, however, these u_j^* correspond to solutions of the Bethe equations in the physical region. Therefore, the contour deformation can be understood as analytically continuing the mirror rapidity u to the physical region to include excitations. These excitations contribute source terms to the TBA and energy equations as in eq. (6.32) as they give rise to singularities. This contour deformation trick was found by Dorey and Tateo [72].

We can further analytically continue the excited TBA eqs. (6.32) back to physical rapidities and evaluate at u_j^*, which yields

$$
i\pi(2n_j+1) = -ip_j L + \Big(\log(1+Y_{Q'})\star K^{Q'Q}\Big)(u_j^*) - \sum_k \log\Big(S^{Q'Q}(u_k^*,u_j^*)\Big)\,, \tag{6.34}
$$

where $n_j \in \mathbb{Z}$ labels the different branches of $\log Y_Q(u_j^*) = \log(-1)$. This equation is also called *exact Bethe equation*, as it contains corrections to the asymptotic part from the convolution of the Y-function with the kernel. Moreover, the Bethe roots u_j^* have to satisfy the exact Bethe equation (6.34).

Again we refer the reader to the reviews [130, 132] for a more detailed discussion of TBA techniques and examples of its application to other models.

6.2. TBA equations in the pure-RR sector

Let us study the mirror TBA equations for $AdS_3 \times S^3 \times T^4$ with pure RR flux, which were worked out in [65]. For pure RR flux the dispersion relation from eq. (4.56) becomes

$$\mathcal{E} = \sqrt{m^2 + h^2 \sin^2 \frac{p}{2}}\,. \tag{6.35}$$

Similarly to the example in Sec. 6.1, the particles involved can organise into Bethe strings. Again, the string hypothesis is assumed, namely that all the relevant solutions are captured by Bethe strings. Let us therefore discuss the relevant types of particles in the following.

Fundamental excitations. The fundamental excitations were given in Sec. 4.5. In comparison with our choice in Sec. 4.2 the grading in ref. [65] is chosen such that the left momentum carrying modes are in the $\mathfrak{sl}(2)$ grading. Hence the right modes are in the $\mathfrak{su}(2)$ grading. This simply amounts to an exchange of what we called left and right before. In the following we will use the choice from [65]. The massless modes are in a fermionic grading. Similarly to the Bethe equations in AdS_5 (or its subsectors as in Sec. 2.2.4) we have auxiliary Bethe roots y here from creating level-II excitations, *i.e.* acting with the lowering operators. These roots transform in the fundamental representation of the $\mathfrak{su}(2)_\bullet$ algebra. The mirror Bethe-Yang equations as well as the two-particle S matrices can be found in [65].

Massive bound states. As mentioned before, the fundamental particles can be organised in Bethe strings forming bound states. While the individual particles may have complex momenta and energies, the corresponding bound states have real mirror momenta and energies. The bound states are created from poles in the S matrix. Considering left particles it turns out, that the pole structure takes such a form, that only left particles can form bound states. Combining Q particles with $\mathfrak{u}(1)$ charge $m = +1$, the bound state will have mass $m = Q$ and hence be denoted as Q-particle [65].

A similar analysis can be done for right particles. However, due to the $\mathfrak{su}(2)$ grading the S matrix has poles and zeros and thus additional zeros and poles from the auxiliary equations are needed to satisfy the Bethe-Yang equations. We will denote right bound states as $\bar{Q}$-particles [65].

There exist no bound states consisting of left and right particles, as the corresponding left-right S matrix does not have poles in the mirror region.

Massless excitations. Massless particles do not form bound states, as the scattering matrix has neither poles nor zeros in the mirror region. Accordingly physical massless excitations have real momenta [63]. Further, there are also no bound states between massive and massless particles [65]. As discussed in Sec. 4.2, there are two massless representations, labelled by the index $\dot{\alpha} = 1, 2$ transforming as a doublet under $\mathfrak{su}(2)_\circ$.

Auxiliary roots. Also the auxiliary roots y do not form bound states. Moreover, they are neither contributing to the momentum nor the energy. These roots are labelled by the index $\alpha = 1, 2$, transforming as a doublet under $\mathfrak{su}(2)_\bullet$.

6.2.1. Parametrisation

Before moving to the study of the mirror TBA equations in the tensionless limit, let us introduce the parametrisation we will be using in the following. The Zhukovsky variables in the string region can be used as introduced in terms of the momenta p in eq. (4.63). Below we will also consider the parametrisation in the mirror region. In addition to the Bethe rapidity u, which obeys

$$u = x^+ + \frac{1}{x^+} - \frac{i}{h}|m| = x^- + \frac{1}{x^-} + \frac{i}{h}|m|\,, \tag{6.36}$$

it will be convenient to introduce the Fontanella-Torrielli parametrisation [137] in terms of γ-rapidities, *cf.* the detailed discussion of the parametrisation in ref. [63].

String region. In terms of the rapidity u and setting $k = 0$, we can write the Zhukovsky variable in the string region as

$$x_s(u) = \frac{u}{2}\left(1 + \sqrt{1 - \frac{4}{u^2}}\right)\,, \tag{6.37}$$

which has cuts for $-2 < u < 2$ and are therefore called *short cuts*. Further, for massive excitations we then have

$$x_s^\pm(u) = x_s(u \pm \frac{i}{h}|m|)\,, \tag{6.38}$$

where the subscript indicates that we consider particles in the string region here. For physical particles in the string region the rapidities u are real. As in Sec. 4.5 we can take the $m \to 0$ limit to obtain the parametrisation for massless particles. Let us define $x_s(u) = x_s(u + i0)$, which then satisfies the constraint

$$x_s(u + i0) = \frac{1}{x_s(u - i0)}\,, \tag{6.39}$$

with the rapidity taking values just above the short cut $-2 < u < 2$ for real momenta p. Hence, we have $(x_s(u))^2 = e^{ip}$. It follows from this parametrisation, that x_s lies on the upper half-circle for massless particles with real momentum.

Moreover, it will be useful to work in the γ-parametrisation introduced in [137]. For massive excitations we then have [63]

$$x_s^\pm(\gamma_s) = \frac{i \mp e^{\gamma^\pm}}{i \pm e^{\gamma^\pm}}\,. \tag{6.40}$$

Since we should have $|x^\pm| > 1$ in the string region (or physical region), we pick the region $-\pi < \mathrm{Im}(\gamma^+) < 0$ for γ^+, while for γ^- we choose $0 < \mathrm{Im}(\gamma^-) < \pi$, following [63]. Then we have

$$\gamma^\pm = \log\left(\mp i\frac{x^\pm - 1}{x^\pm + 1}\right)\,. \tag{6.41}$$

Finally, in this parametrisation the energy can be written as

$$\mathcal{E}(\gamma_s^\pm) = h\left(\frac{1}{\cosh\gamma_s^+} + \frac{1}{\cosh\gamma_s^-}\right)\,. \tag{6.42}$$

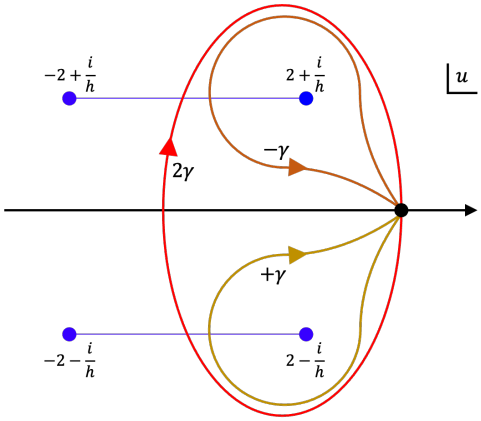

Figure 6.2.: The crossing transformation can be understood as an analytical continuation to the complex rapidity plane. The short cuts are depicted for $x_s^{\pm}(u)$ between the branch points at $u = \pm 2 + \frac{i}{h}$ for the upper and $u = \pm 2 - \frac{i}{h}$ for the lower cut. Note, that in the figure γ refers to the mirror transformations.

Similarly, we have for massless particles

$$x_s(\gamma_s) = \frac{i - e^{\gamma_s}}{i + e^{\gamma_s}}\,, \qquad \gamma_s = \log\left(-i\frac{x_s - 1}{x_s + 1}\right)\,. \tag{6.43}$$

As stated above, for real momenta, the variable $x_s(\gamma_s)$ takes values on the upper half of the unit circle and hence γ is real. The energy can be written as

$$\mathcal{E}^0(\gamma_s) = \frac{2h}{\cosh\gamma_s}\,. \tag{6.44}$$

Mirror region. In Sec. 4.7 we considered the crossing transformation, which takes a particle to its antiparticle. Here we will consider *mirror transformations*, which are sometimes referred to as *half crossing*. The name will become clear in the following. As noted above, the Zhukovsky parametrisation in eq. (6.37) has short cuts at $-2 < u < 2$. Let us begin with massive particles $x_s^{\pm}(u)$. The mirror transformation then corresponds to analytically continuing $x_s^+(u)$ to the complex u plane and around the branch points, see Fig. 6.2. This continuation is also denoted by u^γ and under the mirror transformation we have

$$u^\gamma: \quad x_s^+(u^\gamma) = \frac{1}{x_s^+(u)}\,, \tag{6.45}$$

for massive particles. As discussed in Sec. 6.1, by going to the mirror theory we obtain the mirror energy $\tilde{\mathcal{E}}$ and mirror momentum $\tilde{p}$ as

$$\tilde{\mathcal{E}} = -ip\,, \qquad \tilde{p} = -i\mathcal{E}\,. \tag{6.46}$$

As we are interested in the mirror TBA equations, we will mostly work with the mirror theory in the remainder of this section. Therefore, let us introduce a more suitable mirror Zhukovsky parametrisation given by

$$x(u) = \frac{1}{2}\left(u - i\sqrt{4 - u^2}\right)\,, \tag{6.47}$$

which has cuts on the real u-line for $|u| > 2$ and are hence also called *long cuts*. Again, for massive particles we can write

$$x^{\pm}(u) = x(u \pm \tfrac{i}{h}|m|)\,. \tag{6.48}$$

In the mirror region the momentum for a Q-particle is given by

$$\tilde{p}^{Q}(u) = h\left(x(u - \tfrac{i}{h}Q) - x(u + \tfrac{i}{h}Q)\right) + iQ\,, \tag{6.49}$$

while the mirror energy for a Q-particle is

$$\tilde{\mathcal{E}}^{Q}(u) = \log\frac{x(u - \frac{i}{h}Q)}{x(u + \frac{i}{h}Q)}\,, \tag{6.50}$$

and analogously for $\bar{Q}$-particles [65]. Similarly to the string region, particles with real mirror momentum $\tilde{p}^{Q}$ are defined for real rapidities $u \in \mathbb{R}$.

Like in the string region, for massless particles we define

$$x(u) = x(u + i0) = \frac{1}{x(u - i0)}\,. \tag{6.51}$$

Here, we have u just above the long cut on the real u-line with $|u| > 2$. In the mirror theory $x(u + i0)$ also lies on the real axis and takes the values $-1 \leq x \leq 1$.

Let us also introduce the parametrisation in terms of the γ-rapidities here. For the massive particles it is given by [63]

$$\gamma^{+} = \frac{1}{2}\log\left(-\frac{u + \frac{iQ}{2} - 2}{u + \frac{iQ}{2} + 2}\right) - i\pi\,, \qquad \gamma^{-} = \frac{1}{2}\log\left(-\frac{u - \frac{iQ}{2} - 2}{u - \frac{iQ}{2} + 2}\right). \tag{6.52}$$

Analogously, for the massless case we have

$$\gamma(u) = \frac{1}{2}\log\left(-\frac{u - 2}{u + 2}\right) + \frac{i\pi}{2}\,. \tag{6.53}$$

Further, for massless mirror particles, the relation between the γ-parameter and the Zhukovsky variable x in the mirror theory is

$$x(\gamma) = -\tanh\frac{\gamma}{2}\,, \qquad \gamma(x) = -2\,\mathrm{arctanh}(x)\,. \tag{6.54}$$

Moreover, by directly comparing the definition of γ given here with the one given for the string region we see that

$$\gamma_s = \gamma - \frac{i\pi}{2}\,. \tag{6.55}$$

where $\gamma(u)$ is defined in the mirror region by eq. (6.53) and $\gamma_s(u) = \gamma(x_s(u))$ in the string region by eq. (6.43). In particular, we can use the shifted rapidities to obtain the relation given in eq. (6.46)

$$\mathcal{E}^{0}(\gamma - \tfrac{i\pi}{2}) = -i\,\tilde{p}^{0}(\gamma)\,, \qquad p^{0}(\gamma - \tfrac{i\pi}{2}) = -i\,\tilde{\mathcal{E}}^{0}(\gamma)\,. \tag{6.56}$$

In what follows, we will use the notation introduced here and indicate whenever a

variable is defined in the string region by the resepective subscript.

Anti-string region. Going from the string to the anti-string region corresponds to a crossing transformation, as discussed in Sec. 4.7. However, it can also be understood as the analytic continuation through the cuts for $x_s^+(u)$ and $x_s^-(u)$, as depicted in Fig. 6.2. The 2γ crossing transformations for massive and massless particles are then given by the rules presented in Sec. 4.7.

More on massless particles. In the following we will focus on massless particles in particular. Hence, it will be convenient to explicitly give the parametrisation of the physical quantities in terms of the γ- and γ_s-rapidities in the mirror and string region, respectively. In the string region we have

$$\mathcal{E}^0 = \frac{2h}{\cosh\gamma_s}\,, \qquad p^0 = -i\log\left(\frac{i-e^{\gamma_s}}{i+e^{\gamma_s}}\right)^2, \tag{6.57}$$

where we choose the branches of the logarithm in such a way, that

$$p^0 = \begin{cases} -2i\log\left(+\frac{i-e^{\gamma_s}}{i+e^{\gamma_s}}\right), & \gamma_s > 0 \quad (-\pi \le p \le 0), \\ -2i\log\left(-\frac{i-e^{\gamma_s}}{i+e^{\gamma_s}}\right), & \gamma_s < 0 \quad (0 \le p \le +\pi). \end{cases} \tag{6.58}$$

The gapless dispersion relation for massless particles makes this choice of different branches for positive and negative momentum necessary, *cf.* also the discussion in ref. [138]. Taking γ slightly above the real axis, we have for the mirror particles

$$\tilde{p}^0 = -\frac{2h}{\sinh\gamma}\,, \qquad \widetilde{\mathcal{E}}^0 = -\log\left(\frac{1-e^{\gamma}}{1+e^{\gamma}}\right)^2. \tag{6.59}$$

Again we choose the branches of the logarithm as in [138] and distinguish positive and negative mirror momentum modes

$$\widetilde{\mathcal{E}}^0(\gamma) = \begin{cases} -2\log\left(\frac{1-e^{\gamma}}{1+e^{\gamma}}\right) + 2\pi i, & \gamma > 0 \quad (i.e.\ \tilde{p}^0 < 0), \\ -2\log\left(\frac{1-e^{\gamma}}{1+e^{\gamma}}\right), & \gamma < 0 \quad (i.e.\ \tilde{p}^0 > 0), \end{cases} \tag{6.60}$$

and the variables γ take values just above the real line. Note, that the mirror energy is not analytic around $\gamma = 0$ or equivalently $p = 0$, as discussed in [138].

Auxiliary roots. Finally, we need to parametrise the auxiliary particles. We only need to consider them in the mirror theory here. They can be described by Zhukovsky variables taking values on the unit circle [65]. Moreover, it turns out, that for the parametrisation of the mirror kinematics of auxiliary particles, the string kinematics of massless particles can be used. In contrast, to the massless particles however, the auxiliary particles have neither energy nor momentum associated to the auxiliary roots. Another difference is, that the auxiliary particles can take values on the upper or lower half circle. Hence, it is customary to introduce two types of auxiliary roots as in the following table [65]:

Auxiliary	Parametrisation
y^+ *particles*	$1/x(u)$ on the upper half circle with $-2 < u < 2$; we will use $x_s(u)$
y^- *particles*	$x(u)$ on the lower half circle with $-2 < u < 2$; we will use $1/x_s(u)$

The parametrisation in terms of the γ-rapidities is then analogous to the parametrisation of the massless particles in the string region as well.

6.2.2. Mirror TBA equations

The mirror TBA equations were derived in [65]. As in Sec. 6.1, the kernels are defined by taking the logarithmic derivative of the corresponding S matrix in the mirror-mirror kinematics, *i.e.*

$$K^{**}(u,u') = \frac{1}{2\pi i}\frac{\mathrm{d}}{\mathrm{d}u}\log S^{**}(u,u')\,, \tag{6.61}$$

where the stars indicate massive, massless or auxiliary particles. For the reader's convenience, we collect the various kernels in App. B. The TBA equations are written in terms of the rapidity variables u, the domains of which are chosen such that all real momenta are covered. In particular, this makes it necessary to introduce the convolutions

$$\star \leftrightarrow \int_{-\infty}^{+\infty}\mathrm{d}u, \qquad \hat{\star} \leftrightarrow \int_{-2}^{+2}\mathrm{d}u, \qquad \check{\star} \leftrightarrow \int_{-\infty}^{-2}\mathrm{d}u + \int_{+2}^{+\infty}\mathrm{d}u\,. \tag{6.62}$$

From the discussion of the parametrisation it becomes clear, that we use $\star$ for Q and $\overline{Q}$ particles, while for massless particles we need to use $\check{\star}$. Finally, for convolutions involving auxiliary particles we use $\hat{\star}$.

Similarly to Sec. 6.1, we can find the excited TBA equations from the ground state equations. In the following, we will consider massless excitations only. By using the Dorey-Tateo contour deformation trick [72], we can pick up an even number of massless excitations with pairs of real momenta $(-p_j, p_j)$. This directly ensures that the level-matching condition is satisfied. Moreover, the Y-functions are symmetric under $u \leftrightarrow -u$. The driving terms for massless excitations stem then from deforming the contour in such a way, that residues are picked up in the convolutions, when for the massless Y-functions we have

$$Y_0^{(\dot{\alpha})}(u_{s,j}^{\dot{\alpha}_j}) = -1\,, \qquad \text{with} \qquad j = 1,\ldots,2M\,. \tag{6.63}$$

The values of $u_{s,j}^{\dot{\alpha}_j}$ lie in the string region, as indicated by the subscript. For massless particles, this means, that $u_{s,j}^{\dot{\alpha}_j}$ takes values between -2 and 2.

The excited state mirror TBA equations are given below in terms of the Y-functions with the driving terms added in grey. As in the example in Sec. 6.1, the driving terms are of the form $\log S^{0_*\,*}(u_{s,j}^{\dot{\alpha}_j},\cdot)$, where the dot indicates the free argument. It is worth stressing, that these S matrix elements have the first argument in the string region. This is further highlighted by the index 0_*.

Moreover, the ground state equations from [65] can be recovered straightforwardly by simply dropping the driving contributions. In the following equations we will explicitly write the dependence on u. However, in order to improve readability we will mostly

leave it implicit in our discussion in Sec. 6.3.

Equation for Q-particles.

$$\begin{aligned}-\log Y_Q(u) = L\tilde{\mathcal{E}}^Q(u) &- \left(\log\left(1+Y_{Q'}\right)\star K_{sl}^{Q'Q}\right)(u) - \left(\log\left(1+\bar{Y}_{Q'}\right)\star \tilde{K}_{su}^{Q'Q}\right)(u) \\ &- \sum_{\dot\alpha=1}^{N_0}\left(\log\left(1+Y_0^{(\dot\alpha)}\right)\check\star K^{0Q}\right)(u) + \sum_{j=1}^{2M}\log S^{0_*Q}(u_{s,j}^{\dot\alpha_j},u) \\ &- \sum_{\alpha=1,2}\left(\log\left(1-\frac{1}{Y_+^{(\alpha)}}\right)\hat\star K_+^{yQ}\right)(u) - \sum_{\alpha=1,2}\left(\log\left(1-\frac{1}{Y_-^{(\alpha)}}\right)\hat\star K_-^{yQ}\right)(u)\,.\end{aligned} \tag{6.64}$$

Equation for $\bar{Q}$-particles.

$$\begin{aligned}-\log \bar{Y}_Q(u) = L\tilde{\mathcal{E}}^Q(u) &- \left(\log\left(1+\bar{Y}_{Q'}\right)\star K_{su}^{Q'Q}\right)(u) - \left(\log\left(1+Y_{Q'}\right)\star \tilde{K}_{sl}^{Q'Q}\right)(u) \\ &- \sum_{\dot\alpha=1}^{N_0}\left(\log\left(1+Y_0^{(\dot\alpha)}\right)\check\star \tilde{K}^{0Q}\right)(u) + \sum_{j=1}^{2M}\log \tilde{S}^{0_*Q}(u_{s,j}^{\dot\alpha_j},u) \\ &- \sum_{\alpha=1,2}\left(\log\left(1-\frac{1}{Y_+^{(\alpha)}}\right)\hat\star K_-^{yQ}\right)(u) - \sum_{\alpha=1,2}\left(\log\left(1-\frac{1}{Y_-^{(\alpha)}}\right)\hat\star K_+^{yQ}\right)(u)\,.\end{aligned} \tag{6.65}$$

Equations for Massless particles.

$$\begin{aligned}-\log Y_0^{(\dot\alpha)}(u) = L\tilde{\mathcal{E}}^0(u) &- \sum_{\dot\beta=1}^{N_0}\left(\log\left(1+Y_0^{(\dot\beta)}\right)\check\star K^{00}\right)(u) + \sum_{j=1}^{2M}\log S^{0_*0}(u_{s,j}^{\dot\alpha_j},u) \\ &- \left(\log\left(1+Y_Q\right)\star K^{Q0}\right)(u) - \left(\log\left(1+\bar{Y}_Q\right)\star \tilde{K}^{Q0}\right)(u) \\ &- \sum_{\alpha=1,2}\left(\log\left(1-\frac{1}{Y_+^{(\alpha)}}\right)\hat\star K^{y0}\right)(u) - \sum_{\alpha=1,2}\left(\log\left(1-\frac{1}{Y_-^{(\alpha)}}\right)\hat\star K^{y0}\right)(u)\,.\end{aligned} \tag{6.66}$$

Equations for auxiliary y^--particles.

$$\begin{aligned}\log Y_-^{(\alpha)}(u) = &-\left(\log\left(1+Y_Q\right)\star K_-^{Qy}\right)(u) + \left(\log\left(1+\bar{Y}_Q\right)\star K_+^{Qy}\right)(u) \\ &+ \sum_{\dot\alpha=1}^{N_0}\left(\log\left(1+Y_0^{(\dot\alpha)}\right)\check\star K^{0y}\right)(u) - \sum_{j=1}^{2M}\log S^{0_*y}(u_{s,j}^{\dot\alpha_j},u)\,.\end{aligned} \tag{6.67}$$

Equations for auxiliary y^+-particles.

$$\begin{aligned}\log Y_+^{(\alpha)}(u) = &-\Big(\log\left(1+Y_Q\right)\star K_+^{Qy}\Big)(u)+\Big(\log\left(1+\bar{Y}_Q\right)\star K_-^{Qy}\Big)(u)\\ &-\sum_{\dot\alpha=1}^{N_0}\Big(\log\left(1+Y_0^{(\dot\alpha)}\right)\check{\star}K^{0y}\Big)(u)+\sum_{j=1}^{2M}\log S^{0\star y}(u_{s,j}^{\dot\alpha_j},u)\,.\end{aligned}\tag{6.68}$$

Note that we wrote the equations with a sum over the N_0 massless modes. In the original proposal [65] the value is $N_0 = 2$. However, in the recent work [139] a comparison of the ground state energy with a direct computation from string theory suggests, that only one massless mode should be included, *i.e.* $N_0 = 1$. We will keep the following analysis as general as possible by writing N_0.

Energy and momentum. Similar to the example in Sec. 6.1, we can compute the energy from the Y-functions. However, here we have to consider the contributions from the massive as well as the massless Y-functions.

$$\begin{aligned}\mathcal{E}(L) = &-\int_{-\infty}^{\infty}\frac{\mathrm{d}u}{2\pi}\frac{\mathrm{d}\tilde{p}^Q(u)}{\mathrm{d}u}\log\big((1+Y_Q(u))(1+\bar{Y}_Q(u))\big)\\ &-\int_{|u|>2}\frac{\mathrm{d}u}{2\pi}\frac{\mathrm{d}\tilde{p}^0(u)}{\mathrm{d}u}\sum_{\dot\alpha=1}^{N_0}\log\Big(1+Y_0^{(\dot\alpha)}(u)\Big)+\sum_{j=1}^{2M}\mathcal{E}^0(u_{s,j}^{\dot\alpha_j})\,.\end{aligned}\tag{6.69}$$

The auxiliary Y-functions do not contribute to the energy. It is also useful to write a similar formula to impose that the total-momentum of the (ground) state vanishes, namely

$$\begin{aligned}0 = &-\int_{-\infty}^{\infty}\frac{\mathrm{d}u}{2\pi}\frac{\mathrm{d}\tilde{\mathcal{E}}^Q(u)}{\mathrm{d}u}\log\big((1+Y_Q(u))(1+\bar{Y}_Q(u))\big)\\ &-\int_{|u|>2}\frac{\mathrm{d}u}{2\pi}\frac{\mathrm{d}\tilde{\mathcal{E}}^0(u)}{\mathrm{d}u}\sum_{\dot\alpha=1}^{N_0}\log\Big(1+Y_0^{(\dot\alpha)}(u)\Big)+\sum_{j=1}^{2M}p(u_{s,j}^{\dot\alpha_j})\,.\end{aligned}\tag{6.70}$$

This is the level-matching condition in string theory (without winding around the lightcone, see [111]). Since we chose pairs of momenta $(-p_j, p_j)$ with $j = 1, \ldots, M$, the last sum does not contribute.

Exact Bethe equations. The rapidities $u_{s,j}^{\dot\alpha_j}$ have to satisfy the exact Bethe equations. Similarly to the example in Sec. 6.1, we can write them by analytically continuing the

massless TBA eq. (6.66) to the string region. Introducing the label $n_k^{\dot\alpha} \in \mathbb{Z}$ we get

$$
\begin{aligned}
&i\pi(2n_k^{\dot\alpha}+1) = \\
&\quad - iLp_k^{\dot\alpha_k} - \sum_{\dot\beta=1}^{N_0} \left(\log\left(1+Y_0^{(\dot\beta)}\right)\star K^{00_*}\right)(u_{s,k}^{\dot\alpha_k}) + \sum_{j=1}^{2M} \log S^{0_*0_*}(u_{s,j}^{\dot\alpha_j},\, u_{s,k}^{\dot\alpha_k}) \\
&\quad - \left(\log\left(1+Y_Q\right)\star K^{Q0_*}\right)(u_{s,k}^{\dot\alpha_k}) - \left(\log\left(1+\bar Y_Q\right)\star \tilde K^{Q0_*}\right)(u_{s,k}^{\dot\alpha_k}) \\
&\quad - \sum_{\alpha=1,2}\left(\log\left(1-\frac{1}{Y_+^{(\alpha)}}\right)\hat\star K^{y0_*}\right)(u_{s,k}^{\dot\alpha_k}) - \sum_{\alpha=1,2}\left(\log\left(1-\frac{1}{Y_-^{(\alpha)}}\right)\hat\star K^{y0_*}\right)(u_{s,k}^{\dot\alpha_k}),
\end{aligned}
\tag{6.71}
$$

for $k = 1, \ldots, 2M$. Again, the 0_* signals, that the corresponding function is analytically continued to the string region.

6.3. Simplified TBA equations in the tensionless limit

The mirror TBA equations written above can be simplified. In the following, we will begin to rewrite them, dropping the $\mathfrak{su}(2)$ labels and introducing renormalised kernels. Afterwards, we will consider the small-tension limit $h \to 0$. In this limit the massive modes will decouple, allowing us to write TBA equations involving only massless and auxiliary modes.

6.3.1. Rewriting of the TBA equations

We will drop the $\mathfrak{su}(2)$ labels in what follows and will from now on use

$$
Y_0(u) \equiv Y_0^{(1)}(u) = Y_0^{(2)}(u)\,, \qquad \text{and} \qquad Y_\pm(u) \equiv Y_\pm^{(1)}(u) = Y_\pm^{(2)}(u)\,. \tag{6.72}
$$

However, we still have to use the label to distinguish the Bethe roots, as two Bethe roots may take the same value as long as they satisfy the Pauli exclusion principle. This allows us to replace the sum over $\dot\alpha$ by the factor N_0.

Considering the above TBA equations we can identify a potential problem with the auxiliary-massless convolutions. For the corresponding S matrices in the mirror-mirror region we have

$$
S^{0y}(u,u') = \frac{1}{\sqrt{x(u)^2}}\frac{x(u)-x_s(u')}{\frac{1}{x(u)}-x_s(u')}\,, \qquad S^{y0}(u',u) = \frac{1}{S^{0y}(u,u')}\,, \tag{6.73}
$$

with u just above the long cut for a massless mirror particle and u' just above the short cut for the auxiliary particles. Let us consider the source term $S^{0_*y}(u_{s,j}^{\dot\alpha_j}, u')$. As $u_{s,j}^{\dot\alpha_j}$ is in the string region, we have that $x_s(u_{s,j}^{\dot\alpha_j})$ is on the upper half-circle, just like $x_s(u')$. It follows that the source term $S^{0_*y}(u_{s,j}^{\dot\alpha_j}, u')$ has a zero when u' is on the real mirror line. This leads to a logarithmic singularity in the convolutions involving $\log\left(1-\frac{1}{Y_+}\right)$ in eqs. (6.64), (6.65) and (6.66). It is convenient to rewrite the convolution as

$$
-\log\left(1-\frac{1}{Y_+}\right)^2 \hat\star K^{y0} = \left(-\log\left(1-Y_+\right)^2 + \log(Y_+)^2\right)\hat\star K^{y0}\,. \tag{6.74}
$$

Note that the representation of the logarithm is important here. Depending on whether we write $\log z^2$ or $2\log z$, we might obtain an additional $2\pi i$ term. Convoluting this additional term with K^{y0} yields $2i\pi\hat{\star}K^{y0} = i\pi$. This ambiguity can be fixed later on by demanding compatibility of the exact Bethe equations and the asymptotic Bethe equations.

Apparently the first convolution in eq. (6.74) is regular, while the second is still divergent. However, we can now use eq. (6.68) to express the contribution of the latter through multiple convolutions. Using this and leaving the dependence on the rapidity u implicit, we can rewrite the massless TBA equations as

$$\begin{aligned}-\log Y_0 = L\tilde{\mathcal{E}}^0 &- \log(1+Y_0)^{N_0}\check{\star}K^{00}_{\text{ren}} + \sum_{j=1}^{2M}\log S^{0_*0}_{\text{ren}}(u^{\dot\alpha_j}_{s,j},\,\cdot\,)\\ &- \log(1+Y_Q)\star K^{Q0}_{\text{ren}} - \log(1+\bar{Y}_Q)\star\tilde{K}^{Q0}_{\text{ren}}\\ &- \log(1-Y_+)^2\hat{\star}K^{y0} - \log\left(1-\frac{1}{Y_-}\right)^2\hat{\star}K^{y0}\,,\end{aligned} \tag{6.75}$$

where we defined the *renormalised kernels* as

$$\begin{aligned}K^{00}_{\text{ren}} &= K^{00} + 2K^{0y}\hat{\star}K^{y0}\,,\\ K^{Q0}_{\text{ren}} &= K^{Q0} + 2K^{Qy}_{+}\hat{\star}K^{y0}\,,\quad \tilde{K}^{Q0}_{\text{ren}} = \tilde{K}^{Q0} - 2K^{Qy}_{-}\hat{\star}K^{y0}\,,\end{aligned} \tag{6.76}$$

as well as the renormalised source term

$$\log S^{0_*0}_{\text{ren}}(u^{\dot\alpha_j}_{s,j},u') = \log S^{0_*0}(u^{\dot\alpha_j}_{s,j},u') + 2\int_{-2}^{+2}\mathrm{d}v\,\log S^{0_*y}(u^{\dot\alpha_j}_{s,j},v)\,K^{y0}(v,u')\,. \tag{6.77}$$

Analogously, this rewriting can be done for the massive TBA equations (6.64) and (6.65). However, as we will see in the following subsection, these will not be important in the small tension limit. Further, by defining

$$\begin{aligned}K^{00_*}_{\text{ren}} &= K^{00_*} + 2K^{0y}\hat{\star}K^{y0_*}\,,\\ K^{Q0_*}_{\text{ren}} &= K^{Q0_*} + 2K^{Qy}_{+}\hat{\star}K^{y0_*}\,,\quad \tilde{K}^{Q0_*}_{\text{ren}} = \tilde{K}^{Q0_*} - 2K^{Qy}_{-}\hat{\star}K^{y0_*}\,,\end{aligned} \tag{6.78}$$

we can obtain from eq. (6.71) the renormalised exact Bethe equations given as

$$\begin{aligned}i\pi(2n^{\dot\alpha}_k+1) = &-iLp^{\dot\alpha_k}_k - \log(1+Y_0)^{N_0}\check{\star}K^{00_*}_{\text{ren}} + \sum_{j=1}^{2M}\log S^{0_*0_*}_{\text{ren}}(u^{\dot\alpha_j}_{s,j},\,u^{\dot\alpha_k}_{s,k})\\ &- \log(1+Y_Q)\star K^{Q0_*}_{\text{ren}} - \log(1+\bar{Y}_Q)\star\tilde{K}^{Q0_*}_{\text{ren}}\\ &- \log(1-Y_+)^2\hat{\star}K^{y0_*} - \sum_{\alpha=1,2}\log\left(1-\frac{1}{Y_-}\right)^2\hat{\star}K^{y0_*}\,.\end{aligned} \tag{6.79}$$

6.3.2. Analysing the scaling in the small-tension limit

We are interested in the small tension limit $h\to 0$. To find the excited mirror TBA equations as well as the exact Bethe equations and exact energy in this limit, let us start by considering the scaling of the Y-functions. It will turn out, that the massive

modes decouple, giving a simpler set of equations, which can be simplified further.

Assumptions and resulting scaling. Let us begin by considering the scaling behaviour of the massive Y-functions. The TBA equations for Y_Q and $\bar{Y}_Q$ are given in eqs. (6.64) and (6.65), respectively. The mirror energy $\tilde{\mathcal{E}}^Q(u)$ is bounded from below by its value at $\tilde{p} = 0$, that is at $u = 0$. In fact,

$$\tilde{\mathcal{E}}^Q(u) = \log \frac{Q^2}{h^2} + \mathcal{O}(h^2) \qquad \text{for} \qquad Q \neq 0\,. \tag{6.80}$$

Since the mirror energy is divergent for $h \to 0$, we conclude that there is at least one divergent term in the equations for Y_Q and $\bar{Y}_Q$ with $Q \neq 0$. Further, let us assume, that all the remaining terms on the right hand side of the excited state TBA equations for Y_Q and $\bar{Y}_Q$ are finite in the limit $h \to 0$. Then we find from the respective TBA equations that

$$Y_Q(u) = h^{2L}\, y_Q(u)\,, \qquad \bar{Y}_Q(u) = h^{2L}\, \bar{y}_Q(u)\,, \tag{6.81}$$

where we introduced the functions $y_Q(u)$ and $\bar{y}_Q(u)$, which are convergent and finite as $h \to 0$.

Similarly, we can consider the scaling of the massless Y-functions. The mirror energy $\tilde{\mathcal{E}}^0(u)$ is given in eq. (6.59). As it does not explicitly depend on h, it is finite in the $h \to 0$ limit. Let us further assume, that the kernels involving massive particles, *i.e.* K^{Q0} and $\tilde{K}^{Q0}$, are convergent and finite as $h \to 0$. Under these assumptions and using the scaling of Y_Q and $\bar{Y}_Q$ from eq. (6.81), we find

$$-\log(1 + Y_Q) \star K^{Q0} - \log(1 + \bar{Y}_Q) \star \tilde{K}^{Q0} = \mathcal{O}(h^{2L})\,, \tag{6.82}$$

which contributes at a higher order in h than the mirror energy $\tilde{\mathcal{E}}^0(u) = \mathcal{O}(h^0)$. Therefore, we can neglect the contribution from massive modes to the massless TBA equations.

Making similar assumptions about the kernels involving massive modes in the auxiliary equations, namely $K^{Qy}_{\pm}$, and the analytically continued kernels K^{Q0_*} and $\tilde{K}^{Q0_*}$ in the exact Bethe equations, there the massive modes decouple at leading order in the coupling h as well.

After these considerations, we are left with a system of equations for and involving only $Y_0(u)$ and $Y_\pm(u)$. Assuming again, that the remaining kernels are well behaved for $h \to 0$, we find the scaling

$$Y_0(u) = \mathcal{O}(h^0)\,, \qquad \text{and} \qquad Y_\pm(u) = \mathcal{O}(h^0)\,. \tag{6.83}$$

With this, we can consider the scaling of the energy for an excited state. As before, the integrals involving Y_Q and $\bar{Y}_Q$ functions in eq. (6.69) are of the order h^{2L} and hence suppressed. We find for the energy at leading order $\mathcal{O}(h^1)$,

$$\mathcal{E}(L) = -\int\limits_{|u|>2} \frac{\mathrm{d}u}{2\pi} \frac{\mathrm{d}\tilde{p}^0}{\mathrm{d}u} \log(1 + Y_0)^{N_0} + \sum_{j=1}^{2M} \mathcal{E}^0(u_{s,j}^{\dot{\alpha}_j})\,. \tag{6.84}$$

From eqs. (6.44) and (6.59) it is clear, that the dependence on h is introduced through $\mathcal{E}^0(u)$ and $\tilde{p}^0(u)$.

In the following paragraphs we will justify the assumptions made about the kernels. However, we will keep the discussion rather compact due to its technical nature. Our focus is on the simplification of the TBA equations, given that the kernels are sufficiently well-behaved. We will discuss the kernels involved in the convolutions in the TBA equations, but, of course, a similar analysis needs to be done for the source terms and finally the exact Bethe equations. For more details and a more technical discussion, we refer the reader to [4, 5].

Vindicating the assumptions for massive particles. In the $h \to 0$ limit the leading order of the kernels $K_{sl}^{Q'Q}(u', u)$ and $\tilde{K}_{su}^{Q'\bar{Q}}(u', u)$ are given by the contributions from the BES terms, namely $K_{\Sigma}^{Q'Q}(u', u)$ and $\tilde{K}_{\Sigma}^{Q'\bar{Q}}(u', u)$. The kernels are regular for real values of the rapidities u', u.

Next, we consider the massless-massive kernel $K^{0Q}(u_1, u_2)$, that has multiple divergences. Firstly, there are divergences at $u_1 = \pm 2$, which are integrable as long as the kernel is convoluted with a finite function. Further, there are divergencies for $u_1 \to \pm\infty$, as the BES kernel diverges like $1/x(u_1)^2$ for $x(u_1) \to 0$ and $|x(u_1)| \ll h \ll 1$. Therefore, the functions we integrate the kernel against have to vanish around $x(u_1) = 0$. We can also see from the formula for the energy eq. (6.84), that we need $\log(1 + Y_0)$ to vanish around $x(u_1) = 0$. Since the mirror momentum diverges at $x(u_1) = 0$ this is necessary for a well-defined energy. This behaviour of Y_0 follows from the term $L\tilde{\mathcal{E}}^0$ in the massless TBA equations as $Y_0(u_1) \sim x(u_1)^{2L}$ in the vicinity $|x(u_1)| \ll 1$. Hence, it can be concluded, that the convolution is regular and the $h \to 0$ limit can be taken. The analysis of the kernels $K_{\pm}^{yQ}$ is similar. Also these feature singularities, which are integrable as long as the functions $Y_{\pm}(u_1)$ remain finite near the rapidities for which the kernels diverge.

Following these statements, it can be concluded, that all the convolutions in the equations for massive particles are regular for small h. The scaling of Y_Q is therefore solely dictated by the term $L\tilde{\mathcal{E}}^Q$, as assumed above.

Vindicating the assumptions for massless particles. We also have to consider the kernels appearing in the massless TBA equations. Let us begin by stating, that the auxiliary kernel K^{y0} is regular.

Next, the massive-massless kernel $K^{Q0}(u_2, u_1)$ behaves like $K^{0Q}(u_1, u_2)$ considered above. Though the kernel is singular for $x(u_1) \to 0$, *i.e.* $u_1 \to \pm\infty$, its convolution with the massive Y-functions behaves like $h^{2L} \log(x(u_1))$ for $|x(u_1)| \ll h \ll 1$. Hence the contribution from massive particles can be neglected at leading order.

Finally, we have the massless-massless kernel $K^{00}(u_1, u_2)$. For later convenience, let us already state here, that the massless-massless BES kernel $K_{\text{BES}}^{00}(u_1, u_2)$ decouples at leading order in h. Also this kernel is divergent at $x_1 \to 0$. However, the convolution with the massless Y-functions vanishes for $h \to 0$, as long as Y_0 also vanishes in the vicinity of $x_1 = 0$, as discussed above.

With these observations, we see that also for the massless TBA equations most kernels decouple.

6.3.3. Simplifying the TBA equations

Having analysed the leading order at which the Y-functions (at $\mathcal{O}(h^0)$) and the energy (at $\mathcal{O}(h^1)$) contribute, we found, that the massive modes decouple. Hence the excited

mirror TBA equations at leading order in h are given by

$$\begin{aligned}
-\log Y_0 =& L\tilde{\mathcal{E}}_0 - \log(1+Y_0)^{N_0}\check{\star}K^{00}_{\text{ren}} + \sum_{j=1}^{2M}\log S^{0_*0}_{\text{ren}}(u^{\dot\alpha_j}_{s,j},\,\cdot\,)\\
&- \log(1-Y_+)^2\hat{\star}K^{y0} - \log\left(1-\frac{1}{Y_-}\right)^2\hat{\star}K^{y0}\,,\\
\log Y_- =& +\log(1+Y_0)^{N_0}\check{\star}K^{0y} - \sum_{j=1}^{2M}\log S^{0_*y}(u^{\dot\alpha_j}_{s,j},\,\cdot\,)\,,\\
\log Y_+ =& -\log(1+Y_0)^{N_0}\check{\star}K^{0y} + \sum_{j=1}^{2M}\log S^{0_*y}(u^{\dot\alpha_j}_{s,j},\,\cdot\,)\,.
\end{aligned} \tag{6.85}$$

Here we left the dependence of the source terms on the rapidity u implicit and merely indicated it by a dot. Let us now take a closer look at the remaining kernels and S matrices. Further, we will rewrite the equations in terms of the real γ-rapidity. Arguments in the string region can be realised by appropriately shifting the kernels, taking $\gamma_s = \gamma - \frac{i\pi}{2}$ from eq. (6.55) into account. For this purpose, let us introduce the *Cauchy kernel* $s(\gamma)$ and the corresponding S matrix $S(\gamma)$, which are defined as

$$s(\gamma) = \frac{1}{2\pi i}\frac{\mathrm{d}}{\mathrm{d}\gamma}\log S(\gamma) = \frac{1}{2\pi\cosh\gamma}\,, \qquad S(\gamma) = -i\tanh\left(\frac{\gamma}{2}-\frac{i\pi}{4}\right). \tag{6.86}$$

Moreover, since we work in the γ-parametrisation, we will introduce calligraphic kernels, which are related to the kernels from eq. (6.61) through

$$K^{**}(u,u') = \frac{\mathrm{d}\gamma}{\mathrm{d}u}\,\mathcal{K}^{**}(\gamma(u),\gamma(u'))\,, \quad \text{with} \quad \mathcal{K}^{**}(\gamma,\gamma') = \frac{2}{2\pi i}\frac{\mathrm{d}}{\mathrm{d}\gamma}\log S^{**}(\gamma,\gamma')\,. \tag{6.87}$$

Let us now consider the expressions relevant for the TBA equations above. First of all, looking at the auxiliary equations, we can observe that we can rewrite the S matrices involving massless and auxiliary particles as

$$S^{0y}(x(\gamma),x_s(\gamma')) = \frac{-i\,\mathrm{sgn}(\gamma)}{S(\gamma-\gamma')}\,, \qquad S^{y0}(x_s(\gamma),x(\gamma')) = \frac{+i\,\mathrm{sgn}(\gamma')}{S(\gamma-\gamma')}\,, \tag{6.88}$$

so that the respective kernels are given by

$$\mathcal{K}^{0y}(\gamma,\gamma') = -s(\gamma-\gamma') + \frac{1}{2}\delta(\gamma)\,, \qquad \mathcal{K}^{y0}(\gamma,\gamma') = -s(\gamma-\gamma')\,. \tag{6.89}$$

Neglecting the δ-functions[1], the TBA equations for the auxiliary particles become

$$\begin{aligned}
\log Y_-(\gamma) =& -\left(\log(1+Y_0)^{N_0} * s\right)(\gamma) - \sum_{j=1}^{M}\log\left(S_*(-\gamma_j^{\dot\alpha_j}-\gamma)S_*(\gamma_j^{\dot\alpha_j}-\gamma)\right)\,,\\
\log Y_+(\gamma) =& +\left(\log(1+Y_0)^{N_0} * s\right)(\gamma) + \sum_{j=1}^{M}\log\left(S_*(-\gamma_j^{\dot\alpha_j}-\gamma)S_*(\gamma_j^{\dot\alpha_j}-\gamma)\right)\,,
\end{aligned} \tag{6.90}$$

[1]Neglecting $\log(1+Y_0)^{N_0}\check{\star}K^{0y}$ can be justified, as $Y_0(\gamma)$ vanishes at $\gamma=0$ as argued above.

where the analytic continuation of the S matrices in the source term is indicated by the asterisk. We use the definition

$$S_*(\gamma) \equiv S(\gamma + \frac{i\pi}{2}) \,, \tag{6.91}$$

for the continuation of $S(\gamma)$ to the mirror-string region. We also paired the roots of opposite signs in eq. (6.90). Note further, that here we used $*$ for the convolution, since we always integrate the γ-rapidity over the real line, *i.e.*

$$* \leftrightarrow \int_{-\infty}^{+\infty} \mathrm{d}\gamma \,. \tag{6.92}$$

By adding the two lines in eq. (6.90), we see that at leading order in the coupling we have $Y_+(\gamma)Y_-(\gamma) = 1$ and hence we can introduce

$$Y(\gamma) \equiv Y_+(\gamma) = \frac{1}{Y_-(\gamma)} \,. \tag{6.93}$$

This leads to only one equation for the auxiliary particles written in terms of $Y(\gamma)$.

Let us proceed with the massless TBA equations. The renormalised calligraphic kernel $\mathcal{K}^{00}_{\text{ren}}$, as found in eq. (6.76), is given by

$$\mathcal{K}^{00}_{\text{ren}}(\gamma,\gamma') = \mathcal{K}^{00}(\gamma,\gamma') + 2\left(\frac{du}{d\gamma}\right)(K^{0y}\hat{\star}K^{y0})(\gamma,\gamma') \,, \tag{6.94}$$

where the kernel $\mathcal{K}^{00}(\gamma,\gamma')$ is the sum of three terms (*cf.* also eq. (B.5) in App. B)

$$\mathcal{K}^{00}(\gamma,\gamma') = s(\gamma-\gamma') + 2\mathcal{K}_{\text{SG}}(\gamma,\gamma') - 2\mathcal{K}^{00}_{\text{BES}}\Big(x(\gamma),x(\gamma')\Big) \,. \tag{6.95}$$

The last term is related to the BES-phase, which does not contribute at leading order in the coupling h. We can therefore neglect it in the following. Further, the *Sine-Gordon* kernel is of difference form in the rapidities and given by

$$\mathcal{K}_{\text{SG}}(\gamma,\gamma') = \frac{\gamma-\gamma'}{2\pi^2\sinh(\gamma-\gamma')} \,. \tag{6.96}$$

Let us now evaluate the convolution in eq. (6.94). The calculation can be done explicitly and yields

$$\begin{aligned} K^{0y}\hat{\star}K^{y0}(u,u') &= \int_{-2}^{2} du''\, K^{0y}(u,u'')K^{y0}(u'',u') \\ &= -\int_{-\infty}^{\infty} d\gamma''\, K^{0y}(u(\gamma),u_s(\gamma''))\,\frac{du''}{d\gamma''}\,K^{y0}(u_s(\gamma''),u(\gamma')) \\ &= \left(\frac{d\gamma}{du}\right)\left(-\mathcal{K}_{\text{SG}}(\gamma,\gamma') + \frac{1}{4}\delta(\gamma)\right) \,. \end{aligned} \tag{6.97}$$

Substituting this into eq. (6.94) and again neglecting the δ-functions, we see, that at

leading order in the coupling h the renormalised massless kernel becomes

$$\mathcal{K}^{00}_{\text{ren}}(\gamma,\gamma') = s(\gamma-\gamma') + \mathcal{O}(h)\,. \tag{6.98}$$

In a similar way, we can find that the analytically continued renormalised massless S matrix is in the small h limit given by

$$S^{0_*0}_{\text{ren}}(\gamma,\gamma') = -\frac{1}{S_*(\gamma-\gamma')} + \mathcal{O}(h)\,. \tag{6.99}$$

Equipped with these results, we can finally write the TBA equations from eq. (6.85) in the simplified form

$$\begin{aligned} -\log Y_0(\gamma) &= L\tilde{\mathcal{E}}^0(\gamma) - \left(\log\left(1+Y_0\right)^{N_0} * s\right)(\gamma) - \sum_{j=1}^{M} \log\Big(S_*(-\gamma_j^{\dot\alpha_j}-\gamma)\,S_*(\gamma_j^{\dot\alpha_j}-\gamma)\Big) \\ &\quad - \left(\log\left(1-Y\right)^{4} * s\right)(\gamma)\,, \\ \log Y(\gamma) &= \left(\log\left(1+Y_0\right)^{N_0} * s\right)(\gamma) + \sum_{j=1}^{M} \log\Big(S_*(-\gamma_j^{\dot\alpha_j}-\gamma)S_*(\gamma_j^{\dot\alpha_j}-\gamma)\Big)\,. \end{aligned} \tag{6.100}$$

It is worth noting, that picking the pairs of rapidities $(-\gamma_j^{\dot\alpha_j}, \gamma_j^{\dot\alpha_j})$ introduces a sign into the source term of the auxiliary TBA equations, given by $\operatorname{sgn}(-\gamma_j^{\dot\alpha_j})\operatorname{sgn}(\gamma_j^{\dot\alpha_j}) = -1$. However, there is also another factor $i^2 = -1$ from eq. (6.88) compensating the sign from the Signum function. Hence, the source terms in the auxiliary TBA equations are identical to the one in the massless TBA equation.

Finally, we also have the exact Bethe equation, which reads

$$\begin{aligned} i\pi(2n_k^{\dot\alpha}+1) =& -iLp(\gamma_k^{\dot\alpha_k}) - \left(\log\left(1+Y_0\right)^{N_0} * s_*\right)(\gamma_k^{\dot\alpha_k}) + \sum_{j=1}^{2M} \log S(\gamma_j^{\dot\alpha_j}-\gamma_k^{\dot\alpha_k}) \\ &- \left(\log\left(1-Y\right)^{4} * s_*\right)(\gamma_k^{\dot\alpha_k})\,. \end{aligned} \tag{6.101}$$

Let us emphasise again, that the pairs of Bethe roots $\pm\gamma_j^{\dot\alpha_j}$ need to satisfy the exact Bethe equation.

One can now attempt to solve this set of eqs. (6.100) and (6.101), to obtain the Y-functions Y_0 and Y as well as the Bethe roots $\pm\gamma_j^{\dot\alpha_j}$. Using the solutions together with eq. (6.84), the exact energy can be calculated. By rewriting eq. (6.84) in terms of the γ-rapidities, we obtain

$$\mathcal{E}(L) = -\int_{-\infty}^{+\infty} \frac{\mathrm{d}\gamma}{2\pi}\frac{\mathrm{d}\tilde{p}^0}{\mathrm{d}\gamma}\log\left(1+Y_0(\gamma)\right)^{N_0} + \sum_{j=1}^{2M}\mathcal{E}(\gamma_j^{\dot\alpha_j})\,. \tag{6.102}$$

We can see that there is no contribution to the energy at $\mathcal{O}(h^0)$, as both $\tilde{p}^0(\gamma)$ and $\mathcal{E}(\gamma_s)$ are of order $\mathcal{O}(h^1)$. Hence, at this order, massless states have zero energy and are highly degenerate. Further, since $\log\left(1+Y_0(\gamma)\right)^{N_0} \sim \mathcal{O}(h^0)$, the massless Y-functions contribute to the energy at $\mathcal{O}(h^1)$. This indicates, that wrapping correction start contributing at the earliest order possible. This also lifts the degeneracy of the massless states. From our discussion around eq. (6.81), we can then expect wrapping corrections

to the energy from the massive Y-functions contributing at $\mathcal{O}(h^{2L})$.

Ground state solution. Let us study the ground state TBA equations, which we can obtain from eq. (6.100) by simply dropping the source terms. Since the equations are written over a BPS vacuum, the ground state energy must vanish. Let us consider this more explicitly. The TBA equation for Y_0 is singular and we need to regularise it by introducing a small chemical potential μ, as it was done for $\mathrm{AdS}_5 \times \mathrm{S}^5$ in [140]. A similar analysis for the TBA equations at hand has been performed in [139] including the massive modes. Let us repeat the analysis here for the equations obtained in the small tension limit given in eq. (6.100). We introduce μ in the following way

$$\begin{aligned} -\log Y_0(\gamma) &= L\tilde{\mathcal{E}}^0(\gamma) - \left(\log\left(1+Y_0\right)^{N_0} * s\right)(\gamma) - \left(\log\left(1-Y\right)^4 * s\right)(\gamma)\,, \\ \log Y(\gamma) &= \quad \mu \quad + \left(\log\left(1+Y_0\right)^{N_0} * s\right)(\gamma)\,. \end{aligned} \tag{6.103}$$

We can now make an ansatz for the Y-functions as a series in the chemical potential of the form

$$Y_0(\gamma) = \sum_{k=0} \mu^k y_0^{(k)}(\gamma)\,, \qquad Y(\gamma) = \sum_{k=0} \mu^k y^{(k)}(\gamma)\,, \tag{6.104}$$

and substitute it into the ground state TBA equations (6.103). Expanding in μ, we can solve for the coefficient functions $y_0^{(k)}(\gamma)$ and $y^{(k)}(\gamma)$ up to a certain order. For $N_0 = 1, 2$ we find

$$\begin{aligned} Y_0(\gamma) &= \mu^2 e^{-L\tilde{\mathcal{E}}_0(\gamma)} + \mu^3 \left(e^{L\tilde{\mathcal{E}}_0(\gamma)} + N_0\, e^{-2L\tilde{\mathcal{E}}_0(\gamma)}\right) + \mathcal{O}(\mu^4)\,, \\ Y(\gamma) &= 1 + \mu + \frac{\mu^2}{2}\left(1 + N_0\, e^{-L\tilde{\mathcal{E}}_0(\gamma)}\right) + \mathcal{O}(\mu^3)\,. \end{aligned} \tag{6.105}$$

For the solutions the exact energy evaluates at leading order in μ to

$$\begin{aligned} \mathcal{E}(L) &= -\frac{h}{\pi}\int_{-\infty}^{\infty} d\gamma\, \frac{\cosh\gamma}{\sinh^2\gamma}\, \log(1+Y_0(\gamma))^{N_0} \\ &= -\mu^2 \frac{N_0 h L}{L^2 - \frac{1}{4}} + \mathcal{O}(\mu^3)\,. \end{aligned} \tag{6.106}$$

As expected, in the limit $\mu \to 0$ we find that the ground state energy of a BPS state vanishes. This result agrees with the massless contribution in eq. (3.12) of [139], in which a term related to the massive modes is also present. Further, this means, that the ground state Y-functions are given by $Y_0 = 0$ and $Y = 1$.

Comments on solutions for excited states. In order to solve the simplified TBA equations (6.100) in the tensionless limit numerical methods need to be used. This can be done iteratively. Making an ansatz for the Y-functions, the TBA equations are evaluated numerically and the result is used to update the Y-functions. If the iteration is convergent, the resulting function for Y_0 can be used to calculate the correction to the energy. The TBA equations given in eq. (6.100) were solved to high precision in [4, 5]. Fig. 6.3 is taken from [4] and shows the anomalous dimensions for states of lengths $L = 4, 8, 16, 256$, for which we find $L/2$ distinct energies labelled by ν_1. We see, that the anomalous dimensions are rather well-approximated by the asymptotic result and quite close to the energies of the *free* model given by eq. (6.35) with $p_1 = 2\pi\nu_1/L$.

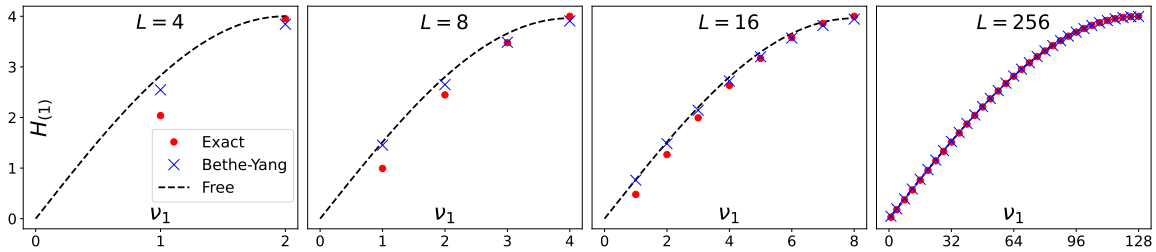

Figure 6.3.: This figure shows the anomalous dimensions for states with rapidities $\gamma_1 = -\gamma_2$ and is taken from [4]. Expanding the energy as $\mathcal{E} = H_{(1)}h + \mathcal{O}(h^2)$, the plots show the leading contribution $H_{(1)}$ for lengths $L = 4, 8, 16, 256$. These results are compared with the predictions from the Bethe-Yang equation $e^{ip_1 L}\prod_{k=1}^{2} S^{00}(p_1, p_k) = -1$ and the energy of a free model with the dispersion relation given in eq. (6.35).

This suggests that in the weak-coupling limit this model becomes similar to one of free particles with a massless periodic dispersion relation $\mathcal{E}(p) \sim |\sin(p/2)|$. It is worth stressing, that this similarity is not exact, implying that we have an interacting model already at leading order in h.

6.4. Chapter summary

In this chapter we considered the thermodynamic Bethe ansatz, which allows us to describe integrable models in a thermodynamic setting. In Sec. 6.1 we reviewed the TBA for the Heisenberg XXX spin chain and familiarised with the concepts involved. In particular, we considered the formation of bound states and the free energy. Going to the mirror TBA allows then to capture wrapping corrections. Further, we introduced the contour deformation trick [72] to consider excited states as well.

In Sec. 6.2 we turned to the mirror TBA equations for the pure Ramond-Ramond sector of $\mathrm{AdS}_3 \times \mathrm{S}^3 \times \mathrm{T}^4$, which were derived in [65]. Here we introduced the relevant particles as well as a parametrisation for the different kinematical regions. Moreover, the parametrisation used here can be conveniently rewritten using γ-rapidities. Finally, we gave the excited TBA equations, where we considered the excitation of massless modes only.

The simplification of the excited TBA equations was studied in Sec. 6.3. Dropping the $\mathfrak{su}(2)$ labels of the Y-functions, we rewrote the equations and introduced renormalised kernels. From analysing the scaling behaviour of the Y-functions in the small-tension limit, we concluded, that the massive modes decouple, leaving us only with the massless and auxiliary equations. Finally, we rewrote the remaining kernels and S matrix elements in terms of the γ-rapidities, yielding the simplified small tension TBA equations (6.100). From these we could see, that wrapping corrections from massless modes start contributing at the earliest order possible, *i.e.* at $\mathcal{O}(h^1)$.

Chapter 7.

Conclusions

In this thesis we worked on different aspects of integrability in $\mathrm{AdS}_5/\mathrm{CFT}_4$ as well as $\mathrm{AdS}_3/\mathrm{CFT}_2$. In the following we summarise the results and discuss possible directions of future research. Since we considered integrability in two different models, let us also discuss the results of the different parts respectively.

Part I: Integrability in $\mathcal{N} = 4$ SYM

We began this part with a review of integrability in $\mathcal{N} = 4$ SYM theory. In particular integrability provides powerful tools and methods to solve the spectral problem of the planar theory. These can even be extended to three- and higher-point functions by using the hexagon formalism [38]. Over the last years this machinery was further developed and used for the calculation of loop-corrections as well as non-planar corrections. Moreover, most of the hexagon results in the literature are for operators in rank-one sectors, as the formalism can be straightforwardly applied in these sectors.

Higher-rank sectors. An application of the hexagon form factor to higher-rank cases is more involved due to the more complicated structure of the physical states and scattering processes involved. Therefore, in Sec. 3.2 we considered this extension with the goal to maintain the operator structure of the formalism, while importing only the necessary minimum of information from the nested Bethe ansatz into the hexagon. This allows us to consider operators from higher-rank sectors at all three points. We dubbed this procedure *hybrid picture*, as we need the nested Bethe wave function to find the coefficients of the multi-component Bethe wave function, on which we act with the hexagon in the usual matrix formalism. In the examples we considered, these coefficients capture the information supplied by the auxiliary rapidities from the nested ansatz. The evaluation of the hexagon depends only on the momentum carrying rapidities. Hence, our hybrid approach eclipses local details of the wave functions, as all relevant information is hidden in the Bethe rapidities.

In [104] a nested hexagon was introduced. For instance, eq. (19) there resembles our expressions for the coefficients g_Ψ, though it does not contain the creation amplitudes for higher-level magnons of the nested Bethe ansatz. Moreover, the construction in [104] relies heavily on the construction of the Bethe wave functions. Since already in the spectral problem the wave functions can have a complicated local structure, we aimed at avoiding this route. What is more, the hexagon operator features poles between conjugate particles at different edges due to crossing. Dissolving the matrix structure of the hexagon, it is hard to see how the correct crossing properties could be recovered from a nested Bethe ansatz wave function. The only part of the Beisert S matrix occurring

there is the $\mathcal{A}(u_1, u_2)$ element [97], which does not yield the right pole structure under crossing. However, when considering multiple higher-rank operators, this structure is crucial. Finally, when using the hexagon for the computation of higher-point functions, the construction of a single wave function for the correlator seems discouraging. Despite these differences in the construction, it would be interesting to use the hybrid picture considering three-point functions with only one higher-rank operator and compare the results with [104].

Marginal deformations. In Sec. 3.3 we aimed to generalise the hexagon formalism of $\mathcal{N} = 4$ SYM to the β-deformed theory. Since marginal deformations can be incorporated into the nested Bethe ansatz for the spectral problem by introducing deformation factors as in [97], our approach tried to introduce deformation factors into the undeformed hexagons. Already when studying the splitting factors we observed that they are dressed by such factors due to the deformation of the nested Bethe ansatz. We considered three-point functions with operators in the SU(1|2) sector and were able to fix these deformation factors. Further, the deformation is implicitly put into the hexagon through the Bethe roots characterising the three operators. However, there is a caveat when we choose the R-charges of the outer operators. There must be no effective vacuum-vacuum propagators $\langle \hat{Z}\hat{Z} \rangle$ between the two non-trivial operators on the three-point function. Such propagators exist in the undeformed theory as a result of the twisted translation. The underlying symmetry is broken by the deformations and the defining axioms from the undeformed theory cannot easily be adapted to the deformed case. While one could hope that the symmetry somehow survives, it is hard to see how to repair the twisted translation. Though a coproduct structure as in [141] can be used to carry out the bootstrap of a deformed hexagon, it does not map single-trace operators to their descendants as it does not respect cyclic symmetry. As long as we restrict to such sets of operator lengths that the problematic propagators are not present, the undeformed twisted translation can lead to correct results. Thus we can use the $\mathcal{N} = 4$ hexagon amplitudes dressed as in our non-trivial examples. Moreover, although we restricted to the real β-deformation in this thesis, in [2] this analysis was extended to PSU(1, 1|2) sectors using the more general three-parameter γ-deformation. While the β-deformation cannot be implemented in the way described here, it was however possible to reproduce results involving only one γ-parameter, sensitive to two of the R-charges.

Further, the SU(1|2) sector only contains transversal excitation, *i.e.* they cannot be contracted on the rotated vacuum $\hat{Z}$ and thus their one-particle hexagon form factor vanishes. The mentioned problems with the twisted translation will be most prominent when the longitudinal scalar excitations $Y, \bar{Y}$ are involved, since effective propagators $\langle \hat{Y}\hat{Z} \rangle$ and $\langle \hat{\bar{Y}}\hat{Z} \rangle$ exist with the rotated vacuum. In Sec. 3.3.2 we considered examples from the β-deformed SU(2) sector. The asymptotic part of the coupling dependence of these correlators could be recovered from the hexagon computations even in the presence of the deformations. We only considered the asymptotic contribution at one-loop order, but it should be possible to recover it to higher orders and also for operators from the SU(1|2) sector, as the dependence is captured by the Zhukowsky variables. An open and interesting question is how the gluing prescription of [38] can be adapted. Since additional non-trivial deformation factors need to be introduced into the splitting factor for longitudinal excitations, *cf.* eq. (3.34), we need a better understanding of these in order to consider gluing corrections.

More generally, it would be desirable to obtain a first principle derivation of a deformed hexagon formalism. A first step could be to investigate, whether a tailoring picture for spin chains similar to the one developed in [37] does also exist for deformed theories. Building on that, one might think of a more intricate bootstrap procedure for these less supersymmetric theories. Hitherto, we did only muse about the introduction of twist factors for the hexagon operator in a similar spirit as for the S-matrix in [142]. Finally, considering a γ-deformed hexagon formalism, it would be interesting to take a particular limit of the deformation, trying to make contact with the hexagon introduced for fishnet theories in [143].

Double excitations. As discussed, fixing the vacuum breaks the symmetry algebra to a $\mathfrak{su}(2|2) \times \mathfrak{su}(2|2)$ subalgebra and the magnons in the spin chain picture can be considered as bi-fundamental excitations transforming under this subalgebra. However, this picture excludes some of the $\mathcal{N} = 4$ SYM fields, such as the conjugate vacuum $\bar{Z}$, half of the fermions $\Psi^{\alpha 1}, \Psi^{\alpha 2}, \bar{\Psi}^{\dot{\alpha}}_{\dot{3}}, \bar{\Psi}^{\dot{\alpha}}_{\dot{4}}$, as well as the chiral and anti-chiral field strength $\mathcal{F}^{\alpha\beta}, \bar{\mathcal{F}}^{\dot{\alpha}\dot{\beta}}$. In Sec. 3.4 we regained these as double excitations. Since we need a description in the hybrid picture to carry out hexagon calculations, we considered both, the nested and the matrix picture. In both pictures *double excitation creation amplitudes* are necessary. Restricting to tree-level, we also provided an illustrative example with Konishi operators in the SO(6) sector.

In the nested ansatz a double excitation $\bar{Z}$ is created by allowing the combination of simple roots $\mathfrak{R}^1{}_2, \mathfrak{R}^2{}_{\dot{3}}, \mathfrak{R}^{\dot{3}}{}_{\dot{4}}, \mathfrak{R}^2{}_{\dot{3}}$ to act on the same vacuum site. The inclusion of higher-loop effects should also be possible by considering certain gradings of the symmetry algebra [23]. While the creation amplitude in the nested Bethe ansatz depends on the excitations involved, in the matrix picture, we found a universal creation amplitude $\hat{e}(u_1, u_2)$. The structure of these amplitudes suggests, that a dependence on the coupling constant may be introduced by rewriting them in terms of the Zhukovsky variables. The results presented here were worked out from rather simple examples. However, they should be put to more involved tests. For instance, we would like to study local terms also in the Bethe wave functions with multiple derivatives as excitations.

Lagrangian insertion method. Combining the hybrid formalism with the concept of double excitations, we considered the chiral Yang-Mills Lagrangian $\mathrm{tr}\big(\mathcal{F}_{\alpha\beta}\mathcal{F}^{\alpha\beta}\big)$ in Sec. 3.5. At least at tee-level, the existence of double excitations allows to describe the chiral field strength $\mathcal{F}^{\alpha\beta}$ as a site with two fermions. The Yang-Mills Lagrangian of length $L = 2$ carries consequentially four fermionic excitations. Since the Lagrangian is a vacuum descendant, the fermions feature infinite level-I rapidities.

The on-shell field theory Lagrangian further contains admixtures in form of a Yukawa term and the scalar superpotential. In the integrability picture these should be captured by coupling corrections to elements of the respective Bethe ansatz and the relevant solution. We wish to study the implications of this constructions more deeply and hope to clarify this point in future work.

Furthermore, we considered this construction in order to apply the Lagrangian insertion method [68, 69] to the hexagon formalism. Magnificently, since the double excitations are hidden in the local structure of the wave function, the hexagon formalism can be used straightforwardly. This was tested for a simple protected correlator in Sec. 3.5.2. Moreover, as tessellations of higher-point functions are well studied, *cf.* refs. [41, 42, 45], we are confident that loop-corrections for such correlators can

be addressed by these methods. The evaluation of gluing corrections in the hexagon formalism is involved, *cf.* refs. [38, 43, 44], whereas the Lagrangian insertion trades this for the evaluation of a tree-level correlator and an integration. We may hope that this simplifies the explicit calculation. Excitingly, our method would also allow the computation of non-planar corrections to the spectrum problem by placing a Lagrangian on a tiling as in [42, 46, 47, 144]. On the downside, considering more elaborate examples there are some conceptual difficulties to be overcome. For instance, in correlation functions involving physical operators length-changing effects become apparent. We leave these questions for future work.

Part II: Integrability in AdS_3

In this part we considered integrability in $AdS_3 \times S^3 \times T^4$. Though many concepts and methods from integrability were already introduced in Part I, we reviewed the peculiarities of this model in Sec. 4.

Hexagon form factors in AdS_3. Having reviewed the hexagon approach for the computation of three-point functions in $AdS_5 \times S^5$ in Part I, we may wonder, whether such an integrability method can also be devised for $AdS_3 \times S^3 \times T^4$. Our aim in this chapter was to perform the bootstrap procedure for the hexagon form factor and fix its scalar prefactors. This is the first example of such a machinery other than the original. Furthermore, we checked its internal consistency and used it to calculate protected three-point functions, reproducing results from the literature [71].

There are many directions which we may pursue. First of all, our construction can be applied to calculations for backgrounds with a mixture of NSNS and RR background fluxes. Most similar to the case at hand in $AdS_5 \times S^5$ is the consideration of pure RR flux. Moreover, in this case the dressing factors are known [61–63]. On the other hand, restricting to pure NSNS flux should allow us to compare the hexagon results with correlation functions from worldsheet CFT techniques [51]. However, there are two obstructions when trying to find the pure NSNS hexagon. Firstly, the central charges from eq. (4.52) vanish identically for all values of the momentum p. The bootstrap constraints from Sec. 5.2 are then too weak to fix the two-particle from factors. One might expect the hexagon to be related to the two-particle S matrix, although also the S matrix cannot be fixed from symmetry arguments. A proposal for the two-particle S matrix of pure NSNS backgrounds was introduced in [64]. Secondly, even the scalar dressing factors at the pure NSNS point are unknown. Finally, we have the most general case of background supporting both NSNS and RR flux. Unfortunately, this case will possibly be very challenging, as once again the scalar factors are unknown.

For the simple calculation performed here, the asymptotic part of the hexagon was sufficient. Nonetheless, it would be interesting to study the incorporation of mirror corrections into this machinery. A first step into this direction was taken in [127], considering the class of correlators we also studied here. However, due to the presence of massless modes [145] the evaluation may generally be more complicated than in $AdS_5 \times S^5$.

As mentioned several times, the hexagon formalism can also be used to calculate higher-point correlation functions [41, 42, 45] as well as non-planar correlators [42, 46, 47, 144]. For correlation functions of BPS operators wrapping corrections may be controllable. In [127] four-point functions were considered. However, in order to

apply the formalism for such computations, there are still some conceptual issues to be overcome. For instance, there is no clear prescription for the Z-markers yet.

To sum up, though there are missing pieces and open questions, this formalism yields nonetheless the potential to contribute to the understanding of AdS_3/CFT_2. Moreover, one may wonder whether there are further backgrounds allowing for this bootstrap procedure. An important feature so far seems the factorisation of the symmetry algebra of these backgrounds. For instance, with respect to the spectral problem $AdS_4 \times CP^3$ [146] and $AdS_3 \times S^3 \times S^3 \times S^1$ [147] are integrable, though neither of these backgrounds has a factorised symmetry algebra. It would be very interesting to study the possibility of bootstrapping correlation functions for these models.

TBA for AdS_3. We considered the mirror TBA equations for $AdS_3 \times S^3 \times T^4$ with pure RR flux, which were derived in [65] and used the contour deformation trick [72] to excite massless modes. In particular we were interested in the weak tension limit. Given that the kernels behave sufficiently well the equations simplify significantly. The massive modes decouple and the resulting TBA equations given in eq. (6.100) are of difference form, featuring only the Cauchy kernel. In [4, 5] the simplified equations were also solved numerically and we saw that the anomalous dimensions are rather well-approximated by the asymptotic result and quite close to the energies of the free model. One may ask, what the dual CFT of $AdS_3 \times S^3 \times T^4$ string theory with pure RR flux at small-tension is and wonder whether it would be related to the symmetric product orbifold of a free theory. In the case of $AdS_3 \times S^3 \times T^4$ with one unit of pure NSNS flux the dual theory is indeed $\mathrm{Sym}^N(T^4)$. However, our results show, that for pure RR flux already at leading order in the tension h we have an interacting model. Hence, it would be interesting to study the dynamics of the system at hand more closely. In doing so, we may also hope to obtain a better understanding of the dual CFT.

Further, for a particular set of states one may consider interpolating from small tension to finite and possibly large tension. Comparing with perturbative results provides further testing ground. In [139] this was initiated by studying the ground state energy in the semi-classical approximation, where L and h are large, but their ratio is kept fixed. Agreement with the mirror TBA equations was found, including only one of the massless modes, *i.e.* setting $N_0 = 1$. Furthermore, it would be fascinating, trying to make contact with the *Quantum Spectral Curve* (QSC) conjectured in [66, 67]. In [148] such an investigation was initiated for some massive states. Comparing results obtained from the mirror TBA and QSC would help to test whether the two descriptions match and may further settle the question of what role massless modes play in the QSC. These questions may also be answered by deriving the QSC from the mirror TBA in a similar fashion to [149, 150]. Finally, one may wonder whether the mirror TBA can also be extended to mixed flux backgrounds. Once again, the main obstacle here is that the dressing factors for this setting are unknown.

Appendix A.

Evaluation of the $\mathcal{N} = 4$ SYM hexagon

A.1. Parametrisation and crossing

We introduce the Zhukovsky variables $x^{\pm}(u)$ used for $\mathcal{N} = 4$ SYM through the relation

$$\frac{u}{g} = x(u) + \frac{1}{x(u)} \quad \text{and} \quad x^{\pm}(u) = x(u \pm \frac{i}{2}) \,. \tag{A.1}$$

We choose the branch which has $|x(u)| > 1$ as the physical branch and hence find the solution

$$x(u) = \frac{u}{2g}\left(1 + \sqrt{1 - \frac{4g^2}{u^2}}\right) . \tag{A.2}$$

This solution has branch points for $u = \pm 2g$. Therefore, $x^-(u)$ has a short cut between $-2g + \frac{i}{2}$ and $2g + \frac{i}{2}$ in the complex u-plane. Similarly, for $x^+(u)$ the short cut is between $-2g - \frac{i}{2}$ and $2g - \frac{i}{2}$.

Continuing the rapidity u along a closed path across the cuts one gets to another sheet. This analytic continuation of taking the rapidity u into the complex plane and across the branch cuts is also called a 2γ transformation. Similarly, one could only cross one of the cuts. If only the cut for x^+ is crossed, the transformation is denoted as γ transformation or *mirror transformation*. The action of the mirror transformations on the Zhukowsky variables is given by

$$\begin{aligned}
u^{\gamma} \;&: \qquad x^+ \to \frac{1}{x^+} \,, \quad x^- \to x^- \,, \\
u^{2\gamma} \;&: \qquad x^+ \to \frac{1}{x^+} \,, \quad x^- \to \frac{1}{x^-} \,, \\
u^{3\gamma} \;&: \qquad x^+ \to x^+ \,, \quad x^- \to \frac{1}{x^-} \,, \\
u^{4\gamma} \;&: \qquad x^+ \to x^+ \,, \quad x^- \to x^- \,.
\end{aligned} \tag{A.3}$$

Hence, two mirror transformations result in a crossing transformation, taking a particle into an antiparticle. Further, two crossing transformations take the particle back to itself. Functions with a simple dependence on the variables $x^{\pm}$ are not affected by two crossing or four mirror transformations, respectively. In Appendix A.2 we will consider the hexagon phase, which has non-trivial monodromies under crossing.

Finally, there is also a crossing rule for moving magnons from edge to edge. These rules were worked out in [38]. For bosonic excitations $X, Y, \bar{X}, \bar{Y}$ and derivatives $\mathcal{D}^{\alpha\dot{\beta}}$ they read

$$\Phi^{a\dot{b}} \overset{2\gamma}{\to} -\Phi^{b\dot{a}} \,, \qquad \mathcal{D}^{\alpha\dot{\beta}} \overset{2\gamma}{\to} -\mathcal{D}^{\beta\dot{\alpha}} \,, \tag{A.4}$$

while for fermionic magnons the rule is

$$\Psi^{a\dot{\beta}} \overset{2\gamma}{\to} -\Psi^{\beta\dot{a}}\,, \qquad \Psi^{\alpha\dot{b}} \overset{2\gamma}{\to} +\Psi^{b\dot{\alpha}}\,. \tag{A.5}$$

A.2. Dressing phase and measure factor

The dressing phase for hexagon form factors in $\mathcal{N}=4$ SYM was proposed in [38]. It is given by

$$h(u_1,u_2) = \frac{x^-(u_1)-x^-(u_2)}{x^-(u_1)-x^+(u_2)}\,\frac{1-\frac{1}{x^-(u_1)x^+(u_2)}}{1-\frac{1}{x^+(u_1)x^+(u_2)}}\,\frac{1}{\sigma(u_1,u_2)}\,, \tag{A.6}$$

where the $\sigma(u_1,u_2)$ is the Beisert-Eden-Staudacher dressing phase [21]. Further, from the unitarity condition it follows that $\sigma(u_1,u_2)=\frac{1}{\sigma(u_2,u_1)}$. The crossing equation for the BES phase is given by [151]

$$\sigma(u_1^{2\gamma},u_2)\,\sigma(u_1,u_2) = \frac{1-\frac{x^-(u_1)}{x^+(u_2)}}{1-\frac{x^-(u_1)}{x^-(u_2)}}\,\frac{1-\frac{1}{x^+(u_1)x^+(u_2)}}{1-\frac{1}{x^+(u_1)x^-(u_2)}}\,. \tag{A.7}$$

For the scalar h factor, an analogous crossing equation can be obtained straightforwardly [38]

$$h(u_1^{2\gamma},u_2)\,h(u_1,u_2) = \frac{1-\frac{1}{x^+(u_1)x^-(u_2)}}{1-\frac{1}{x^+(u_1)x^+(u_2)}}\,\frac{x^-(u_1)-x^-(u_2)}{x^-(u_1)-x^+(u_2)}\,. \tag{A.8}$$

Further useful relations are given by

$$h(u_1^{2\gamma},u_2^{2\gamma}) = h(u_1,u_2)\,, \qquad h(u_1^{4\gamma},u_2) = \frac{1}{h(u_2,u_1)}\,, \tag{A.9}$$

where the first reflects the invariance of a hexagon amplitude under crossing the full set of excitations from one edge to another.

Finally, there is also the *measure factor* $\mu(u)$. Considering a form factor featuring a particle-antiparticle pair, the measure factor is given by [38]

$$\operatorname*{Res}_{u_1=u_2}\,\langle \mathbf{h}|\bar{\Xi}(u_1^{2\gamma})\Xi(u_2)\rangle = \frac{i}{\mu(u_1)}\,. \tag{A.10}$$

A.3. String and spin chain frame

In Chapter 3, we match the results for correlation functions obtained from the hexagon formalism against field theory results. However, for the evaluation of hexagon form factors it is convenient to use the string frame applying the crossing rules given above. To compare with weak coupling results from field theory, we need to map the result to the spin chain frame. A suitable map was introduced in [38, 100] dressing the magnons with Z-markers as

$$\mathcal{D}_{\rm s} = \mathcal{D}_{\rm s.c.}\,, \quad \Psi_{\rm s} = Z^{\frac{1}{4}}\Psi_{\rm s.c.}Z^{\frac{1}{4}}\,, \quad \Phi_{\rm s} = Z^{\frac{1}{2}}\Phi_{\rm s.c.}Z^{\frac{1}{2}}\,, \tag{A.11}$$

where the subscript s refers to string and *s.c.* to spin chain frame. These factors then introduce momentum dependent phase factors, which map between the different frames. In order to do so all the Z-markers are moved to the very left using $|Z^{\pm}X\rangle = e^{\mp ip}\,|XZ^{\pm}\rangle$. The Z-markers can then be pulled out of the hexagon by using the rule [38]

$$\langle \mathbf{h}|Z^n\alpha\rangle_{\text{s.c.}} = e^{-i\frac{n}{2}P}\,\langle \mathbf{h}|\alpha\rangle_{\text{s.c.}}\ , \tag{A.12}$$

with P the total momentum of the state α. The map for a generic state with excitation on all three edges is then given by

$$\langle \mathbf{h}|\alpha_1\rangle\,|\alpha_2\rangle\,|\alpha_3\rangle_{\text{s.c.}} = (F_{\{p\}}F_{\{q\}}F_{\{r\}})^{-1}e^{\frac{i}{4}[P(l+m-n)+Q(m+n-l)+R(n+l-m)]}\,\langle \mathbf{h}|\alpha_1\rangle\,|\alpha_2\rangle\,|\alpha_3\rangle_{\text{s}}\ , \tag{A.13}$$

where P, Q, R are the total momenta of the excitations on the respective edges $\alpha_1, \alpha_2, \alpha_3$. The factors $F_{\{p\}}$ arise by moving the Z-markers and are given as

$$F_{\{p\}} = \exp\left(i\sum_{k=1}^{|\alpha|}\frac{n_k}{2}\left(\frac{p_k}{2}+\sum_{j=1}^{k-1}p_j\right)\right), \tag{A.14}$$

where n_k characterises the k-th particle in α. We have $n_k = 2$ for a boson, $n_k = 1$ for a fermion and $n_k = 0$ for a derivative. Analogously, we have the factors $F_{\{q\}}, F_{\{r\}}$ for α_2, α_3 with m_k and l_k. Finally, the numbers n, m, l in eq. (A.13) are given by the sums $n = \sum_{k=1}^{|\alpha|} n_k$ and accordingly for m and l. Using this rule, we can evaluate the correlators considered in Sec. 3 in the spin chain frame and compare against field theory results.

Appendix B.

S Matrices and kernels for AdS_3

For the reader's convenience, we list here the various S matrices needed for the mirror TBA equations in Sec. 6.2. The kernels are then obtained by taking the logarithmic derivative. The material listed here was derived in [63, 65].

B.1. S matrices

All the S matrices given here can be found in Appendix B of ref. [65]. We will use a similar notation. Further, we always take the $u + i0$ prescription, when the u-rapidity lies on the branch cut.

The standard bound state S matrix is given by

$$S^{QQ'}(u-u') = S^{Q+Q'}(u-u')S^{Q-Q'}(u-u')\prod_{j=1}^{Q'-1}\Big(S^{Q-Q'+2j}(u-u')\Big)^2\,, \tag{B.1}$$

where the rational S matrix S^Q reads

$$S^Q(u,u') = \frac{u-u'-\frac{iQ}{h}}{u-u'+\frac{iQ}{h}} \tag{B.2}$$

Left-anything scattering:

$$\begin{aligned}
S_{sl}^{Q_aQ_b}(u_a,u_b) &= S^{Q_aQ_b}(u_a-u_b)^{-1}(\Sigma_{ab}^{Q_aQ_b})^{-2}\,,\\
\tilde{S}_{sl}^{Q_a\bar{Q}_b}(u_a,u_b) &= e^{ip_a}\frac{1-\frac{1}{x_a^+x_b^+}}{1-\frac{1}{x_a^-x_b^-}}\frac{1-\frac{1}{x_a^+x_b^-}}{1-\frac{1}{x_a^-x_b^+}}(\tilde{\Sigma}_{ab}^{Q_a\bar{Q}_b})^{-2}\,,\\
S^{Q_a0}(u_a,x_j) &= ie^{-\frac{i}{2}p_a}\frac{x_a^+x_j-1}{x_a^--x_j}\frac{(\Sigma_{\rm BES}^{Q_a0}(x_a^\pm,x_j))^{-2}}{\Phi_{\rm SG}(\gamma_{aj}^{+\circ})\Phi_{\rm SG}(\gamma_{aj}^{-\circ})}\,,\\
S_+^{Q_ay}(u,v) &= e^{\frac{i}{2}p_a}\frac{x^-(u_a)-x(v)}{x^+(u_a)-x(v)}\,,\\
S_-^{Q_ay}(u,v) &= e^{\frac{i}{2}p_a}\frac{x^-(u_a)-\frac{1}{x(v)}}{x^+(u_a)-\frac{1}{x(v)}}\,.
\end{aligned} \tag{B.3}$$

Here we use the notation $\gamma_{aj}^{\pm\circ} = \gamma_a^\pm - \gamma_j$. Moreover, the phases include the improved BES dressing factors such as $\Sigma_{ab}^{Q_aQ_b}$ and $\Sigma_{\rm BES}^{Q_a0}$ which will be given in Appendix B.2.1. Further, the phases also feature the Sine-Gordon factor $\Phi_{\rm SG} = e^{\varphi_{\rm SG}}$, which is given below in Appendix B.2.2.

Right-anything scattering:

$$
\begin{aligned}
S_{su}^{\bar{Q}_a\bar{Q}_b}(u_a,u_b) &= e^{ip_a}e^{-ip_b}\left(\frac{x_a^+-x_b^-}{x_a^--x_b^+}\right)^{-2} S^{\bar{Q}_a\bar{Q}_b}(u_a-u_b)^{-1}(\Sigma_{ab}^{\bar{Q}_a\bar{Q}_b})^{-2}\,,\\
\tilde{S}_{su}^{\bar{Q}_aQ_b}(u_a,u_b) &= e^{-ip_b}\frac{1-\frac{1}{x_a^-x_b^-}}{1-\frac{1}{x_a^+x_b^+}}\frac{1-\frac{1}{x_a^+x_b^-}}{1-\frac{1}{x_a^-x_b^+}}(\tilde{\Sigma}_{ab}^{\bar{Q}_aQ_b}(u_a,u_b))^{-2}\,,\\
\tilde{S}^{\bar{Q}_a0}(u_a,x_j) &= ie^{+\frac{i}{2}p_a}\frac{x_a^--x_j}{x_a^+x_j-1}\frac{(\Sigma_{\rm BES}^{\bar{Q}_a0}(x_a^\pm,x_j))^{-2}}{\Phi_{\rm SG}(\gamma_{aj}^{+\circ})\Phi_{\rm SG}(\gamma_{aj}^{-\circ})}\,.
\end{aligned}
\tag{B.4}
$$

Massless-anything scattering:

$$S^{00}(u_j,u_k) = a(\gamma_{jk})\Phi_{\rm SG}(\gamma_{jk})^2(\Sigma_{\rm BES}^{00}(x_j,x_k))^{-2}\,, \tag{B.5}$$

$$S^{0Q_b}(x_j,u_b) = \frac{1}{S^{Q_b0}(u_b,x_j)}\,, \tag{B.6}$$

$$\tilde{S}^{0\bar{Q}_b}(x_j,u_b) = \frac{1}{\tilde{S}^{\bar{Q}_b0}(u_b,x_j)}\,, \tag{B.7}$$

$$S^{0y}(u,v) = \frac{1}{\sqrt{x(u+i0)^2}}\frac{x(u+i0)-x_s(v+i0)}{\frac{1}{x(u+i0)}-x_s(v+i0)}\,. \tag{B.8}$$

The auxiliary factor $a(\gamma)$ was introduced in [63] and is given by

$$a(\gamma) = -i\tanh\left(\frac{\gamma}{2}-\frac{i\pi}{4}\right) \equiv S(\gamma)\,. \tag{B.9}$$

Auxiliary-anything scattering:

$$S_-^{yQ}(v,u_j) = e^{+\frac{i}{2}p_j}\frac{\frac{1}{x(v)}-x^-(u_j)}{\frac{1}{x(v)}-x^+(u_j)} = \frac{1}{S_-^{Qy}(u_j,v)}\,, \tag{B.10}$$

$$S_+^{yQ}(v,u_j) = e^{-\frac{i}{2}p_j}\frac{x(v)-x^+(u_j)}{x(v)-x^-(u_j)} = \frac{1}{S_+^{Qy}(u_j,v)}\,, \tag{B.11}$$

$$S^{y0}(v,u_j) = \frac{1}{\sqrt{x(u_j+i0)^2}}\frac{x(v)-x(u_j+i0)}{x(v)-\frac{1}{x(u_j+i0)}} = \frac{1}{S^{0y}(u_j,v)}\,. \tag{B.12}$$

We note that $S_\mp^{yQ}(v,u)$ are identical to $S_\pm^{yQ}(v,u)$ in [152]. The corresponding kernels are positive in the mirror-mirror region.

Kernels. The kernels are defined by taking the logarithmic derivative with respect to the rapidity u of the corresponding S matrix in the mirror-mirror kinematics, *i.e.*

$$K^{**}(u,u') = \frac{1}{2\pi i}\frac{\rm d}{{\rm d}u}\log S^{**}(u,u')\,. \tag{B.13}$$

The asterisks indicate massive, massless or auxiliary particles. For instance, the kernel associated to the massive S matrix $S_{sl}^{Q'Q}(u',u)$ will be denoted as $K_{sl}^{Q'Q}(u',u)$ and similarly for the other matrices.

B.2. Dressing factors

The S matrices and kernels encountered in Sec. 6.2 contain the matrix part, but also the dressing phases. The dressing factors given here were proposed in [65].

B.2.1. The BES phase

The improved BES factor in the mirror-mirror region for QQ' particles [65] is the same as in [153],

$$\begin{aligned}\frac{1}{i}\log\Sigma_{\text{BES}}^{QQ'}(x_1^\pm,x_2^\pm) &= \Phi(x_1^+,x_2^+)-\Phi(x_1^+,x_2^-)-\Phi(x_1^-,x_2^+)+\Phi(x_1^-,x_2^-)\\ &\quad-\frac{1}{2}\big(\Psi(x_1^+,x_2^+)+\Psi(x_1^-,x_2^+)-\Psi(x_1^+,x_2^-)-\Psi(x_1^-,x_2^-)\big)\\ &\quad+\frac{1}{2}\big(\Psi(x_2^+,x_1^+)+\Psi(x_2^-,x_1^+)-\Psi(x_2^+,x_1^-)-\Psi(x_2^-,x_1^-)\big)\\ &\quad+\frac{1}{i}\log\frac{i^Q\,\Gamma\big[Q'-\frac{i}{2}h\big(x_1^+-\frac{1}{x_1^+}-x_2^+-\frac{1}{x_2^+}\big)\big]}{i^{Q'}\Gamma\big[Q+\frac{i}{2}h\big(x_1^+-\frac{1}{x_1^+}-x_2^+-\frac{1}{x_2^+}\big)\big]}\frac{1-\frac{1}{x_1^+x_2^-}}{1-\frac{1}{x_1^-x_2^+}}\sqrt{\frac{x_1^+x_2^-}{x_1^-x_2^+}}\,.\end{aligned} \tag{B.14}$$

Here, the functions $\Phi(x_1,x_2)$ and $\Psi(x_1,x_2)$ were introduced, which are given by

$$\begin{aligned}\Phi(x_1,x_2) &= i\oint\frac{\mathrm{d}w_1}{2\pi i}\oint\frac{\mathrm{d}w_2}{2\pi i}\frac{1}{(w_1-x_1)(w_2-x_2)}\log\frac{\Gamma\big[1+\frac{i}{2}h\big(w_1+\frac{1}{w_1}-w_2-\frac{1}{w_2}\big)\big]}{\Gamma\big[1-\frac{i}{2}h\big(w_1+\frac{1}{w_1}-w_2-\frac{1}{w_2}\big)\big]}\,,\\ \Psi(x_1,x_2) &= i\oint\frac{\mathrm{d}w}{2\pi i}\frac{1}{w-x_2}\log\frac{\Gamma\big[1+\frac{i}{2}h\big(x_1+\frac{1}{x_1}-w-\frac{1}{w}\big)\big]}{\Gamma\big[1-\frac{i}{2}h\big(x_1+\frac{1}{x_1}-w-\frac{1}{w}\big)\big]}\,,\end{aligned} \tag{B.15}$$

where the integration contour is the unit circle. The function $\Phi(x_1,x_2)$ is defined for all values of x_1,x_2 with $|x_1|\neq 1$ and $|x_2|\neq 1$.

B.2.2. Sine-Gordon dressing factor

The Sine-Gordon dressing factor is given by [63]

$$\Phi_{\text{SG}}(\gamma)=e^{\varphi_{\text{SG}}(\gamma)}\,, \tag{B.16}$$

with

$$\varphi_{\text{SG}}(\gamma)=\frac{i}{\pi}\text{Li}_2(-e^{-\gamma})-\frac{i}{\pi}\text{Li}_2(e^{-\gamma})+\frac{i\gamma}{\pi}\log\big(1-e^{-\gamma}\big)-\frac{i\gamma}{\pi}\log\big(1+e^{-\gamma}\big)+\frac{i\pi}{4}\,. \tag{B.17}$$

This expression is valid for values of γ with $-\pi<\text{Im}\{\gamma\}<\pi$. Further, for real values of γ, the function $\varphi_{\text{SG}}(\gamma)$ takes purely imaginary values. The functions is defined in such a way, that it satisfies

$$\Phi_{\text{SG}}(\gamma)\Phi_{\text{SG}}(-\gamma)=1\,,\quad \Phi_{\text{SG}}(\gamma)^*=\frac{1}{\Phi_{\text{SG}}(\gamma^*)}\,,\quad \Phi_{\text{SG}}(\gamma)\Phi_{\text{SG}}(\gamma+i\pi)=i\tanh\frac{\gamma}{2}\,. \tag{B.18}$$

Note also, that the Sine-Gordon kernel is then given by

$$\mathcal{K}_{\rm SG}(\gamma) = \frac{1}{2\pi i}\frac{\mathrm{d}}{\mathrm{d}\gamma}\varphi_{\rm SG}(\gamma) = \frac{\gamma}{2\pi^2\sinh\gamma}\,. \tag{B.19}$$

B.2.3. Massive dressing factors

The massive dressing factors in the mirror-mirror kinematics, with $Q, Q' = 1, 2, \ldots$ are given in appendix C of [65] and read

$$\begin{aligned}(\Sigma_{12}^{QQ'})^{-2} &= -\frac{\sinh\frac{\gamma_{12}^{-+}}{2}}{\sinh\frac{\gamma_{12}^{+-}}{2}}e^{\varphi^{\bullet\bullet}(\gamma_1^\pm,\gamma_2^\pm)}(\Sigma_{\rm BES}^{QQ'}(x_1^\pm,x_2^\pm))^{-2}\,,\\ (\tilde{\Sigma}_{12}^{QQ'})^{-2} &= +\frac{\cosh\frac{\gamma_{12}^{+-}}{2}}{\cosh\frac{\gamma_{12}^{-+}}{2}}e^{\tilde{\varphi}^{\bullet\bullet}(\gamma_1^\pm,\gamma_2^\pm)}(\Sigma_{\rm BES}^{QQ'}(x_1^\pm,x_2^\pm))^{-2}\,,\end{aligned} \tag{B.20}$$

where the rapidities with two indices are defined as their difference, *i.e.* $\gamma_{12}^{\pm\mp} = \gamma_1^\pm - \gamma_{12}^\mp$. As defined in eq. (B.13), the corresponding kernels are given as

$$\begin{aligned}K_\Sigma^{Q_1Q_2}(u_1,u_2) &= \frac{1}{2\pi i}\frac{\partial}{\partial u_1}\log\Sigma_{12}^{Q_1Q_2}(x_1^\pm,x_2^\pm),\\ \tilde{K}_\Sigma^{Q_1Q_2}(u_1,u_2) &= \frac{1}{2\pi i}\frac{\partial}{\partial u_1}\log\tilde{\Sigma}_{12}^{Q_1Q_2}(x_1^\pm,x_2^\pm).\end{aligned} \tag{B.21}$$

The phases $\varphi^{\bullet\bullet}$ and $\tilde{\varphi}^{\bullet\bullet}$ are given by eqs. (5.6) and (5.7) in [63]. There the phases are written as

$$\begin{aligned}e^{\varphi^{\bullet\bullet}(\gamma_1^\pm,\gamma_2^\pm)} &= \exp\Big(\varphi_+(\gamma_{12}^{--}) + \varphi_+(\gamma_{12}^{++}) + \varphi_-(\gamma_{12}^{-+}) + \varphi_-(\gamma_{12}^{+-})\Big),\\ e^{\tilde{\varphi}^{\bullet\bullet}(\gamma_1^\pm,\gamma_2^\pm)} &= \exp\Big(\varphi_-(\gamma_{12}^{--}) + \varphi_-(\gamma_{12}^{++}) + \varphi_+(\gamma_{12}^{-+}) + \varphi_+(\gamma_{12}^{+-})\Big),\end{aligned} \tag{B.22}$$

where the functions $\varphi_\pm$ are given through

$$\begin{aligned}\varphi_-(\gamma) &= +\frac{i}{\pi}\mathrm{Li}_2\left(+e^\gamma\right) - \frac{i}{4\pi}\gamma^2 + \frac{i}{\pi}\gamma\,\log\left(1-e^\gamma\right) - \frac{i\pi}{6}\,,\\ \varphi_+(\gamma) &= -\frac{i}{\pi}\mathrm{Li}_2\left(-e^\gamma\right) + \frac{i}{4\pi}\gamma^2 - \frac{i}{\pi}\gamma\,\log\left(1+e^\gamma\right) - \frac{i\pi}{12}\,.\end{aligned} \tag{B.23}$$

B.2.4. Mixed-mass and massless dressing factors

The mixed-mass dressing factors are given by the Sine-Gordon dressing factor $\Phi_{\rm SG}$ as well as the corresponding BES phases. The mixed-mass BES dressing factor can be obtained from eq. (B.14) by setting $Q = 0$ or $Q' = 0$ as needed and the massless ones by setting both to zero. For massless particles in the mirror region the x variable takes values on the real axis with $-1 < x < 1$. Hence, it does not lie on the integration contour and there is no ambiguity in taking the massless limit. As stated in the main text, the BES phase diverges around $x = 0$. However, the convolutions with the massless Y-functions are still finite, if Y_0 vanishes around $x = 0$.

Further, exciting massless modes in the TBA equations, we also need to consider the string-mirror and mirror-string kinematics, where the massless excitation is in

the string region. For instance, let us consider $\Sigma^{0Q'}_{\text{BES}}(x, y^{\pm})$ where we set $Q = 0$. For massless particles in the string region, the Zhukovsky variable x lies on the upper-half circle. Considering the functions Φ and Ψ from eq. (B.15) this appears problematic. As the massless particle lies on the integration contour, this seems to lead to a pole. For our example of $\Sigma^{0Q'}_{\text{BES}}(x, y^{\pm})$ the potential issues arise from the integrals in the functions $\Phi(x, y^{\pm})$, $\Phi(\frac{1}{x}, y^{\pm})$, $\Psi(y^{\pm}, x)$, and $\Psi(y^{\pm}, \frac{1}{x})$. However, the integrals can be continued inside the unit circle as long as h is finite, as no singularities occur outside a disk of radius $(\sqrt{1 + (2h)^{-2}} - (2h)^{-1})$. For a detailed discussion of the analytic properties we refer the reader to ref. [153]. In practice, also a principal-value prescription can be used. Here the relevant residues at the poles are added, when we want to compute the explicit values of the BES dressing factor.

Bibliography

[1] B. Eden, D. le Plat and A. Sfondrini, *Integrable bootstrap for AdS_3/CFT_2 correlation functions*, *JHEP* **08** (2021) 049 [2102.08365].

[2] B. Eden, D. le Plat and A. Spiering, *Higher-rank sectors in the hexagon formalism and marginal deformations*, 2212.03211.

[3] B. Eden, D. le Plat and A. Spiering, *Double excitations in the AdS(5)/CFT(4) integrable system and the Lagrange operator*, 2302.02961.

[4] A. Brollo, D. le Plat, A. Sfondrini and R. Suzuki, *Tensionless Limit of Pure–Ramond-Ramond Strings and AdS3/CFT2*, *Phys. Rev. Lett.* **131** (2023) 161604 [2303.02120].

[5] A. Brollo, D. le Plat, A. Sfondrini and R. Suzuki, *More on the tensionless limit of pure-Ramond-Ramond AdS3/CFT2*, 2308.11576.

[6] G. 't Hooft, *A planar diagram theory for strong interactions*, *Nucl. Phys.* **B72** (1974) 461.

[7] J. M. Maldacena, *The large N limit of superconformal field theories and supergravity*, *Adv. Theor. Math. Phys.* **2** (1998) 231 [hep-th/9711200].

[8] N. Beisert, C. Ahn, L. F. Alday, Z. Bajnok, J. M. Drummond, L. Freyhult et al., *Review of AdS/CFT Integrability: An Overview*, *Lett. Math. Phys.* **99** (2012) 3 [1012.3982].

[9] O. Aharony, O. Bergman, D. L. Jafferis and J. Maldacena, *$\mathcal{N} = 6$ superconformal Chern-Simons-matter theories, M2-branes and their gravity duals*, *JHEP* **0810** (2008) 091 [0806.1218].

[10] A. Sfondrini, *Towards integrability for AdS_3/CFT_2*, *J. Phys.* **A48** (2015) 023001 [1406.2971].

[11] S. S. Gubser, I. R. Klebanov and A. M. Polyakov, *Gauge theory correlators from non-critical string theory*, *Phys. Lett.* **B428** (1998) 105 [hep-th/9802109].

[12] E. Witten, *Anti-de Sitter space and holography*, *Adv. Theor. Math. Phys.* **2** (1998) 253 [hep-th/9802150].

[13] D. E. Berenstein, J. M. Maldacena and H. S. Nastase, *Strings in flat space and pp waves from $\mathcal{N} = 4$ super Yang Mills*, *JHEP* **0204** (2002) 013 [hep-th/0202021].

[14] J. A. Minahan and K. Zarembo, *The Bethe-ansatz for $\mathcal{N} = 4$ super Yang-Mills*, *JHEP* **0303** (2003) 013 [hep-th/0212208].

[15] H. Bethe, *On the theory of metals. 1. Eigenvalues and eigenfunctions for the linear atomic chain*, *Z. Phys.* **71** (1931) 205.

[16] N. Beisert and M. Staudacher, *The $\mathcal{N} = 4$ SYM integrable super spin chain*, *Nucl. Phys.* **B670** (2003) 439 [hep-th/0307042].

[17] N. Beisert, *The complete one-loop dilatation operator of $\mathcal{N} = 4$ super Yang-Mills theory*, *Nucl. Phys.* **B676** (2004) 3 [hep-th/0307015].

[18] N. Beisert, C. Kristjansen and M. Staudacher, *The dilatation operator of conformal $\mathcal{N} = 4$ super Yang-Mills theory*, *Nucl. Phys.* **B664** (2003) 131 [hep-th/0303060].

[19] N. Beisert, *The $\mathfrak{su}(2|2)$ dynamic S-matrix*, *Adv. Theor. Math. Phys.* **12** (2008) 945 [hep-th/0511082].

[20] A. B. Zamolodchikov and A. B. Zamolodchikov, *Factorized s-matrices in two dimensions as the exact solutions of certain relativistic quantum field theory models*, *Annals of Physics* **120** (1979) 253.

[21] N. Beisert, B. Eden and M. Staudacher, *Transcendentality and crossing*, *J. Stat. Mech.* **0701** (2007) P01021 [hep-th/0610251].

[22] N. Beisert, V. Dippel and M. Staudacher, *A novel long range spin chain and planar $\mathcal{N} = 4$ super Yang- Mills*, *JHEP* **0407** (2004) 075 [hep-th/0405001].

[23] N. Beisert and M. Staudacher, *Long-range* PSU$(2, 2|4)$ *Bethe ansaetze for gauge theory and strings*, *Nucl. Phys.* **B727** (2005) 1 [hep-th/0504190].

[24] J. Ambjørn, R. A. Janik and C. Kristjansen, *Wrapping interactions and a new source of corrections to the spin-chain/string duality*, *Nucl. Phys.* **B736** (2006) 288 [hep-th/0510171].

[25] A. B. Zamolodchikov, *Thermodynamic Bethe ansatz in relativistic models. Scaling three state Potts and Lee-Yang models*, *Nucl. Phys.* **B342** (1990) 695.

[26] G. Arutyunov and S. Frolov, *On string S-matrix, bound states and TBA*, *JHEP* **0712** (2007) 024 [0710.1568].

[27] D. Bombardelli, D. Fioravanti and R. Tateo, *Thermodynamic Bethe ansatz for planar AdS/CFT: a proposal*, *J. Phys.* **A42** (2009) 375401 [0902.3930].

[28] G. Arutyunov and S. Frolov, *Thermodynamic Bethe ansatz for the $AdS_5 \times S^5$ mirror model*, *JHEP* **0905** (2009) 068 [0903.0141].

[29] G. Arutyunov and S. Frolov, *Simplified TBA equations of the AdS(5) x S**5 mirror model*, *JHEP* **11** (2009) 019 [0907.2647].

[30] N. Gromov, V. Kazakov, S. Leurent and D. Volin, *Quantum spectral curve for AdS_5/CFT_4*, *Phys. Rev. Lett.* **112** (2014) 011602 [1305.1939].

[31] N. Gromov, V. Kazakov, S. Leurent and D. Volin, *Quantum spectral curve for arbitrary state/operator in AdS_5/CFT_4*, *JHEP* **09** (2015) 187 [1405.4857].

[32] C. Marboe and D. Volin, *Quantum spectral curve as a tool for a perturbative quantum field theory*, *Nucl. Phys. B* **899** (2015) 810 [1411.4758].

[33] N. Beisert, *The S-matrix of AdS / CFT and Yangian symmetry*, *PoS* **SOLVAY** (2006) 002 [0704.0400].

[34] R. G. Leigh and M. J. Strassler, *Exactly marginal operators and duality in four-dimensional N=1 supersymmetric gauge theory*, *Nucl. Phys. B* **447** (1995) 95 [hep-th/9503121].

[35] R. Roiban, *On spin chains and field theories*, *JHEP* **09** (2004) 023 [hep-th/0312218].

[36] O. Lunin and J. M. Maldacena, *Deforming field theories with U(1) x U(1) global symmetry and their gravity duals*, *JHEP* **05** (2005) 033 [hep-th/0502086].

[37] J. Escobedo, N. Gromov, A. Sever and P. Vieira, *Tailoring three-point functions and integrability*, *JHEP* **1109** (2010) 028 [1012.2475].

[38] B. Basso, S. Komatsu and P. Vieira, *Structure constants and integrable bootstrap in planar $\mathcal{N} = 4$ SYM theory*, 1505.06745.

[39] B. Eden and A. Sfondrini, *Three-point functions in $\mathcal{N} = 4$ SYM: the hexagon proposal at three loops*, *JHEP* **02** (2016) 165 [1510.01242].

[40] B. Basso, V. Goncalves, S. Komatsu and P. Vieira, *Gluing Hexagons at Three Loops*, *Nucl. Phys.* **B907** (2016) 695 [1510.01683].

[41] T. Fleury and S. Komatsu, *Hexagonalization of Correlation Functions*, *JHEP* **01** (2017) 130 [1611.05577].

[42] B. Eden, Y. Jiang, D. le Plat and A. Sfondrini, *Colour-dressed hexagon tessellations for correlation functions and non-planar corrections*, *JHEP* **02** (2018) 170 [1710.10212].

[43] T. Fleury and S. Komatsu, *Hexagonalization of Correlation Functions II: Two-Particle Contributions*, *JHEP* **02** (2018) 177 [1711.05327].

[44] M. De Leeuw, B. Eden, D. le Plat, T. Meier and A. Sfondrini, *Multi-particle finite-volume effects for hexagon tessellations*, *JHEP* **09** (2020) 039 [1912.12231].

[45] B. Eden and A. Sfondrini, *Tessellating cushions: four-point functions in $\mathcal{N} = 4$ SYM*, *JHEP* **10** (2017) 098 [1611.05436].

[46] T. Bargheer, J. Caetano, T. Fleury, S. Komatsu and P. Vieira, *Handling Handles I: Nonplanar Integrability*, 1711.05326.

[47] B. Eden and T. Scherdin, *Tilings and Twist at $1/N^4$*, 2203.09399.

[48] O. Ohlsson Sax and B. Stefański, *Closed strings and moduli in AdS_3/CFT_2*, *JHEP* **05** (2018) 101 [1804.02023].

[49] J. M. Maldacena and H. Ooguri, *Strings in AdS_3 and $\mathrm{SL}(2,R)$ WZW model. I*, *J. Math. Phys.* **42** (2001) 2929 [hep-th/0001053].

[50] J. M. Maldacena, H. Ooguri and J. Son, *Strings in AdS_3 and the $\mathrm{SL}(2,R)$ WZW model. II: Euclidean black hole*, *J. Math. Phys.* **42** (2001) 2961 [hep-th/0005183].

[51] J. M. Maldacena and H. Ooguri, *Strings in AdS_3 and the $\mathrm{SL}(2,R)$ WZW model. III: Correlation functions*, *Phys. Rev.* **D65** (2002) 106006 [hep-th/0111180].

[52] G. Giribet, C. Hull, M. Kleban, M. Porrati and E. Rabinovici, *Superstrings on AdS_3 at $k = 1$*, *JHEP* **08** (2018) 204 [1803.04420].

[53] M. R. Gaberdiel and R. Gopakumar, *Tensionless string spectra on AdS_3*, *JHEP* **05** (2018) 085 [1803.04423].

[54] L. Eberhardt, M. R. Gaberdiel and R. Gopakumar, *The Worldsheet Dual of the Symmetric Product CFT*, *JHEP* **04** (2019) 103 [1812.01007].

[55] A. Babichenko, B. Stefański, jr. and K. Zarembo, *Integrability and the AdS_3/CFT_2 correspondence*, *JHEP* **1003** (2010) 058 [0912.1723].

[56] A. Cagnazzo and K. Zarembo, *B-field in AdS_3/CFT_2 correspondence and integrability*, *JHEP* **1211** (2012) 133 [1209.4049].

[57] B. Hoare and A. A. Tseytlin, *On string theory on $AdS_3 \times S^3 \times T^4$ with mixed 3-form flux: tree-level S-matrix*, *Nucl. Phys.* **B873** (2013) 682 [1303.1037].

[58] B. Hoare, A. Stepanchuk and A. Tseytlin, *Giant magnon solution and dispersion relation in string theory in $AdS_3 \times S^3 \times T^4$ with mixed flux*, *Nucl. Phys.* **B879** (2014) 318 [1311.1794].

[59] T. Lloyd, O. Ohlsson Sax, A. Sfondrini and B. Stefański, jr., *The complete worldsheet S matrix of superstrings on $AdS_3 \times S^3 \times T^4$ with mixed three-form flux*, *Nucl. Phys.* **B891** (2015) 570 [1410.0866].

[60] R. Borsato, O. Ohlsson Sax, A. Sfondrini and B. Stefański, jr, *The complete $AdS_3 \times S^3 \times T^4$ worldsheet S-matrix*, *JHEP* **1410** (2014) 66 [1406.0453].

[61] R. Borsato, O. Ohlsson Sax, A. Sfondrini, B. Stefański, jr. and A. Torrielli, *Dressing phases of AdS_3/CFT_2*, *Phys. Rev.* **D88** (2013) 066004 [1306.2512].

[62] R. Borsato, O. Ohlsson Sax, A. Sfondrini, B. Stefański, jr. and A. Torrielli, *On the dressing factors, Bethe equations and Yangian symmetry of strings on $AdS_3 \times S^3 \times T^4$*, *J. Phys.* **A50** (2017) 024004 [1607.00914].

[63] S. Frolov and A. Sfondrini, *New dressing factors for AdS3/CFT2*, *JHEP* **04** (2022) 162 [2112.08896].

[64] M. Baggio and A. Sfondrini, *Strings on NS-NS Backgrounds as Integrable Deformations*, *Phys. Rev.* **D98** (2018) 021902 [1804.01998].

[65] S. Frolov and A. Sfondrini, *Mirror thermodynamic Bethe ansatz for AdS3/CFT2*, *JHEP* **03** (2022) 138 [2112.08898].

[66] A. Cavaglià, N. Gromov, B. Stefański, Jr., Jr. and A. Torrielli, *Quantum Spectral Curve for AdS_3/CFT_2: a proposal*, *JHEP* **12** (2021) 048 [2109.05500].

[67] S. Ekhammar and D. Volin, *Monodromy bootstrap for SU(2|2) quantum spectral curves: from Hubbard model to AdS_3/CFT_2*, *JHEP* **03** (2022) 192 [2109.06164].

[68] B. Eden, P. S. Howe and P. C. West, *Nilpotent invariants in N=4 SYM*, *Phys. Lett. B* **463** (1999) 19 [hep-th/9905085].

[69] B. Eden, A. C. Petkou, C. Schubert and E. Sokatchev, *Partial nonrenormalization of the stress tensor four point function in N=4 SYM and AdS / CFT*, *Nucl. Phys. B* **607** (2001) 191 [hep-th/0009106].

[70] R. Borsato, O. Ohlsson Sax and A. Sfondrini, *A dynamic $\mathfrak{su}(1|1)^2$ S-matrix for AdS_3/CFT_2*, *JHEP* **1304** (2013) 113 [1211.5119].

[71] A. Pakman and A. Sever, *Exact $\mathcal{N} = 4$ correlators of AdS_3/CFT_2*, *Phys. Lett.* **B652** (2007) 60 [0704.3040].

[72] P. Dorey and R. Tateo, *Excited states by analytic continuation of TBA equations*, *Nucl. Phys.* **B482** (1996) 639 [hep-th/9607167].

[73] F. Gliozzi, J. Scherk and D. Olive, *Supersymmetry, supergravity theories and the dual spinor model*, *Nuclear Physics B* **122** (1977) 253.

[74] L. Brink, J. H. Schwarz and J. Scherk, *Supersymmetric yang-mills theories*, *Nuclear Physics B* **121** (1977) 77.

[75] V. K. Dobrev and V. B. Petkova, *All positive energy unitary irreducible representations of extended conformal supersymmetry*, *Phys. Lett.* **B162** (1985) 127.

[76] M. Gunaydin and N. Marcus, *The spectrum of the s5 compactification of the chiral n=2, d=10 supergravity and the unitary supermultiplets of u(2,2/4)*, *Classical and Quantum Gravity* **2** (1985) L11.

[77] N. Beisert, *The dilatation operator of $\mathcal{N} = 4$ super Yang-Mills theory and integrability*, *Phys. Rept.* **405** (2004) 1 [hep-th/0407277].

[78] M. F. Sohnius and P. C. West, *Conformal invariance in n = 4 supersymmetric yang-mills theory*, *Physics Letters B* **100** (1981) 245.

[79] S. Mandelstam, *Light-cone superspace and the ultraviolet finiteness of the n=4 model*, *Nuclear Physics B* **213** (1983) 149.

[80] L. Brink, O. Lindgren and B. E.W. Nilsson, *The ultra-violet finiteness of the n=4 yang-mills theory*, *Physics Letters B* **123** (1983) 323.

[81] V. Arnold, *Mathematical methods of classical mechanics*, vol. 60. Springer, 1989.

[82] O. Babelon, D. Bernard and M. Talon, *Introduction to Classical Integrable Systems*, Cambridge Monographs on Mathematical Physics. Cambridge University Press, 2003, 10.1017/CBO9780511535024.

[83] A. Torrielli, *Lectures on Classical Integrability*, *J. Phys. A* **49** (2016) 323001 [1606.02946].

[84] S. Driezen, *Modave Lectures on Classical Integrability in 2d Field Theories*, *PoS* **Modave2021** (2022) 002 [2112.14628].

[85] V. E. Korepin, *Calculation of norms of Bethe wave functions*, *Communications in Mathematical Physics* **86** (1982) 391 .

[86] M. Gaudin, *DIAGONALISATION D'UNE CLASSE D'HAMILTONIENS DE SPIN*, pp. 301–312. EDP Sciences, Les Ulis, 1996. doi:10.1051/978-2-7598-0254-8.c018.

[87] C. N. Yang, *Some exact results for the many-body problem in one dimension with repulsive delta-function interaction*, *Phys. Rev. Lett.* **19** (1967) 1312.

[88] O. Aharony and S. S. Razamat, *Exactly marginal deformations of N=4 SYM and of its supersymmetric orbifold descendants*, *JHEP* **05** (2002) 029 [hep-th/0204045].

[89] D. Berenstein and S. A. Cherkis, *Deformations of N=4 SYM and integrable spin chain models*, *Nucl. Phys. B* **702** (2004) 49 [hep-th/0405215].

[90] D. Bundzik and T. Mansson, *The General Leigh-Strassler deformation and integrability*, *JHEP* **01** (2006) 116 [hep-th/0512093].

[91] L. V. Bork, D. I. Kazakov, G. S. Vartanov and A. V. Zhiboedov, *Conformal Invariance in the Leigh-Strassler deformed N=4 SYM Theory*, *JHEP* **04** (2008) 003 [0712.4132].

[92] A. Mauri, S. Penati, A. Santambrogio and D. Zanon, *Exact results in planar N=1 superconformal Yang-Mills theory*, *JHEP* **11** (2005) 024 [hep-th/0507282].

[93] J. Fokken, C. Sieg and M. Wilhelm, *Non-conformality of γ_i-deformed $\mathcal{N} = 4$ SYM theory*, *J. Phys.* **A47** (2014) 455401 [1308.4420].

[94] J. Fokken, C. Sieg and M. Wilhelm, *The complete one-loop dilatation operator of planar real β-deformed $\mathcal{N} = 4$ SYM theory*, *JHEP* **1407** (2014) 150 [1312.2959].

[95] T. Filk, *Divergencies in a field theory on quantum space*, *Physics Letters B* **376** (1996) 53.

[96] V. V. Khoze, *Amplitudes in the beta-deformed conformal Yang-Mills*, *JHEP* **02** (2006) 040 [hep-th/0512194].

[97] N. Beisert and R. Roiban, *Beauty and the twist: The Bethe ansatz for twisted N=4 SYM*, *JHEP* **08** (2005) 039 [hep-th/0505187].

[98] Z. Bajnok and R. A. Janik, *String field theory vertex from integrability*, *JHEP* **04** (2015) 042 [1501.04533].

[99] N. Drukker and J. Plefka, *Superprotected n-point correlation functions of local operators in $\mathcal{N} = 4$ super Yang-Mills*, *JHEP* **04** (2009) 052 [0901.3653].

[100] J. Caetano and T. Fleury, *Fermionic Correlators from Integrability*, *JHEP* **09** (2016) 010 [1607.02542].

[101] V. Gonçalves, *Extracting OPE coefficient of Konishi at four loops*, *JHEP* **03** (2017) 079 [1607.02195].

[102] B. Eden and F. Paul, *Half-BPS half-BPS twist two at four loops in N=4 SYM*, 1608.04222.

[103] B. Basso, V. Goncalves and S. Komatsu, *Structure constants at wrapping order*, 1702.02154.

[104] B. Basso, F. Coronado, S. Komatsu, H. T. Lam, P. Vieira and D.-l. Zhong, *Asymptotic Four Point Functions*, 1701.04462.

[105] T. McLoughlin, R. Pereira and A. Spiering, *One-loop non-planar anomalous dimensions in super Yang-Mills theory*, *JHEP* **10** (2020) 124 [2005.14254].

[106] L. F. Alday, J. R. David, E. Gava and K. S. Narain, *Structure constants of planar N = 4 Yang Mills at one loop*, *JHEP* **09** (2005) 070 [hep-th/0502186].

[107] J. R. David and A. Sadhukhan, *Structure constants of β deformed super Yang-Mills*, *JHEP* **10** (2013) 206 [1307.3909].

[108] B. Eden, P. Heslop, G. P. Korchemsky and E. Sokatchev, *Hidden symmetry of four-point correlation functions and amplitudes in N=4 SYM*, *Nucl. Phys. B* **862** (2012) 193 [1108.3557].

[109] B. Eden, P. Heslop, G. P. Korchemsky and E. Sokatchev, *Constructing the correlation function of four stress-tensor multiplets and the four-particle amplitude in N=4 SYM*, *Nucl. Phys. B* **862** (2012) 450 [1201.5329].

[110] B. Eden, P. Heslop, G. P. Korchemsky and E. Sokatchev, *The super-correlator/super-amplitude duality: Part I*, *Nucl. Phys. B* **869** (2013) 329 [1103.3714].

[111] G. Arutyunov and S. Frolov, *Foundations of the $AdS_5 \times S^5$ superstring. part I*, *J. Phys. A* **A42** (2009) 254003 [0901.4937].

[112] R. Borsato, O. Ohlsson Sax, A. Sfondrini, B. Stefański, jr. and A. Torrielli, *The all-loop integrable spin-chain for strings on $AdS_3 \times S^3 \times T^4$: the massive sector*, *JHEP* **1308** (2013) 043 [1303.5995].

[113] G. Arutyunov, S. Frolov, J. Plefka and M. Zamaklar, *The off-shell symmetry algebra of the light-cone $AdS_5 \times S^5$ superstring*, *J. Phys.* **A40** (2007) 3583 [hep-th/0609157].

[114] R. Borsato, O. Ohlsson Sax and A. Sfondrini, *All-loop Bethe ansatz equations for AdS_3/CFT_2*, *JHEP* **1304** (2013) 116 [1212.0505].

[115] R. Borsato, O. Ohlsson Sax, A. Sfondrini and B. Stefański, jr., *Towards the all-loop worldsheet S matrix for $AdS_3 \times S^3 \times T^4$*, *Phys. Rev. Lett.* **113** (2014) 131601 [1403.4543].

[116] J. Plefka, F. Spill and A. Torrielli, *On the Hopf algebra structure of the AdS/CFT S-matrix*, *Phys. Rev.* **D74** (2006) 066008 [hep-th/0608038].

[117] A. Torrielli, *Review of AdS/CFT integrability, Chapter VI.2: Yangian algebra*, *Lett. Math. Phys.* **99** (2010) 547 [1012.4005].

[118] N. Drukker and J. Plefka, *The Structure of n-point functions of chiral primary operators in N=4 super Yang-Mills at one-loop*, *JHEP* **04** (2009) 001 [0812.3341].

[119] K. M. Watson, *Some general relations between the photoproduction and scattering of π mesons*, *Phys. Rev.* **95** (1954) 228.

[120] F. A. Smirnov, *Form-factors in completely integrable models of quantum field theory*, *Adv. Ser. Math. Phys.* **14** (1992) 1.

[121] M. Baggio, J. de Boer and K. Papadodimas, *A non-renormalization theorem for chiral primary 3-point functions*, *JHEP* **07** (2012) 137 [1203.1036].

[122] M. Baggio, O. Ohlsson Sax, A. Sfondrini, B. Stefański, jr. and A. Torrielli, *Protected string spectrum in AdS_3/CFT_2 from worldsheet integrability*, *JHEP* **04** (2017) 091 [1701.03501].

[123] A. Dei and A. Sfondrini, *Integrable spin chain for stringy Wess-Zumino-Witten models*, *JHEP* **07** (2018) 109 [1806.00422].

[124] M. R. Gaberdiel and I. Kirsch, *Worldsheet correlators in AdS_3/CFT_2*, *JHEP* **0704** (2007) 050 [hep-th/0703001].

[125] A. Dabholkar and A. Pakman, *Exact chiral ring of AdS_3/CFT_2*, *Adv. Theor. Math. Phys.* **13** (2009) 409 [hep-th/0703022].

[126] M. Baggio, V. Niarchos and K. Papadodimas, *On exact correlation functions in SU(N) $\mathcal{N} = 2$ superconformal QCD*, *JHEP* **11** (2015) 198 [1508.03077].

[127] M. Fabri, *Hexagonalization in AdS3×S3×T4: Mirror corrections*, *Phys. Rev. D* **106** (2022) 126008 [2209.01959].

[128] R. Borsato, O. Ohlsson Sax, A. Sfondrini and B. Stefański, *On the spectrum of $AdS_3 \times S^3 \times T^4$ strings with Ramond-Ramond flux*, *J. Phys.* **A49** (2016) 41LT03 [1605.00518].

[129] M. Lüscher, *Volume dependence of the energy spectrum in massive quantum field theories. 1. Stable particle states*, *Commun. Math. Phys.* **104** (1986) 177.

[130] S. J. van Tongeren, *Integrability of the $AdS_5 \times S^5$ superstring and its deformations*, *J. Phys.* **A47** (2014) 433001 [1310.4854].

[131] S. J. van Tongeren, *Introduction to the thermodynamic Bethe ansatz*, *J. Phys. A* **49** (2016) 323005 [1606.02951].

[132] Z. Bajnok, *Review of AdS/CFT integrability, Chapter III.6: Thermodynamic Bethe ansatz*, *Lett. Math. Phys.* **99** (2010) 299 [1012.3995].

[133] F. Woynarovich, *On the sz=0 excited states of an anisotropic heisenberg chain*, *Journal of Physics A: Mathematical and General* **15** (1982) 2985.

[134] F. Woynarovich, *On the eigenstates of a heisenberg chain with complex wavenumbers not forming strings*, *Journal of Physics C: Solid State Physics* **15** (1982) 6397.

[135] O. Babelon, H. de Vega and C. Viallet, *Analysis of the bethe ansatz equations of the xxz model*, *Nuclear Physics B* **220** (1983) 13.

[136] A. Tsvelick and P. Wiegmann, *Exact results in the theory of magnetic alloys*, *Advances in Physics* **32** (1983) 453.

[137] A. Fontanella and A. Torrielli, *Geometry of Massless Scattering in Integrable Superstring*, *JHEP* **06** (2019) 116 [1903.10759].

[138] S. Frolov and A. Sfondrini, *Massless S matrices for AdS3/CFT2*, *JHEP* **04** (2022) 067 [2112.08895].

[139] S. Frolov, A. Pribytok and A. Sfondrini, *Ground state energy of twisted $AdS_3 \times S^3 \times T^4$ superstring and the TBA*, 2305.17128.

[140] S. Frolov and R. Suzuki, *Temperature quantization from the TBA equations*, *Phys. Lett. B* **679** (2009) 60 [0906.0499].

[141] A. Garus, *Untwisting the symmetries of β-deformed Super-Yang–Mills*, *JHEP* **10** (2017) 007 [1707.04128].

[142] C. Ahn, Z. Bajnok, D. Bombardelli and R. I. Nepomechie, *Twisted Bethe equations from a twisted S-matrix*, *JHEP* **1102** (2011) 027 [1010.3229].

[143] B. Basso, J. Caetano and T. Fleury, *Hexagons and Correlators in the Fishnet Theory*, 1812.09794.

[144] T. Bargheer, F. Coronado and P. Vieira, *Octagons I: Combinatorics and Non-Planar Resummations*, *JHEP* **08** (2019) 162 [1904.00965].

[145] M. C. Abbott and I. Aniceto, *Massless Lüscher terms and the limitations of the AdS_3 asymptotic Bethe ansatz*, *Phys. Rev.* **D93** (2016) 106006 [1512.08761].

[146] T. Klose, *Review of AdS/CFT integrability, Chapter IV.3: $\mathcal{N} = 6$ Chern-Simons and strings on $AdS_4 \times CP^3$*, *Lett. Math. Phys.* **99** (2010) 401 [1012.3999].

[147] R. Borsato, O. Ohlsson Sax, A. Sfondrini and B. Stefański, jr., *The $AdS_3 \times S^3 \times S^3 \times S^1$ worldsheet S matrix*, *J. Phys.* **A48** (2015) 415401 [1506.00218].

[148] A. Cavaglià, S. Ekhammar, N. Gromov and P. Ryan, *Exploring the Quantum Spectral Curve for AdS_3/CFT_2*, 2211.07810.

[149] D. Bombardelli, A. Cavaglià, D. Fioravanti, N. Gromov and R. Tateo, *The full quantum spectral curve for AdS_4/CFT_3*, *JHEP* **09** (2017) 140 [1701.00473].

[150] R. Klabbers and S. J. van Tongeren, *Quantum Spectral Curve for the eta-deformed AdS_5xS^5 superstring*, *Nucl. Phys.* **B925** (2017) 252 [1708.02894].

[151] R. A. Janik, *The $AdS_5 \times S^5$ superstring worldsheet S-matrix and crossing symmetry*, *Phys. Rev.* **D73** (2006) 086006 [hep-th/0603038].

[152] G. Arutyunov, S. Frolov and R. Suzuki, *Exploring the mirror TBA*, *JHEP* **1005** (2010) 031 [0911.2224].

[153] G. Arutyunov and S. Frolov, *The dressing factor and crossing equations*, *J. Phys.* **A42** (2009) 425401 [0904.4575].